Vehicle vibration analysis

J van Wyngaardt
20717202

Dissertation submitted in fulfilment of the requirements for the degree *Magister in Mechanical Engineering* at the Potchefstroom Campus of the North-West University

Supervisor: Dr CB Nel

May 2014

SUMMARY

Engine noise and vibration harshness is a big concern in the competitive automotive vehicle manufacturing industry. It is very important to limit the vibration and noise levels for the general pleasure of driving. Vibration could cause human discomfort as experienced by the vehicle driver and the passengers. Vibration transmitted from the engine to the vehicle's support structure is also a disadvantage from a material fatigue point of view.

For this literature survey done, no previous work could be found where a vibration absorber was used at an engine of a vehicle. The feasibility of an engine vibration absorber to reduce vibration levels at a vehicle for several driving conditions was examined in this study. An Engine Vibration Absorber was successfully designed, manufactured and also experimentally characterised and evaluated. The design involved the development of mathematical models to determine mainly responses and natural frequencies. The mathematical models were implemented in computer programs developed. The design included the choices that were made regarding size, layout, position, mass, stiffness and damping properties for this Absorber. All the parameters required as input data for the computer programs were experimentally characterised. The dynamic properties of rubber mounts used at the Absorber were amplitude excitation dependant and thus complicated the analysis and the characterisation, but these stiffness and damping magnitudes were successfully determined and used in the computer simulations.

The Engine Vibration Absorber was successfully tuned for a frequency that corresponded to the vertical bounce mode natural frequency of the Engine mount system. The predicted and measured natural frequency magnitudes of the two-degree-of-freedom system were compared.

As criteria of vibration transmitted, the dynamic force magnitudes transmitted through the Engine mounts to the vehicle's support structure were computed with the programs developed. These dynamic force magnitudes transmitted were also experimentally determined. These predicted and measured dynamic force magnitudes were compared for several operational conditions.

Various operational conditions were theoretically and experimentally investigated. Steady state conditions included responses from road input forces, as well as from internal engine shaking forces. Transient conditions included responses resulting from road impact forces, engine starting, and engine stopping conditions.

The study shows that the Engine Vibration Absorber reduced the noise levels measured inside the vehicle's compartment. The Engine Vibration Absorber very effectively reduced the dynamic force magnitudes (vibration) transmitted to the vehicle's support structure for all the different road input conditions at or near resonance. The Engine Vibration Absorber significantly reduced the significantly larger vibration amplitudes caused by road inputs, but with no significant negative effect regarding any additional dynamic forces transmitted when the Engine was running at several speeds.

Keywords: Vehicle vibration, absorber, tunable, resonance, reduced vibration

---

OPSOMMING

Enjin geraas en vibrasie intensiteit is 'n groot kommer in die mededingende motorbedryf. Dit is baie belangrik om die vibrasie- en geraasvlakke te beperk ter wille van die algemene plesier van bestuur. Vibrasie kan menslike ongemak veroorsaak, soos ervaar deur die voertuigbestuurder en die passasiers. Vibrasie wat oorgedra word na die voertuig se ondersteuningstruktuur vanaf die enjin is verder 'n nadeel vanuit 'n materiaal vermoeidheid oogpunt.

Vir hierdie literatuurstudie kon geen vorige studies gevind word waar 'n vibrasie absorbeerder op 'n enjin van 'n voertuig gebruik was nie. Die uitvoerbaarheid van 'n Enjin Vibrasie Absorbeerder wat vibrasievlakke vir verskeie operasionele toestande van 'n voertuig verminder, is in hierdie studie ondersoek. 'n Enjin Vibrasie Absorbeerder is suksesvol ontwerp, vervaardig en ook eksperimenteel gekarakteriseer en geëvalueer. Die ontwerp behels die ontwikkeling van wiskundige modelle om hoofsaaklik respons en natuurlike frekwensies te bepaal. Die wiskundige modelle is geïmplementeer in rekenaarprogramme wat ontwikkel is. Die ontwerp sluit in die keuses wat met betrekking tot grootte, uitleg, posisie, massa, styfheid- en demping-eienskappe vir hierdie Absorbeerder gemaak is. Al die parameters wat benodig is om as insetdata vir die rekenaarprogramme te gebruik, is eksperimenteel gekarakteriseer. Die dinamiese eienskappe van die rubber monteerstukke wat vir die Absorbeerder gebruik is, is afhanklik aan die amplitude opwekking en het dus die analise en die karakterisering gekompliseer, maar hierdie styfheid- en demping-waardes is suksesvol bepaal en in die rekenaarsimulasies gebruik.

Die Enjin Vibrasie Absorbeerder is suksesvol gestem vir 'n frekwensie wat ooreenstem met die vertikale hop modevorm natuurlike frekwensie van die Enjin se monteerstelsel. Die voorspelde en gemete natuurlike frekwensie groottes van die twee-vryheidgraad stelsel is vergelyk.

As kriteria vir die vibrasie oorgedra, is die dinamiese kraggroottes wat oorgedra word deur die Enjin se monteerstelsel na die voertuig se ondersteuningstruktuur bereken met die rekenaarprogramme wat ontwikkel is. Hierdie dinamiese kraggroottes wat oorgedra is, is ook eksperimenteel bepaal. Hierdie voorspelde en gemete dinamiese kraggroottes is vir verskeie operasionele toestande vergelyk.

Verskeie operasionele toestande is teoreties en eksperimenteel ondersoek. Gestadigde toestande het respons as gevolg van die padinset kragte, sowel as die interne enjin skudkragte ingesluit. Oorgangsgedrag het respons ingesluit wat afkomstig was van pad impakkragte, die aanskakeling van die enjin, en die afsluiting van die enjin.

Die studie toon dat die Enjin Vibrasie Absorbeerder die geraasvlakke wat in die voertuig se kompartement gemeet is, verminder het. Die Enjin Vibrasie Absorbeerder het die dinamiese kraggroottes (vibrasie) wat na die voertuig se ondersteuningstruktuur oorgedra is vir al die verskillende insette van die padtoestande by of naby aan resonansie baie effektief verminder. Die Enjin Vibrasie Absorbeerder het die aansienlik groter vibrasie amplitudes wat veroorsaak word deur die pad insette aansienlik verminder, maar geen beduidende negatiewe uitwerking gehad ten opsigte van enige addisionele dinamiese kragte wat oorgedra is wanneer die enjin teen verskeie snelhede gehardloop het nie.

Sleutelwoorde: Voertuig vibrasie, absorbeerder, verstelbaar, resonansie,
verminderde vibrasie

DECLARATION

I, Johann van Wyngaardt, hereby declare that the material used in this study is my own original work, except where specifically referred to by name, or in the form of a reference. This work is not submitted at another university.

Johann van Wyngaardt

Student number: 20717202

Identity number: 880616 5050 08 1

ACKNOWLEDGEMENTS

- God almighty for everything.
- My mother Mari van Wyngaardt and father Jaap van Wyngaardt for all of their love and support.
- Dr. Carl Nel for his guidance, advice and support during this study.
- Quintin Crous for the manufacturing of parts.
- Lourens Joubert and Stephan Grobler for their help during the road tests.
- Mr. Willem van Tonder and Mr. Thabo Diobe for their help during the characterisation of the Engine.
- Mique van der Merwe for the proofreading of this dissertation and her support.
- Mr. Sarel Naudé for the use of the laboratory facilities.
- Family and friends for their assistance and support.

TABLE OF CONTENTS

LIST OF TABLES

LIST OF FIGURES

LIST OF SYMBOLS AND ABBREVIATIONS (NOMENCLATURE)

Capitalised Letters

A	Amplitude of dynamic force at the base of the Shaker test setup	N
F_e	Amplitude of dynamic internal engine shaking force	N
F_r	Amplitude of dynamic road force	N
F_T	Amplitude of dynamic force transmitted to vehicle's structure	N
X_a	Displacement amplitude of Absorber mass	m
X_e	Displacement amplitude of Engine mass	m
X_S	Displacement amplitude of Absorber mass at Shaker test setup	m
$\ddot{X}_a$	Acceleration amplitude of Absorber mass	m/s^2
$\ddot{X}_e$	Acceleration amplitude of Engine mass	m/s^2
$\ddot{X}_S$	Acceleration amplitude of Absorber mass at Shaker test setup	m/s^2
Y	Displacement amplitude at the wheels	m
Y_S	Displacement amplitude at the base of the Shaker test setup	m
$\ddot{Y}$	Acceleration amplitude at the wheels	m/s^2
$\ddot{Y}_S$	Acceleration amplitude at the base of the Shaker test setup	m/s^2

Lowercase Letters

c_a	Equivalent damping coefficient of Absorber mounts	Ns/m
c_c	Equivalent critical damping coefficient of Absorber mounts	Ns/m
c_e	Equivalent damping coefficient of Engine mounts	Ns/m
k_a	Equivalent dynamic stiffness coefficient of Absorber mounts	N/mm
k_e	Equivalent dynamic stiffness coefficient of Engine mounts	N/mm
f	Forced frequency	Hz
f_{n_1}	First natural frequency of Modified system	Hz
f_{n_2}	Second natural frequency of Modified system	Hz
f_{n_a}	Absorber natural frequency	Hz
f_{n_e}	Engine bounce mode natural frequency	Hz

f_r	Forced frequency of dynamic road force	Hz
f_e	Forced frequency of dynamic internal engine shaking force	Hz
f_S	Forced frequency at the Shaker test setup	Hz
g	Absorber and Engine's centre of gravity	
m_a	Absorber mass	kg
m_e	Engine mass	kg
t	Time	sec
x_a	Displacement of Absorber mass	m
x_e	Displacement of Engine mass	m
x_S	Displacement of Absorber mass at Shaker test setup	m
$\dot{x}_a$	Velocity of Absorber mass	m/s
$\dot{x}_e$	Velocity of Engine mass	m/s
$\dot{x}_S$	Velocity of Absorber mass at Shaker test setup	m/s
$\ddot{x}_a$	Acceleration of Absorber mass	m/s^2
$\ddot{x}_e$	Acceleration of Engine mass	m/s^2
$\ddot{x}_S$	Acceleration of Absorber mass at Shaker test setup	m/s^2
y	Displacement at the wheels	m
y_S	Displacement at the base of the Shaker test setup	m
$\dot{y}_S$	Velocity at the base of the Shaker test setup	m/s

Greek symbols

α	Phase angle between stiffness- and viscous damping force vectors	rad
π	Radians	
ϕ	Phase angle between Z_1 and Z_2 vectors or phase angle between the excitation displacement and response vectors	rad
ω	Forced frequency	rad/s
ζ_a	Equivalent damping ratio of Absorber mounts	
ζ_e	Equivalent damping ratio of Engine mounts	

Abbreviations

rpm	Revolutions per minute
VSD	Variable Speed Drive
dB	Sound intensity in decibels

1 INTRODUCTION AND LITERATURE REVIEW

1.1 INTRODUCTION

Engine noise and vibration harshness is a big concern in the competitive automotive vehicle manufacturing industry. A comfortable ride condition is of utmost importance. Excessive noise and vibration can cause problems such as discomfort, annoyance and even chronic health problems. According to earlier investigations in the field of human response to stationary random vibration, the frequency below 25 Hz is classified as the ride frequency (Kim *et al.*, 1994). Within this frequency range, the engine mount system of a vehicle was studied as exposed to vibration inputs from the uneven road surface, the wheels and internal engine shaking forces (Bretl, 1993; Ishihama *et al.*, Kim *et al.*, 1994; 1995; Nel, 2000; Singh *et al.*, 1992).

One of the major concerns in vehicle vibration is the bounce mode of a typical engine mount system, which is around 10 to 13 Hz. The natural frequency of a vehicle's front suspension is also typically around 10 to 13 Hz, which is excited by the uneven road surface through the wheels (Barak, 1991; Ishihama *et al.*, 1995; Kim *et al.*, 1994; Nel, 2000). Thus, resonance may occur at the engine mount system that causes undesired vibrations and an unpleasant boom noise inside the vehicle's compartment (La Civita & Sestieri, 1999). If an automotive vehicle is moving forward at around 80 km/h, the forced frequency of the wheels is also in the range of 10 to 13 Hz, thus causing an additional resonance condition (Steyn, 2011).

As for any other dynamic system, the human body has been found to show signs of resonances when exposed to vibration such as ground transportation vehicles. While the tolerance of humans to the same level of vibration varies from individual to individual, an increased sensitivity is experienced when exposed to vibrations in the range of 2 to 13 Hz for most humans (Barak, 1991; Rao, 2011). This frequency range falls within the bounce mode of a typical engine mount system, thus causing a further resonance condition, which can be perceived by the driver as an uncomfortable and poor ride condition (Kim *et al.*, 1994; Nel, 2000).

It would thus be feasible to reduce the vibration at the engine mount system excited by the uneven road surface and the wheels of the vehicle. If the engine vibration could be

reduced, the dynamic forces transmitted to the vehicle's structure will be reduced, as well as the noise levels inside the vehicle's compartment.

One of the most common techniques to reduce vibration transmitted is with the use of engine rubber mounts with low stiffness as for vibration isolators. This technique is mainly limited by the allowable static and dynamic deflection of the engine mounts (Nel, 2000; Rao, 2011). A hydraulic engine mount was used by Steyn (2011) to reduce engine vibration transmitted to the vehicle. The hydraulic engine mount provided large damping in the low-frequency range that reduced the engine vibration caused by road input forces transmitted through the vehicle's suspension. The hydraulic engine mount also provided low stiffness with low damping in the high-frequency range, which provided good engine vibration isolation.

Other techniques contain the use of sub-frames and counterweights. These techniques add a great deal of mass and cost to the structure (Du Plooy, 1999).

1.2 ENGINE MOUNT SYSTEMS

The first engine mounts manufactured from rubber made its appearance in March 1932. Three rubber mounts supported the engine of a new Plymouth manufactured by Chrysler that were used for improved vibration isolation (Steyn, 2011). The result was that the noise and vibration was considerably reduced. Hydraulic engine mounts have been developed in the past few years which offered an even better result as ordinary rubber mounts (Hwang *et al.*, 2009; Nakahara *et al.*, 2008; Steyn, 2011; West, 1987). The engine mount system is a significant characteristic to obtain vibration isolation, and has an extremely important effect on the ride standards and noise inside a vehicle's compartment (Steyn, 2011).

An engine mount should be soft and provide large damping in the low-frequency range to limit the engine movement normally caused by road input forces transmitted through the vehicle's suspension. Nevertheless, the engine mount should provide low stiffness with low damping for proper vibration isolation in the high-frequency range as well (Nel, 2000; Nel & Heyns, 1996; Steyn, 2011).

Elastomers are widely used in the society to control structural vibration and sound radiation. Elastomers consist of good damping properties, which is especially an advantage at transient conditions. The dynamic properties of elastomeric materials are

difficult to determine due to their visco-elastic behaviour. In general, the dynamic properties of elastomers depend on static pre-load, vibration amplitude, temperature and the excitation frequency (De-Wei *et al.*, 2011; Karlsson & Persson, 2003; Lin *et al.,* 2005; Sjöberg, 2002; Steyn, 2011).

The dynamic properties of elastomeric materials are more amplitude dependent than frequency dependent in the low frequency regions below 50 Hz (Austrell & Olsson, 2012; Garcia, 2006; Karlsson & Persson, 2003; Lin *et al.,* 2005; Ooi & Ripin, 2011; Sjöberg, 2002). The dynamic stiffness of elastomeric materials is normally larger compared to the static stiffness (Wang *et al.*, 2010).

Amplitude dependency of the dynamic characteristics of engine rubber mounts was investigated because of different excitation levels caused by multiple engine operational conditions at vehicles (Kim & Singh, 1992; Nel, 2000; Nel & Heyns, 1996). These dynamic stiffness coefficients and mount loss factors were obtained by measuring the load-deflection properties of an individual mount by using a dynamic testing machine, comprising a hydraulic actuator, a load cell and digital read-out instrumentation. Other researchers also used servo controlled hydraulic actuators, and some used electromagnetic Shakers for excitation to do experimental characterization of dynamic properties of rubber mounts (Austrell & Olsson, 2012; Colgate *et al.*, 1995; De-Wei *et al.*, 2011; Kim & Singh, 1992; Sing *et al.*, 1992).

1.3 DYNAMIC EXCITATION FORCES AT ENGINE MOUNT SYSTEMS

There are mainly three types of dynamic amplitude excitations exerted on the engine mount system, namely (Nel, 2000; Nel & Heyns, 1996; Singh *et al.*, 1992; Steyn, 2011; West, 1987):

1. Mass imbalances of the engine reciprocating and rotating parts: In a four-stroke engine these forces occur in the same direction as the cylinder movement that normally varies from 20 to 200 Hz (Nel, 2000).

2. Cylinder gas pressure differences: Pressure differences within the engine's cylinders cause a variable dynamic moment around the crankshaft (Nel, 2000).

3. Road input forces: Dynamic forces from the road surface through the wheel suspension play an imperative role in the transmission of dynamic forces through the engine mounts to the vehicle's support structure, which occurs in the region of 10 to 13 Hz (Barak, 1991; Ishihama *et al.*, 1995; Kim *et al.*, 1994; Nel, 2000).

The forced frequency of the vehicle's wheels also transmits dynamic forces through the wheel suspension to the engine mount system. These dynamic forces are particularly very large at resonance when the forced frequency of the wheels coincide with the bounce mode natural frequency of a typical engine mount system around 10 to 13 Hz (Nel, 2000; Steyn, 2011).

Engine mount vibration responses can usually fluctuate between 0.01 to 0.25 mm in the vertical direction, and for very large road inputs up to 3 mm (Colgate *et al.*, 1995; Nel, 2000; Sing *et al.*, 1992; Steyn, 2011).

1.4 THE EFFECTS OF NOISE AND VIBRATION ON THE HUMAN BODY

The human body consists of several natural frequencies. In the frequency range of 4 to 8 Hz, it has been established that human tolerance of whole-body vibration is at its lowest. Mainly the spinal cord, but also the legs and the buttocks fall within the frequency range of a typical vehicle's wheel suspension natural frequency, which is around 10 Hz (Rao, 2011). The bounce mode natural frequency of an engine mount system is also typically in the range of 10 to 13 Hz (Barak, 1991; Demic, 1990; Ishihama *et al.*, 1995; Kim *et al.*, 1994; Nel, 2000; Steyn, 2011). Thus an additional resonance condition is present if these frequencies should coincide, which could be perceived as an uncomfortable and poor ride condition by the driver.

The effect of vibration on the human body depends on the direction at which the vibration occurs (Griffin, 2004). Numerous studies on the health and safety of operators and drivers confirmed that extensive exposure to low frequency vibrations could cause irritation and fatigue (Prasad *et al.*, 1995). Vibration has an undesirable effect on the human body, which is why it is important that the vibration exposure should be limited (Griffin, 1981; Steyn, 2011). If the bounce mode of the engine mount system is excited by the vehicle's wheel suspension due to the uneven road surface or the wheels, resonance may occur. This could cause an increase in sensitivity within the human body due to the large vibration levels present.

Low frequency noise in vehicles is mostly the result of structural borne excitation, and is becoming progressively widespread and increasingly annoying. Engine mount systems, wheel suspensions and exhaust hangers are potential contributors to the low frequency noise in vehicle compartments (Meillier & Mairesse, 1996; Roggenkamp & Marcella-O'Leary, 1996; Van der Linden & Fun, 1993; Wyckaert & Van der Auweraer, 1995).

According to Van der Linden & Varet (1996), the low frequency noise spectrum inside the vehicle's compartment is usually dominated by the noise from the engine mount system and wheel suspension. When the frequency content of the transmitted energy coincides with structural resonances, the interior noise level is amplified (Gielen *et al.*, 1996). When the dynamic forces transmitted through the engine mounts are reduced, the sound pressure and thus the noise level inside the vehicle's compartment could be reduced (La Civita & Sestieri, 1999; Steyn, 2011).

Steyn (2011) measured noise levels inside a vehicle's compartment while driving on a gravel road, and measured a noise level of 85 dB. According to Levak *et al.* (2008) noise levels in the range of 71 to 90 dB are severe to human beings and levels from 90 dB and higher are profound. Research showed that cumulative exposure to moderate levels, such as 70 dB, could lead to permanent loss of hearing. The harmful effects of noise on human beings are usually of a psychological nature. The physical effects of noise are more frequently examined than the psychological ones, which could be seen in the forms of aggravation, anxiety, anger and attention disorders as well as difficulties in resting and perception (Atmaca *et al.*, 2005; Cheung, 2004; Levak *et al.*, 2008; Mndeme & Mkoma, 2012). An increase of 3 dB indicates double the sound intensity, whereas an increase of 10 dB means that the human ear perceives the sound as twice as loud (Alison *et al.*, 2011).

1.5 DYNAMIC VIBRATION ABSORBERS

Dynamic vibration absorbers effectively reduce vibration levels at resonance conditions (Canales et al, 2008; Megahed & Abd El-Razik, 2010; Rao, 2011; Yang *et al.*, 2011). It consists of an additional relatively small mass with a stiffness- and damping element attached to the main system that needs to be protected from vibration (Rao, 2011). In an extensive literature survey that has been done, reports on the use of vibration absorbers at vehicle engines could not be found.

Dynamic vibration absorbers adjust a system's dynamics with the aim to improve the response. Vibration absorbers reduce unwanted dynamic vibration responses of a system by introducing a new mode of vibration. Therefore, the main system with the attached absorber forms a two-degree-of-freedom system; thus the system will contain two natural frequencies (Brogan *et al.*, 2003; Du Plooy, 1999; Fortgang & Singhose, 2005; Rao, 2011). A vibration absorber is designed to have a natural frequency equal to the excitation frequency of the main system (Du Plooy, 1999; Megahed & Abd El-Razik, 2010).

The earliest theoretical work simply considered the ideal undamped case for a vibration absorber. With the arrival of computational techniques, it has been feasible to design an absorber for a selection of situations and criteria, as well as non-linearity and damping in both the absorber and main system (Brogan *et al.*, 2003; Fortgang & Singhose, 2005; Hartog, 1956; Hunt, 1979).

Numerous studies investigated the optimisation of the performance of vibration absorbers. The optimisation techniques used for an absorber attached to a single-degree-of-freedom undamped main system is based on the existence of two fixed invariant points. For damped main systems, this theory is not suitable. The optimal values of stiffness and damping coefficients of a vibration absorber may be determined by means of the method presented in the well-known book of Den Hartog (1956). A damped vibration absorber attached to a primary system consisting no damping was considered by Den Hartog (1956). His study used the feature of "fixed-point" frequencies, i.e., frequencies at which the response amplitude of the primary mass is independent of the absorber damping element. Based on the "fixed-points" theory, Den Hartog (1956) found the optimum tuning parameter as the damping element of the absorber.

Since this established work, a number of contributions have been made that considered undamped single- and multi-degree-of-freedom systems. A smaller number of studies were done on damped vibration absorbers attached to a damped single-degree-of-freedom main system (Megahed & Abd El-Razik, 2010; Yang *et al.*, 2011).

The two most important characteristic parameters for a vibration absorber is the tuning ratio of the natural frequencies and the absorber's relative mass (Du Plooy, 1999; Heyns & Van Niekerk, 1997; Rao, 2011). A graph of transmissibility against the forced

frequency ratio for several values of the damping coefficient shows that a wider operating range can be achieved with a damped vibration absorber (Rao, 2011, p.841).

The following factors are important to consider with the design of a vibration absorber (Rao, 2011):

- The amplitudes that the absorber mass will experience is always a lot larger than that of the main mass. Thus, the design must be able to accommodate the large amplitudes of the absorber mass.

- Given that the amplitudes of the absorber mass are estimated to be large, the absorber's spring- and damping element should be designed from a fatigue point of view.

- Nearly all vibration absorbers reported in this literature survey consist of almost zero damping. If more damping is added to the absorber, the reduction of vibration on the main mass will be less effective. Damping is to be added only in situations in which the frequency band in which the absorber is effective is too narrow for operation.

1.6 DYNAMIC VIBRATION ABSORBER APPLICATIONS

The use of vibration absorbers has crossed an extensive variety of applications (Brogan *et al.*, 2003; Fortgang & Singhose, 2005; Hunt, 1979; Sun *et al.*, 1995), including:

- *Architecture:* Buildings, chimneys, bridges, windmills, communication towers, etc.
- *Rotational machinery:* Pumps, generators, engines, etc.
- *Consumer goods:* Dishwashers, refrigerators, passenger seating, etc.

One of the applications for a passive vibration absorber is on high-voltage power transmission lines (Rao, 2011). The wind (normally between 1 m/s and 7 m/s) causes the cables to swing and weaken the cables. Fatigue failure becomes a concern with the vibrating cables. This motion is an oscillation and the whole line along with the structures vibrates at a certain frequency. Because the acting force (wind) doesn't have a forced frequency, the cables and structure vibrate at one of their natural frequencies. The vibration found on these lines has a high frequency but low amplitude. The frequency

range of the vibrations is typically between 3 Hz and 150 Hz (Verma, 2002). An absorber consisting two masses and mounted to a cable is attached to the transmission line. This type of vibration absorber is called a Stockbridge-Damper. The masses are attached to cables with a typical length of 0.15 to 0.25 m, which provide the necessary stiffness. There are two masses typically weighing 1 to 20 kg on each side of the vibration absorber (Canales *et al.*, 2008).

One of the larger applications for vibration absorbers is at skyscrapers in countries with a history of earthquakes, for instance the Taipei 101 building in Taiwan (Eddy, 2005). When an earthquake occurs, the ground shakes in all kind of directions. This can cause the building to vibrate and resonance may occur. To prevent catastrophic failure a pendulum absorber was installed at the top of the building, at the 91st floor which is 390.60 m from the ground, with the bottom of the vibration absorber at the 87th floor. As the building starts to swing, the mass counters the movement by swinging in the opposite direction, which reduces the building's vibrating response. The mass of the vibration absorber is in the form of a 726 ton sphere of stacked steel plates which is 0.26% of the building's mass (Joseph *et al.,* 2006). Another problem with skyscrapers is that the wind can cause the building to oscillate. In some cases it was recorded that the building's top floors moved one meter from side to side. The vibration absorber contributes in reducing these vibration responses as well.

Excessive vibrations in high rise elevators can cause discomfort to the people in the bucket (Fortgang *et al.*, 2006). With the reduction of vibrations, the elevator can travel at much greater speeds. The length of the cables can cause problems in high rise elevators due to their elastic behaviour, which can cause excessive vibrations in the elevator. A whole elevator setup is represented by several masses, springs and dampers, with the vibration absorber attached to the cab. Since the vibration absorber can only be tuned to a specific frequency, the natural frequencies were determined on each floor for a high rise elevator to determine the most common resonating frequency. The settling time of the elevator was observed at every floor and the main problem occurred on the 90th floor. The absorber was designed for the conditions on the 90th floor, but it brought the settling time of the bucket down in the entire building. The vibration absorber's mass was designed on the Hartog criteria which stated that the absorber mass must be 10 % of the original system's mass.

All motorcycles operate at a wide range of frequencies (Fasana & Giorcelli, 2009). The handlebars cause a lot of discomfort to the rider when it vibrates. These vibrations are generated by the road or the unbalance of the motorcycle engine. The vibrations not only cause discomfort, but also cause fatigue on the parts of the motorcycle. A vibration absorber was considered which had to fit on the motorbike handlebars without disturbing the rider. The frequency which the absorber was designed for was the first mode of the handlebars, which was the bending mode. This mode is easy to determine on motorbike handlebars. The vibration absorber was designed for a 4-cylinder sport motorbike. The natural frequencies of the handlebars were determined by operating the bike on a running road in its highest gear. This frequency was confirmed at around 170 Hz in a lab test where the handlebars were attached to a shaker. The absorber was in the form of a small mass of 55 g attached to each side of the handlebars with a rubber mounting which provided a stiffness of about 62.8 kN/m. The absorber's natural frequency was not exactly on the handlebars natural frequency, but it was not a problem because the left and right hand side handle was not exactly the same. The damping ratio was varied between 2%, 5% and 10% for the absorber and all three these damping ratios provided very good results in the vibration reduction of the handlebars. In the worst case of 2 % damping there was still a 4 dB loss achieved. The vibrations on the handlebars just had to be decreased to a suitable level.

Wind could cause excessive vibrations in structures such as antenna towers, bridge cables, ventilation stacks etc. (Fischer, 2007). These vibrations increase the stresses in the structures above the designed rating for static loads. There are a few types of vibration absorbers to handle this problem. Due to the cost of vibration absorbers, the passive vibration absorbers are the best type for these applications. The optimal absorber is a mass and spring setup. The spring can be in the form of a helical or leaf. The spring stiffness can be determined so that the absorber is tuned in to the exact problem frequency. Another absorber type is used when the structure moves in more than one direction. This is done by using a mass in the shape of a plate and to attach not one spring to the mass, but a spring at each corner. This setup is a little more complex to be tuned, since the absorber must be tuned in more than one direction. This type of absorber can also be used on rotating machinery.

In modern day living, emissions are a big concern in the automotive industry. Car manufacturers are pressured to keep new models' emissions to a minimum. Nester *et al.* (2003) considered a V8 engine, where the engine could run in both V8 and V4 modes by means of valve deactivation. From an emission point of view this was a good idea, but it had vibration concerns, especially when the engine was running in V4 mode. Excessive vibration occurred at idling speeds and there was a significant increase in vibrations when a load was coupled to the engine. The vibrations were caused by the second order fluctuating torque originated at the crankshaft of the engine. This became a problem because the crankshaft was designed for the fourth order running speed of the engine. After consideration, it was decided that the best solution for this problem was to design and install a vibration absorber on the crankshaft of the engine. The vibration absorber was in the form of a pendulum absorber. These absorbers are masses attached to the flange of the crankshaft with rollers. This results in an absorber movement relative to the path of the crankshaft. The vibration absorber was tuned by using the product of the engine speed and the mode of vibration, which was at the second order running speed of the engine for this case. This type of tuning is acceptable for small absorber amplitudes only, thus the absorber would experience large vibration amplitudes and the vibration levels of the crankshaft would actually increase from the original system without an absorber. This problem was overcome by tuning the vibration absorber above the problem frequency. The absorber was tested and the vibration amplitudes were compared to a similar engine. A reduction of vibration amplitudes were obtained for the engine with the vibration absorber attached to the crankshaft. The tests were done at idling speeds only, but with different loads.

A vibration problem occurred at the propellers of a turboprop type aircraft (Keye *et al.*, 2009). The blade pass frequency is a big problem to be considered in these types of aircrafts. It results in problems such as excessive vibrations and noise in the airplane. A passive vibration absorber is not very effective at this type of application due to the broad range of engine running speeds. Using more than one vibration absorber would result in a great deal of mass added to the engines. There are a lot of active vibration absorbers that are already fitted on fixed wing airplanes as well as helicopters, but they are constructed of too many mechanical parts. This results in an absorber that is difficult to manufacture and they are expensive. A different type of absorber had to be designed for this application. It was decided that a tunable vibration absorber would be the best solution. A vibration absorber was designed and manufactured which was efficient in the

range of 87.3 to 97.4 Hz. It was in the form of masses attached to a leaf spring which was controlled by a piezo-electric actuator. The vibrating masses were in the range of 0.9 kg and the complete vibration absorber only weighed 1.08 kg. The piezo-electric actuator varied the spring stiffness of the leaf spring as the frequencies changed. The vibration absorber was tested on an Airbus A400M military aircraft. To eliminate manufacturing uncertainties the frequencies that were designed for was a little higher than needed and was tuned down to specifics after the manufacturing process.

Optical disc drives such as CD-ROM and DVD drives are widely used in everyday living. The biggest concern with these types of drives is off-tracking and off-focusing (Heo & Chung, 2002; Kim *et al.*, 2007). The servo controls on the drive address these issues when the vibration levels are low, but for larger vibration levels another solution had to be found. The vibrations are caused by a deformed or wavy disk at resonating frequencies. Heo & Chung (2002) measured excessive vibration levels at a DVD drive when a disc was spinning at approximately 58 Hz, which was identified as the fundamental resonance frequency. The equipment used for the measuring of the vibration levels was a laser vibrometer and an acceleration meter. A vibration absorber consisting only 2% of the main mass was designed to suppress the vibration levels at this critical frequency. The absorber was in the form of a steel ring and a rubber bobbin, consisting a damping ratio of 20%. A considerable reduction in vibration as well as noise levels was achieved with the use of this vibration absorber.

From this literature survey done no previous work could be found where a vibration absorber was used at an engine mount system of an automotive vehicle.

1.7 CONCLUSIONS

From the literature it is clear that a vibration absorber could contribute to reduce the vibrations of an engine mount system excited by the vehicle's wheel suspension, because of the resonance with the engine mount system.

From the literature it has been noted that a vibration absorber has not yet been developed for a vehicle's engine mount system. Vibration absorbers work well at resonance, and could be beneficial at an engine mount system.

A proper engine vibration absorber should limit the dynamic motion of the engine under various operational conditions such as engine idling, starting, stopping, maximum torque, maximum power, maximum engine speed with load, and wheel suspension force excitations from the uneven road surface as well as the wheels. Acceptable translational Absorber displacement amplitudes must also be obtained under the above-mentioned dynamic conditions and static conditions.

In the following chapter different mathematical models as developed for the engine vibration absorber are discussed.

1.8 PROBLEM STATEMENT

The problem of this study is to investigate the reduction engine vibration transmitted to the structure of an automotive vehicle during different operational conditions. The literature survey clearly identified four different resonance conditions at an engine mount system of a typical front-wheel-drive vehicle. These resonance conditions include:

- The wheel hop suspension natural frequency normally coincides with the engine mount system bounce mode natural frequency (10 to 13 Hz).
- The wheel rotation forced frequency coincides with the engine mount system bounce mode natural frequency (10 to 13 Hz) at a certain vehicle speed.
- The uneven road surface normally causes engine vertical excitation on its rubber mounts (10 to 13 Hz).
- Human body natural frequencies (10 to 13 Hz), for example the spinal cord is in this same range and when excited could lead to discomfort.

From the literature it is clear that vibration absorbers used at several other structural applications where resonance takes place, perform extremely well to reduce vibration levels. For this literature survey done, no previous work could be found where a vibration absorber was used at an engine of a vehicle. The feasibility of an engine vibration absorber should be examined in this study.

1.9 SCOPE OF STUDY

The scope of this study is to simulate, design and manufacture as well as experimentally characterise an engine vibration absorber. The vibration absorber attached to an engine should be experimentally evaluated for several operational conditions.

The main focus areas of this study were identified as follows:

- A literature survey.
- The development of mathematical models for the design of an engine vibration absorber.
- Mathematical models implemented in computer programs.
- Characterisation of input parameters for computer programs.
- Prediction of natural frequencies and displacement responses.
- Criteria for vibration transmitted to the vehicle structure.

- Experimental evaluation of engine vibration absorber for various operational conditions.
- Determine advantages of the vibration absorber regarding the forces excited by the wheel suspension, as well as possible disadvantages regarding internal engine shaking forces.

2 MATHEMATICAL MODELS

2.1 INTRODUCTION

For this study, five different mathematical models were developed. The first model is applicable for the characterisation of the equivalent stiffness- and damping element of the Engine Vibration Absorber. This model is essential to determine the dynamic properties of the Absorber. The remaining models are used to make certain theoretical predictions with and without the presence of the Absorber.

2.2 CHARACTERISATION OF ABSORBER'S DYNAMIC PROPERTIES

A rigid body mass m_a, which represents the mass of the Absorber and is supported by an equivalent stiffness element k_a and equivalent viscous damping element c_a, which is firmly bolted on the base of an Electro-dynamic Shaker is considered, as shown in Figure 2.1 (Nel & Steyn, 2012; Nel & Van Wyngaardt, 2014a; Rao, 2011):

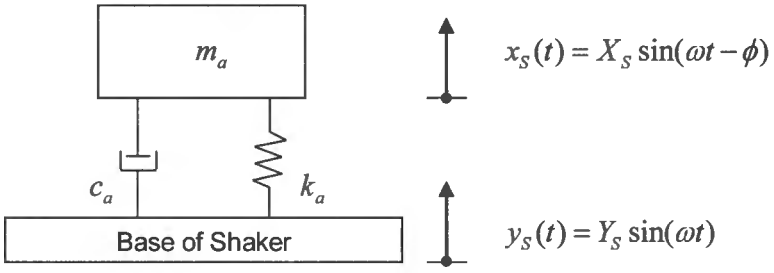

Figure 2.1: Shaker test representation.

When $y_S(t)$ denotes the displacement of the base of the Shaker table, and $x_S(t)$ the rigid body mass displacement from an equilibrium position at time t, the relative displacement of the stiffness element will be $(x_S - y_S)$ and the relative velocity of the two ends at the damper $(\dot{x}_S - \dot{y}_S)$.

The response of a viscous damped system under harmonic motion of the base can be described by the following equation of motion:

$$m_a\ddot{x}_S + c_a(\dot{x}_S - \dot{y}_S) + k_a(x_S - y_S) = 0 \tag{2.1}$$

with Y_S the displacement amplitude of the Shaker base and ω the forced frequency

$$y_S(t) = Y_S \sin(\omega t) \tag{2.2}$$

Equation (2.1) becomes

$$\begin{aligned} m_a\ddot{x}_S + c_a\dot{x}_S + k_a x_S = k_a y_S + c_a\dot{y}_S = k_a Y_S \sin(\omega t) + c_a \omega Y_S \cos(\omega t) \\ = A\sin(\omega t - \alpha) \end{aligned} \tag{2.3}$$

where the excitations from the base are equivalent to a harmonic force with amplitude A applied to the mass, and is described as follows:

$$A = Z_2\sqrt{k_a^2 + (c_a\omega)^2} \tag{2.4}$$

The phase angle α is defined by the angle between the viscous damped- and stiffness vector, and is described as follows:

$$\alpha = \tan^{-1}\left[-\frac{c_a\omega}{k_a}\right] \tag{2.5}$$

Also

$$x_S(t) = X_S \sin(\omega t - \phi) \tag{2.6}$$

where the amplitude ratio is given by

$$\frac{X_S}{Y_S} = \left[\frac{k_a^2 + (c_a\omega)^2}{(k_a - m_a\omega^2)^2 + (c_a\omega)^2}\right]^{1/2} \tag{2.7}$$

and the phase angle

$$\phi = \tan^{-1}\left[\frac{m_a c_a \omega^3}{k_a(k_a - m_a\omega^2) + (c_a\omega)^2}\right] \tag{2.8}$$

The response X_S represents the amplitude of excitation and ϕ represents the phase angle between these X_S and Y_S displacement vectors.

The displacement amplitudes X_S and Y_S can also be written as

$$X_S = \frac{\ddot{X}_S}{\omega^2} \tag{2.9}$$

and

$$Y_S = \frac{\ddot{Y}_S}{\omega^2} \tag{2.10}$$

with

$$\omega = 2\pi f_S \tag{2.11}$$

where $\ddot{X}_S$ and $\ddot{Y}_S$ are the corresponding acceleration amplitudes at a forced frequency f_S.

The critical damping coefficient is defined as

$$c_c = 2\sqrt{k_a m_a} \tag{2.12}$$

where the damping ratio ζ_a is defined as the ratio between the actual damping coefficient c_a and the critical damping coefficient c_c as

$$\zeta_a = \frac{c_a}{c_c} \tag{2.13}$$

2.3 SINGLE-DEGREE-OF-FREEDOM SYSTEM – ROAD FORCES

The Engine as supported by its three mounts is considered as a single-degree-of-freedom system with a rigid body mass m_e, which is supported by an equivalent stiffness element with stiffness coefficient k_e and an equivalent damping element with viscous damping coefficient c_e as shown in Figure 2.2. This system is subject to a harmonic displacement $y(t)$ from the base in the vertical direction with amplitude Y at a forced frequency f_r at a time t due to dynamic road inputs.

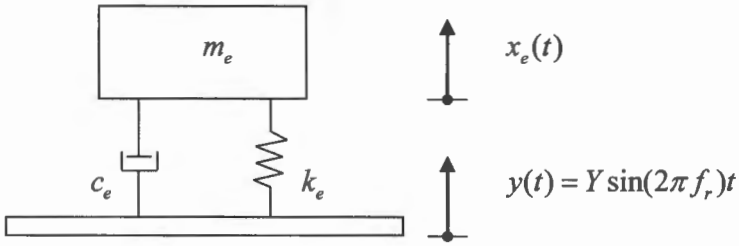

Figure 2.2: Single-degree-of-freedom system – road forces.

For the Engine mount system under harmonic forced conditions from the base the equation of motion is (Rao, 2011):

$$m_e\ddot{x}_e + c_e\dot{x}_e + k_e x_e = k_e Y\sin(2\pi f_r)t + c_e(2\pi f_r)Y\cos(2\pi f_r)t \tag{2.14}$$

where $\ddot{x}_e$, $\dot{x}_e$ and x_e represent the harmonic acceleration, velocity and displacement of the Engine mass respectively.

The road force amplitude F_r is related to Y and can be described as

$$Y = \frac{F_r}{\sqrt{k_e^2 + (2\pi f_r c_e)^2}} \tag{2.15}$$

The displacement amplitudes X_e and Y can also be written as

$$X_e = \frac{\ddot{X}_e}{(2\pi f_r)^2} \tag{2.16}$$

and

$$Y = \frac{\ddot{Y}}{(2\pi f_r)^2} \tag{2.17}$$

where $\ddot{X}_e$ and $\ddot{Y}$ are the corresponding acceleration amplitudes at a forced frequency f_r.

This equation of motion can be solved with a numerical integration technique namely Runge-Kutta. More detail regarding this technique is provided in Chapter 3.

2.4 TWO-DEGREE-OF-FREEDOM SYSTEM – ROAD FORCES

A Vibration Absorber comprising a mass m_a and an equivalent stiffness element with stiffness coefficient k_a, as well as an equivalent damping element with viscous damping coefficient c_a, is attached to the Engine mount system discussed in the previous section with the same harmonic displacement $y(t)$ at the base. A two-degree-of-freedom system is thus considered here as shown in Figure 2.3.

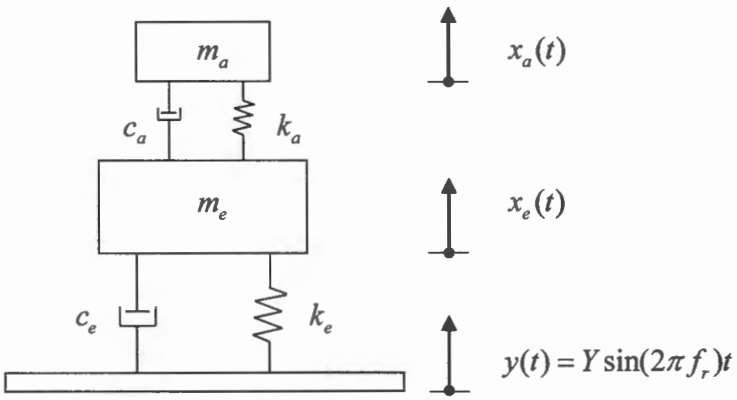

Figure 2.3: Two-degree-of-freedom system – road forces.

For this two-degree-of-freedom system the equations of motion are:

$$m_e\ddot{x}_e + (c_e + c_a)\dot{x}_e - c_a\dot{x}_a + (k_e + k_a)x_e - k_a x_a = k_e Y\sin(2\pi f_r)t + c_e(2\pi f_r)Y\cos(2\pi f_r)t \quad (2.18)$$

and

$$m_a\ddot{x}_a - c_a\dot{x}_e + c_a\dot{x}_a - k_a x_e + k_a x_a = 0 \quad (2.19)$$

where $\ddot{x}_a$, $\dot{x}_a$ and x_a represent the harmonic acceleration, velocity and displacement of the Absorber mass respectively.

The displacement amplitude X_a can also be written as

$$X_a = \frac{\ddot{X}_a}{(2\pi f_r)^2} \quad (2.20)$$

where $\ddot{X}_a$ is the corresponding acceleration amplitude at a forced frequency f_r.

These equations represent a system of two coupled second-order differential equations, which can also be solved with the numerical integration technique namely Runge-Kutta, which is explained in Chapter 3.

2.5 SINGLE-DEGREE-OF-FREEDOM SYSTEM – INTERNAL ENGINE SHAKING FORCES

In this case, the single-degree-of-freedom system in Section 2.3 is firmly attached to a rigid foundation with a harmonic unbalanced load $F_e(t)$ that acts at the centre of gravity of the Engine mass with a magnitude F_e at a forced frequency f_e at a time t, as considered for internal engine shaking forces. Movement of the Engine mass is considered in the vertical direction as shown in Figure 2.4.

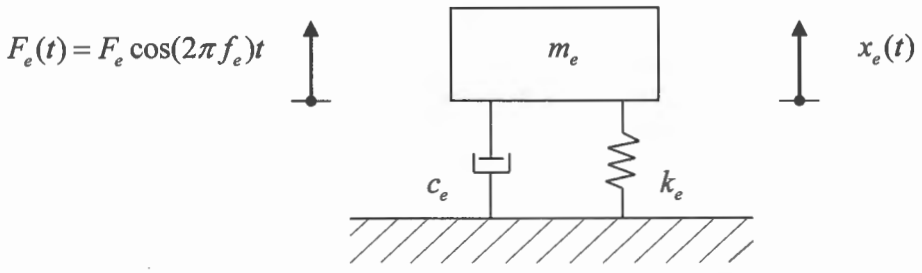

Figure 2.4: Single-degree-of-freedom system – internal engine shaking forces.

For the Engine mount system under harmonic forced conditions at the Engine mass the equation of motion is (Rao, 2011):

$$m_e\ddot{x}_e + c_e\dot{x}_e + k_e x_e = F_e \cos(2\pi f_e)t \tag{2.21}$$

The natural frequency of the Engine mount system

$$f_{n_e} = \sqrt{\frac{k_e}{4\pi^2 m_e}} \tag{2.22}$$

where free vibration takes place.

The displacement amplitude X_e can also be written as

$$X_e = \frac{\ddot{X}_e}{(2\pi f_e)^2} \tag{2.23}$$

where $\ddot{X}_e$ is the corresponding acceleration amplitude at a forced frequency f_e.

These internal engine shaking forces occur at entirely different frequencies compared to the frequencies of the road forces. These forces are related to Engine running speeds. This equation of motion can also be solved with a numerical integration technique namely Runge-Kutta.

2.6 TWO-DEGREE-OF-FREEDOM SYSTEM – INTERNAL ENGINE SHAKING FORCES

With the same Absorber that is discussed in Section 2.4 attached to the Engine mount system that is firmly attached to a rigid foundation, a two-degree-of-freedom system is considered with the same harmonic unbalanced load $F_e(t)$ that acts at the centre of gravity of the Engine mass, as shown in Figure 2.5.

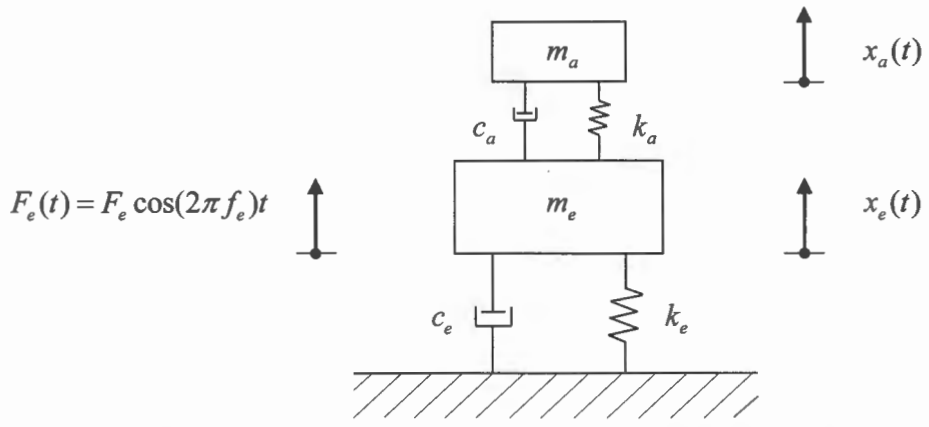

Figure 2.5: Two-degree-of-freedom system – internal engine shaking forces.

For this two-degree-of-freedom system the equations of motion are (Rao, 2011):

$$m_e\ddot{x}_e + (c_e + c_a)\dot{x}_e - c_a\dot{x}_a + (k_e + k_a)x_e - k_a x_a = F_e \cos(2\pi f_e)t \tag{2.24}$$

and

$$m_a\ddot{x}_a - c_a\dot{x}_e + c_a\dot{x}_a - k_a x_e + k_a x_a = 0 \tag{2.25}$$

When the Absorber is considered as a single-degree-of-freedom system that is firmly attached to a rigid foundation, the natural frequency of the Absorber

$$f_{n_a} = \sqrt{\frac{k_a}{4\pi^2 m_a}} \tag{2.26}$$

where free vibration takes place.

The displacement amplitude X_a can also be written as

$$X_a = \frac{\ddot{X}_a}{(2\pi f_e)^2} \tag{2.27}$$

where $\ddot{X}_a$ is the corresponding acceleration amplitude at a forced frequency f_e.

The two new natural frequencies f_{n_1} and f_{n_2} for the two-degree-of-freedom system can be described as

$$f_{n_1} = \left\{ \frac{\left[k_a m_e + (k_e + k_a) m_a\right] - \sqrt{\left[k_a m_e + (k_e + k_a) m_a\right]^2 - 4(m_e m_a)\left[(k_e + k_a)(k_a) - k_a^2\right]}}{8\pi^2 m_e m_a} \right\}^{1/2} \tag{2.28}$$

and

$$f_{n_2} = \left\{ \frac{\left[k_a m_e + (k_e + k_a) m_a\right] + \sqrt{\left[k_a m_e + (k_e + k_a) m_a\right]^2 - 4(m_e m_a)\left[(k_e + k_a)(k_a) - k_a^2\right]}}{8\pi^2 m_e m_a} \right\}^{1/2} \tag{2.29}$$

where free vibration takes place.

These equations were implemented in a computer program in a Matlab environment to compute the magnitudes of these two natural frequencies. The equations of motion can also be solved with the numerical integration technique namely Runge-Kutta discussed in Chapter 3.

2.7 DYNAMIC FORCES TRANSMITTED

As criteria of vibration transmitted, a simplified force function is proposed as follows (Nel, 2000; Nel & Heyns, 1996):

$$F_T = \sqrt{(k_e X_e)^2 + ((2\pi f) c_e X_e)^2} \tag{2.30}$$

where F_T represents the amplitude of the dynamic force transmitted through the Engine mounts to the vehicle's support structure. The equivalent stiffness coefficient of the Engine mounts are represented by k_e, and the equivalent viscous damping coefficient by c_e. The displacement amplitude at the Engine is represented by X_e at a forced frequency f, which is either the forced frequency f_r at which road forces occur, or the forced frequency f_e at which internal engine shaking forces occur. Equation (2.30) was used to evaluate the performance of the Absorber at several operational conditions discussed in Chapter 5. The dynamic forces transmitted to the vehicle's support structure during these conditions were compared between the single-degree-of-freedom system and the two-degree-of-freedom system.

2.8 CONCLUSIONS

The mathematical models were successfully formulated in order to determine the dynamic properties of the Absorber, as well as to predict the dynamic movement of the Engine and Absorber for several operational conditions. The following chapter briefly describes the computer implementation of these mathematical models, as well as the numerical integration technique used.

3 COMPUTER IMPLEMENTATION

3.1 INTRODUCTION

The mathematical models explained in Chapter 2 were implemented in a Matlab environment. The mathematical model described in Section 2.2 was used to characterise the Vibration Absorber's equivalent stiffness- and damping element, which is explained in detail in Chapter 4. The mathematical models described in Section 2.3 to Section 2.6 were also implemented in a Matlab environment, and the differential equations of motion were solved with the use of the Matlab built-in numerical integration algorithm namely *ode45.m*. This algorithm implements a Runge-Kutta method with a variable time increment for efficient computation. This procedure entails that a second-order differential equation is reduced to a series of two first-order differential equations, which is then solved. The modulation of these equations is used to judge different properties of the Absorber, by computation of the response of the Engine as well as the Absorber for certain operational conditions. The computer program for each mathematical model is included in Appendix B.

3.2 CHARACTERISATION OF ABSORBER'S DYNAMIC PROPERTIES

The following flowchart describes the characterisation procedure, which was used to characterise the Absorber's equivalent stiffness- and damping element for several relative displacement amplitudes. A computer program was developed in a Matlab environment for the mathematical model described in Section 2.2 and the measured data recorded with an FFT Analyser was used as input data. The dynamic stiffness as well as the damping properties were computed with the use of the measured amplitudes of the two acceleration signals, as well as the phase difference between these two time signals at several excitation amplitudes where equations (2.7) and (2.8) were solved simultaneously. A detailed example of this characterisation procedure is described in Section 4.5.5.

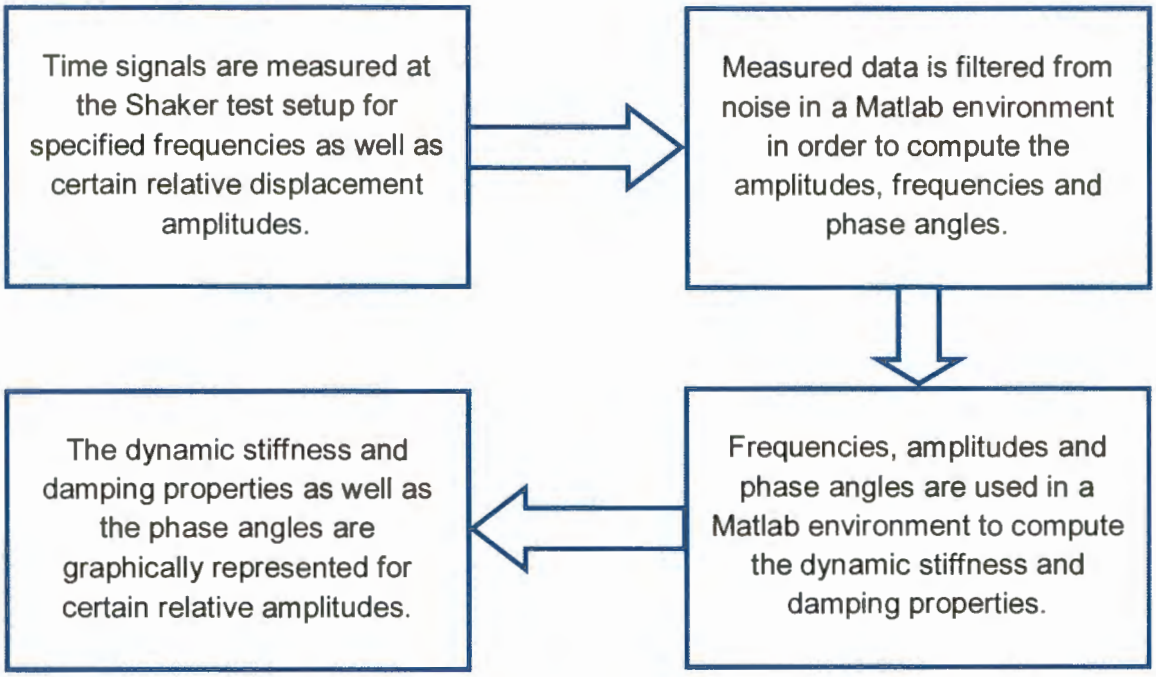

3.3 SINGLE-DEGREE-OF-FREEDOM SYSTEM – ROAD FORCES

The following flowchart describes the Runge-Kutta procedure for the mathematical model described in Section 2.3. The Engine mass supported by its three rubber mounts with stiffness and damping is considered a single-degree-of-freedom system. This system is subject to harmonic movement from the base due to road forces. The second-order differential equation (see equation (2.14)) is reduced to a series of two first-order differential equations, which are then solved with the Matlab built-in numerical integration algorithm namely *ode45.m*.

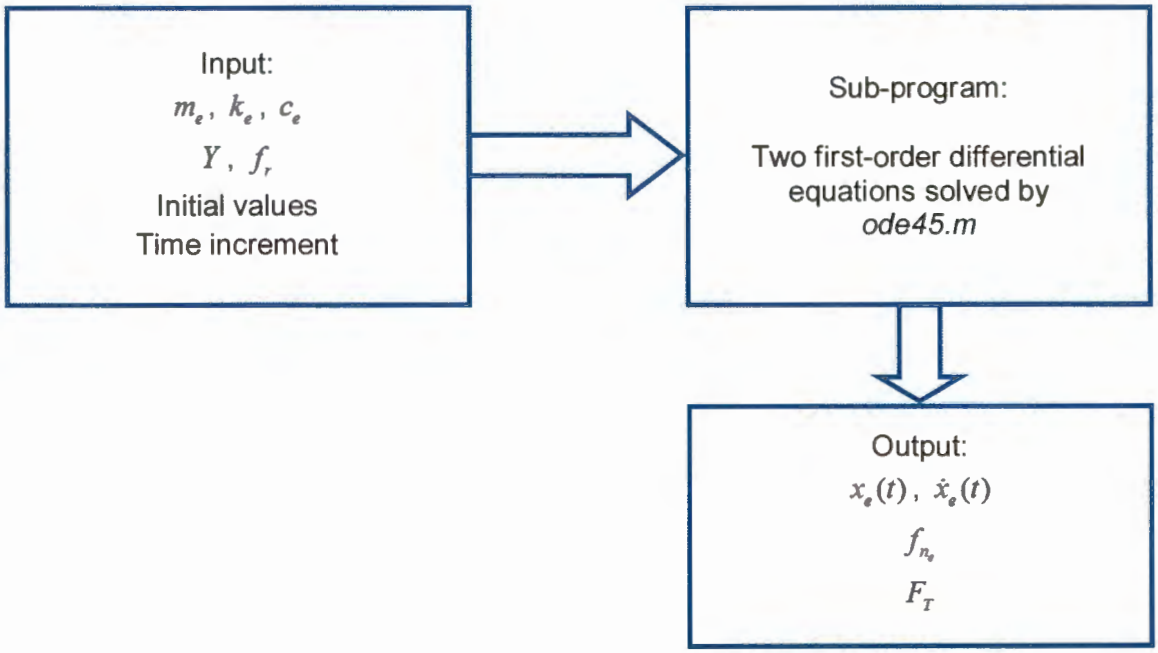

With reference to the flowchart, the initial values taken for the numerical integration process were that the response was zero at the starting time. This procedure was used to obtain theoretical graphical representations for this system and to predict the natural frequency, the response and the dynamic force transmitted for certain operational conditions described in Section 5.7.

3.4 TWO-DEGREE-OF-FREEDOM SYSTEM – ROAD FORCES

The following flowchart describes the Runge-Kutta procedure for the mathematical model described in Section 2.4. The Absorber mass with stiffness- and damping element is attached to the Engine mount system that was discussed in the previous section, hence a two-degree-of-freedom system is considered here. The two second-order differential equations (see equations (2.18) and (2.19)) are reduced to a series of four first-order differential equations, which are then solved with the Matlab built-in numerical integration algorithm namely *ode45.m*.

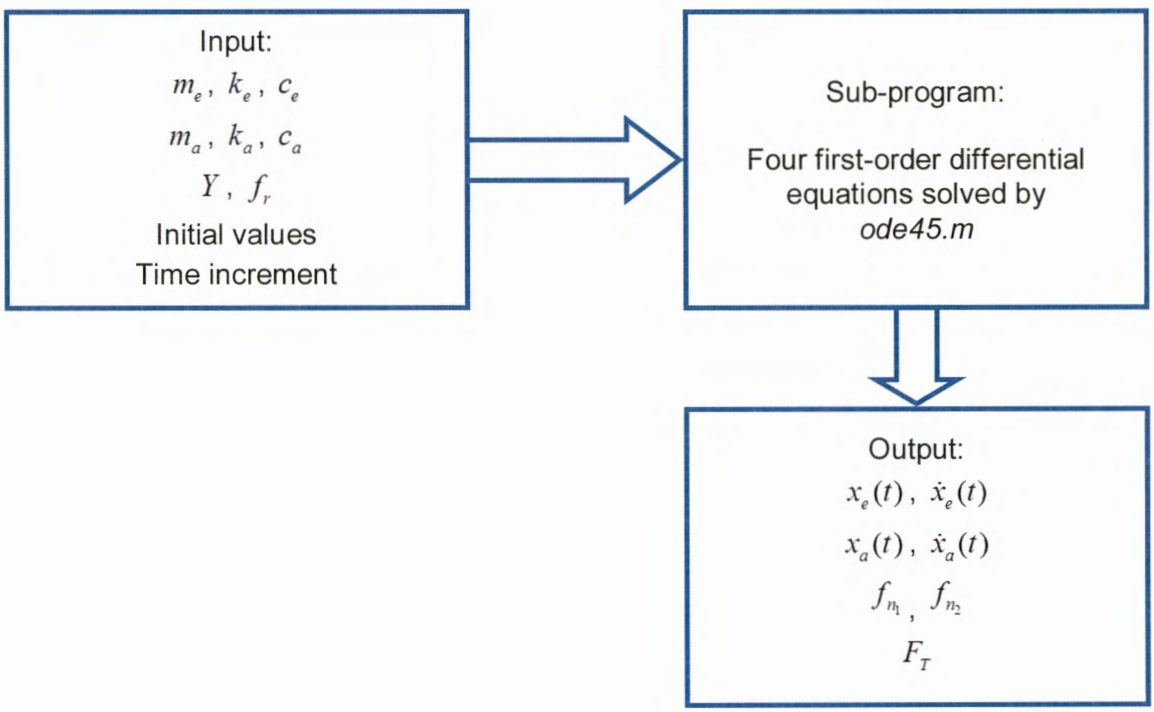

With reference to the flowchart, the initial values taken for the numerical integration process were that the response was zero at the starting time. This procedure was used to obtain theoretical graphical representations for this system and to predict the natural frequencies, the Engine and Absorber response, and the dynamic force transmitted for certain operational conditions described in Section 5.7.

3.5 SINGLE-DEGREE-OF-FREEDOM SYSTEM – INTERNAL ENGINE SHAKING FORCES

The following flowchart describes the Runge-Kutta procedure for the mathematical model described in Section 2.5. The Engine mass supported by its three rubber mounts with stiffness and damping is considered as a single-degree-of-freedom system. In this case, this system is firmly attached to a rigid foundation with a harmonic unbalanced load acting at the Engine's centre of gravity, as considered for internal engine shaking forces. The second-order differential equation (see equation (2.21)) is reduced to a series of two first-order differential equations, which are then solved with the Matlab built-in numerical integration algorithm namely *ode45.m*.

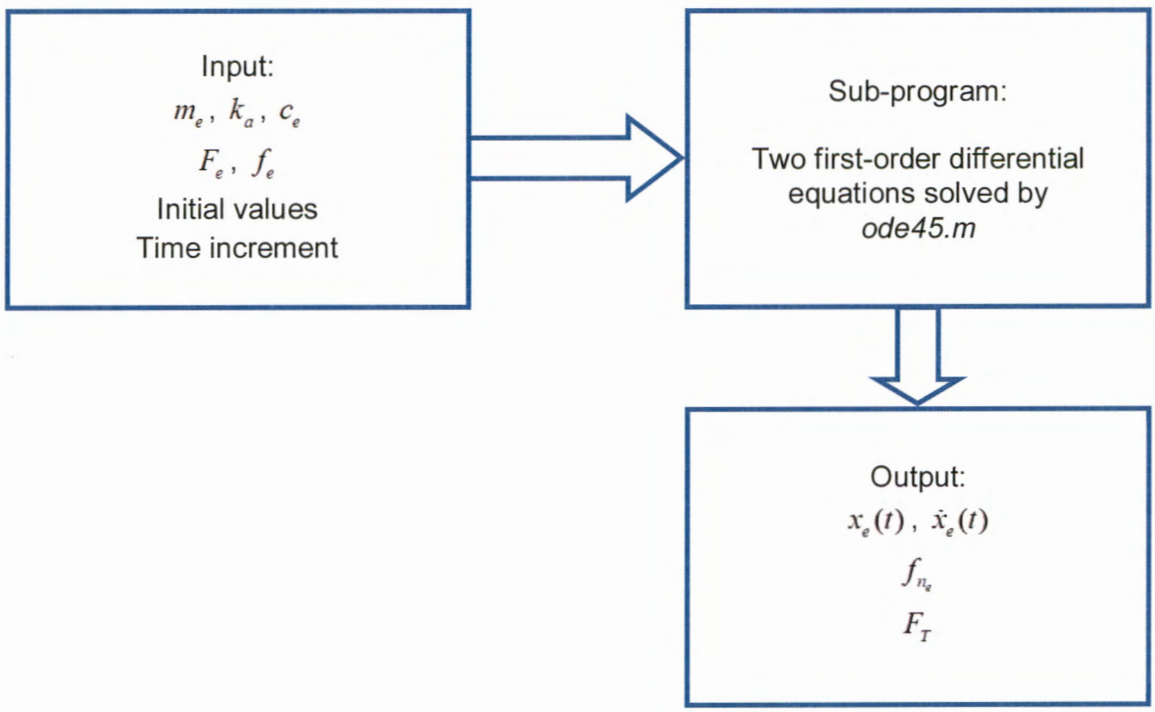

With reference to the flowchart, the initial values taken for the numerical integration process were that the response was zero at the starting time. This procedure was used to obtain theoretical graphical representations for this system and to predict the natural frequency, the response and also the dynamic force transmitted for certain operational conditions described in Section 5.7.

3.6 TWO-DEGREE-OF-FREEDOM SYSTEM – INTERNAL ENGINE SHAKING FORCES

The following flowchart describes the Runge-Kutta procedure for the mathematical model described in Section 2.6. The Absorber mass with stiffness- and damping element is attached to the Engine mount system discussed in the previous section, hence a two-degree-of-freedom system is here considered. The two second-order differential equations (see equations (2.24) and (2.25)) are reduced to a series of four first-order differential equations, which are then solved with the Matlab built-in numerical integration algorithm namely *ode45.m*. The two new natural frequencies as well as the dynamic force transmitted are also computed.

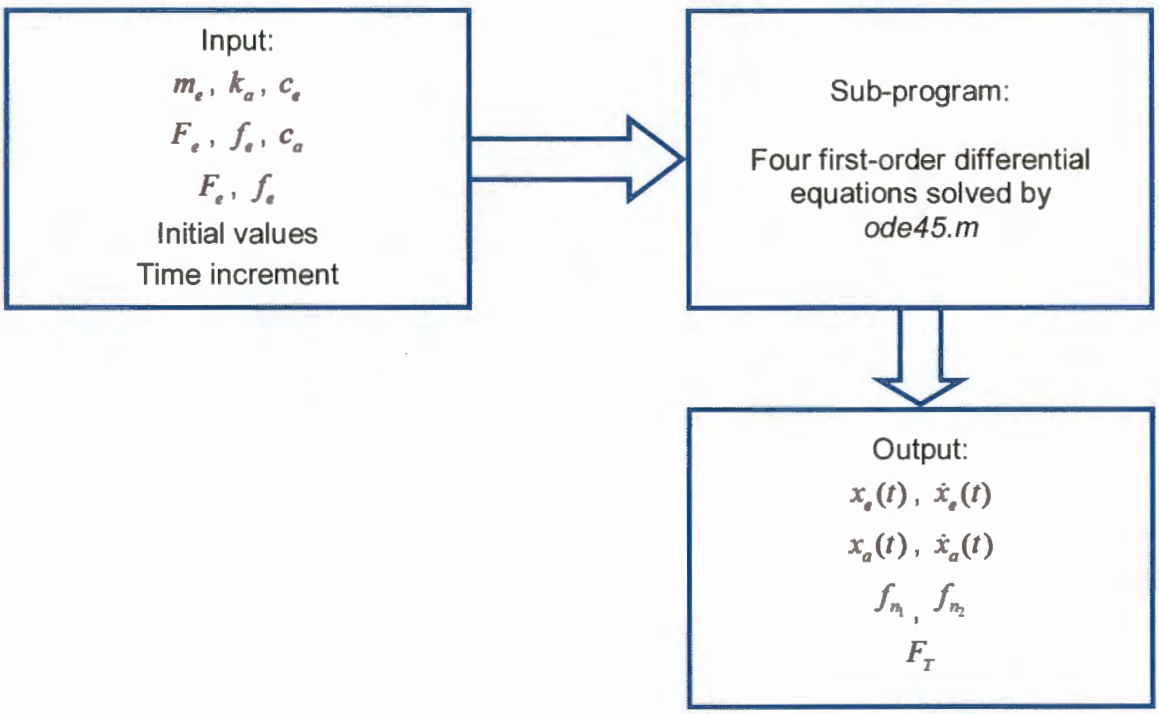

With reference to the flowchart, the initial values taken for the numerical integration process were that the response was zero at the starting time. This procedure was used to obtain theoretical graphical representations for this system and to predict the natural frequencies, the Engine and Absorber response, and also the dynamic force transmitted for certain operational conditions described in Section 5.7.

3.7 CONCLUSIONS

The mathematical models were successfully implemented in a Matlab environment in order to compute the dynamic properties of the Absorber, as well as to predict the Engine and Absorber responses and also dynamic forces transmitted to the vehicle's support structure for certain operational conditions. The final design for the Absorber is described in Chapter 4, Section 4.2. The test setup and instrumentation used for the characterisation of the Absorber's equivalent stiffness- and damping element are also discussed in Chapter 4.

4 EXPERIMENTAL CHARACTERISATION

4.1 INTRODUCTION

The dynamic characteristics of the Vibration Absorber are important for vibration control of the Engine, as well as to provide a comfortable ride condition for the general pleasure of driving. The design of the Vibration Absorber is thoroughly discussed in Section 4.2. The Vibration Absorber was characterised with the use of a Ling Dynamic Systems V724 Electro-dynamic Shaker with a DPA4 Amplifier and SPC4 Signal Controller, which allowed different amplitude excitation levels (Nel & Van Wyngaardt, 2014a). The test assembly as well as the Electro-dynamic Shaker are displayed in Figure 4.11. The Vibration Absorber was first roughly tuned for the bounce mode frequency of the Engine mount system before it was characterised. Linear guide bearings, along with two guide shafts guided the Absorber mass during the up and down movement in the vertical direction. Three rubber mounts arranged in parallel were mounted between the basis of the Absorber and the Absorber mass to represent the equivalent stiffness- and damping element of the Absorber. Two 100 mV/g PCB acceleration meters connected to a Diagnostic Instruments 2200 FFT Analyser were used to measure two acceleration signals simultaneously at the moving mass and the base of the Electro-dynamic Shaker. The data from these signals were used as input data in the computer program described in Section 3.2. These equations were solved in a Matlab environment in order to determine the equivalent dynamic properties of the three rubber mounts at the Absorber.

4.2 ENGINE VIBRATION ABSORBER

A basic schematic layout of the Engine Vibration Absorber is displayed in Figure 4.1. The Absorber's effective mass could be adjusted by adding or removing small masses at the main mass in order to change the natural frequency of the Absorber which allowed tuning. For this study three rubber mounts arranged in parallel were used to provide the equivalent stiffness- and damping element of the Absorber. The equivalent dynamic properties were experimentally characterised. The different components of the Vibration Absorber are discussed respectively in Section 4.2.1 to Section 4.2.6.

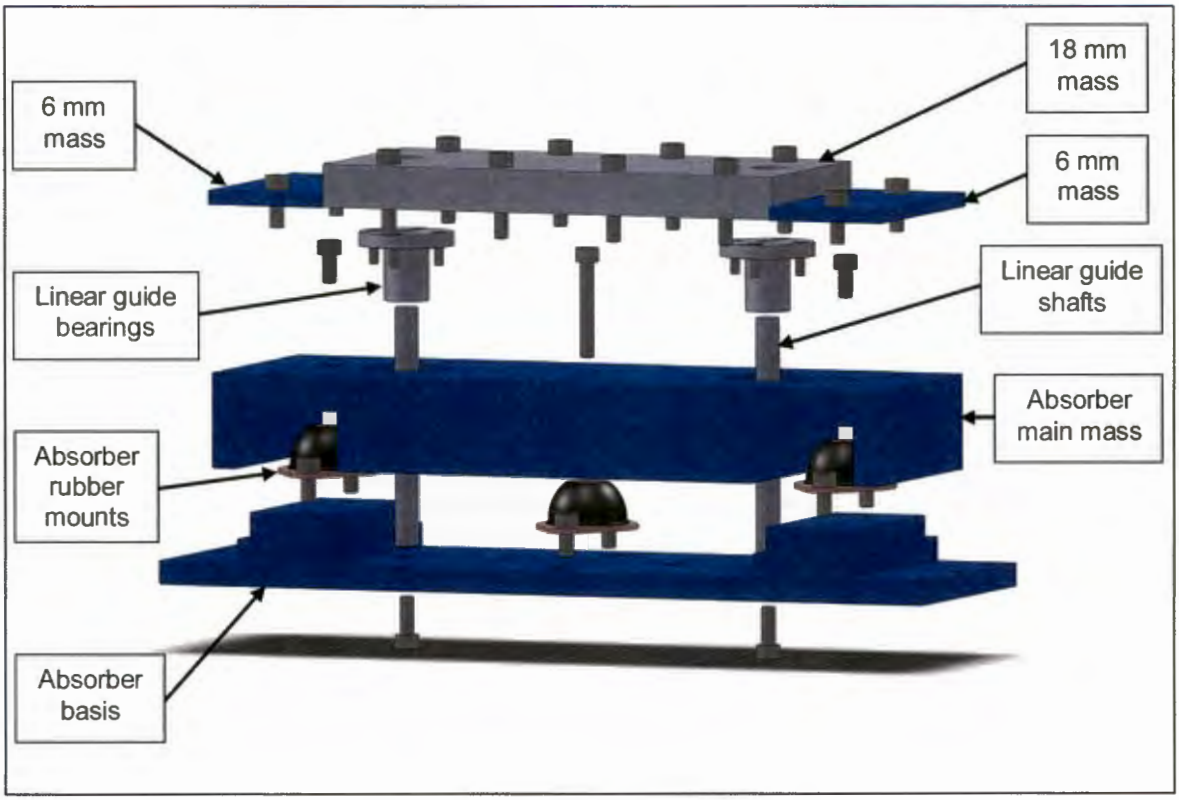

Figure 4.1: View of Engine Vibration Absorber.

4.2.1 Absorber basis

The basis of the Vibration Absorber is manufactured from mild steel as displayed in Figure 4.2. The four ∅ 9 holes in the middle were used to attach the Absorber to the Electro-dynamic Shaker while the three ∅ 6.5 holes on each side were used to attach the assembly to the Engine attachment bracket. The two linear guide shafts as well as the three Absorber rubber mounts were also attached on this basis. A detailed drawing is included in Appendix C.

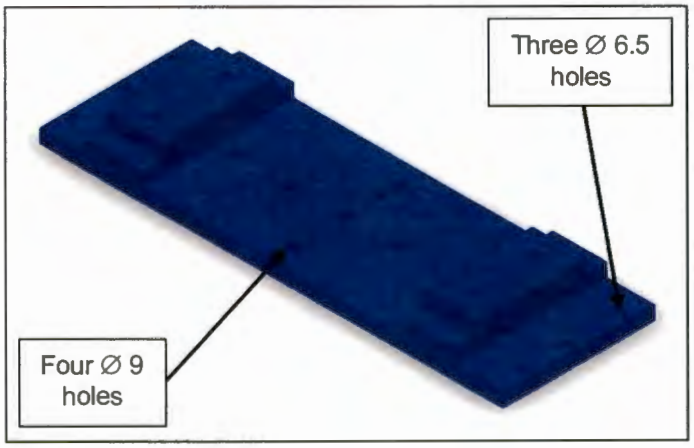

Figure 4.2: Absorber basis.

4.2.2 Absorber rubber mounts

Three rubber mounts were used as the equivalent stiffness- and damping element of the Absorber. These mounts are standard industrial rubber mounts as displayed in Figure 4.3.

Figure 4.3: Absorber rubber mounts.

The two rubber mounts on each side of the Absorber are both M7A Novibra rubber mounts, while the one in the middle is a M7B Novibra rubber mount (see Figure 4.1). The dynamic properties of these two mounts are different, but the geometry is exactly the same. More information regarding these standard industrial mounts is included in Appendix A.

4.2.3 Absorber main mass

Figure 4.4 displays the Vibration Absorber's main mass, which is manufactured from mild steel and is attached on top of the three rubber mounts. A detailed drawing is included in Appendix C.

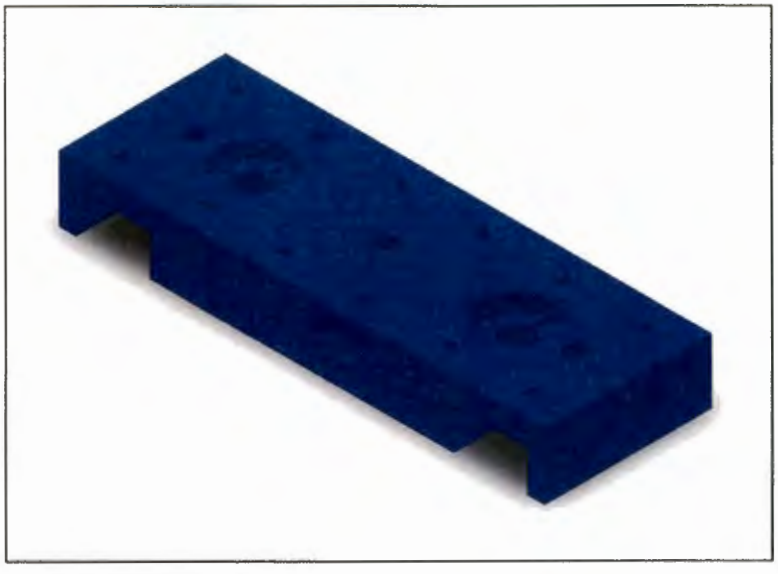

Figure 4.4: Absorber main mass.

The Absorber main mass was specially designed to allow that the Absorber's effective mass could be adjusted by adding or removing masses to the Absorber main mass. As a result the natural frequency of the Absorber could be changed and thus be tuned to the bounce mode frequency of the Engine mount system. The two linear guide bearings were also attached at the Absorber main mass to allow vertical movement (see Figure 4.1).

4.2.4 Linear guide bearings

Two LMF 10 UU linear guide bearings along two linear guide shafts (see Section 4.2.5) were used to guide the movement of the Absorber mass. These bearings consists of a closed flanged cast iron housing as displayed in Figure 4.5, and is a standard bearing which was available from G-Man Traders. More information regarding these standard bearings is shown in Appendix A.

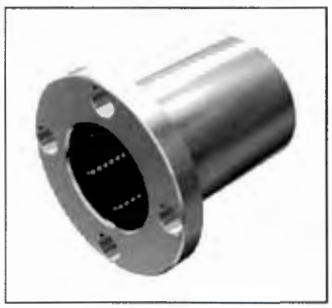

Figure 4.5: Linear guide bearings.

4.2.5 Linear guide shafts

Two linear guide shafts along the two linear guide bearings guided the vertical movement of the Absorber mass. The outside diameter of these standard guide shafts correspond to the inner diameter of the linear guide bearings, which is ∅ 10 mm. These shafts are induction hardened and the surface is polished until the correct diameter is achieved as displayed in Figure 4.6.

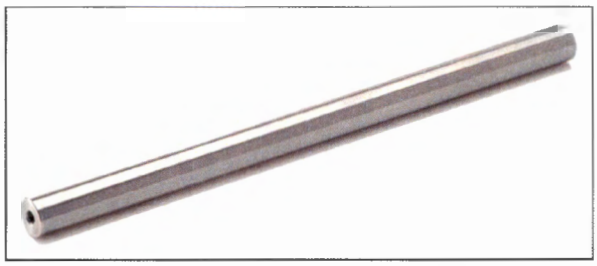

Figure 4.6: Linear guide shafts.

The two guide shafts were specially manufactured by SKF according to a detailed drawing provided where the length was specified (see Appendix C). Furthermore, these shafts possess exceptionally high dimensional stability and are designed for a long service life, and standard linear guide shafts are also available from SKF (see Appendix A).

4.2.6 Engine attachment bracket

A bracket manufactured from mild steel was used to attach the Vibration Absorber to the Engine block as displayed in Figure 4.7. The Absorber was attached to this bracket with three M6 bolts on each side.

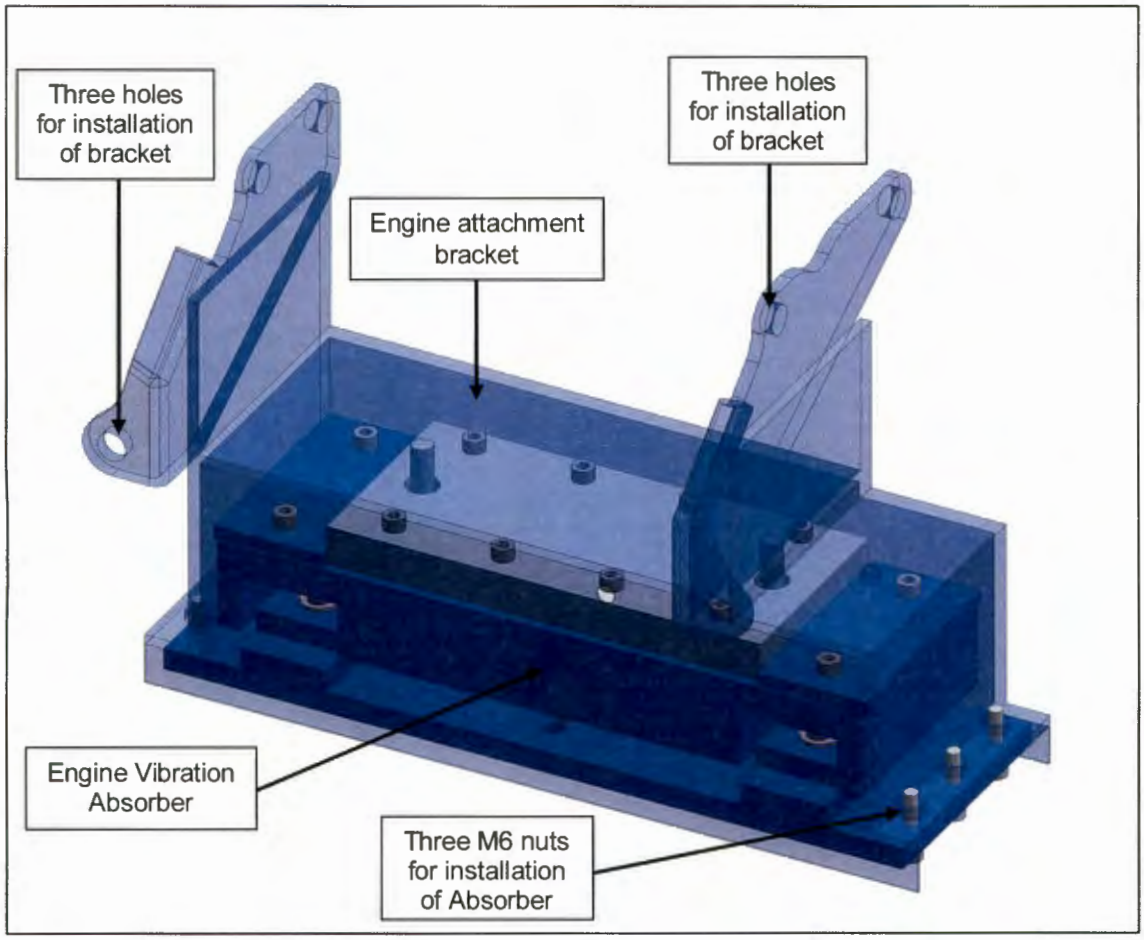

Figure 4.7: Engine attachment bracket.

The casing was also firmly bolted to the Engine block with three M8 bolts on each side (also see Section 5.4, Figure 5.2). By using this enclosed casing, it is ensured that none of the Absorber parts could fall out in the case of a catastrophic failure while driving. A detailed drawing of the Engine attachment bracket is included in Appendix C.

4.3 ABSORBER POSITION

Figure 4.8 displays a schematic top view of the Engine used in this study with the positions of the three Engine rubber mounts. The Vibration Absorber's centre of gravity was positioned to coincide with the Engine's centre of gravity g to allow a two-degree-of-freedom system with movement considered only in the vertical direction. The same Engine with its engine mount positions that was used in this study was previously characterised by Steyn (2011) as well as by Nel and Heyns (1996). More detail regarding these Engine mount dynamic properties is provided in Section 4.8. The position of the Absorber is displayed in blue.

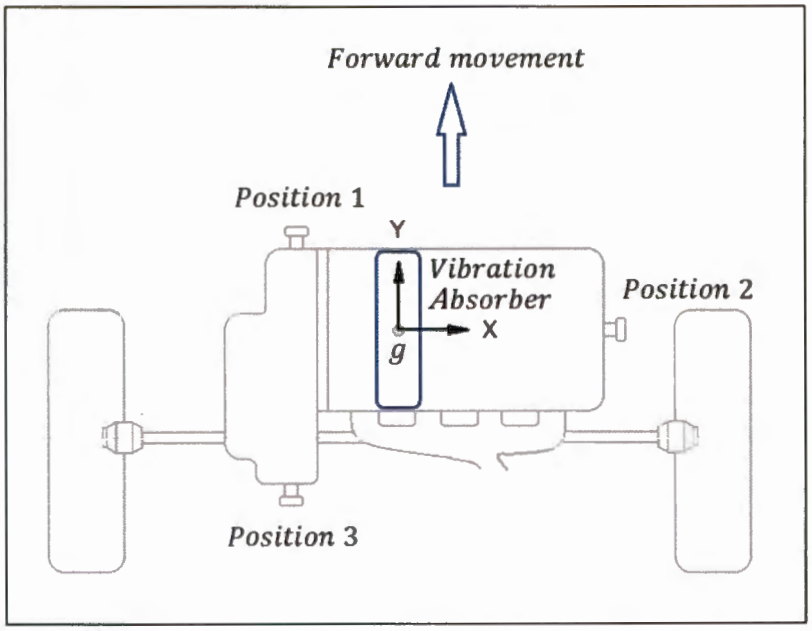

Figure 4.8: Top view of Engine with Vibration Absorber.

The coordinates are provided as the position of each Engine mount relative to the centre of gravity of the Engine, in the X as well as the Y direction, as indicated in Table 4.1 (Nel & Heyns, 1996; Steyn, 2011).

Table 4.1: Coordinates of Engine and Absorber centre of gravity.

Mount	Coordinates [m]	
	X	Y
Engine mount at position 1	-0.1460	0.2645
Engine mount at position 2	0.4230	-0.0520
Engine mount at position 3	-0.2430	-0.3210

4.4 INSTRUMENTATION

4.4.1 Acceleration meter

An acceleration meter is an electromechanical mechanism that measures acceleration caused by dynamic forces (Figure 4.9). It uses a pizo crystal to convert the mechanical motion into electrical signals. Two 100 mV/g PCB acceleration meters connected to an FFT Analyser with a coaxial cable each were simultaneously used to characterise the equivalent stiffness- and damping element of the Vibration Absorber. These acceleration meters were also used for the evaluation of the Absorber in Chapter 5.

Figure 4.9: 100 mV/g PCB acceleration meter.

4.4.2 FFT Analyser

An FFT Analyser was used to measure time- and frequency domain response signals. Figure 4.10 displays the FFT Analyser that was used for this study, which is a two channel Diagnostic Instruments 2200 Real Time FFT Analyser. Time- and frequency domain signals obtained from the two acceleration meters were recorded by the FFT Analyser and the data was downloaded to a personal computer, which was used as input data for the characterisation of the Absorber's equivalent rubber mount.

Figure 4.10: FFT Analyser.

4.4.3 Experimental setup

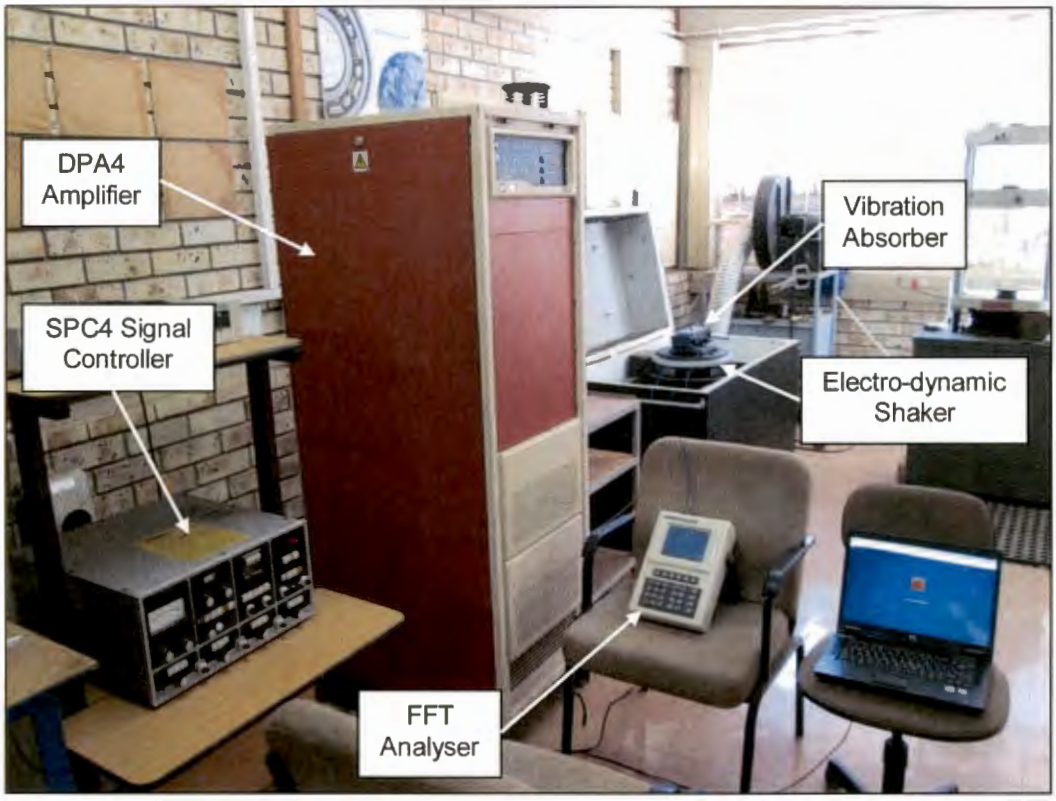

Figure 4.11: Experimental setup.

Figure 4.11 displays the experimental setup that was used for the characterisation of the Vibration Absorber's dynamic properties mounts for different excitation amplitudes (Nel & Van Wyngaardt, 2014a). The equivalent rubber mount supported the mass of the Absorber, while the two linear guide bearings with guide shafts guided the moving Absorber mass to allow movement only in the vertical direction. Two acceleration meters coupled to a FFT Analyser were used to measure the acceleration signals simultaneously at the base and at the Absorber mass. During all Shaker tests in the laboratory, safety shoes as well as hearing protection were worn. Two people were always present in case of a possible emergency.

4.4.4 Electro-dynamic Shaker

The Vibration Absorber was firmly attached to the table of a Ling Dynamic Systems V724 Electro-dynamic Shaker with four M8 Allen cap steel bolts as displayed in Figure 4.12. This test apparatus consists of three main components, namely an Electro-dynamic Shaker, Amplifier and a Signal Controller. The desired amplitude- and frequency

excitations were adjusted with the SPC4 Signal Controller. This signal was sent through a DPA4 Amplifier that controlled the selected amplitude and frequency at the Electro-dynamic Shaker as shown in Figure 4.11.

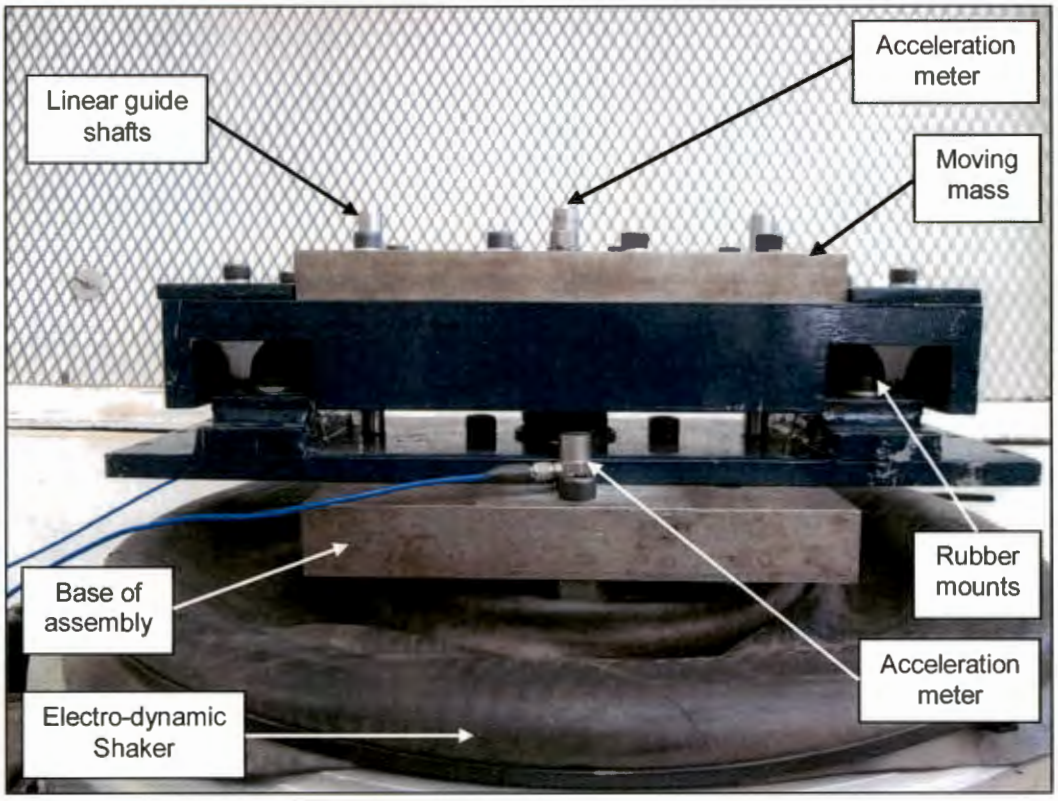

Figure 4.12: Vibration Absorber attached to Electro-dynamic Shaker.

4.5 DYNAMIC TEST PROCEDURE

4.5.1 Natural frequency of Engine mount system

The bounce mode frequency of the Engine mount system was experimentally excited and measured with an acceleration meter that was firmly attached at the Engine's centre of gravity. The natural frequency was excited by impact loads applied on the Engine with the use of a rubber mallet as shown in Figure 4.13.

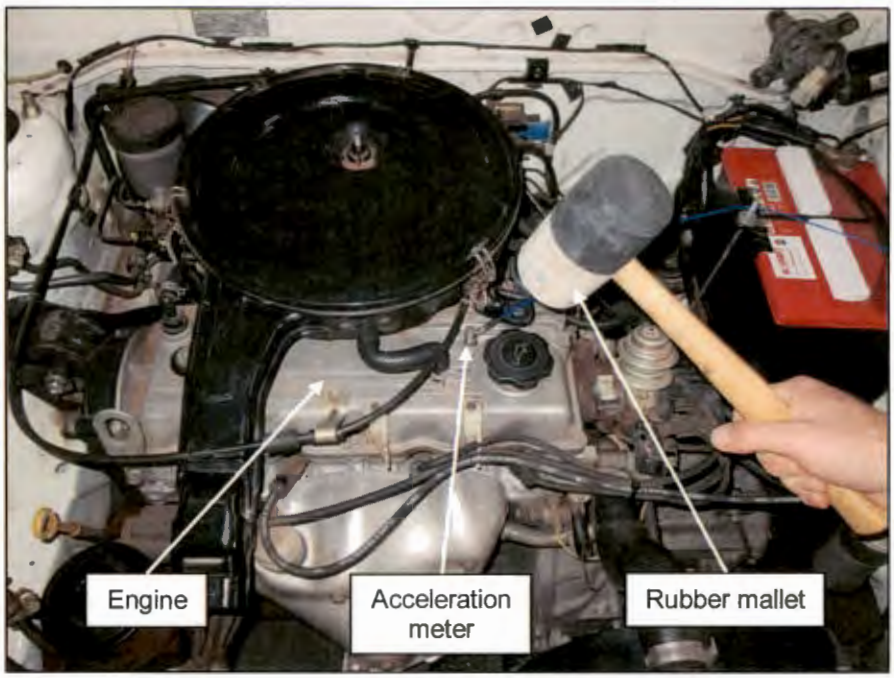

Figure 4.13: Bounce mode natural frequency excitation of Engine mount system.

Figure 4.14 displays the measured bounce mode natural frequency of the Engine mount system as example, which was an average of 13 Hz in this case. The amplitude dependency on stiffness was investigated in Section 4.8.

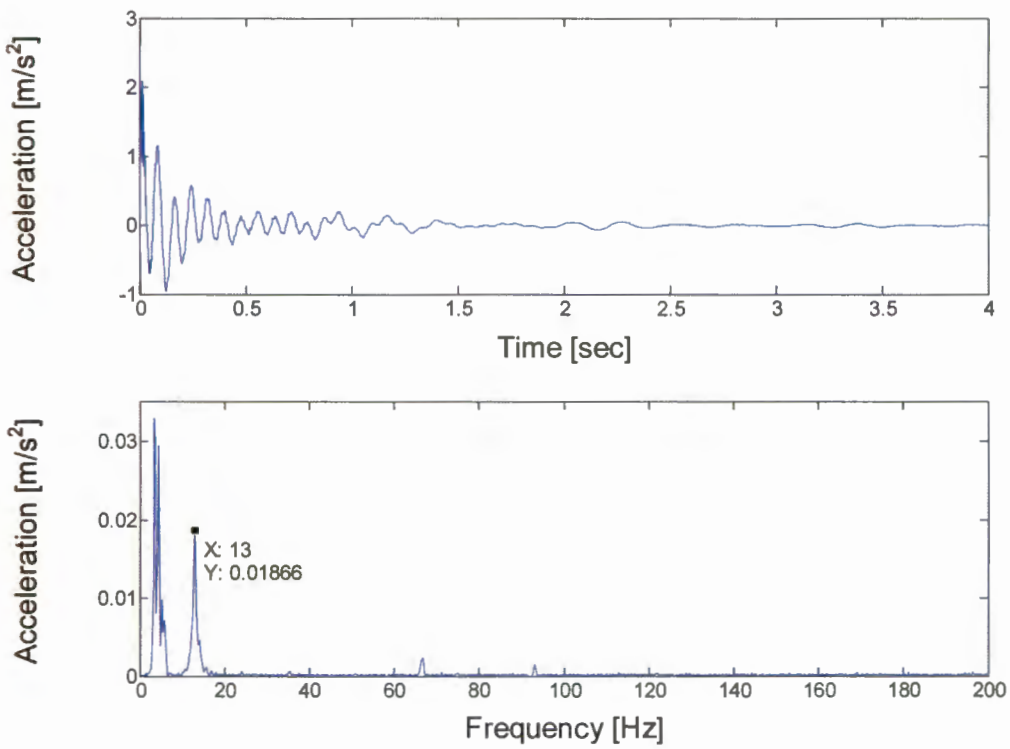

Figure 4.14: Measured bounce mode natural frequency of Engine mount system.

The bounce mode natural frequency of the Engine mount system may shift slightly due to the amplitude dependency of the stiffness of the three Engine rubber mounts (Nel & Van Wyngaardt, 2014a). Table 4.9 in Section 4.9 shows the natural frequency of the Engine mount system at several relative displacement amplitudes. The characterised dynamic stiffness properties of the Engine rubber mounts and the Engine mass was used to compute the corresponding natural frequency at each relative displacement amplitude. This was done with the use of equation (2.22).

4.5.2 Mass of Engine mount system

The mass of the Engine was measured with the use of a calibrated Loadtech LT2002 Load Cell connected to a TDC/I/0400 Microprocessor Load Indicator, as displayed in Figure 4.15. The engine with gearbox (Engine) was loosened from its three rubber mounts and lifted slightly with the use of an overhead crane. The exhaust pipe was still attached to the Engine in order to obtain an equivalent mass for the Engine mount system. A mass magnitude of 170.5 kg for the Engine was obtained.

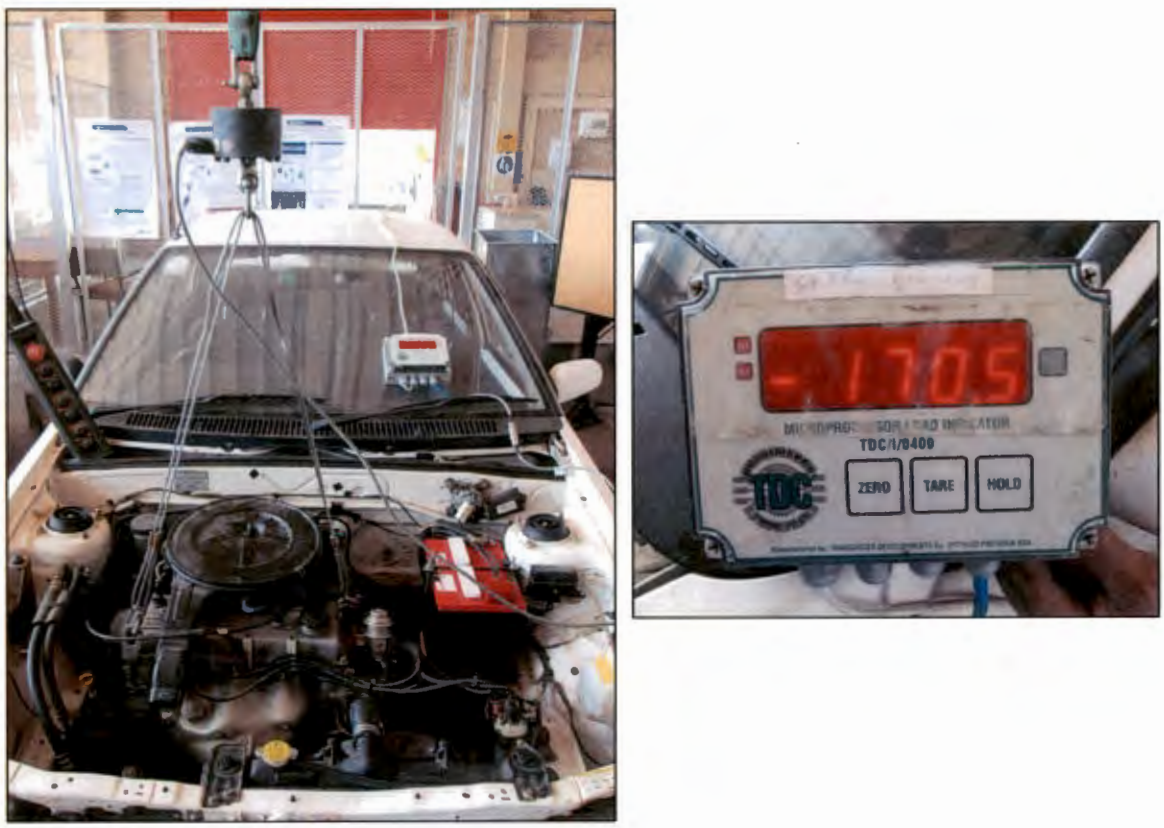

Figure 4.15: Mass of Engine mount system.

The mass magnitude of the Engine attachment bracket as well as the Absorber basis with the two linear guide shafts were also measured with a calibrated PRW-30 T-Scale as displayed in Figure 4.16.

Figure 4.16: Mass of Engine attachment bracket and Absorber basis.

The mass magnitudes of these components were added to the mass of the Engine, which provided a total equivalent Engine mass of 179.1 kg as shown in Table 4.2.

Table 4.2: Equivalent Engine mass.

Component	Mass [kg]
Engine with exhaust pipe attached	170.5
Engine attachment bracket	4.5
Absorber basis with two linear guide shafts	4.1
Total equivalent Engine mass: 179.1 kg	

4.5.3 Natural frequency of Vibration Absorber

The basis of the Absorber was firmly bolted to a rigid foundation and the natural frequency excited by impact loads applied at the Absorber mass with the use of a rubber mallet (Nel & Van Wyngaardt, 2014a). The natural frequency of the Absorber was tuned to be the same as the bounce mode frequency of the Engine mount system by adding the required additional masses on top of the Absorber main mass. This natural frequency was measured with an acceleration meter placed at the centre of gravity of the Absorber and coupled to an FFT Analyser as indicated in Figure 4.17.

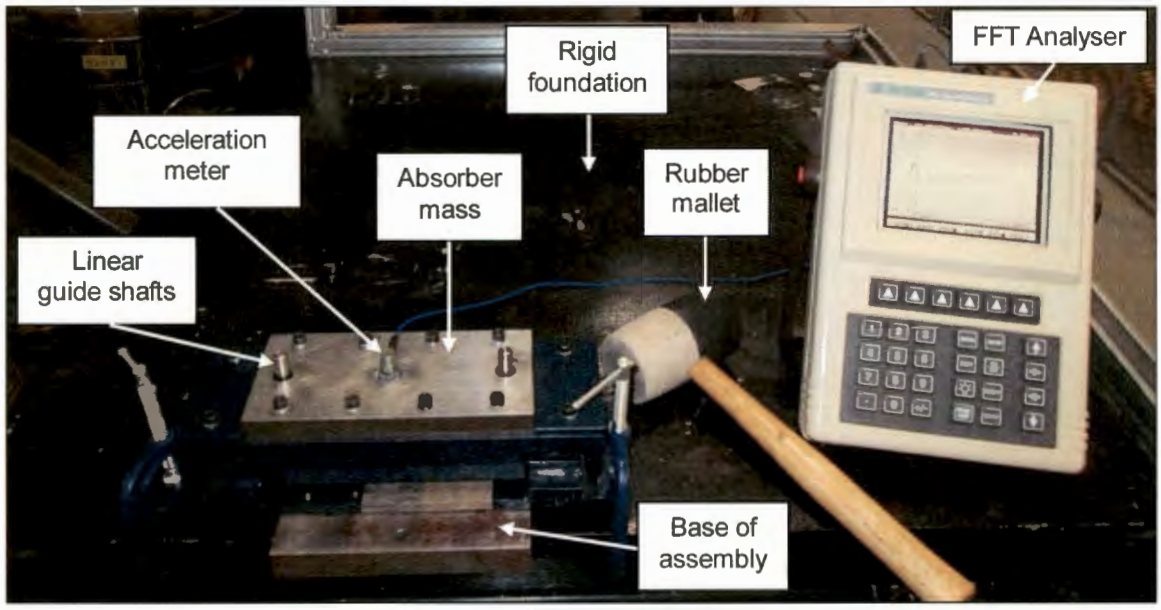

Figure 4.17: Natural frequency excitation of Vibration Absorber.

Figure 4.18 displays the measured natural frequency of the Absorber in the vertical direction as example, which was tuned to correspond to the bounce mode natural frequency of the Engine mount system at 13 Hz (see Figure 4.14). The natural frequency of the Absorber may shift due to the amplitude dependency of the stiffness of the three Absorber rubber mounts (Nel & Van Wyngaardt, 2014a). Table 4.9 in Section 4.9 shows the natural frequency magnitude of the Absorber at several relative displacement amplitudes. The dynamic stiffness properties of the Absorber's mounts as characterised in Section 4.6 and the Absorber mass were used to compute the corresponding natural frequency at each relative displacement amplitude. This was done with the use of equation (2.26).

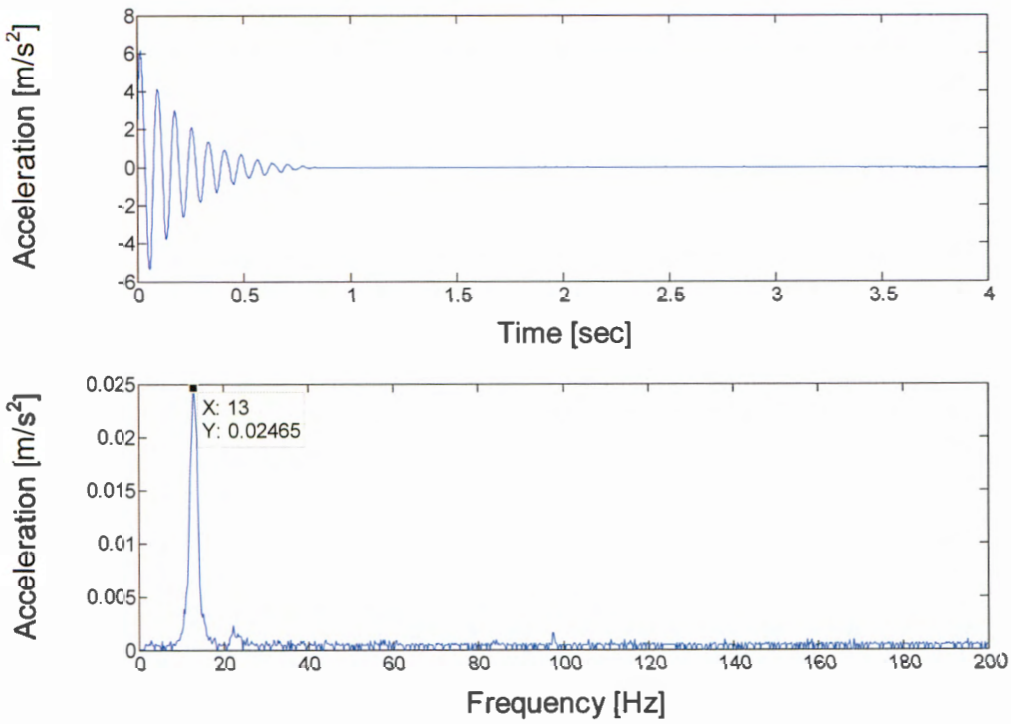

Figure 4.18: Natural frequency of Vibration Absorber.

4.5.4 Moving mass of Vibration Absorber

The Vibration Absorber's moving mass and all its moving components used for the characterisation were also measured with the calibrated PRW-30 T-Scale as displayed in Figure 4.19.

Figure 4.19: Moving mass of Vibration Absorber.

Table 4.3 displays the mass magnitudes for various moving parts of the Absorber that were used to determine the total moving mass. Detailed drawings for these components are included in Appendix C. The mass of the Engine attachment bracket as well as the Absorber basis with the two linear guide shafts (not moving with Absorber's moving parts) were added to the mass of the Engine (see Section 4.5.2).

Table 4.3: Moving mass for various Vibration Absorber parts.

Component	Quantity	Mass [kg]
6 mm thick tuning mass	2	0.2239
18 mm thick tuning mass	1	2.5315
Linear guide bearing	2	0.0617
M6 bolt (16 mm long)	2	0.0056
M6 bolt (30 mm long)	8	0.0076
M6 bolt (40 mm long)	1	0.0101
M4 bolt (10 mm long)	8	0.0017
Main mass	1	7.2110
Total Absorber moving mass: 10.41 kg		

The total moving mass of the Absorber was thus 5.8% of the total equivalent Engine mass. A sensitivity study indicated that an Absorber dynamic mass at around 6% of the total equivalent Engine mass could be effective to reduce Engine vibration, and this mass magnitude will efficiently limit the dynamic movement of the Absorber's moving mass. For small mass magnitudes these dynamic movements will become too large and thus unsafe.

4.5.5 Example of characterisation from time signal at 27 Hz

The Absorber was characterised at a frequency approximately two times higher than its natural frequency, since the dynamic properties of elastomeric materials are more amplitude dependent than frequency dependent in the low frequency region below 50 Hz (Austrell & Olsson, 2012; Garcia, 2006; Karlsson & Persson, 2003; Lin *et al.*, 2005; Ooi & Ripin, 2011; Sjöberg, 2002). The mathematical model described in Section 2.2 was implemented in a computer program in a Matlab environment, and the data recorded by an FFT Analyser was used as the input data (also see Section 3.2). With the measured acceleration amplitudes and the phase difference between the two acceleration signals, the dynamic stiffness and damping properties were computed by solving equations (2.7) and (2.8) simultaneously for different excitation amplitudes.

Two acceleration meters were connected to an FFT Analyser in order to measure the two time signals simultaneously at the base and the mass on top of the Absorber. For example, Figure 4.20 displays two measured time domain acceleration signals used to obtain the acceleration amplitudes $\ddot{X}_S$ and $\ddot{Y}_S$, as well as the phase angle at 27 Hz for a relative displacement amplitude of 0.02 mm. The measured acceleration amplitudes were converted to the corresponding displacement amplitudes by means of equations (2.9) and (2.10). $\ddot{X}_S$ represents the movement at the Absorber mass while $\ddot{Y}_S$ represents the movement at the basis.

Figure 4.20 displays the two time domain signals measured at the test setup. The upper time domain signal was measured on top of the Absorber mass, while the lower time domain signal was measured at the base with some noise from the Electro-dynamic Shaker observed. The noise was filtered out in a Matlab environment with the use of a computer program developed specifically for this purpose. The main influence on the time signals was from the base. However, there were a few measured time signals where noise had no significant effect on the measured signals. Time domain signals were converted into frequency domain signals, and the corresponding acceleration amplitudes and phase angles were determined, as indicated in Figure 4.21 and Figure 4.22. With the use of the Fourier coefficients that were determined, the original interference frequency could be removed. The Fourier coefficients consist of amplitude, frequency and phase angle. This interference was then reconstructed into a time signal without noise, as shown in Figure 4.24. Figure 4.23 displays the time signals with noise, as well as without noise. The computer source code for the reconstruction of time signals is included in Appendix B.

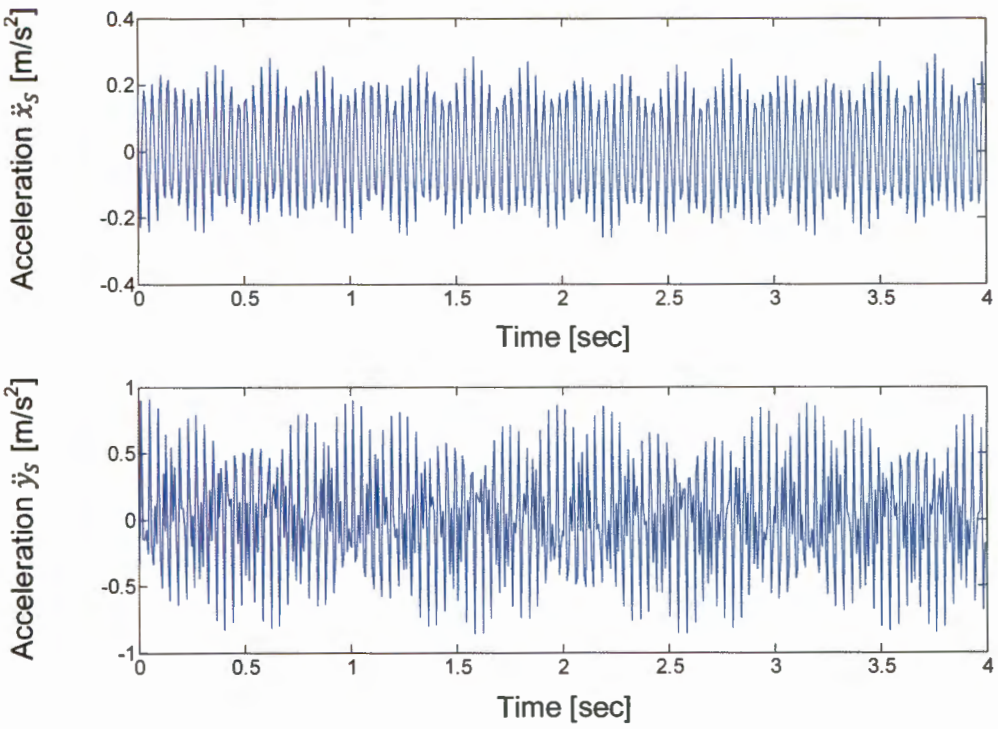

Figure 4.20: Time signals with noise.

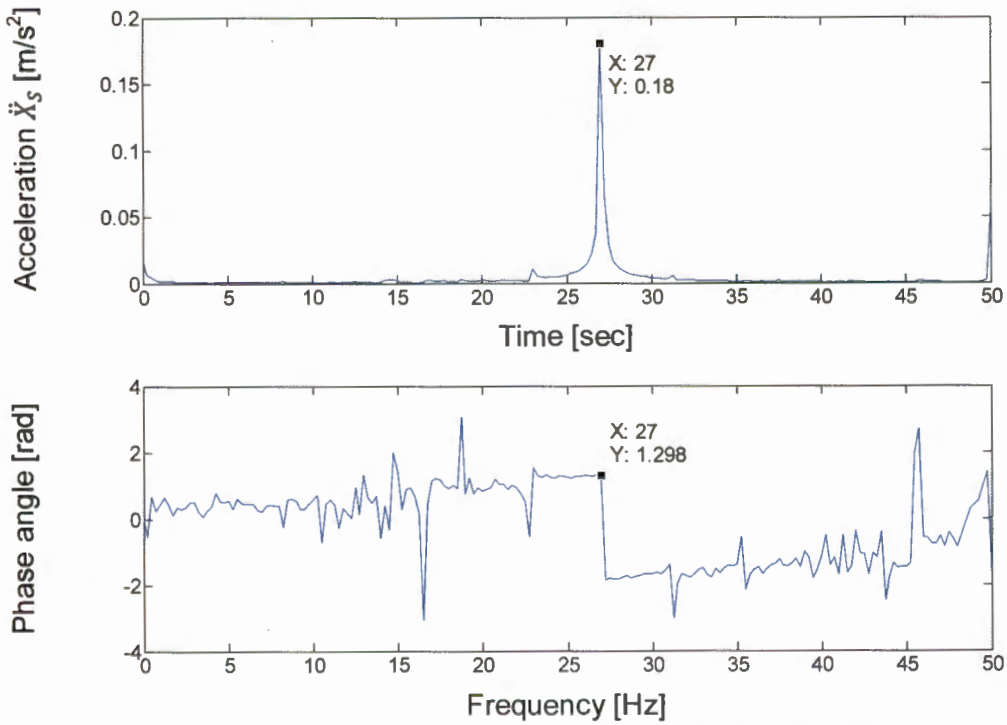

Figure 4.21: FFT and phase angle of the signal on the Absorber mass.

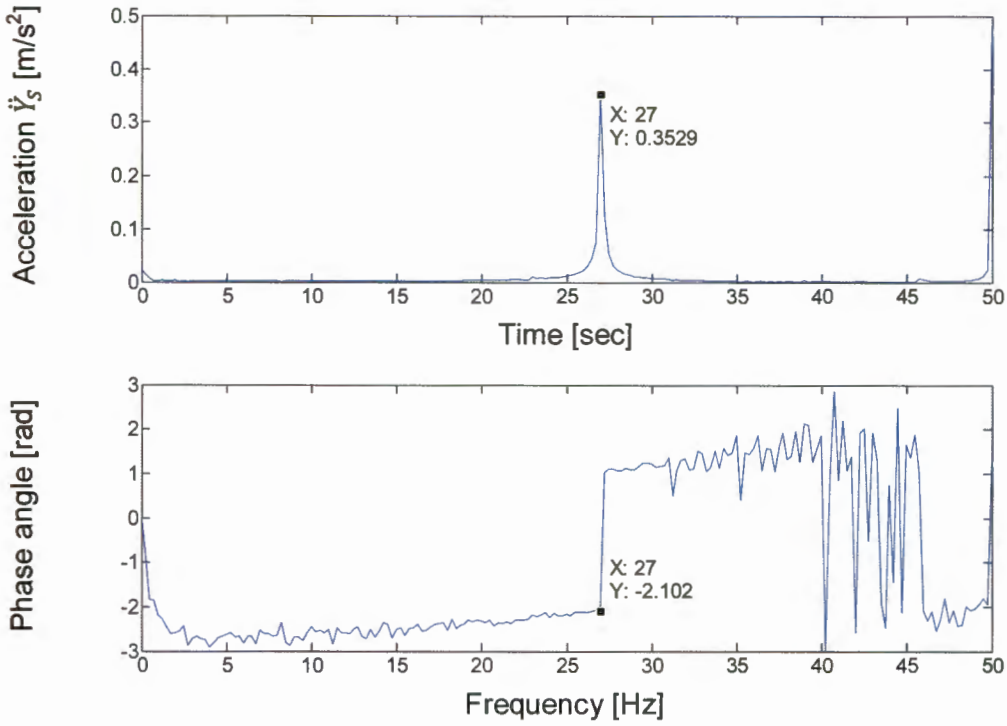

Figure 4.22: FFT and phase angle of the signal on the basis.

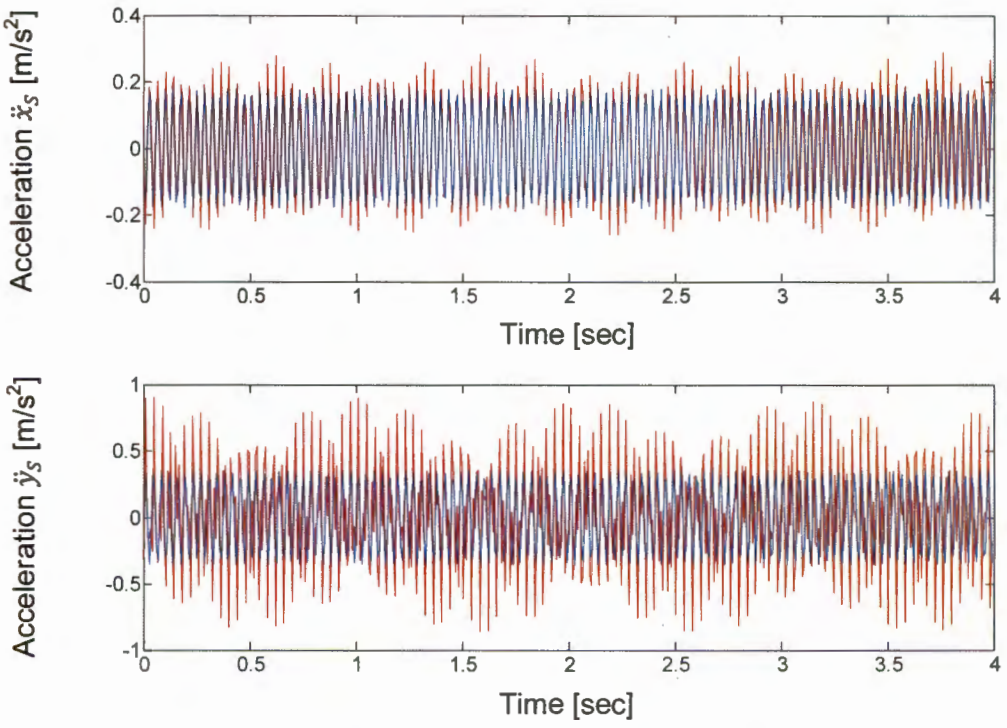

Figure 4.23: Reconstruction with noise and without noise.

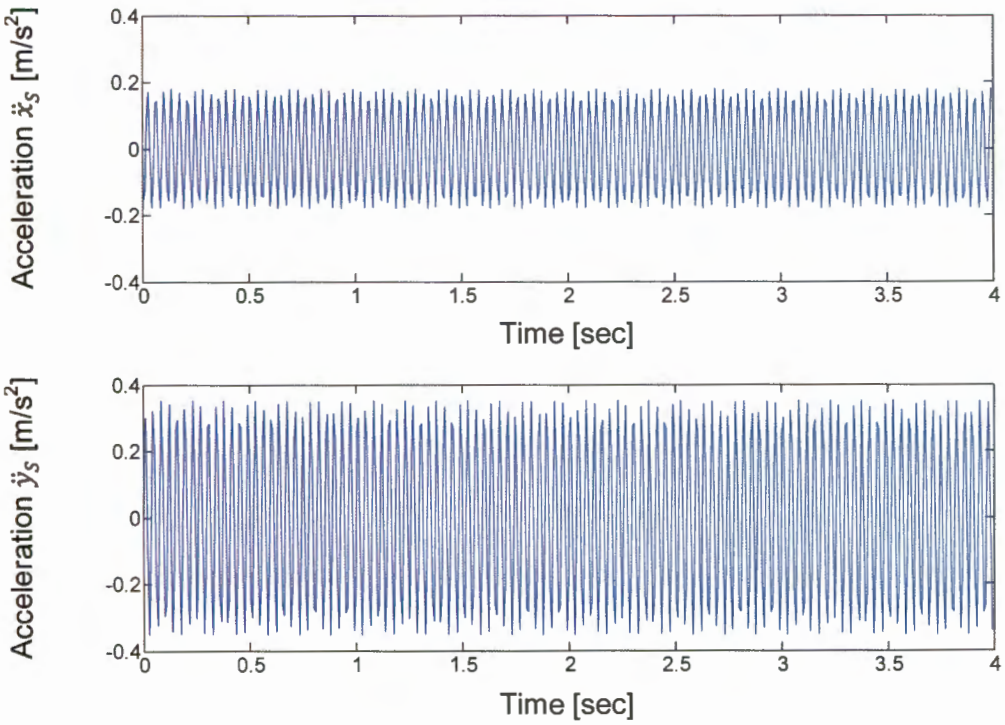

Figure 4.24: Measured time domain acceleration signals without noise.

The values obtained from the time signals are indicated in Table 4.4.

Table 4.4: Fourier coefficients at 27 Hz.

	Absorber mass	Base
Acceleration amplitude [m/s^2]	0.180	0.353
Phase angle [rad]	1.298	-2.102

The difference in phase angle is obtained from Figure 4.21 and Figure 4.22 respectively. The difference in phase angle is $\phi = -3.4$ rad. The measured acceleration amplitudes $\ddot{X}_S$ and $\ddot{Y}_S$ were converted to the corresponding displacement amplitudes by means of equations (2.9) and (2.10). With the displacement amplitudes at the Absorber mass X_S and at the base Y_S, as well as the phase angle ϕ between the two measured time domain signals, equations (2.7) and (2.8) were used to compute the dynamic stiffness k_a and viscous damping c_a as indicated in Table 4.5. These values were computed with the use of a Matlab program described in Chapter 3, Section 3.2, of which the source code is included in Appendix B. The characterisation was done with an Absorber moving mass of 10.41 kg.

Table 4.5: Absorber dynamic properties.

Relative displacement amplitude [mm]	Dynamic stiffness k_a [N/mm]	Viscous damping c_a [Ns/m]	Damping ratio ζ_a
0.02	100.49	102.74	0.050

The computer program was also used to compute the critical damping coefficient, the damping ratio ζ_a, as well as the dynamic vectors. The dynamic force magnitudes were computed respectively and are indicated in Table 4.6.

Table 4.6: Dynamic force magnitudes.

$k_a X_S$ [N]	$c_a \omega X_S$ [N]	$m_a \omega^2 X_S$ [N]	$k_a Y_S$ [N]	$c_a \omega Y_S$ [N]	ϕ [Degrees]	α [Degrees]
0.63	0.11	1.87	1.23	0.21	165.16	174.16

The information in Table 4.6 was used to construct a vector diagram as shown in Figure 4.25. The information indicated in Table 4.6 is only applicable for one set of measured data as an example. Many more measured data sets were used for the other excitation amplitudes (0.01 to 4 mm) regarding the characterisation (see Section 4.6). This characterisation procedure differs from standard methods for elastomeric materials, where a phase angle α is normally utilised. Most literature uses the phase angle α, which is related to ϕ, as described in Section 2.2 (Kim & Singh, 1992; Nel & Steyn, 2012; Steyn, 2011). The phase angle ϕ and α differ since the angles are between different vectors. The characterisation setup as well as the instrumentation differs from what other researchers used for characterisation, therefore the phase angle α is not applicable.

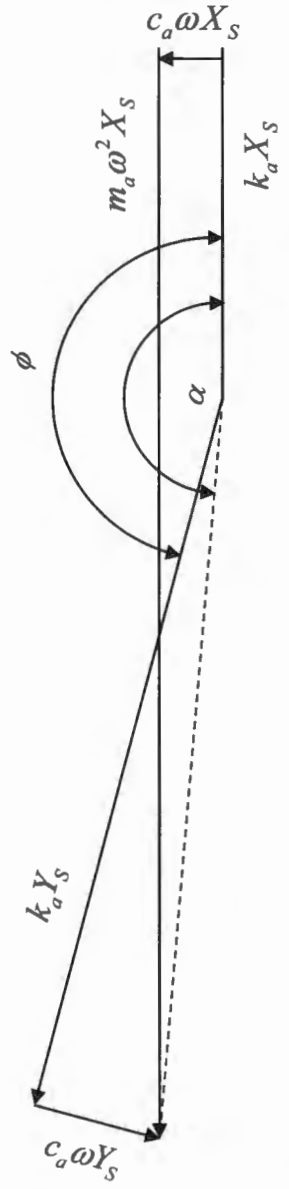

Figure 4.25: Vector diagram of dynamic force magnitudes and phase angle.

4.6 DYNAMIC PROPERTIES OF ABSORBER MOUNTS

The dynamic characteristics of the three Absorber rubber mounts were characterised as one equivalent mount with stiffness and damping properties. Table 4.7 displays these dynamic properties of the Vibration Absorber for several relative displacement amplitudes at an excitation frequency of 27 Hz (Nel & Van Wyngaardt, 2014a). The measured acceleration amplitudes were converted to the corresponding displacement amplitudes by means of equations (2.9) and (2.10). The magnitudes obtained for k_a and c_a were used as input data in the computer programs discussed in Section 3.4 and Section 3.6.

Table 4.7: Dynamic properties of the Absorber.

Relative displacement amplitude [mm]	Dynamic stiffness k_a [N/mm]	Viscous damping c_a [Ns/m]	Damping ratio ζ_a	Phase angle ϕ [Degrees]
0.01	104.83	131.51	0.063	161.45
0.02	100.49	102.29	0.050	165.16
0.05	97.73	74.65	0.037	169.05
0.08	92.96	61.61	0.031	170.69
0.10	90.76	60.27	0.031	170.66
0.25	80.61	49.47	0.027	171.85
0.50	68.51	45.95	0.027	171.58
0.75	64.35	44.88	0.027	171.40
1.00	62.38	43.49	0.027	171.47
1.25	60.60	40.72	0.026	171.84
1.50	60.38	40.64	0.026	171.83
1.75	60.20	39.69	0.025	172.01
2.00	59.84	38.34	0.024	172.24
2.25	59.37	36.28	0.023	172.61
2.50	58.54	34.66	0.022	172.87
2.75	57.95	33.56	0.022	173.04
3.00	57.13	33.56	0.022	172.96
4.00	56.95	31.95	0.021	173.28

Figure 4.26 shows a graphical representation of the Absorber stiffness k_a obtained from the tests performed. The dynamic stiffness is a maximum for the lowest relative displacement amplitude of 0.01 mm. The dynamic stiffness magnitude decreases significantly up to a relative displacement amplitude of approximately 0.5 mm, from where it decreases gradually to the largest relative displacement amplitude at 4 mm.

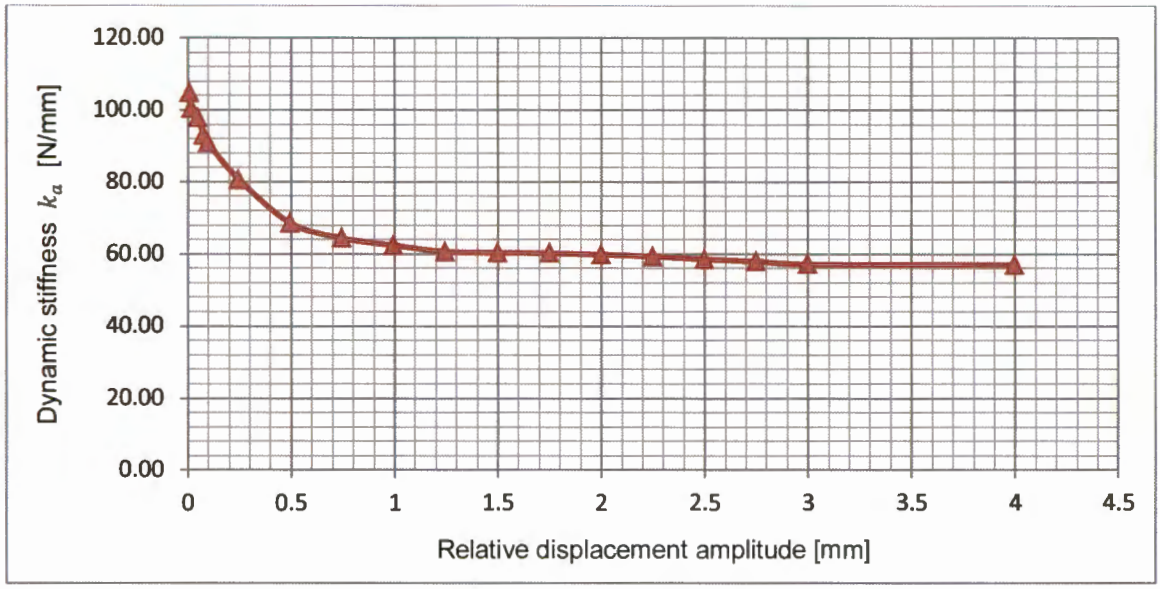

Figure 4.26: Dynamic stiffness of Absorber's equivalent mount.

A graphical representation of the Absorber's damping ratio ζ_a is shown in Figure 4.27. The damping ratio is a maximum for the smallest relative displacement amplitude of 0.01 mm and decreases significantly up to a relative displacement amplitude of approximately 0.25 mm, from where it decreases gradually to the largest relative displacement amplitude at 4 mm.

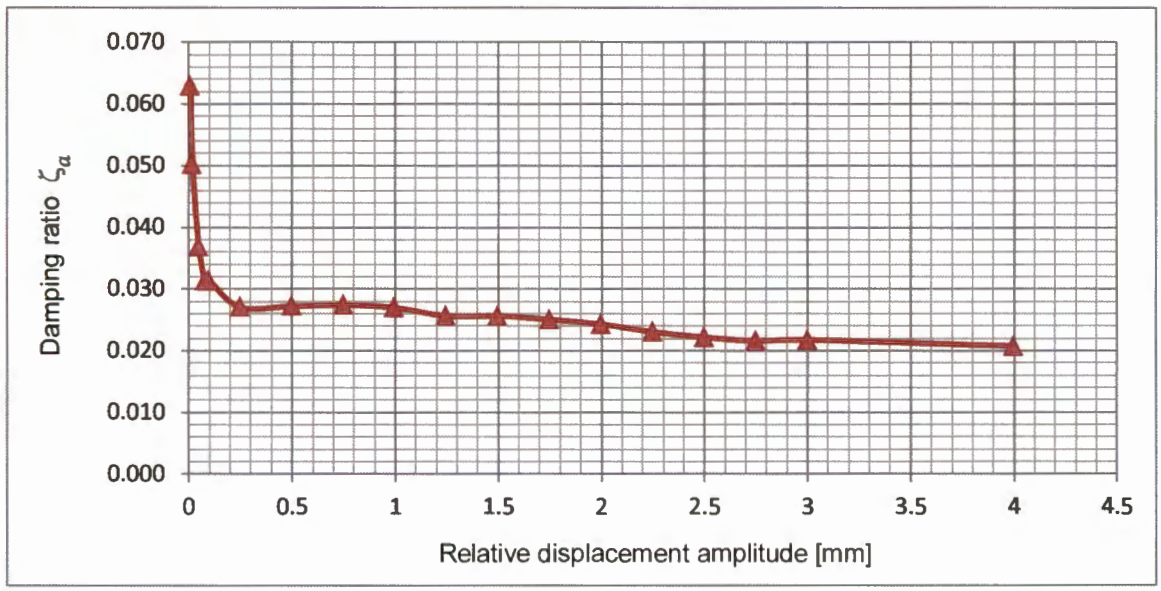

Figure 4.27: Damping ratio of the Absorber.

A graphical representation of the phase angle ϕ is shown in Figure 4.28. The phase angle is the smallest for the lowest relative displacement amplitude of 0.01 mm and increases significantly up to a relative displacement amplitude of approximately 0.25 mm, from where it increases gradually to the largest relative displacement amplitude at 4 mm.

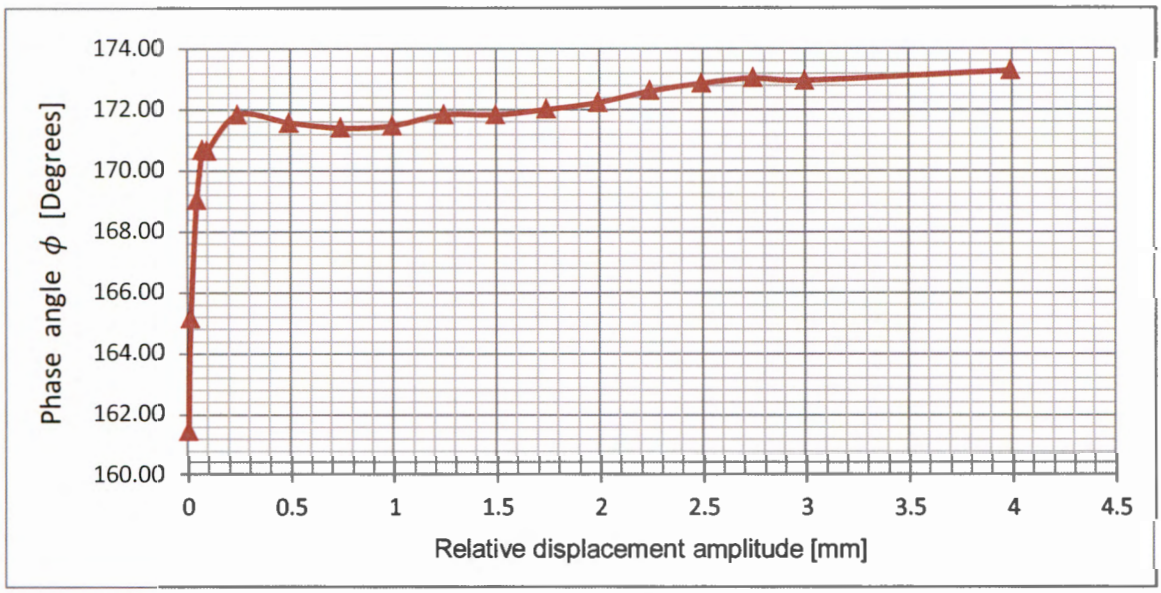

Figure 4.28: Phase angle.

4.7 STATIC TEST FOR ABSORBER

A MTS Landmark Servo hydraulic Test System as shown in Figure 4.29 was used to measure the static load-deflection properties of the equivalent rubber mount of the Absorber in the vertical direction (Nel & Van Wyngaardt, 2014a). The same range of amplitudes for the dynamic tests was used to characterise the static stiffness of the Absorber's equivalent stiffness- and damping element, which varied between 0.01 and 4 mm. Figure 4.30 shows a graphical representation of the equivalent Absorber rubber mount stiffness obtained from the dynamic and static tests performed. The static stiffness magnitudes varied at an average of approximately 20% lower compared to the magnitudes obtained from the Electro-dynamic Shaker approach.

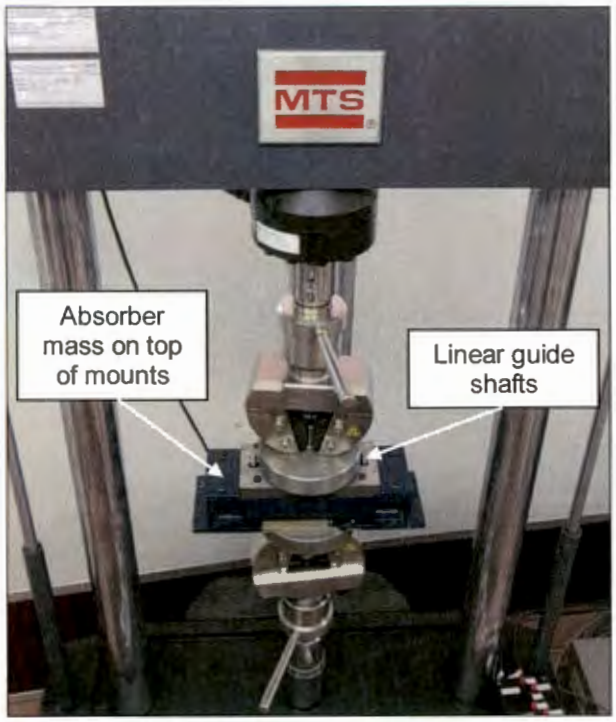

Figure 4.29: Static load-deflection test setup.

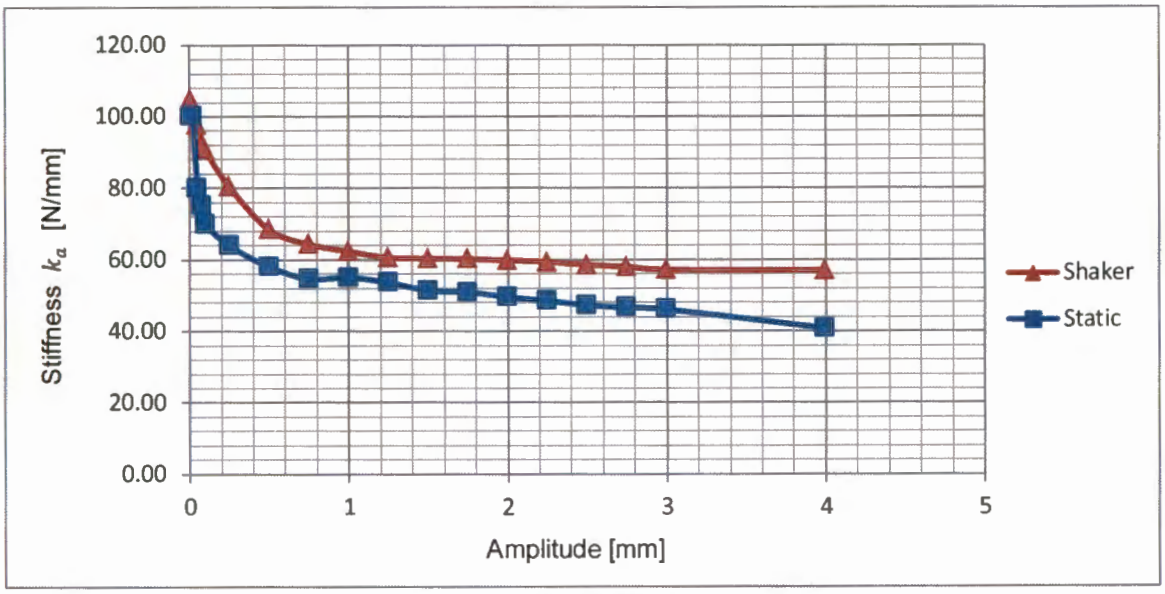

Figure 4.30: Dynamic- and static stiffness properties of Absorber.

It was thus necessary to dynamically characterise the Absorber's equivalent rubber mount, since the stiffness magnitudes obtained from the static tests varied significantly from the magnitudes measured during the dynamic tests.

4.8 DYNAMIC PROPERTIES OF ENGINE MOUNTS

The same three Engine mounts used in this study were previously characterised by Steyn (2011) for certain relative displacement amplitudes at excitation frequencies of 10, 22 and 75 Hz respectively. The same characterisation method was used as in the case of the Absorber mounts (see Section 4.5). These engine mounts were characterised for the same vehicle's Engine that was used in this study. The position of each mount is displayed in Figure 4.8. An equivalent mass of 63.5 kg was used for the Engine mount at position 1 and position 2 for the characterisation, while 56.5 kg was used for the Engine mount at position 3. For this study the three Engine mounts arranged in parallel were considered as one equivalent mount with stiffness- and damping properties, although Steyn (2011) characterised each mount individually. Table 4.8 displays the dynamic properties of the Engine's equivalent mount for several relative displacement amplitudes, and excitation frequencies of 10, 22 and 75 Hz respectively (Steyn, 2011). The magnitudes obtained for k_e and c_e were used as input data in the computer programs discussed in Section 3.3 to Section 3.6.

Table 4.8: Dynamic properties of Engine's equivalent rubber mount.

Relative displacement amplitude [mm]	Dynamic stiffness k_e [N/mm]	Viscous damping c_e [Ns/m]	Damping ratio ζ_e
Frequency at 10 Hz			
0.02	1072.28	1351.45	0.048
0.05	1061.27	1100.98	0.039
0.10	1046.97	1050.94	0.038
0.25	1003.90	1021.54	0.038
0.50	1005.73	1045.09	0.038
Frequency at 22 Hz			
0.02	1097.78	1419.37	0.050
0.05	1119.80	686.87	0.024
0.10	1085.92	813.56	0.029
0.25	1011.88	634.45	0.023
0.50	969.07	556.54	0.021
Frequency at 75 Hz			
0.02	1837.49	1279.61	0.035
0.05	1888.96	1298.46	0.035
0.10	1831.76	1140.14	0.031
0.25	1597.85	742.54	0.022
0.50	1395.26	477.32	0.015

Figure 4.31 shows a graphical representation of the equivalent Engine rubber mount stiffness k_e.

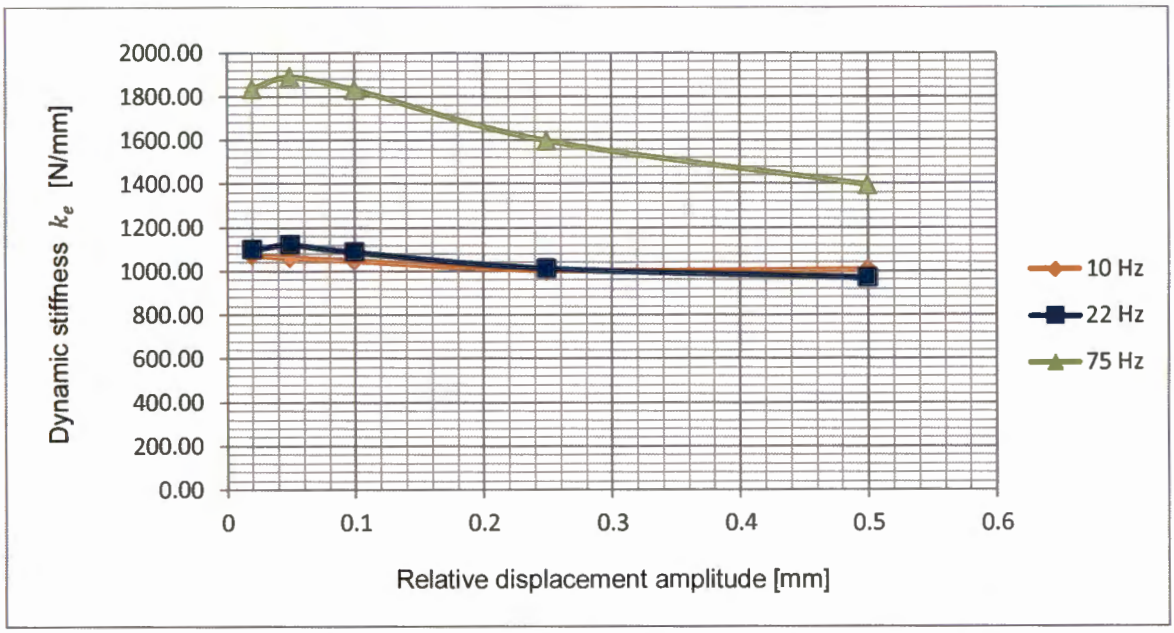

Figure 4.31: Dynamic stiffness of Engine's equivalent rubber mount.

The dynamic stiffness varies only slightly for all relative displacement amplitudes at 10 and 22 Hz. At 75 Hz the dynamic stiffness magnitudes are larger compared to the dynamic stiffness magnitudes at 10 and 22 Hz for all relative displacement amplitudes. The dynamic stiffness at 75 Hz is a maximum at the relative displacement amplitude of approximately 0.05 mm, from where it decreases gradually to the largest relative displacement amplitude at 0.5 mm.

Figure 4.32 shows a graphical representation of the equivalent Engine rubber mount damping ratio ζ_e. The damping ratio is a maximum for the smallest relative displacement amplitude of 0.02 mm at 10 and 22 Hz, and decreases considerably up to a relative displacement amplitude of approximately 0.05 mm, from where it varies slightly to the largest relative displacement amplitude at 0.5 mm. The damping ratio at 75 Hz is a maximum at the relative displacement amplitude of approximately 0.05 mm, from where it decreases gradually to the largest relative displacement amplitude at 0.5 mm.

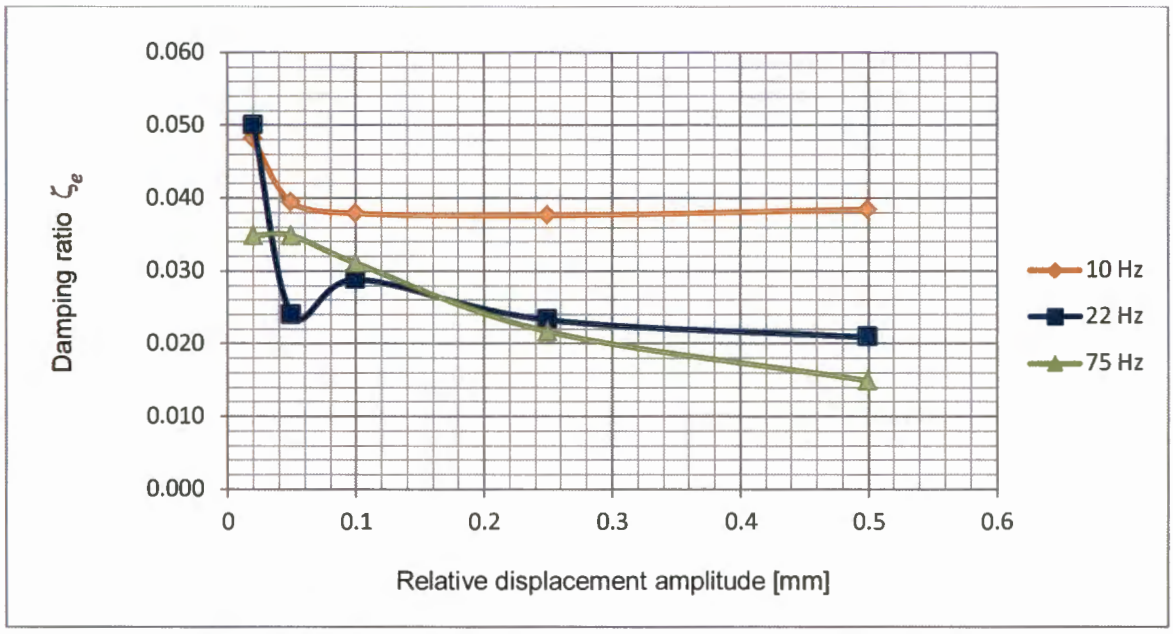

Figure 4.32: Damping ratio of Engine's equivalent rubber mount.

4.9 NATURAL FREQUENCIES

The natural frequency of the Vibration Absorber as well as the Engine mount system changed for different relative displacement amplitudes due to the amplitude dependency of the stiffness of the elastomeric mounts. With the use of the mass and equivalent dynamic stiffness determined at each relative displacement amplitude, the natural frequency was computed for each system respectively with equations (2.22) and (2.26). The natural frequencies of the Absorber as well as the Engine mount system are displayed in Table 4.9 for several excitation amplitudes.

The equivalent dynamic stiffness of the three Engine mounts characterised at 10 Hz was used to compute the natural frequencies for the system at different relative displacement amplitudes, which is typically the frequency range at which the bounce mode of the Engine mount system is excited by road input forces (see Section 5.5.2).

The Absorber was tuned for the larger excitation amplitudes of the Engine mount system at approximately 0.5 mm. In Chapter 5, Section 5.5.2, one of the road forces tests indicated an Engine displacement amplitude of 0.13 mm, and for the Absorber a displacement amplitude of 1.15 mm at 12.25 Hz, which is at resonance of the Engine mount system (also see Figure 5.10 and Table 5.5). Table 4.9 indicates similar relative movement between the Engine and the Absorber mass for comparable displacement amplitudes.

Table 4.9: Natural frequencies of Absorber and Engine mount system.

Relative displacement amplitude [mm]	Absorber natural frequency [Hz]	Engine mount system natural frequency [Hz]
0.01	15.97	-
0.02	15.63	12.31
0.05	15.42	12.25
0.08	15.04	-
0.10	14.86	12.17
0.25	14.00	11.91
0.50	12.91	11.92
0.75	12.51	-
1.00	12.32	-
1.25	12.14	-
1.50	12.12	-
1.75	12.10	-
2.00	12.07	-
2.25	12.02	-
2.50	11.93	-
2.75	11.87	-
3.00	11.79	-
4.00	11.77	-

4.10 CONCLUSIONS

The Vibration Absorber's equivalent rubber mount was successfully characterised with the use of the computer program described in Section 3.2, and the dynamic properties were determined at different excitation amplitudes. The dynamic properties of the three Engine mounts were obtained from previously work done by Steyn (2011) and were converted to properties for one equivalent Engine mount. The mass of the Vibration Absorber as well as the Engine mount system were also experimentally characterised. In the following chapter, the Vibration Absorber's performance was experimentally evaluated for certain operational conditions. This includes forces excited from the road as well as internal engine shaking forces. Transient response as well as the noise levels were also investigated.

5 EXPERIMENTAL EVALUATION

5.1 INTRODUCTION

The experimental evaluation entails the installation and testing of the designed prototype Vibration Absorber attached to the test vehicle. The Vibration Absorber was attached to the Engine with a specially designed Engine attachment bracket. In order to evaluate the performance of the Absorber, vibration response measurements were taken at the Engine's centre of gravity as well as at the Absorber in the vertical direction. The behaviour of the Engine and Absorber were investigated for several operational conditions. Dynamic force magnitudes transmitted to the vehicle's support structure were also computed. Two systems were compared to one another for all of the operational conditions; the Engine without the Absorber as well as the Engine with the Absorber attached. Engine and Absorber vibration responses, as well as natural frequencies predicted with mathematical models as described in Chapter 2 and implemented in computer programs as described in Chapter 3 were compared to the experimental data for all of the operational conditions.

5.2 TWO DIFFERENT EXPERIMENTAL SYSTEMS

Vibration measurements were taken for two different systems at various operational conditions as described below.

5.2.1 Original system

For the Original system, the Engine mounted on its three standard rubber mounts was considered as a single-degree-of-freedom system without the Absorber, as described in Section 2.3 and Section 2.5. Movement of the Engine was only considered in the vertical direction, and the appropriate dynamic properties of the Engine mounts described in Section 4.8 were used here.

5.2.2 Modified system

For the Modified system, the Engine mounted on its three standard rubber mounts with the Vibration Absorber attached to the Engine was considered as a two-degree-of-freedom system, as described in Section 2.4 and Section 2.6. The position of the

Vibration Absorber is indicated in Section 4.3. Movement of the Engine as well as the Absorber was thus only considered in the vertical direction, and the appropriate dynamic properties of the Absorber's stiffness- and damping element described in Section 4.6 were used here.

5.3 TEST VEHICLE

The vehicle that was used for the evaluation of the Absorber is displayed in Figure 5.1. The vehicle is a Mazda 323 Sting, which is equipped with a 1.3 litre four-cylinder front-wheel-drive Engine configuration.

Figure 5.1: Test vehicle.

5.4 INSTALLATION OF ENGINE VIBRATION ABSORBER

The designed Vibration Absorber prototype was attached to the Engine with the use of an Engine attachment bracket. Three M8 bolts on the one side of the Engine block and three on the other side were used to attach the bracket to the Engine as indicated in Figure 5.2. The Vibration Absorber was attached to this bracket with three M6 bolts on each side. A detailed drawing of the Absorber and the Engine attachment bracket is shown in Appendix C.

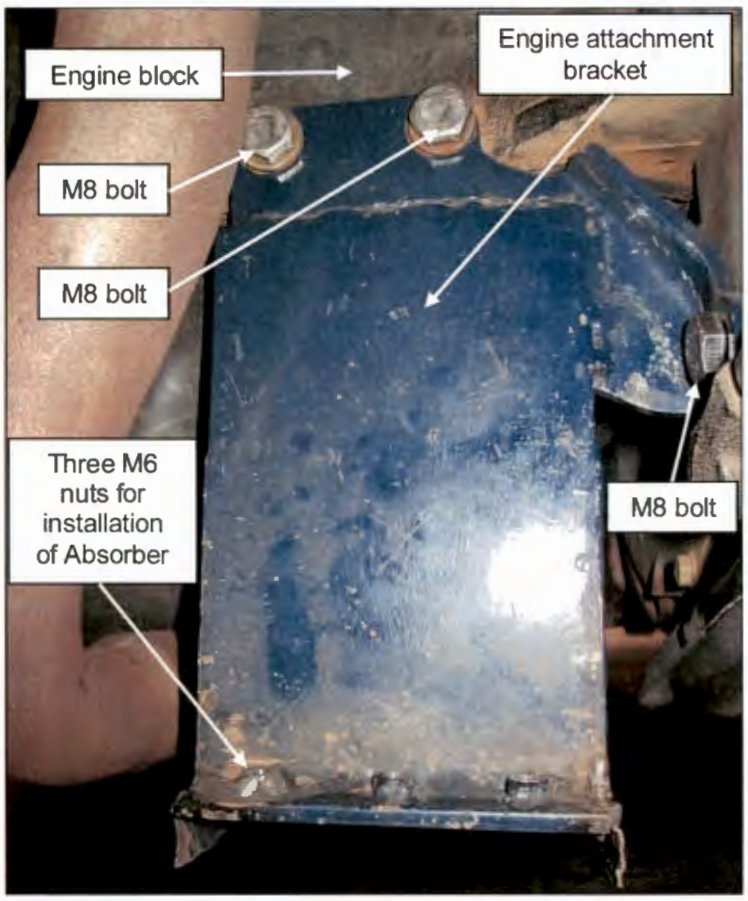

Figure 5.2: Installation of Vibration Absorber at the Engine.

5.5 EXPERIMENTAL EVALUATION OF VIBRATION ABSORBER

Three main operational conditions were experimentally evaluated for the Original- and Modified systems, and are discussed respectively:

1. Road forces, which include forces excited by the uneven road surface through the suspension to the Engine mount system, as well as the centrifugal forces excited by the rotation of the wheels.
2. Internal engine shaking forces, which include the internal shaking forces caused by engine mass imbalances of the engine's reciprocating and rotating parts, as well as gas pressure differences transmitted to the Engine mount system.
3. Transient response, which includes the dynamic forces that are transmitted to the vehicle's support structure due to the large displacements that typically occur during starting, stopping, gear changing, and impact loads from the wheels.

These three main operational conditions were first evaluated for the Original system. Thereafter the Absorber was attached to the Original system and the two new natural frequencies were measured and compared to the predicted natural frequencies. The Modified system was also evaluated for these three main operational conditions and compared to the Original system.

5.5.1 Natural frequencies

The natural frequencies of the Modified system were experimentally measured with acceleration meters that were coupled to an FFT Analyser. These acceleration meters were firmly attached to the Engine near the centre of gravity, as well as the Absorber mass respectively. The same method was used to excite the natural frequencies as displayed in Figure 4.13, Section 4.5.1. Impact loads were applied on the Engine with the use of a rubber mallet as for a bump test.

Figure 5.3 indicates the time- and frequency domain signals obtained from the bump tests performed on the Modified system. In this case, the acceleration meter was placed on the Engine and the response then recorded. The frequency domain signal indicates the amplitudes of the two new natural frequencies of the Modified system for the specific impact load magnitude applied.

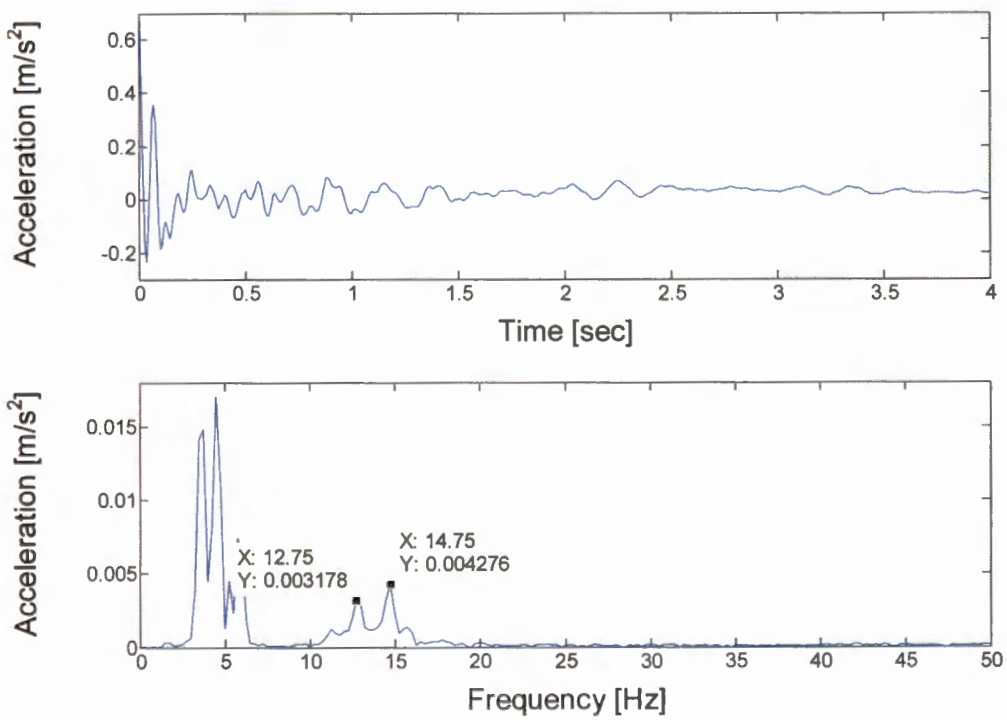

Figure 5.3: Natural frequencies of Modified system (Engine response).

The natural frequencies of the Modified system for the specific impact load magnitude applied were also measured while the acceleration meter was placed at the Absorber mass as displayed in Figure 5.4.

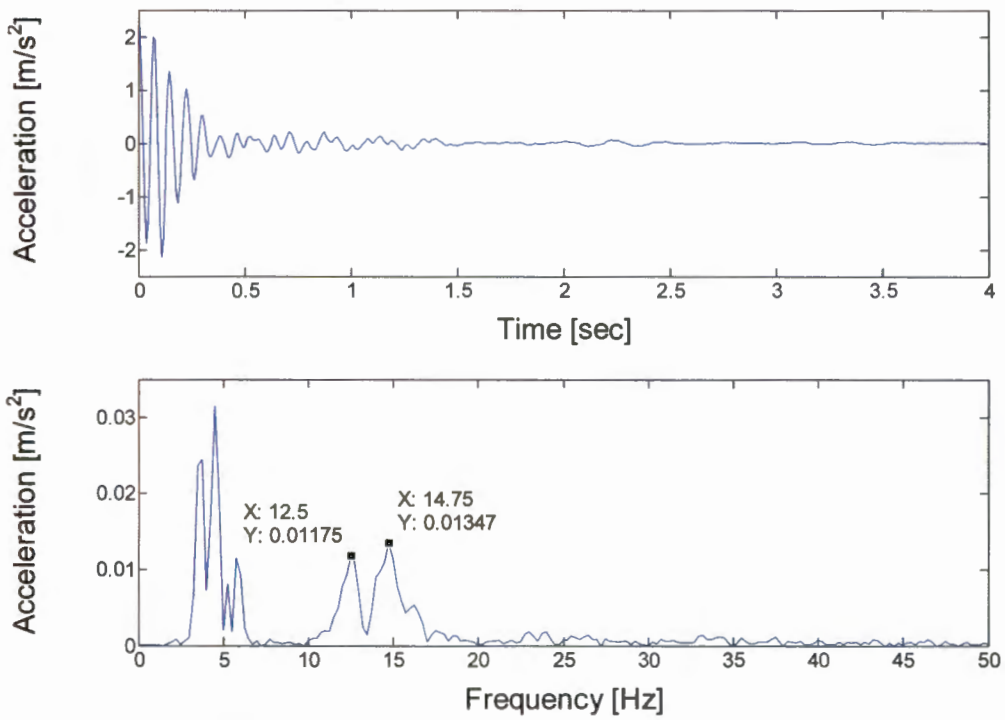

Figure 5.4: Natural frequencies of Modified system (Absorber response).

The comparison between the predicted and measured natural frequencies is displayed in Table 5.1. The measured natural frequencies compare well to the predicted natural frequencies (see Section 2.6). The predicted natural frequencies differ slightly from the measured natural frequencies due to the amplitude dependency on stiffness of the three Engine rubber mounts as well as the rubber mounts of the Absorber.

Table 5.1: Predicted and measured natural frequencies for Modified system.

Operational condition	Measured frequency [Hz]	Predicted frequency [Hz]	Percentage difference [%]
Engine response	12.75	11.38	10.7
	14.75	15.15	2.7
Absorber response	12.5	11.38	8.9
	14.75	15.15	2.7

5.5.2 Road forces

5.5.2.1 Road tests

Before the road tests were conducted, the tyre pressure of each wheel was inflated to around 2.2 bar as prescribed by the vehicle manufacturer. Each wheel was well balanced and proper wheel alignment of the vehicle was done. The tests were conducted for the Original system as well as the Modified system for several different conditions on a reasonably even tar road surface. Another vehicle was used to pull the test vehicle (Mazda) at constant speeds while the Engine was switched off and with the gearbox in a neutral position. Thus internal engine shaking forces were eliminated. The tests were conducted at 80, 100 and 120 km/h. Three conditions were tested at each speed, which included the following:

1. The wheels when they are well balanced.
2. An unbalance mass of 120 g attached to each front wheel.
3. An unbalance mass of 240 g attached to each front wheel.

Figure 5.5 indicate where an unbalance mass of 120 g is attached to one of the front wheels.

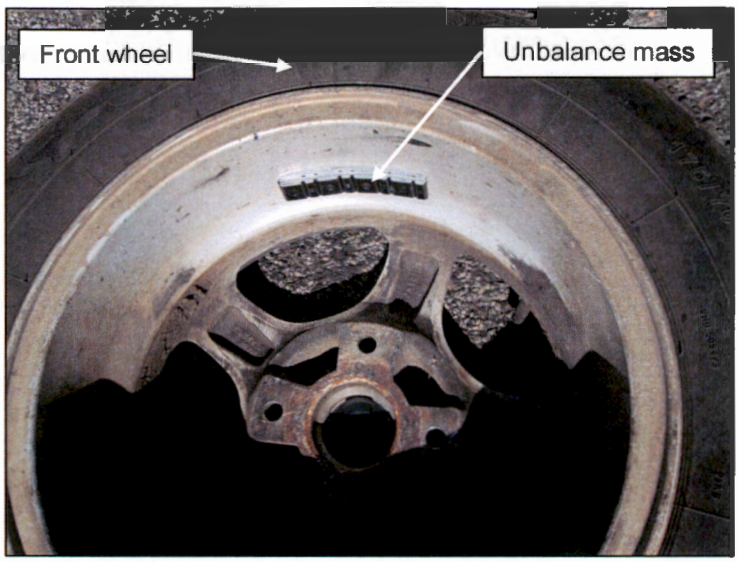

Figure 5.5: Unbalance mass of 120 g attached to front wheel.

A realistic assumption was made with respect to the effective outside diameter of the wheel. From simple calculations, the vehicle's speed was computed in order to match the rotational speed of the wheel (frequency) with the vertical bounce mode frequency of the Engine with no Absorber attached. If the diameter of the wheel is 0.56 m, and the speed

of the vehicle is 82 km/h, the rotational speed of the wheels will be at 13 Hz. The forced frequency will therefore correspond with the bounce mode frequency of the Engine if the vehicle moves at around 82 km/h, which will cause resonance at the Engine mounts for the Original system (see Section 4.5.1). Another resonance condition for the Original system is present when the vertical bounce mode frequency of the Engine mount system is excited by the dynamic forces from the uneven road surface through the wheel suspension. Resonance also occurs when the vertical bounce mode frequency of the Engine mount system coincides with the natural frequency of the wheel suspension (wheel hop natural frequency).

For the Original system, an acceleration meter was attached near the centre of gravity of the Engine and another one at the vehicle's support structure near one of the shock absorbers, as shown in Figure 5.6.

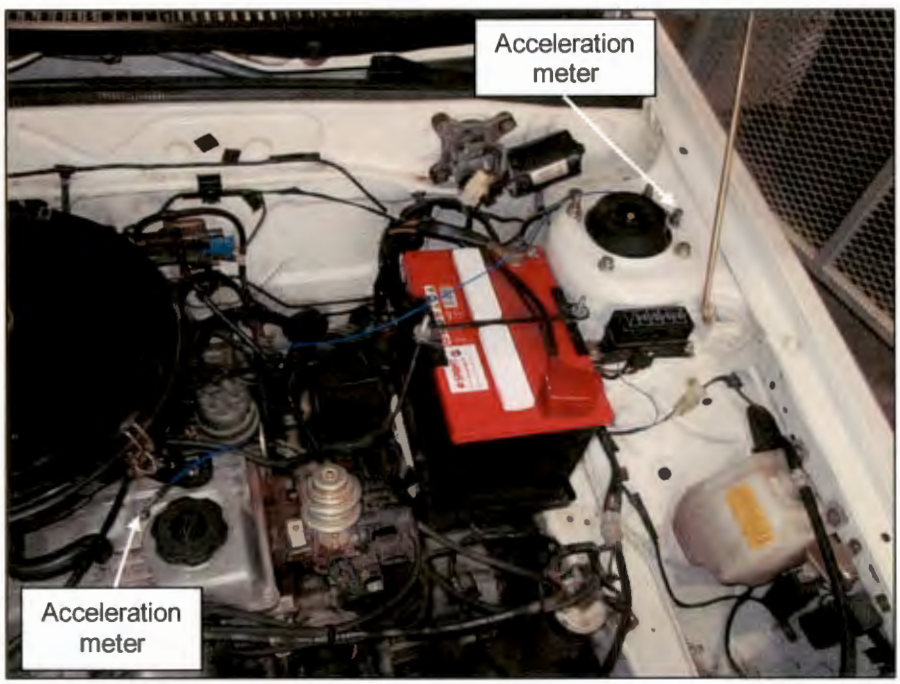

Figure 5.6: Acceleration meter attached to Engine and vehicle's support structure.

Figure 5.7 to Figure 5.9 show as examples the peak frequency domain signals measured at the Engine and the vehicle's support structure for 80, 100 and 120 km/h respectively, with an unbalance mass of 120 g attached to each front wheel for the Original system.

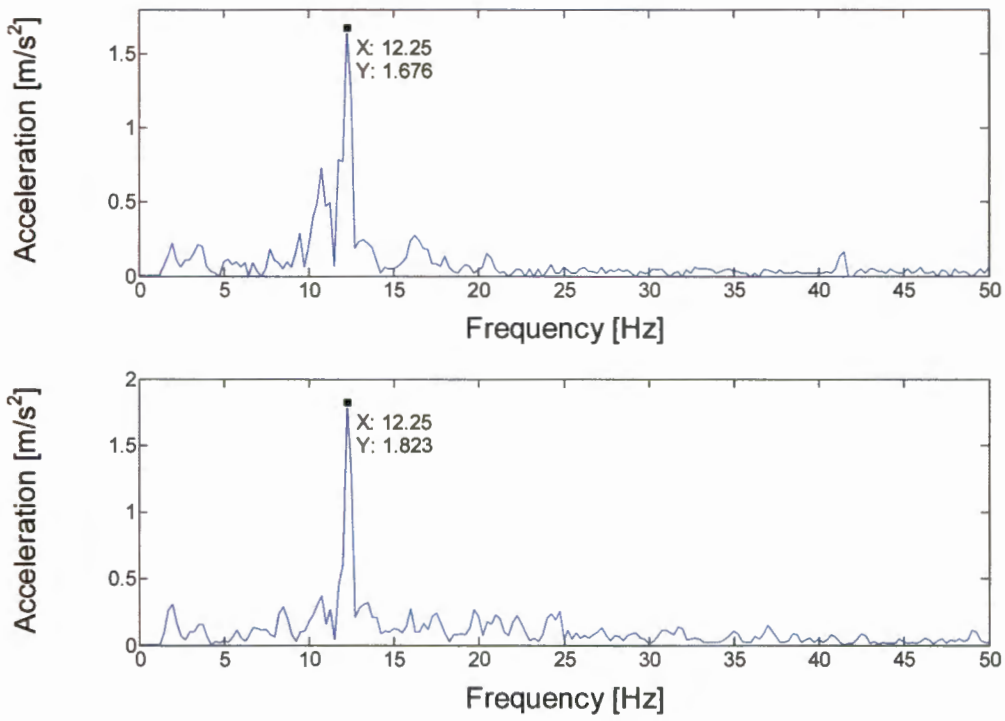

Figure 5.7: Engine (top) and structure (bottom) response at 80 km/h with 120 g unbalance for Original system.

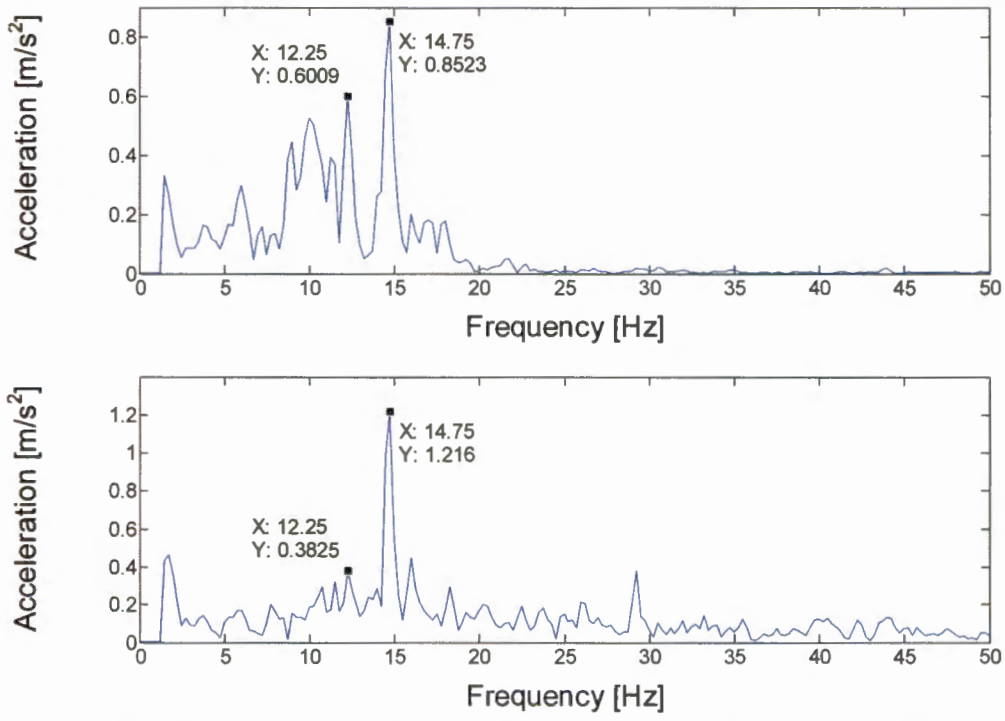

Figure 5.8: Engine (top) and structure (bottom) response at 100 km/h with 120 g unbalance for Original system.

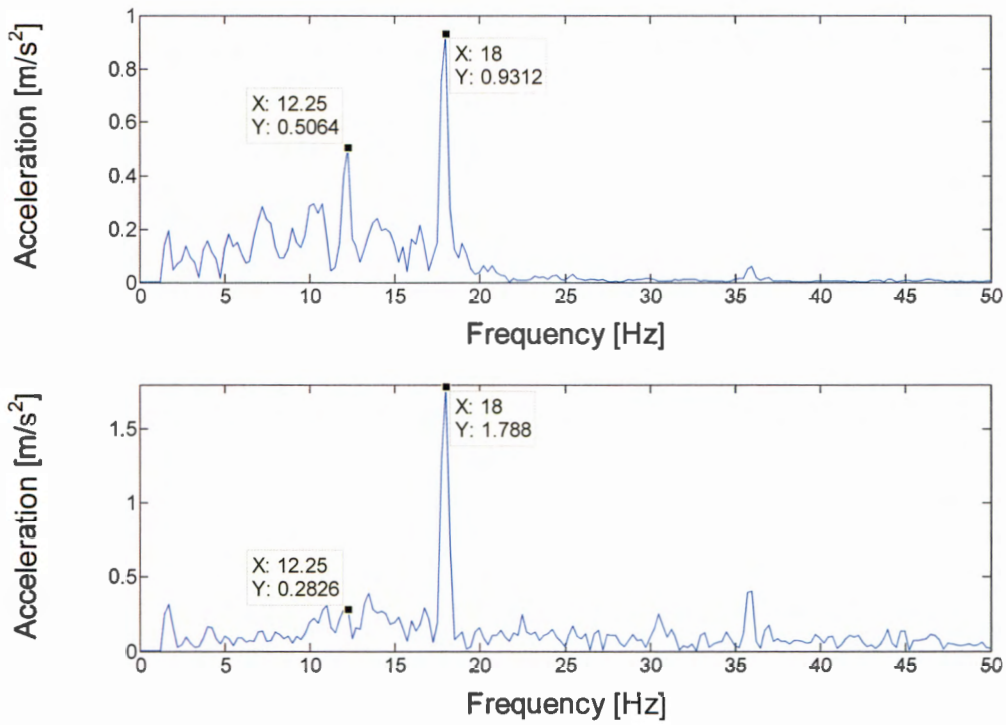

Figure 5.9: Engine (top) and structure (bottom) response at 120 km/h with 120 g unbalance for Original system.

The acceleration amplitudes obtained from the measured frequency domain signals were used to compute the displacement amplitudes with the use of equations (2.16) and (2.17). The displacement amplitudes for the different unbalance mass magnitudes at the front wheels for all the road tests performed for the Original system is shown in Table 5.2 to Table 5.4 when the vehicle was pulled at 80, 100 and 120 km/h respectively. The measured frequency domain signals when the wheels were well-balanced, as well as when a 240 g unbalance mass was attached to each front wheel, and the vehicle pulled at the same constant speeds (80, 100 and 120 km/h respectively) for the Original system are included in Appendix D.

Table 5.2: Road test results for Original system at 80 km/h.

	Wheel suspension frequency = Wheel rotation frequency (12.25 Hz)	
Unbalance mass on each front wheel [g]	Engine displacement amplitude [mm]	Structure displacement amplitude [mm]
Well-balanced wheels	0.151	0.133
120	0.283	0.308
240	0.439	0.436

Table 5.3: Road test results for Original system at 100 km/h.

	Wheel suspension frequency (12.25 Hz)		Wheel rotation frequency (14.75 Hz)	
Unbalance mass on each front wheel [g]	Engine displacement amplitude [mm]	Structure displacement amplitude [mm]	Engine displacement amplitude [mm]	Structure displacement amplitude [mm]
Well-balanced wheels	0.081	0.061	0.068	0.049
120	0.101	0.065	0.100	0.142
240	0.179	0.155	0.171	0.277

Table 5.4: Road test results for Original system at 120 km/h.

	Wheel suspension frequency (12.25 Hz)		Wheel rotation frequency (18 Hz)	
Unbalance mass on each front wheel [g]	Engine displacement amplitude [mm]	Structure displacement amplitude [mm]	Engine displacement amplitude [mm]	Structure displacement amplitude [mm]
Well-balanced wheels	0.071	0.068	0.026	0.036
120	0.085	0.048	0.073	0.140
240	0.116	0.077	0.091	0.181

From Table 5.2 where the vehicle was pulled at 80 km/h, the displacement amplitude at the Engine as well as the structure significantly increased at 12.25 Hz as the unbalance mass on each front wheel increased. From Table 5.3 and Table 5.4 where the vehicle was pulled at 100 and 120 km/h respectively, the displacement amplitude at the Engine and the structure remained relatively the same at 12.25 Hz as the unbalance mass on each front wheel increased, but the response of the structure at 14.75 and 18 Hz increased slightly. The wheel suspension natural frequency is thus excited by the uneven road surface as well as the centrifugal forces from the rotation of the wheels at 12.25 Hz. See Section 5.5.2.2 where the wheel suspension natural frequency were also characterised with the use of an electrical shaker motor.

Figure 5.10 to Figure 5.12 shows as an example the peak frequency domain signals measured at the Engine and the Absorber at 80, 100 and 120 km/h with an unbalance mass of 120 g attached to each front wheel for the Modified system. In this case one acceleration meter was attached near the centre of gravity of the Engine in vertical direction as well as on the Absorber.

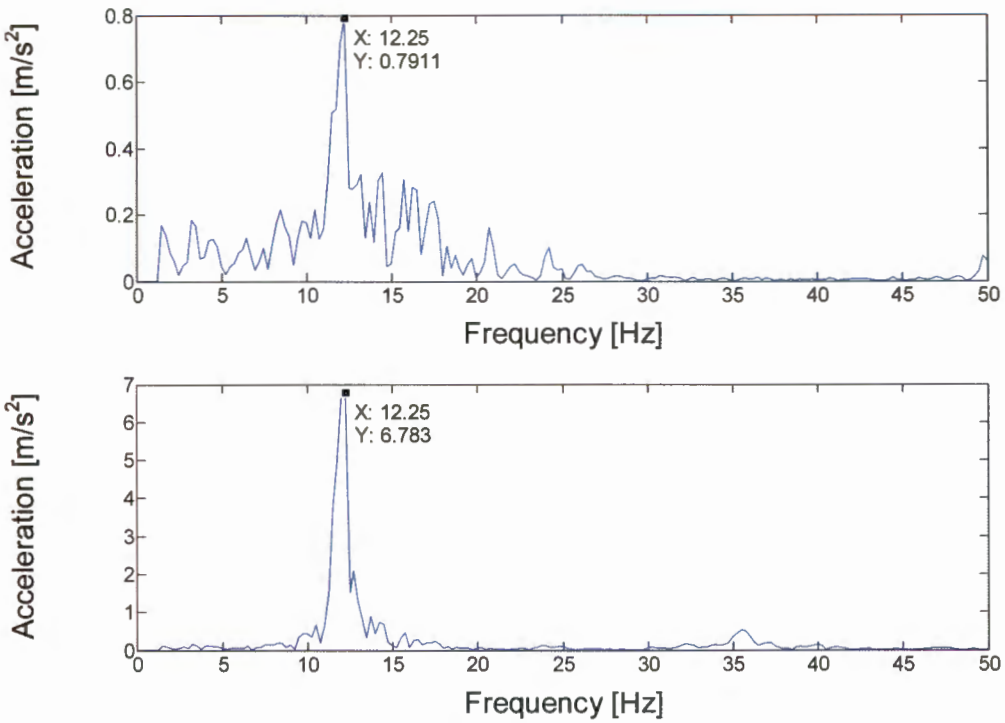

Figure 5.10: Engine (top) and Absorber (bottom) response at 80 km/h with 120 g unbalance for Modified system.

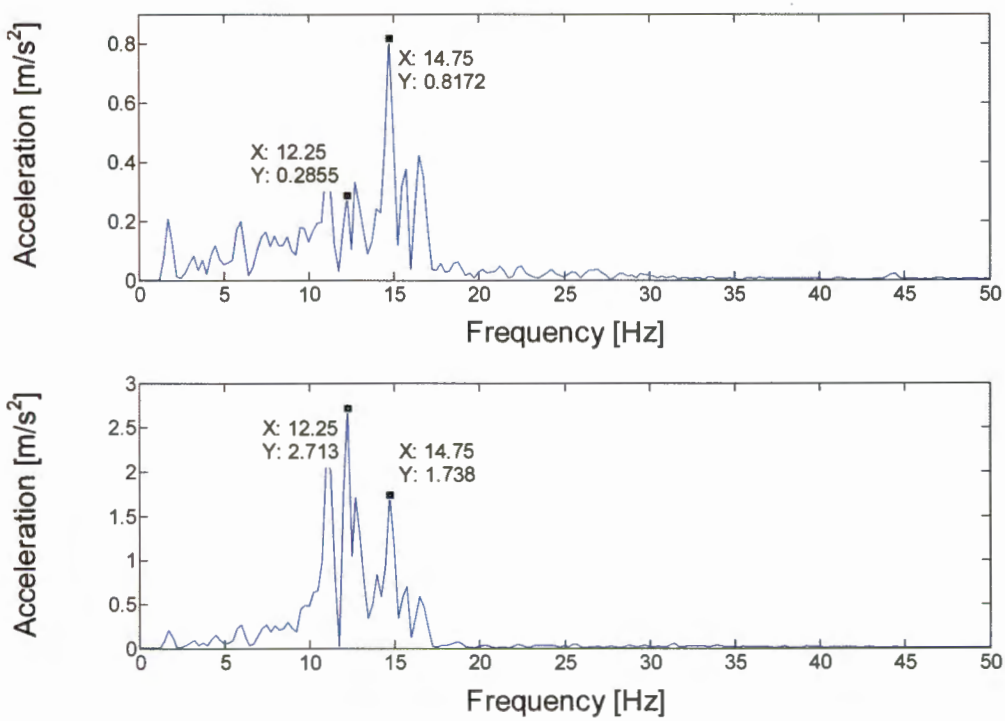

Figure 5.11: Engine (top) and Absorber (bottom) response at 100 km/h with 120 g unbalance for Modified system.

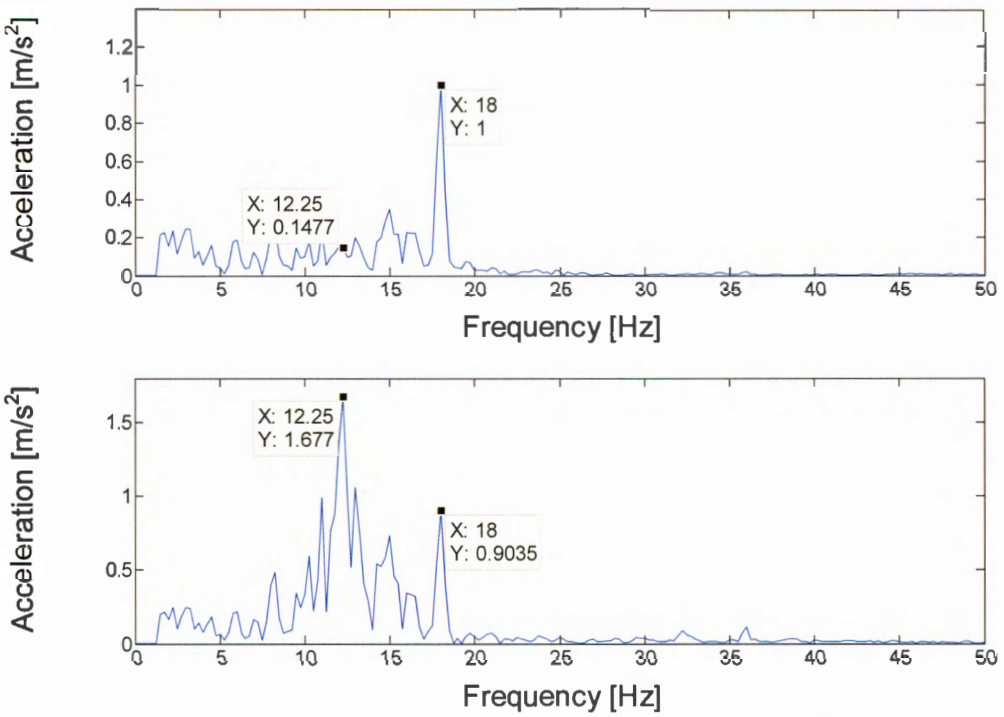

Figure 5.12: Engine (top) and Absorber (bottom) response at 120 km/h with 120 g unbalance for Modified system.

The acceleration amplitudes obtained from the measured frequency domain signals were used to compute the displacement amplitudes with the use of equations (2.16) and (2.20). Table 5.5 to Table 5.7 indicate the displacement amplitudes obtained for the different unbalance mass magnitudes at the front wheels from the road tests for the Modified system when the vehicle was pulled at 80, 100 and 120 km/h respectively. The measured frequency domain signals when the wheels were well-balanced, as well as when a 240 g unbalance mass was attached to each front wheel, and the vehicle pulled at the same constant speeds (80, 100 and 120 km/h respectively) for the Modified system are included in Appendix D.

Table 5.5: Road test results for Modified system at 80 km/h.

	Wheel suspension frequency = Wheel rotation frequency (12.25 Hz)	
Unbalance mass on each front wheel [g]	Engine displacement amplitude [mm]	Absorber displacement amplitude [mm]
Well-balanced wheels	0.066	0.504
120	0.134	1.145
240	0.139	1.560

Table 5.6: Road test results for Modified system at 100 km/h.

	Wheel suspension frequency (12.25 Hz)		Wheel rotation frequency (14.75 Hz)	
Unbalance mass on each front wheel [g]	Engine displacement amplitude [mm]	Absorber displacement amplitude [mm]	Engine displacement amplitude [mm]	Absorber displacement amplitude [mm]
Well-balanced wheels	0.034	0.121	0.066	0.041
120	0.048	0.458	0.095	0.202
240	0.063	0.636	0.152	0.301

Table 5.7: Road test results for Modified system at 120 km/h.

	Wheel suspension frequency (12.25 Hz)		Wheel rotation frequency (18 Hz)	
Unbalance mass on each front wheel [g]	Engine displacement amplitude [mm]	Absorber displacement amplitude [mm]	Engine displacement amplitude [mm]	Absorber displacement amplitude [mm]
Well-balanced wheels	0.029	0.272	0.024	0.023
120	0.024	0.283	0.078	0.071
240	0.044	0.371	0.103	0.082

The Absorber effectively reduced the displacement amplitudes experienced by the Engine when the forces were excited by the wheel suspension natural frequency (wheel hop) and the rotation of the wheels at 12.25 Hz (see Table 5.2 to Table 5.4 for the Original system and Table 5.5 to Table 5.7 for the Modified system). The displacement amplitudes excited by the wheel rotation frequencies at 14.75 and 18 Hz remained more or less the same for all of the conditions.

5.5.2.2 Forced shaker motor response and wheel suspension frequency

An electrical shaker motor connected to a variable speed drive (VSD) was used to represent one of the conditions conducted in the road tests. The electrical motor was attached on top of a bracket with four bolts, which was firmly bolted at the top of each side of the vehicle's front shock absorbers as displayed in Figure 5.13. The advantages of the electrical shaker motor are that it provided harmonic movement on the Engine as well as the Absorber, and the forced frequency of the electrical motor could be changed while the vehicle was stationary. This provided an indication of how the Absorber would perform if the wheel suspension's natural frequency should slightly shift due to heat transfer at the tyres and small tyre pressure changes when the vehicle moved. During all

the forced shaker motor tests the vehicle's wheels were stationary and the Engine was switched off. At all times someone was present at the stop switch of the electrical shaker motor for safety purposes.

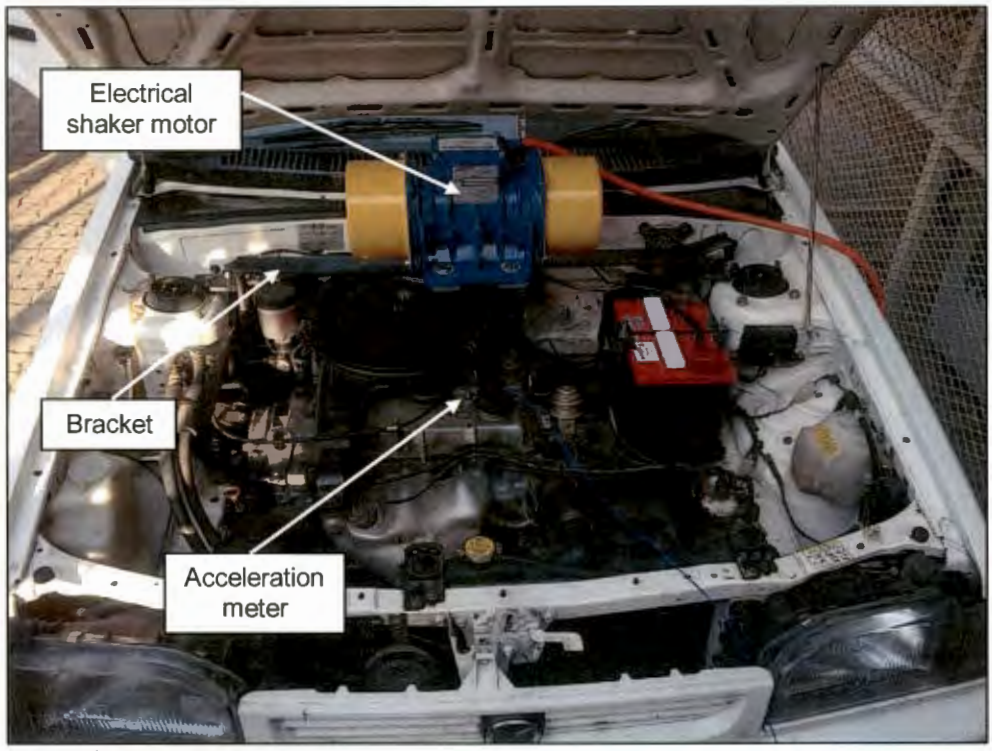

Figure 5.13: Electrical shaker motor test setup.

The condition where each front wheel of the vehicle had an unbalance mass of 120 g attached to them was replicated with the shaker motor. For this condition, the Engine experienced a peak excitation displacement amplitude of 0.28 mm at 12.25 Hz when the vehicle was pulled at a speed of 80 km/h (see Figure 5.7 and Table 5.2).

An acceleration meter was attached to the Engine near the centre of gravity, as well as the Absorber mass in the vertical direction, and coupled to an FFT Analyser in order to record the vibration measurements. The speed of the electrical motor was set by the VSD for three different forced frequencies at 11.75, 12.25 and 12.75 Hz for the Original- and Modified systems respectively. Figure 5.14 to Figure 5.16 show the peak frequency domain signals measured at the three forced frequencies for the Original system.

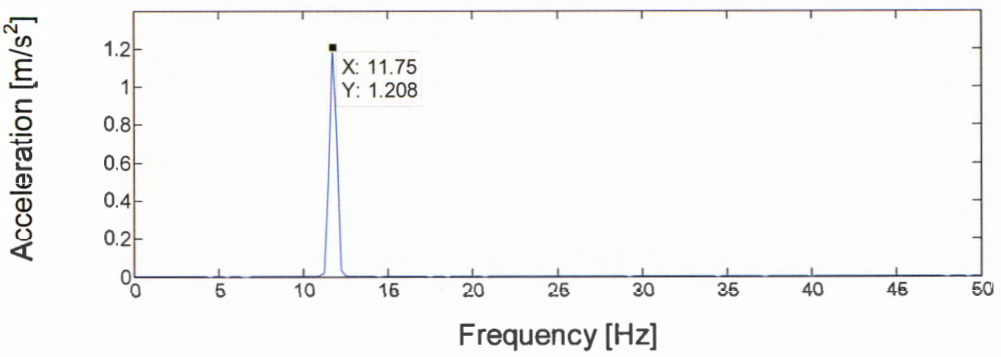

Figure 5.14: Engine response with electrical shaker motor at 11.75 Hz for Original system.

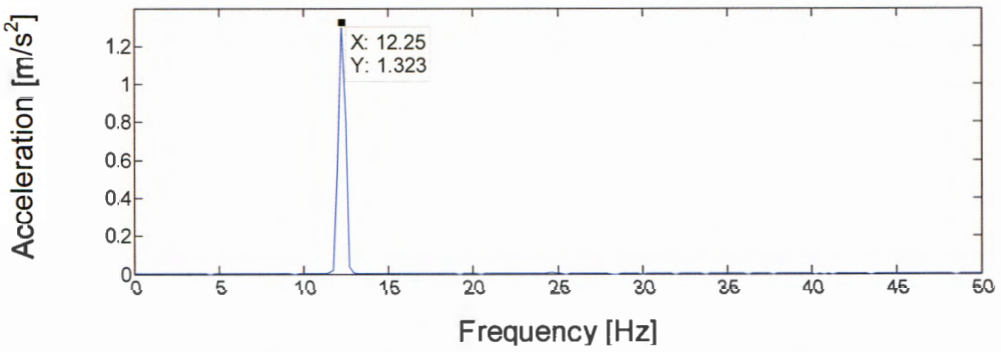

Figure 5.15: Engine response with electrical shaker motor at 12.25 Hz for Original system.

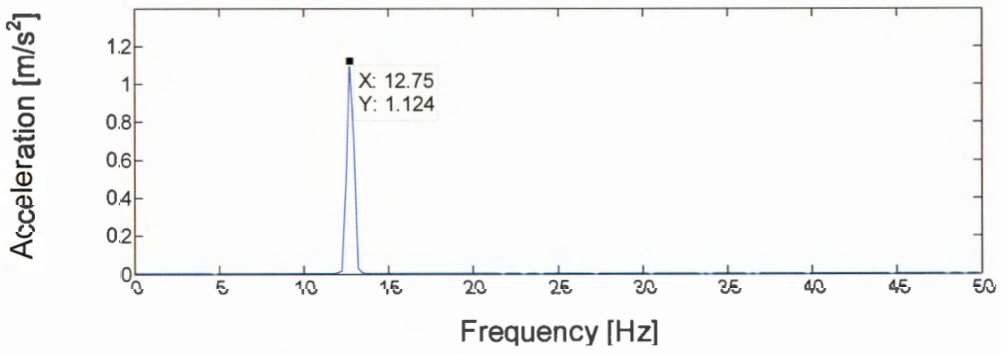

Figure 5.16: Engine response with electrical shaker motor at 12.75 Hz for Original system.

Figure 5.17 to Figure 5.19 indicate the measured peak frequency domain signals for the Modified system.

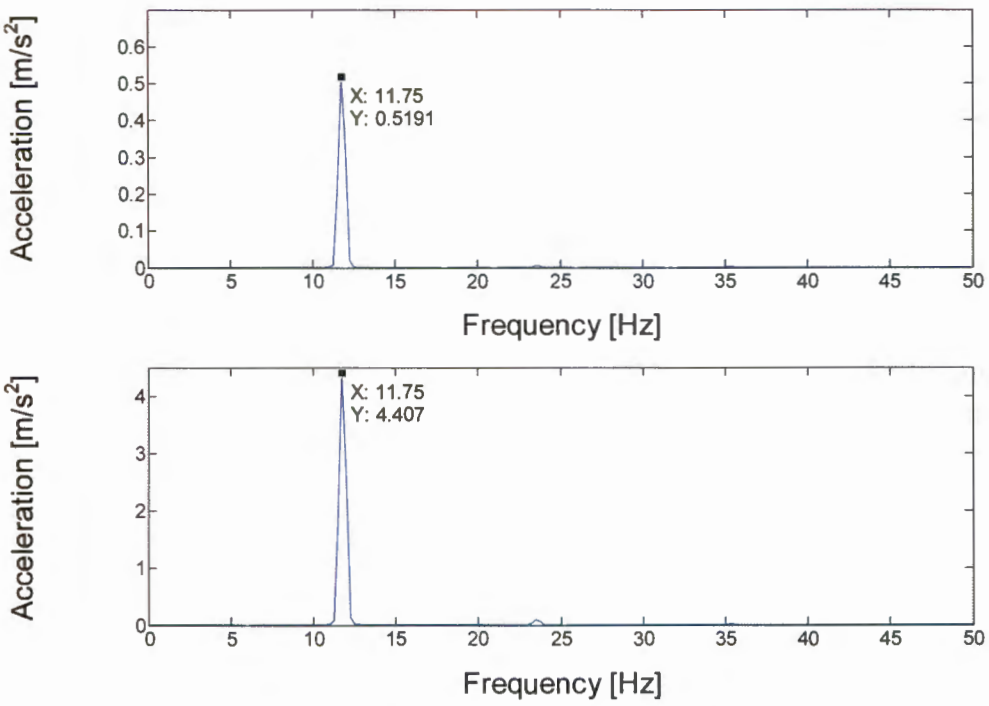

Figure 5.17: Engine (top) and Absorber (bottom) response with electrical shaker motor at 11.75 Hz for Modified system.

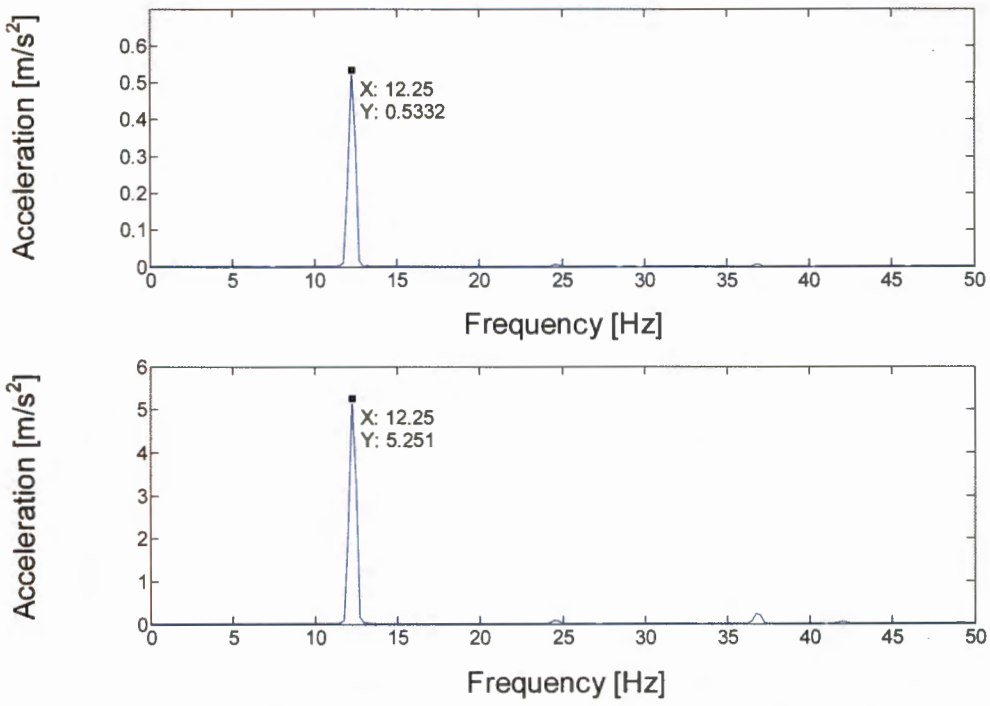

Figure 5.18: Engine (top) and Absorber (bottom) response with electrical shaker motor at 12.25 Hz for Modified system.

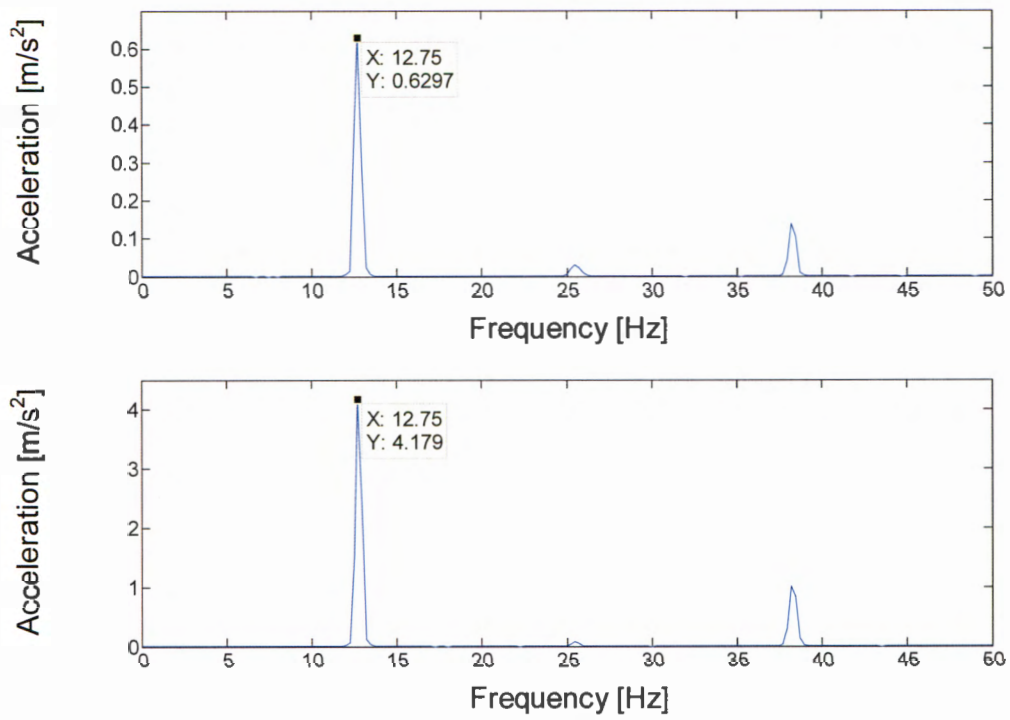

Figure 5.19: Engine (top) and Absorber (bottom) response with electrical shaker motor at 12.75 Hz for Modified system.

The acceleration amplitudes obtained from the measured frequency domain signals were used to compute the displacement amplitudes with the use of equations (2.16) and (2.20). At 12.25 Hz the largest vibration amplitude was observed for the Original system, thus resonance was caused at the Engine mount system for the given vibration displacement amplitude and Engine mount stiffness properties. Table 5.8 indicates the displacement amplitudes obtained for different electrical shaker motor forced frequencies for both the Original- and Modified systems.

Table 5.8: Shaker motor test results for Original- and Modified systems.

	Original system	Modified system	
Forced frequency [Hz]	Engine displacement amplitude [mm]	Engine displacement amplitude [mm]	Absorber displacement amplitude
11.75	0.222	0.095	0.809
12.25	0.223	0.090	0.886
12.75	0.175	0.098	0.651

The Absorber thus effectively reduced the Engine vibration excited by the wheel suspension over this range of frequencies (see Table 5.8). The wheel suspension frequency was characterised with the same electrical shaker motor test setup. The frequency was changed through the VSD at which the electrical motor was running which made it possible to determine the frequency at which the suspension of the vehicle was at resonance (wheel hop natural frequency excited). In order to measure the suspension frequency, an acceleration meter was firmly attached to the rim of one of the front wheels in the vertical direction as shown in Figure 5.20.

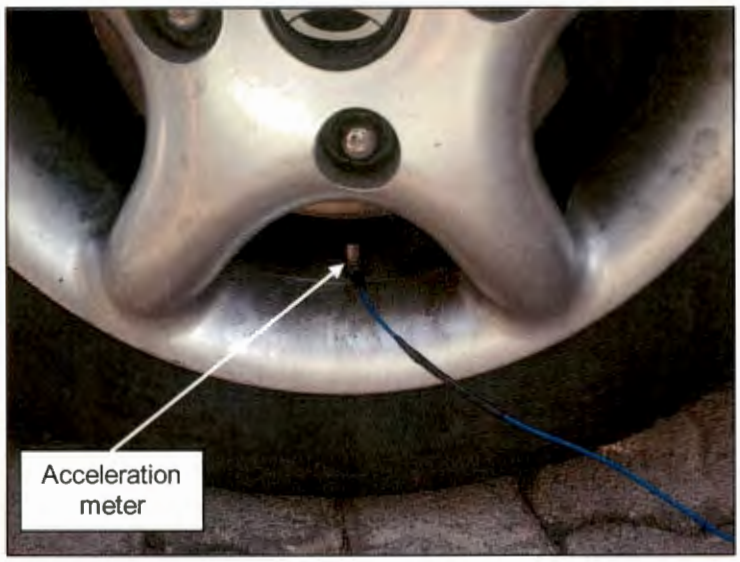

Figure 5.20: Wheel suspension frequency test setup.

Figure 5.21 indicates as example the peak frequency domain signal measured at 10.75 Hz when the suspension was at resonance (also see Table 5.9). The measured frequency domain signals where the forced frequency of the electrical shaker motor was set to 10.25, 10.50, 11.00 and 11.25 Hz respectively, are included in Appendix D.

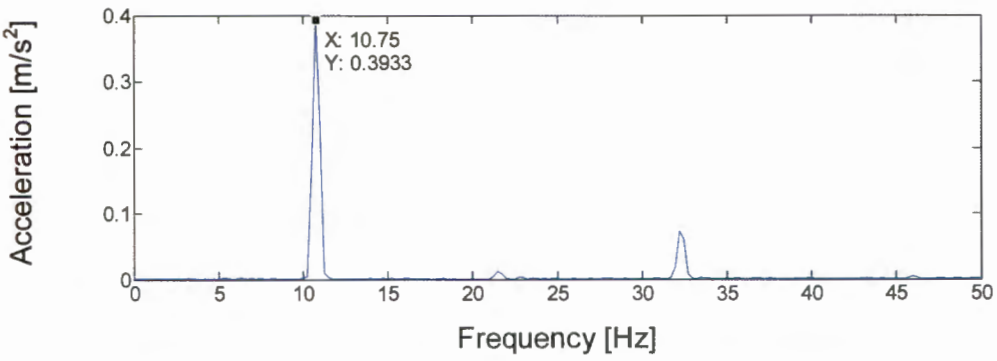

Figure 5.21: Wheel suspension at resonance (10.75 Hz).

The acceleration amplitudes obtained from the measured frequency domain signals were used to compute the displacement amplitudes with the use of equation (2.17). The displacement amplitudes obtained for different electrical shaker motor forced frequencies are shown in Table 5.9.

Table 5.9: Wheel suspension frequency test results.

Frequency [Hz]	Wheel suspension displacement amplitude [mm]
10.25	0.062
10.50	0.085
10.75	0.086
11.00	0.066
11.25	0.034

The frequency at which the wheel suspension is at resonance will differ when the tyres are hot and when it is cold, due to the change in stiffness of the tyres. In this case the tyres were cold, but when the road tests were conducted, the tyres were hot due to the friction between the tar road and the tyres. As a result, different tyre pressures will also slightly change the frequency at which the wheel suspension is at resonance, but for these tests conducted the vehicle's wheels were stationary and the tyre pressures were maintained the same. From the road tests, a wheel suspension natural frequency of 12.25 Hz was obtained when the tyres were hot (see Section 5.5.2.1). From the forced electrical shaker motor tests, a wheel suspension natural frequency of 10.75 Hz was obtained when the tyres were cold and the vehicle was stationary, which indicate a difference of 12.2% compared to the wheel suspension natural frequency obtained from the road tests.

5.5.3 Internal engine shaking forces

The effect of the presence of the Absorber was also evaluated when only internal engine shaking forces were present, which include the internal shaking forces caused by engine mass imbalances and gas pressure differences as transmitted to the Engine mount system. The vehicle was stationary with the gearbox in a neutral position while the Engine was running at an idling speed of 716 rpm and 2000 rpm respectively. This was done for the Original as well as the Modified system sequentially. Vibration measurements were taken only in the vertical direction with an acceleration meter firmly attached near the centre of gravity of the Engine as well as the mass of the Absorber.

Figure 5.22 and Figure 5.23 indicate the measured time- and frequency domain signals for the Original system at 716 rpm and 2000 rpm respectively.

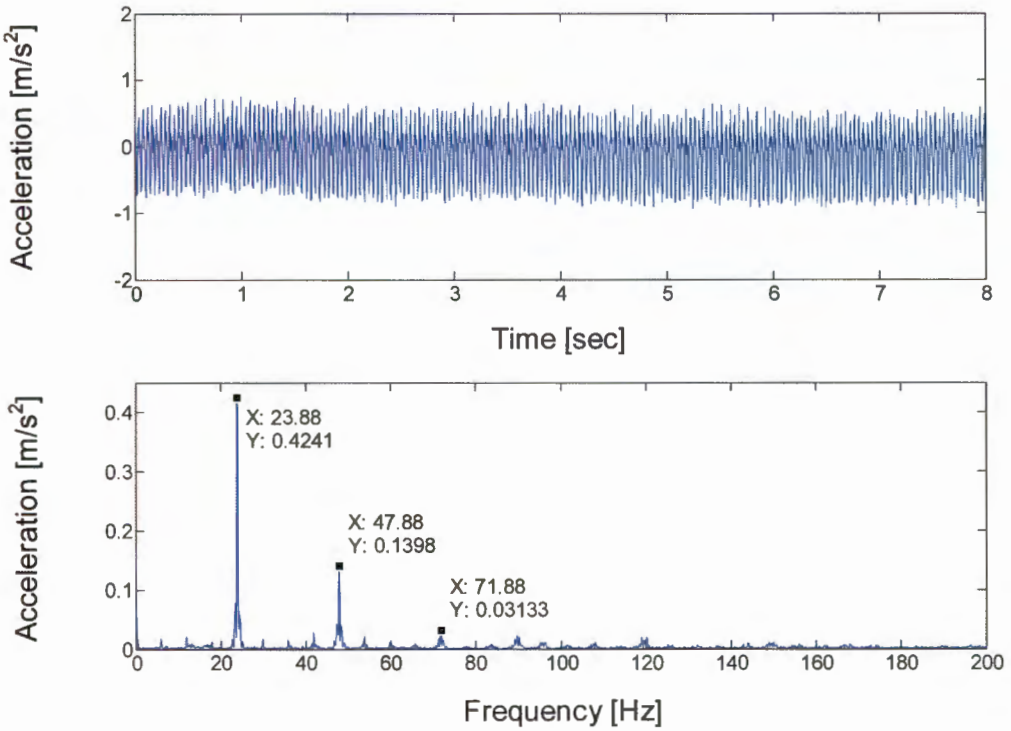

Figure 5.22: Engine response at 716 rpm for Original system.

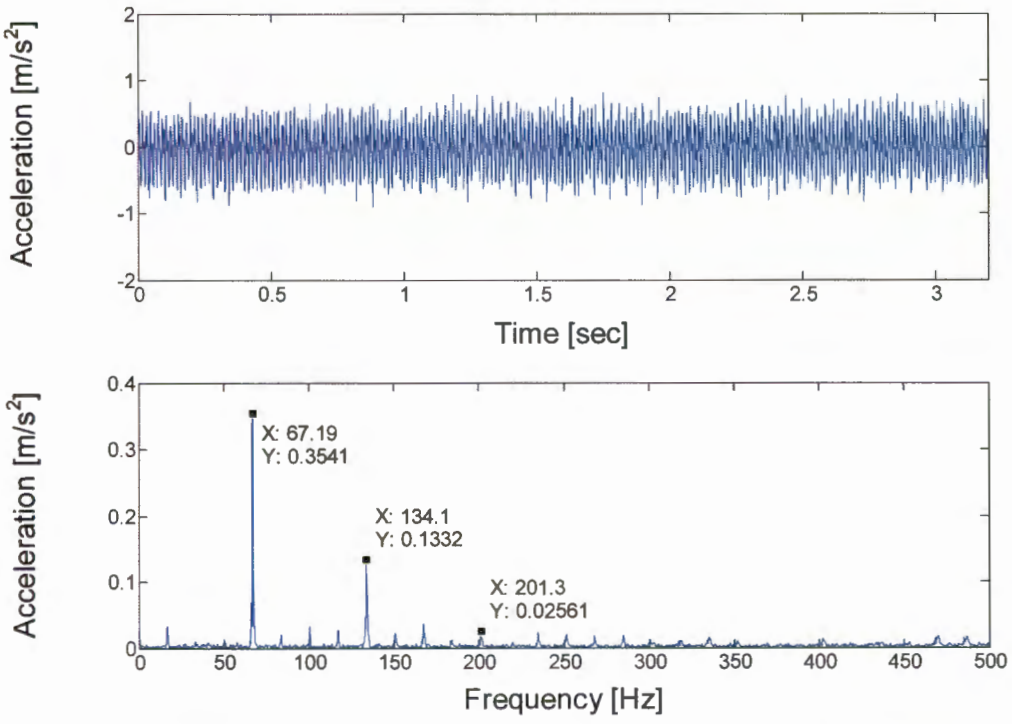

Figure 5.23: Engine response at 2000 rpm for Original system.

Figure 5.24 and Figure 5.25 show the measured frequency domain signals for the Modified system at 716 rpm and 2000 rpm respectively.

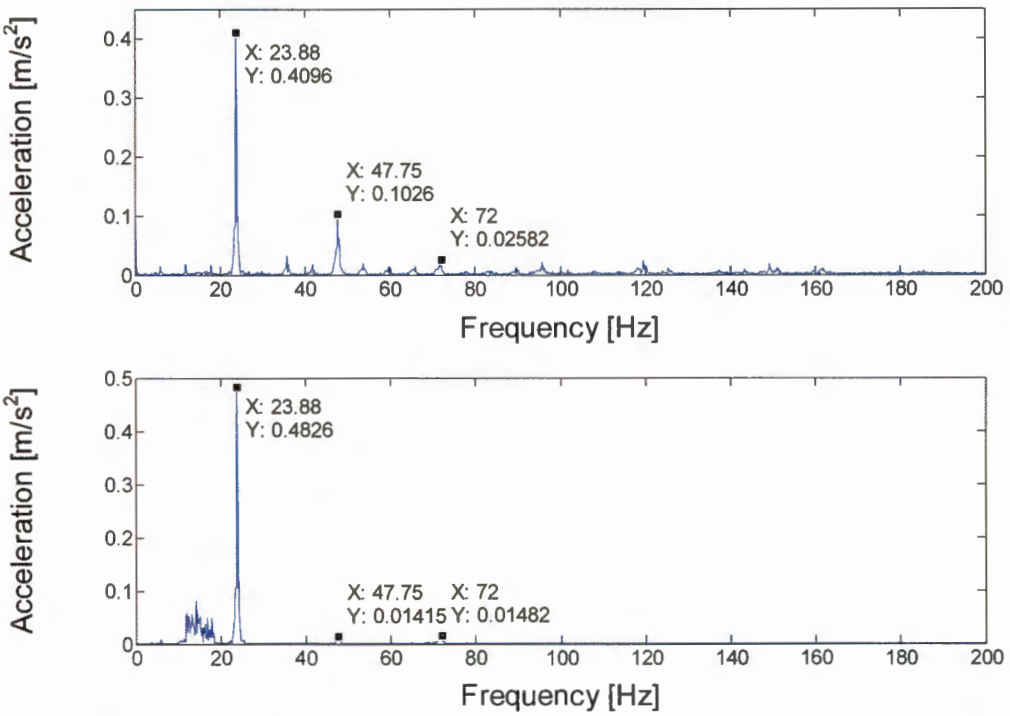

Figure 5.24: Engine (top) and Absorber (bottom) response at 716 rpm for Modified system.

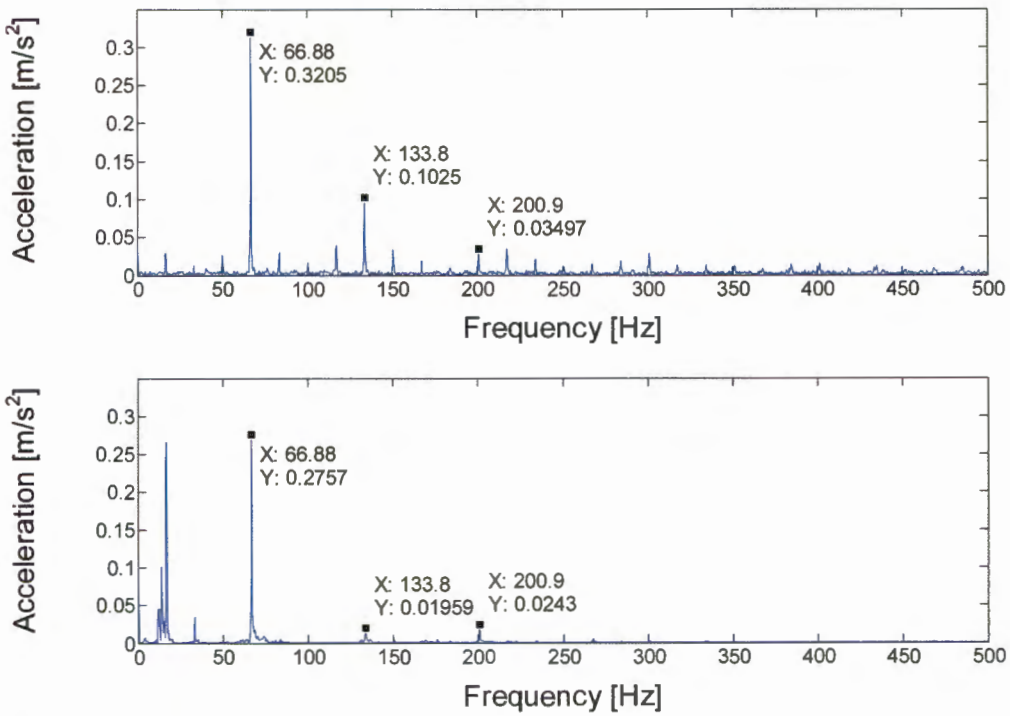

Figure 5.25: Engine (top) and Absorber (bottom) response at 2000 rpm for Modified system.

From Figure 5.22 to Figure 5.25 it is clear that the dominant amplitudes in the frequency domain signals occur at the second, fourth and sixth order running speed of the Engine due to the mass imbalances and gas pressure differences, with the amplitude at second order the largest in relation. The acceleration amplitudes obtained from the measured frequency domain signals were used to compute the displacement amplitudes with the use of equations (2.23) and (2.27). Table 5.10 indicates the displacement amplitudes obtained at different Engine running speeds from these tests for the Original- and Modified systems.

Table 5.10: Internal engine shaking forces test results for Original- and Modified systems.

Operational condition	Original system	Modified system	
Idling speed (716 rpm)	Engine displacement amplitude [mm] x 10^{-3}	Engine displacement amplitude [mm] x 10^{-3}	Absorber displacement amplitude [mm] x 10^{-3}
Second order	18.84	18.19	21.44
Fourth order	1.545	1.140	0.157
Sixth order	0.154	0.126	0.072
2000 rpm	Engine displacement amplitude [mm] x 10^{-3}	Engine displacement amplitude [mm] x 10^{-3}	Absorber displacement amplitude [mm] x 10^{-3}
Second order	1.987	1.815	1.561
Fourth order	0.188	0.145	0.028
Sixth order	0.016	0.022	0.015

Table 5.10 indicates that the presence of the Absorber during idling speed and also at 2000 rpm does not have any significant effect on the Engine's displacement amplitude, because these internal engine shaking forces occur at entirely different frequencies compared to the frequencies for road input forces. The displacement amplitude of the Engine remained relatively the same for the Original- and Modified systems at these operational Engine running speed conditions (see Table 5.10).

From the road tests (Section 5.5.2.1) and internal engine shaking forces tests performed, it is clear that the forces excited through the wheel suspension has a much greater effect on the response of the Engine than for internal engine shaking forces. The average displacement of the Engine due to the forces excited through the wheel suspension at 12.25 Hz is 0.10 mm for the Original system at the Engine's centre of gravity with well-balanced wheels, and 0.25 mm when an unbalance mass of 240 g was attached to each front wheel.

The displacement of the Engine during idling at second order running speed was only 18.84 x 10^{-3} mm for the Original system, which is approximately 5.3 times smaller for the condition where the forces were excited by the well-balanced wheels, and approximately 13.3 times smaller when an unbalance mass of 240 g was attached to each front wheel.

When the Engine was running at 2000 rpm, the displacement of the Engine was only 1.987 x 10^{-3} mm at second order running speed, which is approximately 50.3 times smaller for the condition where the forces were excited by the well-balanced wheels, and approximately 125.8 times smaller when an unbalance mass of 240 g was attached to each front wheel. Thus the Absorber very effectively reduces the large displacement amplitudes experienced by the Engine when the forces are excited by the wheels at 12.25 Hz, but does not greatly affect the system when the small internal engine shaking forces are present.

5.5.4 Transient response

The Absorber's performance was also evaluated for the case of transient response experienced by the Engine. The Engine typically experiences transient response when the gears are changed, when it's switched on and off, as well as when impact forces are excited from an uneven road surface through the suspension to the Engine mount system. The bounce mode frequency of the Engine mount system is thus excited for a short period of time and as a result large transient response is experienced.

Eddy current probes were used to measure the relative displacement of the Engine and the Absorber when they experienced transient response for several transient behaviour conditions. These probes are non-contact type differential expansion transducers that apply eddy currents, and a high frequency power of approximately 1 MHz is provided to the sensors from an oscillator in the drivers, which are powered by 24 VDC output power supplies. Therefore, the sensors produce a high frequency magnetic field so that eddy current flows in the metallic target. The eddy current flow in the target causes a magnetic field generation on the target side, which results in a sensor impedance change. Hence, if the relationship of the gap between the sensor and target vs. sensor impedance is known, the gap between the sensor and target can be attained through sensor impedance measurement. The oscillator output is identified and voltage output linearized with respect to the gap. The output of the drivers is connected to an FFT Analyser with BNC connectors. Figure 5.26 displays the non-contact eddy current probes that were used to evaluate the Absorber's performance for several transient conditions.

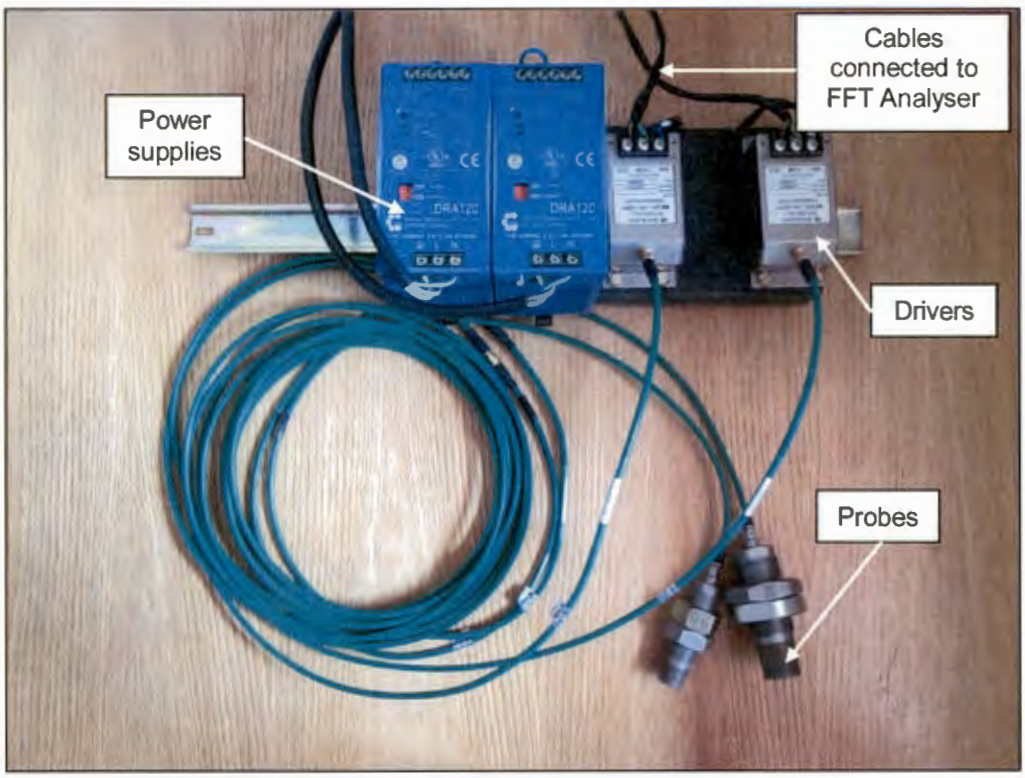

Figure 5.26: Eddy current probes.

The main advantage of eddy current probes is that they can measure the non-periodic excitation response through transient behaviour, while acceleration meters are only good for steady state response measurements.

As an example, Figure 5.27 shows two signals where an acceleration meter and eddy current probe simultaneously measured the transient response of the Engine when it was switched off from idling speed. The eddy current probe measured displacement over time while the acceleration meter measured acceleration over time.

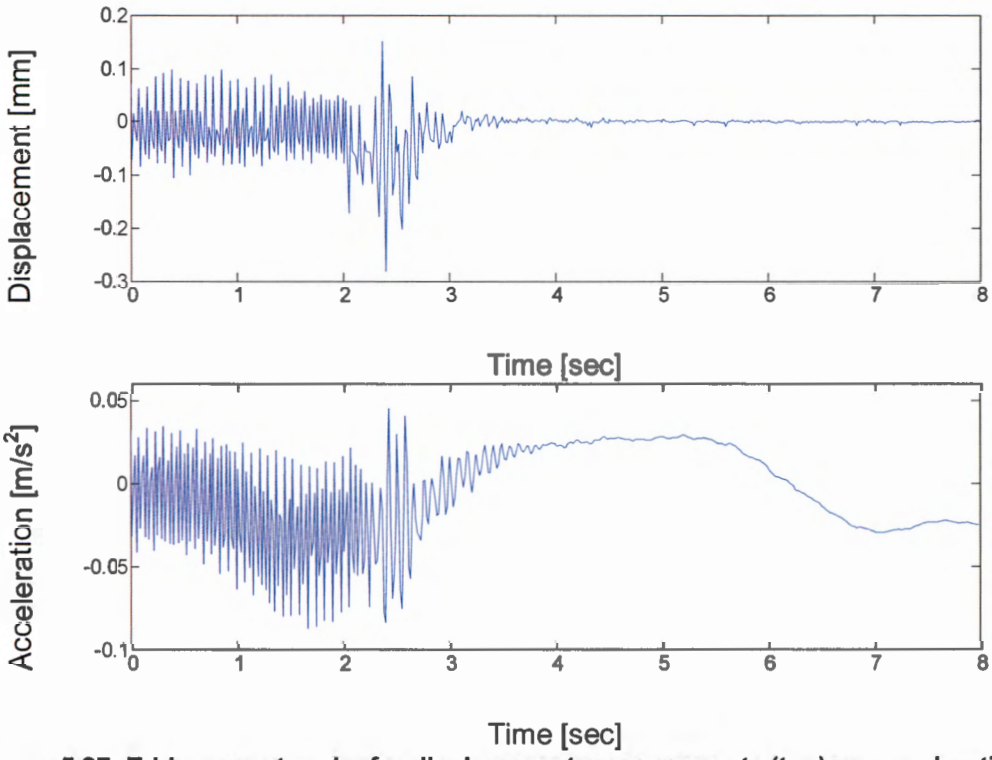

Figure 5.27: Eddy current probe for displacement measurements (top) vs. acceleration meter for acceleration measurements (bottom).

Before the eddy current probes were attached to the Engine and the Absorber, they were calibrated with a lathe consisting a digital output display. An eddy current probe with a tip diameter of ∅ = 18 mm was used to measure the transient behaviour of the Engine relative to the vehicle's support structure, while an eddy current probe with a tip diameter of ∅ = 25 mm was used to measure the transient behaviour of the Absorber mass relative to the Engine.

As an example, the ∅ 25 probe was firmly placed on top of the apron of the lathe, while the Absorber mass was firmly placed on top of the bed. The carriage handwheel of the lathe was then used to move the apron with the ∅ 25 probe on top further away from the Absorber mass (target) while the Absorber mass remained stationary on top of the bed. This probe was connected to an FFT Analyser, and as the probe moved further away from the target, a volt reading was recorded on the FFT Analyser for every 0.1 mm increment. This was done for a relative amplitude range of approximately 0 to 14.9 mm for the ∅ 25 eddy current probe. Figure 5.28 shows the setup used to calibrate the ∅ 25 eddy current probe.

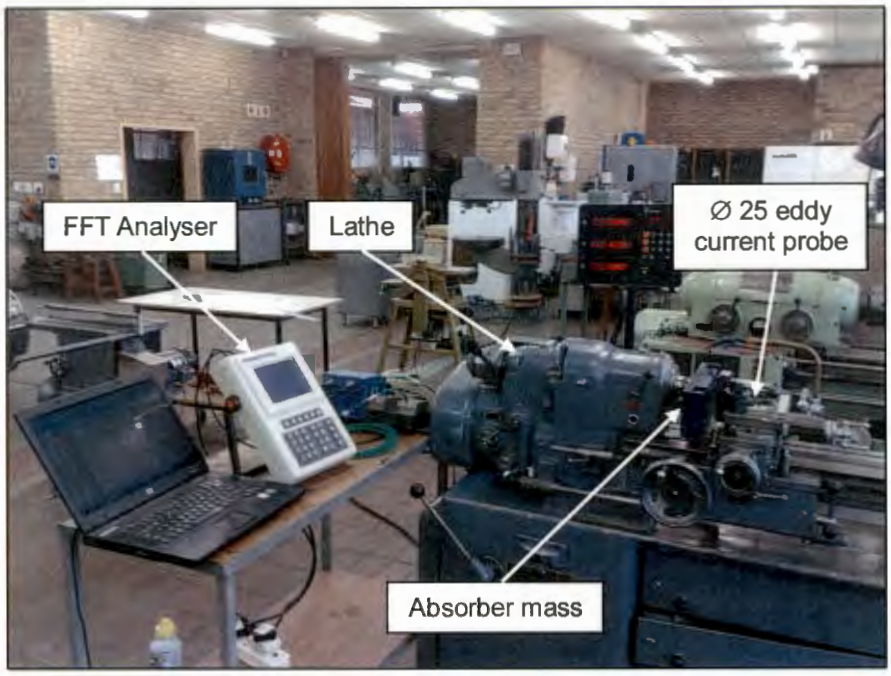

Figure 5.28: Calibration of Ø 25 eddy current probe.

This same calibration technique was used for the Ø 18 eddy current probe for a relative amplitude range of approximately 0 to 3.9 mm. More technical information regarding these eddy current probes is included in Appendix A.

After the calibration, the probes were attached to measure the displacement at the Engine and at the Absorber during transient response conditions. The Ø 18 eddy current probe that measured the Engine's response was attached to the same bracket on which the shaker motor was attached as described in Section 5.5.2.2. The displacement of the Engine was thus measured relative to the vehicle's structure. A small plate was attached to the Engine's gearbox near the Engine's centre of gravity that served as the target for the Ø 18 probe as displayed in Figure 5.29.

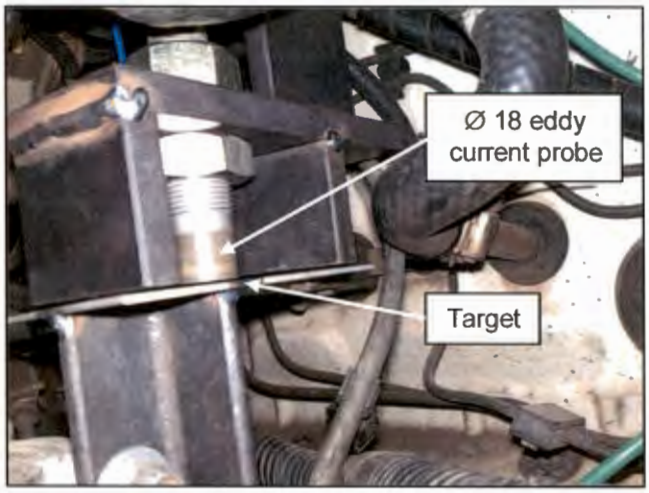

Figure 5.29: Eddy current probe (Ø 18) for Engine displacement measurements.

The Ø 25 eddy current probe that measured the response of the Absorber's mass was attached to the basis of the Absorber. A bracket manufactured from flat steel bar held the probe in place and a 1.6 mm plate protected the probe from the road surface, as displayed in Figure 5.30.

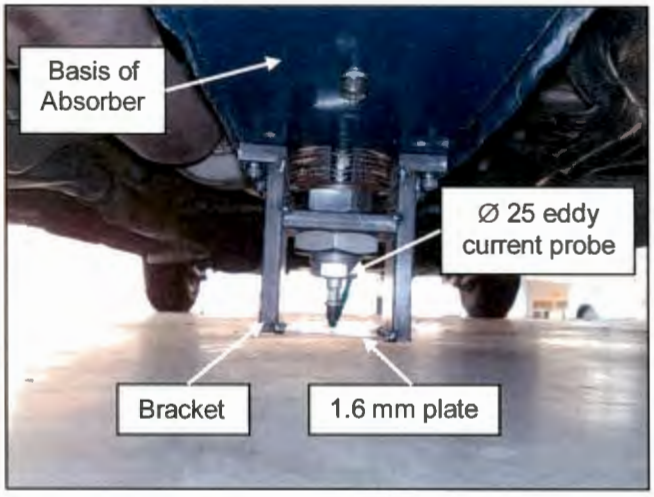

Figure 5.30: Eddy current probe (Ø 25) for Absorber displacement measurements.

The moving mass of the Absorber was the target for the Ø 25 eddy current probe, and measured displacement relative to the movement of the Engine. The vehicle was pulled over different sizes round bars with the gearbox in the neutral position and the Engine switched off, in order to evaluate the Absorber's performance during the wheel impact tests performed as shown in Figure 5.31. This was done for 6, 8 and 12 mm round bars used at the ground surface for the Original as well as for the Modified system sequentially.

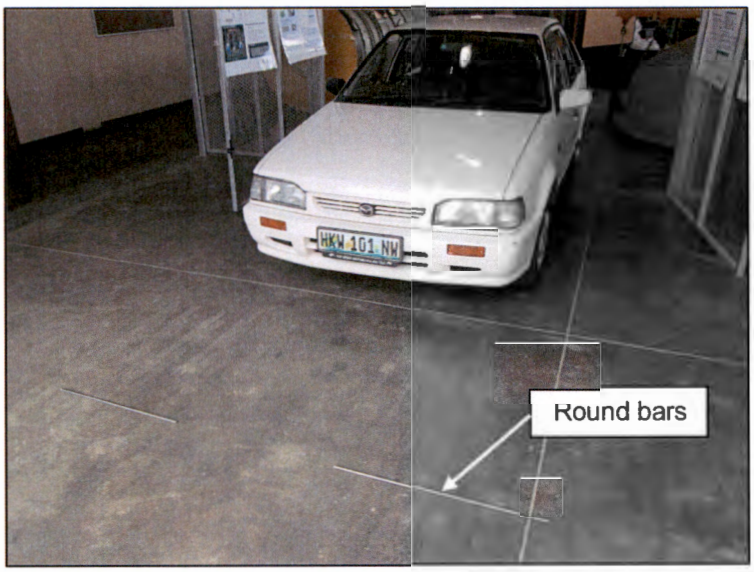

Figure 5.31: Transient response due to road inputs.

Figure 5.32 to Figure 5.34 display the displacement time domain signals obtained for the Original system when the vehicle was slowly moving over the different sizes round bars. The maximum displacement experienced by the Engine relative to the vehicle's support structure during each condition is shown in Figure 5.32 to Figure 5.34 respectively. These maximum values were used to compute the forces transmitted to the vehicle's support structure for these conditions as described in Section 5.6.

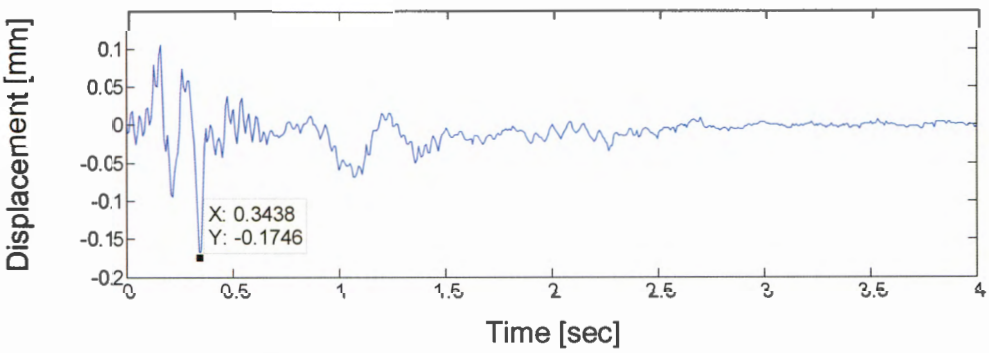

Figure 5.32: Transient response of Engine for 6 mm round bars for Original system.

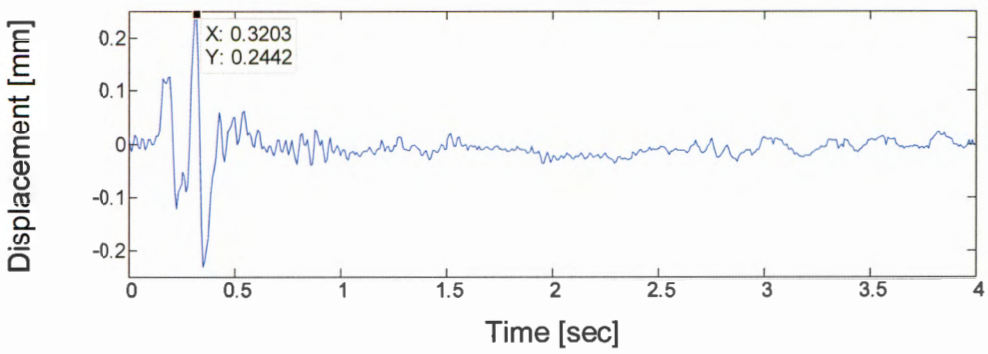

Figure 5.33: Transient response of Engine for 8 mm round bars for Original system.

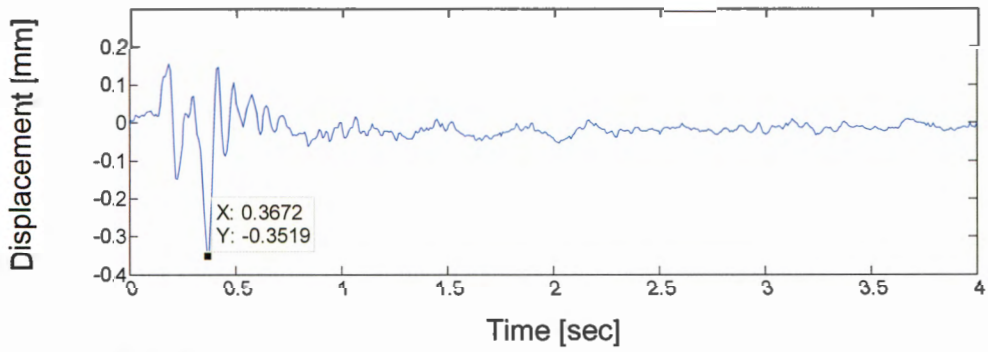

Figure 5.34: Transient response of Engine for 12 mm round bars for Original system.

The displacement time domain signals obtained from the Modified system is shown in Figure 5.35 to Figure 5.37. The top graphs indicate the Engine's displacement time domain response relative to the vehicle's support structure, while the bottom graphs indicate the Absorber mass displacement time domain response relative to the Engine when the vehicle was slowly moving over the different sizes round bars. The maximum displacement experienced by the Engine as well as the Absorber mass during each condition is shown in Figure 5.35 to Figure 5.37 respectively. These maximum values were used to compute the forces transmitted to the vehicle's support structure for these conditions as described in Section 5.6.

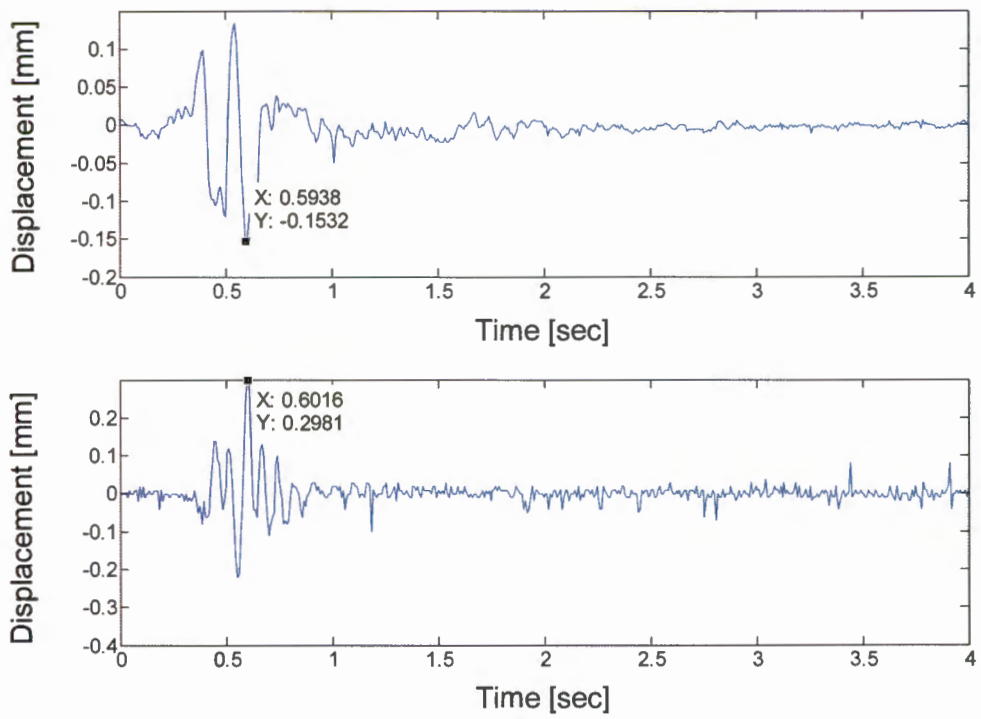

Figure 5.35: Transient response of Engine (top) and Absorber (bottom) for 6 mm round bars for Modified system.

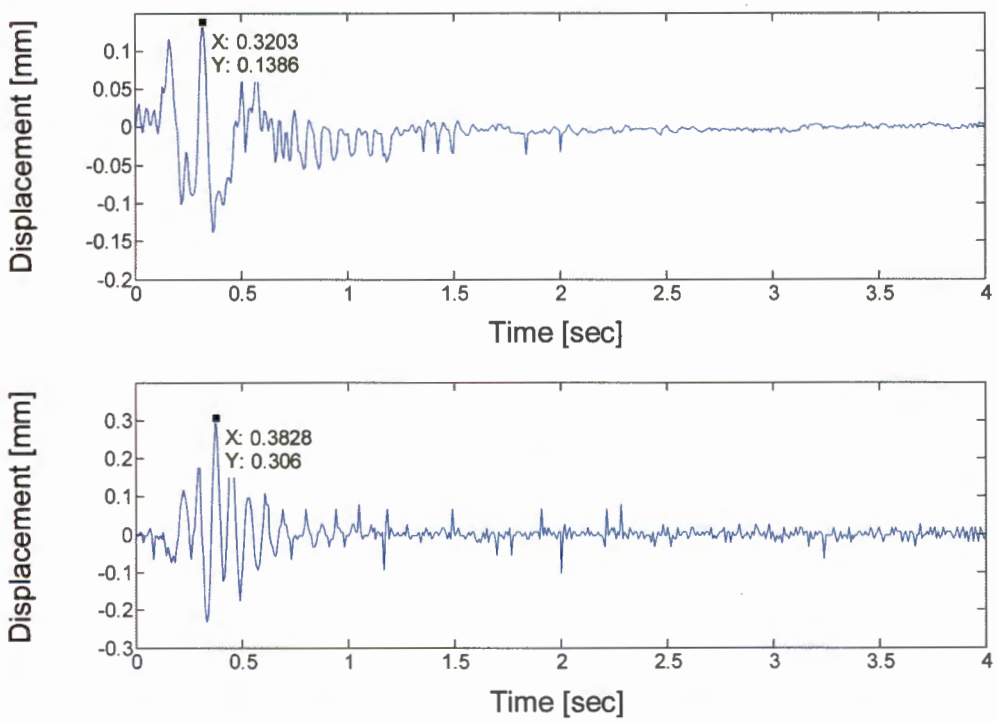

Figure 5.36: Transient response of Engine (top) and Absorber (bottom) for 8 mm round bars for Modified system.

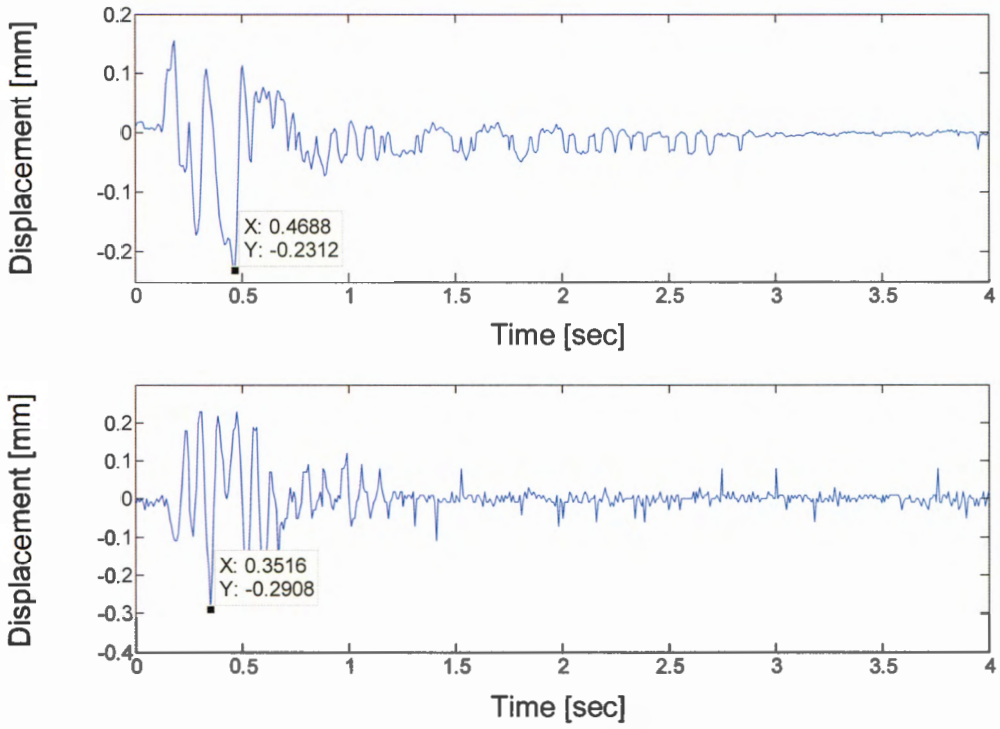

Figure 5.37: Transient response of Engine (top) and Absorber (bottom) for 12 mm round bars for Modified system.

Transient response was also measured for the Original- and Modified systems when the Engine was switched off from idling speed while the vehicle was stationary. The maximum transient displacement response for the Original system during this condition is shown in Figure 5.38.

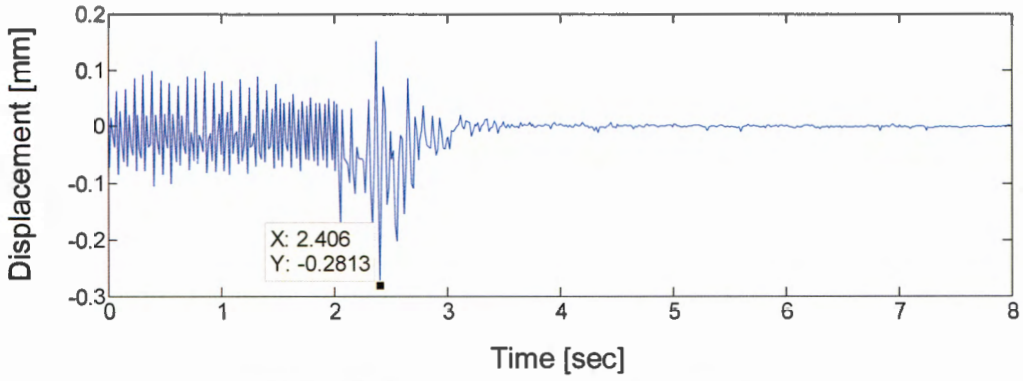

Figure 5.38: Transient response of Engine during shutdown for Original system.

Figure 5.39 indicates the transient displacement response that the Engine as well as the Absorber experienced when the Engine was switched off from idling speed for the Modified system.

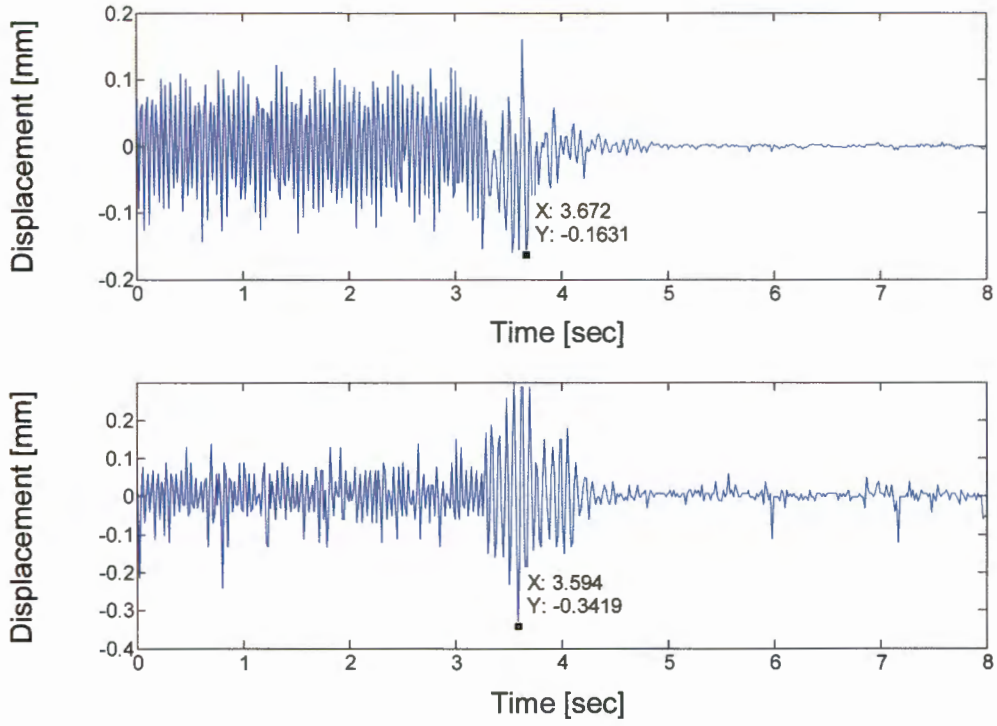

Figure 5.39: Transient response of Engine (top) and Absorber (bottom) during shutdown for Modified system.

The results regarding the maximum displacement amplitudes obtained from all these different time domain graphs (Figure 5.32 to Figure 5.39) are shown in Table 5.11

Table 5.11: Transient response test results for Original- and Modified systems.

	Original system	Modified system	
Operational condition	Engine displacement amplitude [mm]	Engine displacement amplitude [mm]	Absorber displacement amplitude [mm]
6 mm round bars	0.175	0.153	0.298
8 mm round bars	0.244	0.139	0.306
12 mm round bars	0.352	0.231	0.291
Engine switched off from idling speed	0.281	0.163	0.342

The Absorber effectively reduced the transient response that the Engine experienced for all of the above-mentioned conditions. If steady state response is considered during idling speed (see Section 5.5.3), the Engine's displacement response amplitude was 0.019 mm at second order running speed, and when the Engine was switched off the maximum transient displacement response was 0.281 mm (see Figure 5.38), thus

14.8 times larger than the steady state response. The Engine mount system is thus subject to large displacement amplitudes during transient conditions.

The Absorber will therefore contribute significantly to the reduction of the dynamic forces transmitted to the vehicle's structure during transient response conditions. Transient response during start-up of the Engine was not measured due to the presence of the starter motor which complicated modelling, however it was predicted without the starter motor and compared in a comparative context for the Original- and Modified systems (see Table 5.19). However, the advantage in reduction of transmitted forces will be similar to the condition where the Engine is switched off from idling speed.

5.5.5 Noise levels inside the vehicle's compartment

Noise levels were measured inside the vehicle's compartment during the road and Engine running speed tests (Section 5.5.2.1 and Section 5.5.3) for the Original- and Modified systems. Noise levels were also measured while the vehicle was pulled at 40 km/h on a gravel road with the Engine switched off. During the road tests when the test vehicle (Mazda) was pulled by another vehicle, the Engine was switched off and the forces were excited through the wheel suspension from the uneven road surface and the wheels. For the Engine running speed tests the vehicle was stationary and the forces were excited by the internal engine mass imbalances and gas pressure differences.

A calibrated 3M SoundPro SE/DL Series Sound Level Meter was used for all of the noise levels measurements as displayed in Figure 5.40. An average dB value was recorded over a period of 20 seconds for every measurement respectively and the measurements were fairly repeatable. A reduction of noise levels was measured for the Modified system as indicated in Table 5.12 for the mentioned conditions above. The Absorber effectively reduced the noise levels during the road tests, especially at 80 km/h when the forces were excited by the wheel suspension and the rotation of the wheels at 12.25 Hz (resonance, also see Section 5.5.2.1). The noise levels inside the vehicle's compartment were also considerably reduced on the gravel road for the Modified system when the Engine was typically subject to very large displacement amplitudes. During the Engine running speed tests the noise levels were also reduced for the Modified system (also see Section 5.5.3). A difference of 5 dB is the difference between a ringing telephone and an electric shaver. An increase of 3 dB indicates double the sound intensity, whereas an increase of 10 dB means that the human ear perceives the sound as twice as loud (Alison *et al.*, 2011).

Figure 5.40: 3M SoundPro SE/DL Series Sound Level Meter.

Table 5.12: Noise levels measurements inside vehicle compartment for Original- and Modified systems.

Original system		Modified system	
Unbalance mass on each wheel	Noise level [dB]	Unbalance mass on each wheel	Noise level [dB]
Road tests at 80 km/h			
Well-balanced wheels	70.5	Well-balanced wheels	68.5
120 g	71.2	120 g	69.5
240 g	71.7	240 g	70.1
Road tests at 100 km/h			
Well-balanced wheels	71.2	Well-balanced wheels	69.4
120 g	71.7	120 g	70
240 g	71.9	240 g	70.8
Road tests at 120 km/h			
Well-balanced wheels	72.6	Well-balanced wheels	71.6
120 g	73.2	120 g	72.2
240 g	73.5	240 g	73.3
Gravel road (40 km/h)			
Noise level [dB]		Noise level [dB]	
75.3		73.3	
Internal engine shaking forces tests – Idling speed (716 rpm)			
45.5		44.3	
Internal engine shaking forces tests – Engine running at 2000 rpm			
63.3		61.2	

5.6 DYNAMIC FORCE MAGNITUDES TRANSMITTED TO THE VEHICLE'S SUPPORT STRUCTURE

The dynamic force magnitudes transmitted to the vehicle's support structure were computed for several operational conditions evaluated in Chapter 5 (see Table 5.13 to Table 5.18). These computed dynamic force magnitudes transmitted were compared between the Original- and Modified systems, and is summarised in Table 5.19.

The measured acceleration response amplitudes of the Engine obtained from the frequency domain signals were used to compute the displacement amplitudes. The equivalent stiffness and damping coefficient of the three Engine mounts was used to compute the dynamic force magnitudes transmitted to the vehicle's support structure. The dynamic properties of these Engine mounts are shown in Chapter 4. In order to compute the dynamic force magnitudes transmitted to the vehicle's support structure, the closest stiffness coefficient k_e and damping coefficient c_e were chosen for the equivalent Engine mount that experienced similar frequency and amplitude excitations at the Engine. With the use of equation (2.30), the total dynamic force magnitude transmitted to the vehicle's support structure was computed.

5.6.1 Road forces

5.6.1.1 Road tests

Another vehicle was used to pull the test vehicle (Mazda) at constant speeds while the Engine was switched off and with the gearbox in a neutral position. Thus the internal engine shaking forces were eliminated. Dynamic forces were excited by the uneven road surface through the wheel suspension to the Engine mount system, as well as the centrifugal forces excited by the rotation of the wheels. This was done for the Original- and Modified systems respectively (see Section 5.5.2.1). Table 5.13 shows the dynamic force magnitudes transmitted to the vehicle's support structure for the Original- and Modified systems when the vehicle was pulled at 80 km/h with well-balanced wheels, a 120 g unbalance mass attached to each front wheel, and a 240 g unbalance mass attached to each front wheel respectively. Table 5.14 and Table 5.15 show the dynamic force magnitudes transmitted to vehicle's support structure for the Original- and Modified systems for the similar conditions when the vehicle was pulled at 100 km/h and 120 km/h respectively.

As an example, when the vehicle was pulled at 80 km/h with well-balanced wheels for the Original system, the Engine experienced an acceleration amplitude of $\ddot{X}_e$ = 0.89 m/s^2 at an excitation frequency of f_r = 12.25 Hz (see Figure D.1 and Table 5.13). With the use of equation (2.16), a displacement amplitude of X_e = 0.15 mm was computed. The closest stiffness coefficient k_e and damping coefficient c_e was chosen for each Engine mount that experienced similar frequency (12.25 Hz) and amplitude excitations (0.15 mm) at the Engine. An equivalent stiffness coefficient of k_e = 1046.97 N/mm and equivalent damping coefficient of c_e = 1050.94 Ns/m was determined for this displacement amplitude and frequency excitation experienced by the Engine for this condition. The dynamic force magnitude transmitted at the stiffness element was computed as $k_e X_e$ = 158.09 N, while the dynamic force magnitude transmitted at the damping element was computed as $c_e \omega X_e$ = 12.21 N. The resultant of these two force amplitudes was computed with the use of equation (2.30), which provided the total dynamic force magnitude transmitted to the vehicle's support structure as F_T = 158.56 N.

The same method was used to compute the dynamic force magnitudes transmitted to the vehicle's support structure for the Original- and Modified systems for all of the road test conditions mentioned above, as shown in Table 5.13 to Table 5.15.

Table 5.13: Dynamic force magnitudes transmitted during road tests at 80 km/h for Original- and Modified systems.

Frequency f_r [Hz]	Measured displacement amplitude of Engine X_e [mm]	Equivalent stiffness coefficient k_e [N/mm]	Equivalent damping coefficient c_e [Ns/m]	Force amplitude $k_e X_e$ [N]	Force amplitude $c_e \omega X_e$ [N]	Total dynamic force transmitted $\sqrt{(k_e X_e)^2 + (c_e \omega X_e)^2}$ [N]
Original system (well-balanced wheels)						
12.25	0.151	1046.97	1050.94	158.09	12.21	158.56
Modified system (well-balanced wheels)						
12.25	0.066	1061.27	1100.98	70.04	5.59	70.27
Original system (120 g unbalance mass attached to each front wheel)						
12.25	0.283	1003.90	1021.54	284.10	22.25	284.97
Modified system (120 g unbalance mass attached to each front wheel)						
12.25	0.134	1046.97	1050.94	140.29	10.84	140.71
Original system (240 g unbalance mass attached to each front wheel)						
12.25	0.439	1005.73	1009.08	441.52	34.10	442.83
Modified system (240 g unbalance mass attached to each front wheel)						
12.25	0.139	1046.97	1050.94	145.53	11.24	145.96

Table 5.14: Dynamic force magnitudes transmitted during road tests at 100 km/h for Original- and Modified systems.

Frequency f_r [Hz]	Measured displacement amplitude of Engine X_e [mm]	Equivalent stiffness coefficient k_e [N/mm]	Equivalent damping coefficient c_e [Ns/m]	Force amplitude $k_e X_e$ [N]	Force amplitude $c_e \omega X_e$ [N]	Total dynamic force transmitted $\sqrt{(k_e X_e)^2 + (c_e \omega X_e)^2}$ [N]
Original system (well-balanced wheels)						
12.25	0.081	1046.97	1050.94	84.80	6.55	85.06
14.75	0.068	1061.27	1100.98	72.17	6.94	72.50
Modified system (well-balanced wheels)						
12.25	0.034	1072.28	1351.45	36.46	3.54	36.63
14.75	0.066	1061.27	1100.98	70.04	6.73	70.37
Original system (120 g unbalance mass attached to each front wheel)						
12.25	0.101	1046.97	1050.94	105.74	8.17	106.06
14.75	0.100	1046.97	1050.94	104.70	9.74	105.15
Modified system (120 g unbalance mass attached to each front wheel)						
12.25	0.048	1061.27	1100.98	50.94	4.07	51.10
14.75	0.095	1046.97	1050.94	99.46	9.25	99.89
Original system (240 g unbalance mass attached to each front wheel)						
12.25	0.179	1003.90	1021.54	179.70	14.07	180.25
14.75	0.171	1046.97	1050.94	179.03	16.65	179.80
Modified system (240 g unbalance mass attached to each front wheel)						
12.25	0.063	1061.27	1100.98	66.86	5.34	67.07
14.75	0.152	1046.97	1050.94	159.14	14.80	159.83

Table 5.15: Dynamic force magnitudes transmitted during road tests at 120 km/h for Original- and Modified systems.

Frequency f_r [Hz]	Measured displacement amplitude of Engine X_e [mm]	Equivalent stiffness coefficient k_e [N/mm]	Equivalent damping coefficient c_e [Ns/m]	Force amplitude $k_e X_e$ [N]	Force amplitude $c_e \omega X_e$ [N]	Total dynamic force transmitted $\sqrt{(k_e X_e)^2 + (c_e \omega X_e)^2}$ [N]
Original system (well-balanced wheels)						
12.25	0.071	1061.27	1100.98	75.35	6.02	75.59
18	0.026	1097.78	1419.37	28.54	4.17	28.85
Modified system (well-balanced wheels)						
12.25	0.029	1072.28	1351.45	31.10	3.02	31.24
18	0.024	1097.78	1419.37	26.35	3.85	26.63
Original system (120 g unbalance mass attached to each front wheel)						
12.25	0.085	1046.97	1050.94	88.99	6.88	89.26
18	0.073	1119.80	686.87	81.75	5.67	81.94
Modified system (120 g unbalance mass attached to each front wheel)						
12.25	0.024	1072.28	1351.45	25.73	2.50	25.86
18	0.078	1085.92	813.56	84.70	7.18	85.01
Original system (240 g unbalance mass attached to each front wheel)						
12.25	0.116	1046.97	1050.94	121.45	9.38	121.81
18	0.091	1085.92	813.56	98.82	8.37	99.17
Modified system (240 g unbalance mass attached to each front wheel)						
12.25	0.044	1061.27	1100.98	46.67	3.73	46.84
18	0.103	1085.92	813.56	111.85	9.48	112.25

5.6.1.2 Forced electrical shaker motor response

An electrical shaker motor connected to a variable speed drive (VSD) was used to represent one of the conditions conducted in the road tests as described in Section 5.5.2.2. The forced frequency of the electrical motor could be changed when the vehicle was stationary, which provided an indication of how the Absorber would perform if the wheel suspension's natural frequency should shift slightly due to heat transfer at the tyres and small tyre pressure changes when the vehicle moved. During all the forced shaker motor tests the vehicle's wheels were stationary and the Engine was switched off. Table 5.16 shows the dynamic force magnitudes transmitted to the vehicle's support structure for the Original- and Modified systems when the speed of the electrical motor was set by the VSD for three different forced frequencies at 11.75, 12.25 and 12.75 Hz respectively.

As an example, when the electrical shaker motor was running at f_r = 11.75 Hz for the Original system, the Engine experienced an acceleration amplitude of $\ddot{X}_e$ = 1.21 m/s^2 (see Figure 5.14 and Table 5.16). With the use of equation (2.16), a displacement amplitude of X_e = 0.22 mm was computed. The closest stiffness coefficient k_e and damping coefficient c_e was chosen for each Engine mount that experienced similar frequency (11.75 Hz) and amplitude excitations (0.22 mm) at the Engine. An equivalent stiffness coefficient of k_e = 1003.90 N/mm and equivalent damping coefficient of c_e = 1021.54 Ns/m were determined for this displacement amplitude and frequency excitation experienced by the Engine for this condition. The dynamic force magnitude transmitted at the stiffness element was computed as $k_e X_e$ = 222.87 N, while the dynamic force magnitude transmitted at the damping element was computed as $c_e \omega X_e$ = 16.74 N. The resultant of these two force amplitudes was computed with the use of equation (2.30), which provided the total dynamic force magnitude transmitted to the vehicle's support structure as F_T = 223.49 N.

The same method was used to compute the dynamic force magnitudes transmitted to the vehicle's support structure for the Original- and Modified systems for all of the forced electrical shaker motor test conditions mentioned above, as shown in Table 5.16.

Table 5.16: Dynamic force magnitudes transmitted during forced electrical shaker motor tests for Original- and Modified systems.

Frequency f_r [Hz]	Measured displacement amplitude of Engine X_e [mm]	Equivalent stiffness coefficient k_e [N/mm]	Equivalent damping coefficient c_e [Ns/m]	Force amplitude $k_e X_e$ [N]	Force amplitude $c_e \omega X_e$ [N]	Total dynamic force transmitted $\sqrt{(k_e X_e)^2 + (c_e \omega X_e)^2}$ [N]
Original system (11.75 Hz forced electrical shaker motor excitations)						
11.75	0.222	1003.90	1021.54	222.87	16.74	223.49
Modified system (11.75 Hz forced electrical shaker motor excitations)						
11.75	0.095	1046.97	1050.94	99.46	7.37	99.73
Original system (12.25 Hz forced electrical shaker motor excitations)						
12.25	0.223	1003.90	1021.54	223.87	17.53	224.56
Modified system (12.25 Hz forced electrical shaker motor excitations)						
12.25	0.090	1046.97	1050.94	94.23	7.28	94.51
Original system (12.75 Hz forced electrical shaker motor excitations)						
12.75	0.175	1003.90	1021.54	175.68	14.32	176.27
Modified system (12.75 Hz forced electrical shaker motor excitations)						
12.75	0.098	1046.97	1050.94	102.60	8.25	102.93

5.6.2 Internal engine shaking forces

The effect of the presence of the Absorber was also evaluated when only internal engine shaking forces were present (see Section 5.5.3). The vehicle was stationary with the gearbox in a neutral position while the Engine was running at an idling speed of 716 rpm and also at 2000 rpm respectively. This was done for the Original as well as the Modified system respectively. From these measurements it was clear that the dominant amplitudes were at two, four and six times the Engine running speed, with the amplitude at second order the largest in relation. Table 5.17 shows the dynamic force magnitudes transmitted to the vehicle's support structure for the Original- and Modified systems at second, fourth and sixth order when the Engine was running at 716 and 2000 rpm respectively.

As an example, when the Engine was running at 716 rpm for the Original system, the Engine experienced an acceleration amplitude of $\ddot{X}_e$ = 0.42 m/s^2 at second order with an excitation frequency of f_e = 23.88 Hz (see Figure 5.22 and Table 5.17). With the use of equation (2.23), a displacement amplitude of X_e = 18.84 x 10^{-3} mm was computed. The closest stiffness coefficient k_e and damping coefficient c_e was chosen for each Engine mount that experienced similar frequency (23.88 Hz) and amplitude excitations (18.84 x 10^{-3} mm) at the Engine. An equivalent stiffness coefficient of k_e = 1097.78 N/mm and equivalent damping coefficient of c_e = 1419.37 Ns/m were determined for this displacement amplitude and frequency excitation experienced by the Engine for this condition. The dynamic force magnitude transmitted at the stiffness element was computed as $k_e X_e$ = 20.68 N, while the dynamic force magnitude transmitted at the damping element was computed as $c_e \omega X_e$ = 4.01 N. The resultant of these two force amplitudes was computed with the use of equation (2.30), which provided the total dynamic force magnitude transmitted to the vehicle's support structure as F_T = 21.07 N.

The same method was used to compute the dynamic force magnitudes transmitted to the vehicle's support structure for the Original- and Modified systems for all of the Engine running speed conditions mentioned above, as shown in Table 5.17.

Table 5.17: Dynamic force magnitudes transmitted during internal engine shaking forces tests for Original- and Modified systems.

Frequency f_e [Hz]	Measured displacement amplitude of Engine X_e [mm] x10^{-3}	Equivalent stiffness coefficient k_e [N/mm]	Equivalent damping coefficient c_e [Ns/m]	Force amplitude $k_e X_e$ [N]	Force amplitude $c_e \omega X_e$ [N]	Total dynamic force transmitted $\sqrt{(k_e X_e)^2 + (c_e \omega X_e)^2}$ [N]
Original system (Engine running speed - 716 rpm)						
23.88	18.84	1097.78	1419.37	20.68	4.01	21.07
47.88	1.545	1097.78	1419.37	1.70	0.66	1.82
71.88	0.154	1837.49	1279.61	0.28	0.09	0.30
Modified system (Engine running speed - 716 rpm)						
23.88	18.19	1097.78	1419.37	19.97	3.87	20.34
47.75	1.140	1097.78	1419.37	1.25	0.49	1.34
72.00	0.126	1837.49	1279.61	0.23	0.07	0.24
Original system (Engine running speed - 2000 rpm)						
67.19	1.987	1837.49	1279.61	3.65	1.07	3.81
134.1	0.188	1837.49	1279.61	0.35	0.20	0.40
201.3	0.016	1837.49	1279.61	0.03	0.03	0.04
Modified system (Engine running speed - 2000 rpm)						
66.88	1.815	1837.49	1279.61	3.34	0.98	3.47
133.8	0.145	1837.49	1279.61	0.27	0.16	0.31
200.9	0.022	1837.49	1279.61	0.04	0.04	0.05

5.6.3 Transient response

The Engine experienced large displacement amplitudes during the transient response tests performed (see Section 5.5.4). For the transient response conditions where the impact forces were excited by slowly moving the vehicle over the round bars with the Engine switched off, an excitation frequency of 12.25 Hz was assumed, which is the same as the wheel suspension natural frequency obtained from the road tests (see Section 5.5.2.1). When the Engine was switched off from idling speed while the vehicle was stationary, the bounce mode natural frequency of the Engine mount system was excited (see Section 4.5.1). With the use of these excitation frequencies and the dynamic properties of the Engine mounts for certain measured displacement amplitudes, the dynamic force magnitudes transmitted to the vehicle's support structure were computed. Only the maximum displacement amplitude experienced by the Engine during these conditions was used to compute the dynamic force magnitudes transmitted to the vehicle's support structure for the Original- and Modified systems, as shown in Table 5.18.

As an example, when the vehicle was slowly moving over the 6 mm round bars for the Original system, the Engine experienced a maximum displacement amplitude of X_e = 0.17 mm at an assumed excitation frequency of f_r = 12.25 Hz (see Figure 5.32 and Table 5.18). The closest stiffness coefficient k_e and damping coefficient c_e was chosen for each Engine mount that experienced similar frequency (12.25 Hz) and amplitude excitations (0.17 mm) at the Engine. An equivalent stiffness coefficient of k_e = 1046.97 N/mm and equivalent damping coefficient of c_e = 1050.94 Ns/m were determined for this maximum displacement amplitude and assumed frequency excitation experienced by the Engine for this condition. The dynamic force magnitude transmitted at the stiffness element was computed as $k_e X_e$ = 183.22 N, while the dynamic force magnitude transmitted at the damping element was computed as $c_e \omega X_e$ = 14.16 N. The resultant of these two force amplitudes was computed with the use of equation (2.30), which provided the total dynamic force magnitude transmitted to the vehicle's support structure as F_T = 183.77 N for the maximum displacement amplitude.

The same method was used to compute the dynamic force magnitudes transmitted to the vehicle's support structure for the Original- and Modified systems for all the transient response conditions mentioned above, as shown in Table 5.18.

Table 5.18: Dynamic force magnitudes transmitted during transient response tests for Original- and Modified systems.

Frequency [Hz]	Measured displacement amplitude of Engine X_e [mm]	Equivalent stiffness coefficient k_e [N/mm]	Equivalent damping coefficient c_e [Ns/m]	Force amplitude $k_e X_e$ [N]	Force amplitude $c_e \omega X_e$ [N]	Total dynamic force transmitted $\sqrt{(k_e X_e)^2 + (c_e \omega X_e)^2}$ [N]
Original system (6 mm round bars)						
12.25	0.175	1046.97	1050.94	183.22	14.16	183.77
Modified system (6 mm round bars)						
12.25	0.153	1046.97	1050.94	160.19	12.38	160.66
Original system (8 mm round bars)						
12.25	0.244	1003.90	1021.54	244.95	19.19	245.70
Modified system (8 mm round bars)						
12.25	0.139	1046.97	1050.94	145.53	11.24	145.96
Original system (12 mm round bars)						
12.25	0.352	1003.90	1021.54	353.37	27.68	354.45
Modified system (12 mm round bars)						
12.25	0.231	1003.90	1021.54	231.90	18.16	232.61
Original system (Engine switched off from idling speed)						
13.00	0.281	1003.90	1021.54	282.10	23.45	283.07
Modified system (Engine switched off from idling speed)						
13.00	0.163	1046.97	1050.94	170.66	13.99	171.23

5.6.4 Summary of measured test results

Table 5.19 shows the comparison between the dynamic force magnitudes transmitted for the Original- and Modified systems. The Vibration Absorber very effectively reduced the dynamic force magnitudes transmitted to the vehicle's support structure during the road tests when the Engine was not running, especially when the forces were excited through the wheel suspension at 12.25 Hz. The vertical bounce mode natural frequency of the Engine mount system was excited at 12.25 Hz when the forces where excited by the uneven road surface and the wheel rotation forces through the wheel suspension, which is the reason for the excellent performance of the Absorber during these conditions. Resonances occurs when the wheel suspension natural frequency (wheel hop) coincides with the engine mount system bounce mode natural frequency, as well as when the wheel rotation forced frequency coincides with the engine mount system bounce mode natural frequency. An additional resonance condition occurs when the bounce mode natural frequency of the engine mount system is excited by the uneven road surface through the wheel suspension. The dynamic force magnitudes transmitted to the vehicle's support structure remained more or less the same for the forces excited by wheel rotation frequencies at 14.75 and 18 Hz during the road tests (also see Table 5.13 to Table 5.15).

For all of the internal engine shaking forces tests when the vehicle was stationary and only internal shaking forces as well as gas pressure differences were present, the dynamic force magnitudes transmitted were maintained relatively the same for both the Original- and Modified systems (also see Table 5.17). The presence of the Absorber does not have any significant effect on the Engine's displacement amplitude, because these internal engine shaking forces occur at entirely different frequencies compared to the frequencies for road input forces (see Section 5.5.2.1 and 5.5.3).

When the Engine and the Absorber was subjected to harmonic movement from the electrical shaker motor, the force magnitudes transmitted to the vehicle's support structure were also reduced for the Modified system. These tests were conducted with the vehicle's Engine switched off and the wheels were also stationary, while only the electrical motor was running. Although the electrical shaker motor was running at 11.75 and 12.75 Hz respectively, the Absorber still contributed to the reduction of the transmitted force magnitudes, although the motor's forced frequency did not match the

wheel suspension natural frequency at 12.25 Hz (also see Section 5.5.2.2 and Table 5.16).

The Vibration Absorber also effectively reduced the forces transmitted during the transient impact response conditions (also see Table 5.18). The Engine was not running during the road impact tests while the vehicle slowly moved over the different sizes round bars. When the vehicle was stationary with the Engine running at idling speed and then suddenly switched off after a period of time, the Engine experienced large transient displacements. The Absorber significantly reduced the large dynamic force magnitudes transmitted to the vehicle's support structure during this condition.

The Vibration Absorber was tuned to the vertical bounce mode frequency of the Engine, which is the reason for the excellent performance when the forces were transmitted to the Engine mount system at around 12.25 Hz. The Modified system obtained a reduction in the dynamic force magnitudes transmitted to the vehicle's support structure in the range between 50.6% and 71% when the forces were excited through the wheel suspension at 12.25 Hz, with an average reduction of 60%. For the transient conditions the Modified system contributed to the reduction of the large dynamic force magnitudes transmitted to the vehicle's support structure in the range between 12.6% and 40.6%, with an average reduction of 30% (see Table 5.19).

Table 5.19: Comparison between dynamic force magnitudes transmitted for Original- and Modified systems.

Operational condition	Measured dynamic force magnitudes transmitted for Original system [N]	Measured dynamic force magnitudes transmitted for Modified system [N]	Percentage reduction of dynamic force magnitudes transmitted [%]
	Road tests at 80 km/h (12.25 Hz)		
Well-balanced wheels	158.56	70.27	55.68
120 g unbalance	284.97	140.71	50.62
240 g unbalance	442.83	145.96	67.04
	Road tests at 100 km/h (12.25 Hz)		
Well-balanced wheels	85.06	36.63	56.94
120 g unbalance	106.06	51.10	51.82
240 g unbalance	180.25	67.07	62.79
	Road tests at 100 km/h (14.75 Hz)		
Well-balanced wheels	72.50	70.37	2.94
120 g unbalance	105.15	99.89	5.00
240 g unbalance	179.80	159.83	11.11
	Road tests at 120 km/h (12.25 Hz)		
Well-balanced wheels	75.59	31.24	58.67
120 g unbalance	89.26	25.86	71.03
240 g unbalance	121.81	46.84	61.55
	Road tests at 120 km/h (18.00 Hz)		
Well-balanced wheels	28.85	26.63	7.69
120 g unbalance	81.94	85.01	-3.75
240 g unbalance	99.17	112.25	-13.19
	Forced electrical shaker motor response tests		
11.75 Hz	223.49	99.73	55.38
12.25 Hz	224.56	94.51	57.91
12.75 Hz	176.27	102.93	41.61
	Internal engine shaking forces tests – Idling speed (716 rpm)		
Second order	21.07	20.34	3.46
Fourth order	1.82	1.34	26.37
Sixth order	0.30	0.24	20.00
	Internal engine shaking forces tests – Engine running at 2000 rpm		
Second order	3.81	3.47	8.92
Fourth order	0.40	0.31	22.50
Sixth order	0.04	0.05	-25.00
	Transient response tests		
6 mm round bars	183.77	160.66	12.58
8 mm round bars	245.70	145.96	40.59
12 mm round bars	354.45	232.61	34.37
Engine switched off	283.07	171.23	39.51
Engine switched on (Predicted)	373.50	292.38	21.72

5.7 PREDICTED AND MEASURED DYNAMIC FORCE MAGNITUDES TRANSMITTED

The mathematical models discussed in Section 2.3 to Section 2.6 was used for the theoretical predictions and the differential equations of motion was solved with the Matlab built-in numerical integration algorithm namely *ode45.m*. These mathematical models were implemented in respective computer programs discussed in Section 3.3 to Section 3.6. A similar equivalent vertical shaking force magnitude was computed for the Original system, which provided a theoretical response of the Engine mount system that corresponded with the specific measured amplitude response for each experimental condition investigated in this study (Nel & Van Wyngaardt, 2014b). The magnitude of the equivalent vertical shaking force computed for the Original system was then used in the computer simulations for the Modified system. The static mass as well as the equivalent stiffness- and damping element properties of the Engine and the Absorber characterised in Chapter 4 were used in the computer simulations. The closest equivalent stiffness coefficient k_e and k_a as well as the equivalent damping coefficient c_e and c_a were used in the computer simulations that experienced similar measured frequency and displacement amplitude excitations at the Engine and the Absorber respectively. The equivalent Engine mount properties together with the theoretical Engine displacement amplitude computed from the time domain graphs were used to determine the theoretical dynamic force magnitudes transmitted to the vehicle's support structure with the use of equation (2.30). The predicted dynamic force magnitudes transmitted are compared to the measured dynamic force magnitudes transmitted as shown in Table 5.20 for the Modified system. The measured dynamic force magnitudes transmitted is compared between the Original- and Modified systems as shown in Table 5.19.

5.7.1 Road forces

The condition where the vehicle was pulled at 100 km/h with an unbalance mass of 120 g attached to each front wheel while the Engine was not running is theoretically examined as an example for the Original- and Modified systems (see Section 5.5.2.1). The measured frequency domain signal for the Original system is shown in Figure 5.8, while Figure 5.11 shows the measured frequency domain signal for the Modified system. The computer program discussed in Section 3.3, that was developed to solve the differential equation of motion (equation (2.14)), was used to simulate this condition for the Original system. The computer program discussed in Section 3.4, that was developed to solve the differential equations of motion (equation (2.18) and (2.19)), was used to simulate this condition for the Modified system.

The theoretical time domain response of the Engine mount system due to the dynamic force excited by the uneven road surface through the wheel suspension at f_r = 12.25 Hz is shown in Figure 5.41 for the Original system. An equivalent vertical shaking force with a magnitude of F_r = 8.29 N was computed with the use of equation (2.15), which provided the same theoretical time domain response of the Engine as the measured displacement amplitude for this condition (see Figure 5.8). An equivalent stiffness coefficient of k_e = 1046.97 N/mm and equivalent damping coefficient of c_e = 1050.94 Ns/m were determined for the measured displacement amplitude and frequency excitation experienced at the Engine, and were used in the computer simulation for this condition.

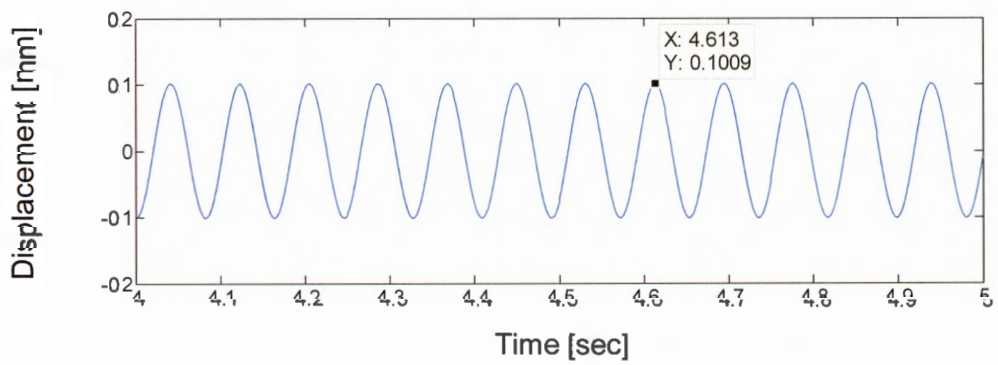

Figure 5.41: Predicted Engine time domain response at 12.25 Hz for Original system.

The same equivalent vertical shaking force with a magnitude of F_r = 8.29 N as characterised, was used for the Modified system at f_r = 12.25 Hz for this condition as shown in Figure 5.42 (also see Figure 5.11). An equivalent stiffness coefficient of k_e = 1061.27 N/mm and equivalent damping coefficient of c_e = 1100.98 Ns/m were determined for the measured displacement amplitude and frequency excitation experienced by the Engine. An equivalent stiffness coefficient of k_a = 90.76 N/mm and equivalent damping coefficient of c_a = 60.27 Ns/m were determined for the measured displacement amplitude and frequency excitation experienced at the Absorber, and were used in the computer simulation for this condition. With the use of equation (2.30), the predicted dynamic force magnitude transmitted to the vehicle's support structure for the Modified system was computed as F_T = 40.88 N (also see Table 5.19 and Table 5.20).

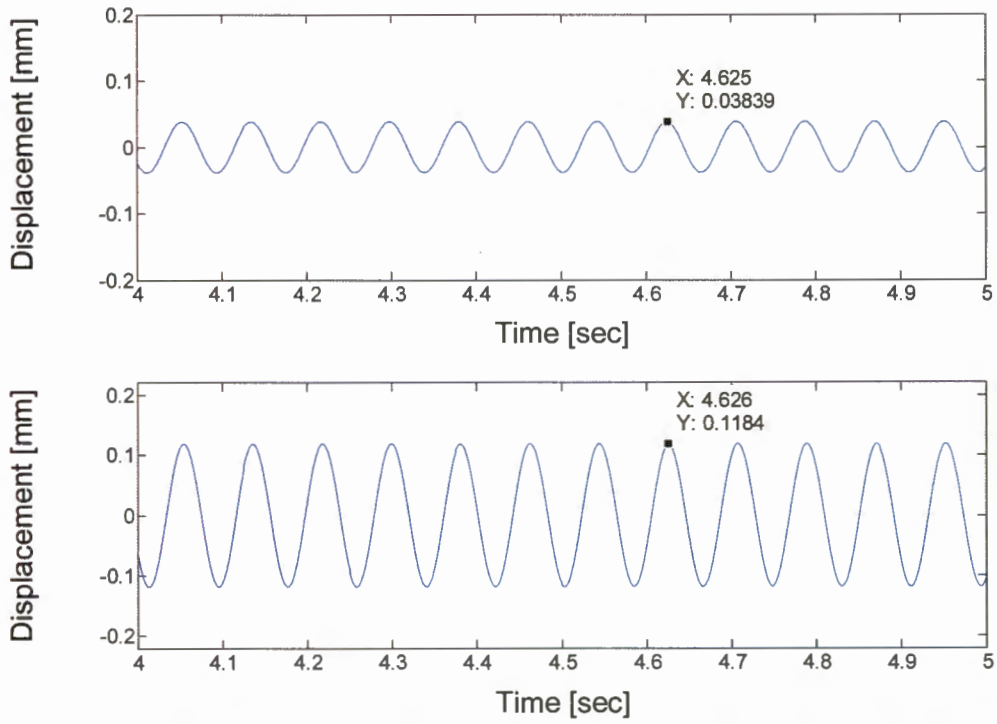

Figure 5.42: Predicted Engine (top) and Absorber (bottom) time domain response at 12.25 Hz for Modified system.

The Absorber mass is subject to large displacement amplitudes while the Engine moves considerably less than for the Original system (see Figure 5.41). The Absorber was tuned to the vertical bounce mode frequency of the Engine mount system, which is the reason for the excellent performance when the forces were transmitted to the Engine mount system at around 12.25 Hz.

For the forces excited by the rotation of the wheels at f_r = 14.75 Hz, an equivalent vertical shaking force with a magnitude of F_r = 50.09 N was computed with the use of equation (2.15), which provided the same theoretical time domain response of the Engine as the measured displacement amplitude for this condition (see Figure 5.8). The theoretical time domain response of the Engine mount system due to the forces excited by the rotation of the wheels at f_r = 14.75 Hz is shown in Figure 5.43 for the Original system. An equivalent stiffness coefficient of k_e = 1046.97 N/mm and equivalent damping coefficient of c_e = 1050.94 Ns/m were determined for the measured displacement amplitude and frequency excitation experienced at the Engine, and were used in the computer simulation for this condition.

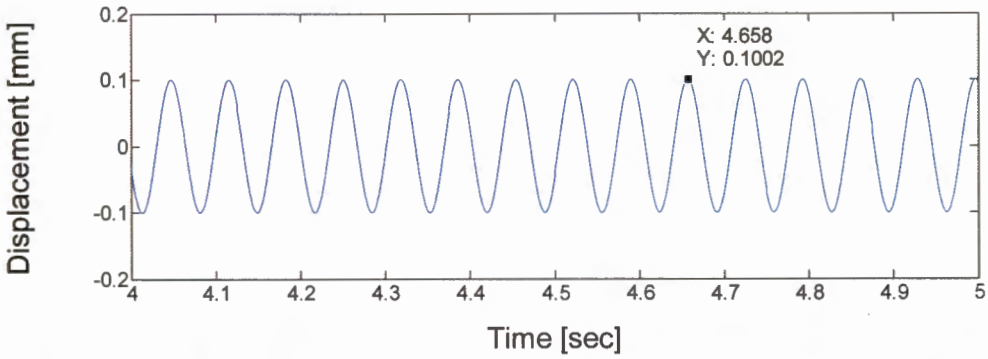

Figure 5.43: Predicted Engine time domain response at 14.75 Hz for Original system.

The same equivalent vertical shaking force with a magnitude of F_r = 50.09 N as characterised, was used for the Modified system at f_r = 14.75 Hz for this condition as shown in Figure 5.44 (also see Figure 5.11). An equivalent stiffness coefficient of k_e = 1046.97 N/mm and equivalent damping coefficient of c_e = 1050.94 Ns/m were determined for the measured displacement amplitude and frequency excitation experienced at the Engine. An equivalent stiffness coefficient of k_a = 80.61 N/mm and equivalent damping coefficient of c_a = 49.47 Ns/m were determined for the measured displacement amplitude and frequency excitation experienced at the Absorber, and were used in the computer simulation for this condition. With the use of equation (2.30) the predicted dynamic force magnitude transmitted to the vehicle's support structure for the Modified system was computed as F_T = 107.85 N (also see Table 5.19 and Table 5.20).

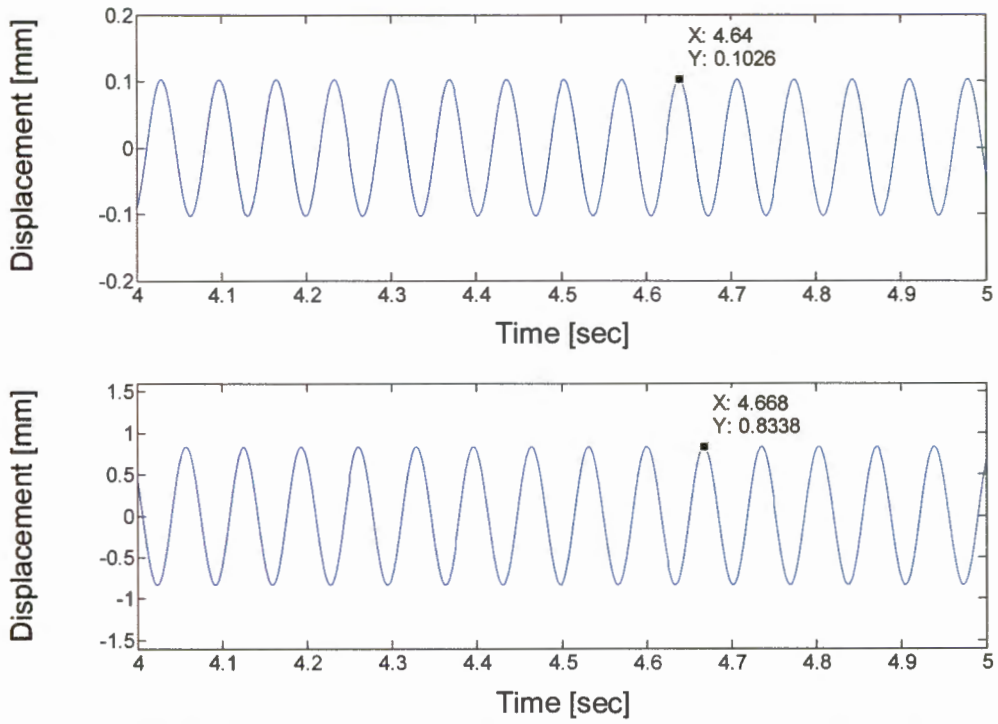

Figure 5.44: Predicted Engine (top) and Absorber (bottom) time domain response at 14.75 Hz for Modified system.

The Engine displacement remained relatively the same for the Modified system compared to the Original system (see Figure 5.43). The Absorber mass is subject to large displacement amplitudes although this wheel rotation force at 14.75 Hz does not occur at the bounce mode frequency of the Engine mount system, which is around 12.25 Hz.

5.7.2 Internal engine shaking forces

The Engine mount system is typically subject to forces excited by the Engine mass imbalances and gas pressure differences when the Engine is running at 716 rpm to 6000 rpm. The condition where the vehicle was stationary with the gearbox in a neutral position and with the Engine idling at 716 rpm is theoretically examined as an example for the Original- and Modified systems at second order running speed (see Section 5.5.3). The measured frequency domain signal for the Original system is shown in Figure 5.22, while Figure 5.24 shows the measured frequency domain signal for the Modified system. The computer program discussed in Section 3.5, that was developed to solve the differential equation of motion (equation (2.21)), was used to simulate this condition for the Original system. The computer program discussed in Section 3.6, that

was developed to solve the differential equations of motion (equation (2.24) and (2.25)), was used to simulate this condition for the Modified system.

The theoretical time domain response of the Engine mount system when subject to internal engine shaking forces at second order running speed (f_e = 23.88 Hz), is shown in Figure 5.45 for the Original system. An equivalent vertical shaking force with a magnitude of F_e = 55.43 N was determined, which provided the same theoretical time domain response of the Engine as the measured displacement amplitude for this condition at second order running speed (see Figure 5.22). An equivalent stiffness coefficient of k_e = 1097.78 N/mm and equivalent damping coefficient of c_e = 1419.37 Ns/m were determined for the measured displacement amplitude and frequency excitation experienced at the Engine, and were used in the computer simulation for this condition.

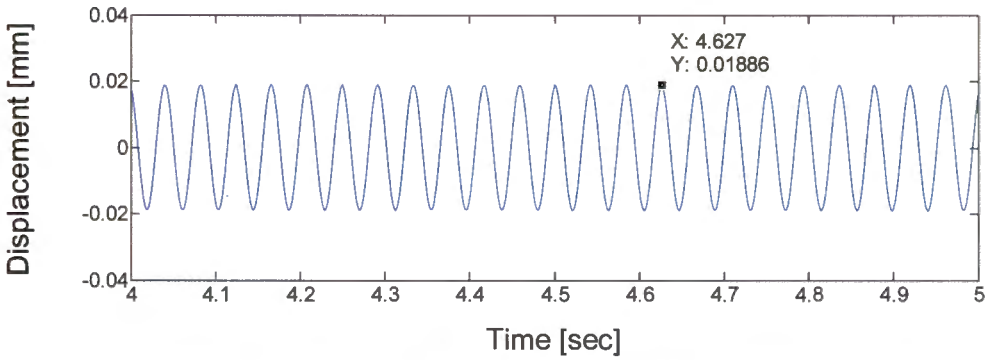

Figure 5.45: Predicted Engine time domain response at 23.88 Hz for Original system.

The same equivalent vertical shaking force with a magnitude of F_e = 55.43 N as characterised, was used for the Modified system at f_e = 23.88 Hz for this condition as shown in Figure 5.46 (also see Figure 5.24). An equivalent stiffness coefficient of k_e = 1097.78 N/mm and equivalent damping coefficient of c_e = 1419.37 Ns/m were determined for the measured displacement amplitude and frequency excitation experienced at the Engine. An equivalent stiffness coefficient of k_a = 100.49 N/mm and equivalent damping coefficient of c_a = 102.29 Ns/m were determined for the measured displacement amplitude and frequency excitation experienced at the Absorber, and were used in the computer simulation for this condition. With the use of equation (2.30), the

predicted dynamic force magnitude transmitted to the vehicle's support structure for the Modified system was computed as F_T = 22.33 N (also see Table 5.19 and Table 5.20).

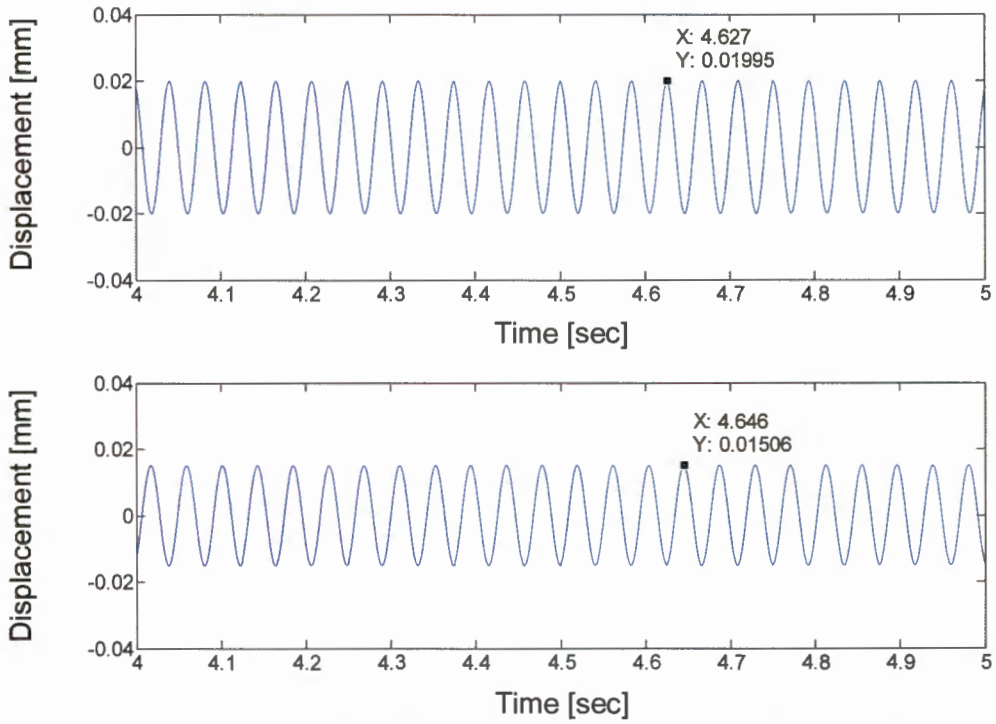

Figure 5.46: Predicted Engine (top) and Absorber (bottom) time domain response at 23.88 Hz for Modified system.

The Engine displacement remained relatively the same for the Modified system compared to the Original system (see Figure 5.45). The Absorber mass displacement is more or less the same as the Engine for the Modified system. The dynamic forces excited through the wheel suspension has a much greater effect on the response of the Engine than for Internal engine shaking forces due to the close resonance condition (see Section 5.5.2 and Section 5.5.3).

5.7.3 Transient response

The Engine typically experiences transient response when the gears are changed, when it is switched on and off, as well as when impact forces are excited from an uneven road surface through the suspension to the Engine mount system. The condition where the vehicle was stationary with the gearbox in a neutral position and the Engine was switched off from idling (f_e = 23.88 Hz) is theoretically examined as an example for the Original- and Modified systems (see Section 5.5.4). The measured time domain signal for the Original system is shown in Figure 5.38, while Figure 5.39 shows the measured

time domain signal for the Modified system. Only the maximum displacement amplitude experienced by the Engine and the Absorber during these conditions was considered. The computer program discussed in Section 3.5, that was developed to solve the differential equation of motion (equation (2.21)), was used to simulate this condition for the Original system. The computer program discussed in Section 3.6, that was developed to solve the differential equations of motion (equation (2.24) and (2.25)), was used to simulate this condition for the Modified system.

The theoretical time domain response of the Engine mount system where the Engine was switched off from idling (f_e = 23.88 Hz) after an integration time of 4 seconds, is shown in Figure 5.47 for the Original system. An equivalent vertical shaking force with a magnitude of F_e = 147.10 N was determined, which provided the same maximum theoretical displacement response of the Engine as the maximum measured displacement response for this transient condition (see Figure 5.38). The magnitude of the equivalent vertical shaking force was thus set to F_e = 0 N in the computer program after an integration time of 4 seconds. An equivalent stiffness coefficient of k_e = 1119.8 N/mm and equivalent damping coefficient of c_e = 686.86 Ns/m were determined for the measured displacement amplitude and frequency excitation experienced at the Engine, and were used in the computer simulation for this condition.

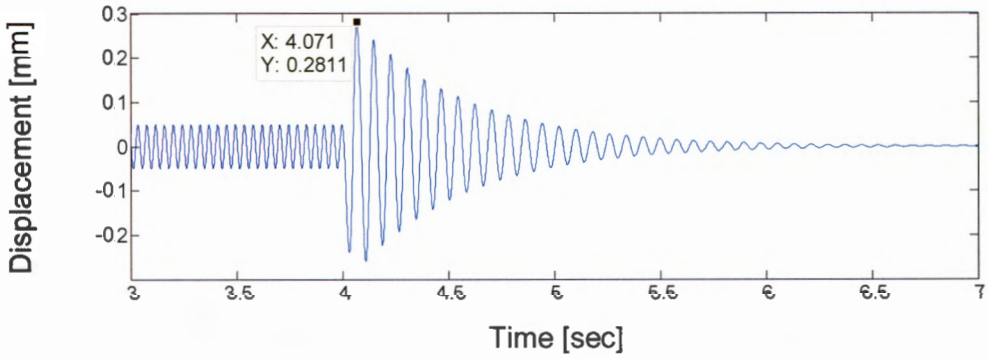

Figure 5.47: Predicted Engine time domain response during shutdown for Original system.

The same equivalent vertical shaking force with a magnitude of F_e = 147.10 N as characterised, was used for the Modified system for this transient condition as shown in Figure 5.48 (also see Figure 5.39). For the Modified system the magnitude of the equivalent vertical shaking force was also set to F_e = 0 N in the computer program after an integration time of 4 seconds. An equivalent stiffness coefficient of k_e = 1119.8 N/mm

and equivalent damping coefficient of c_e = 686.86 Ns/m were determined for the measured displacement amplitude and frequency excitation experienced at the Engine. An equivalent stiffness coefficient of k_a = 97.73 N/mm and equivalent damping coefficient of c_a = 74.65 Ns/m were determined for the measured displacement amplitude and frequency excitation experienced at the Absorber, and were used in the computer simulation for this condition. When the Engine was switched off from idling, transient behaviour occurred, and the bounce mode frequency of the Engine mount system was then excited (see Section 4.5.1 and Section 5.6.3). With the use of equation (2.30) the maximum predicted dynamic force magnitude transmitted to the vehicle's support structure for the Modified system was computed as F_T = 250.73 N (also see Table 5.19 and Table 5.20).

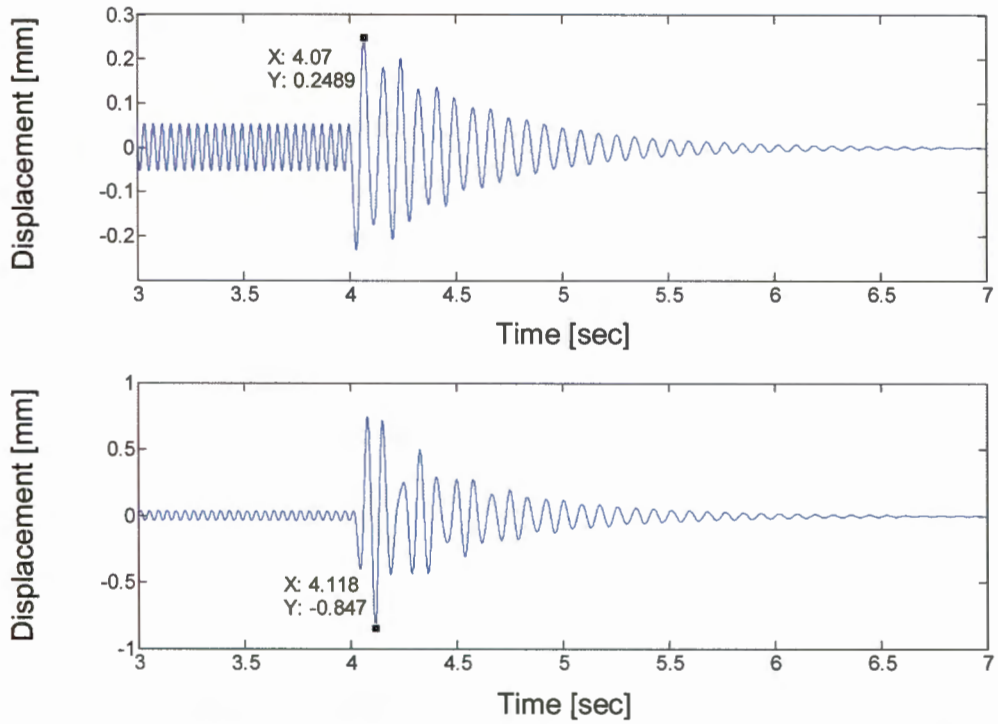

Figure 5.48: Predicted Engine (top) and Absorber (bottom) time domain response during shutdown for Modified system.

The Engine as well as the Absorber is subject to extremely large excitation amplitudes during transient conditions. The Absorber effectively reduced the transient response experienced at the Original system (also see Table 5.19).

5.7.4 Summary of predicted results

From the computer simulations it is clear that the forces excited by the uneven road surface through the wheel suspension is much smaller than the forces excited by the rotation of the wheels or by the Engine imbalance and gas pressure differences, but have a much greater effect on the Engine's displacement due to the close resonance condition (see Section 5.7.1 and Section 5.7.2 as well as Table 5.19). The dynamic force magnitudes transmitted to the vehicle's support structure are thus significantly larger for road forces. During transient conditions, the Engine is subject to large displacement amplitudes, which are also decreased with the presence of the Absorber (see Section 5.7.3 and Table 5.19). The equivalent Engine mount properties together with the theoretical Engine displacement computed from the time domain graphs were used to determine the theoretical dynamic force magnitudes transmitted to the vehicle's support structure with the use of equation (2.30). Table 5.20 indicates the comparison between the measured (also see Table 5.19) and predicted dynamic force magnitudes transmitted to the vehicle's support structure.

The predicted dynamic force magnitudes transmitted correspond well to the measured values. This proves that a simple two-degree-of-freedom system approach is adequate for simulations as a design tool for an Engine Vibration Absorber.

Table 5.20: Measured and predicted dynamic force magnitudes transmitted for the Modified system.

Operational condition	Measured dynamic force magnitudes transmitted for Modified system [N]	Predicted dynamic force magnitudes transmitted for Modified system [N]
	Road tests at 80 km/h (12.25 Hz)	
Well-balanced wheels	70.27	61.11
120 g unbalance	140.71	127.32
240 g unbalance	145.96	107.01
	Road tests at 100 km/h (12.25 Hz)	
Well-balanced wheels	36.63	34.36
120 g unbalance	51.10	40.88
240 g unbalance	67.07	65.54
	Road tests at 100 km/h (14.75 Hz)	
Well-balanced wheels	70.37	78.56
120 g unbalance	99.89	107.38
240 g unbalance	159.83	184.51
	Road tests at 120 km/h (12.25 Hz)	
Well-balanced wheels	31.24	31.09
120 g unbalance	25.86	36.07
240 g unbalance	46.84	46.95
	Road tests at 120 km/h (18.00 Hz)	
Well-balanced wheels	26.63	38.32
120 g unbalance	85.01	101.04
240 g unbalance	112.25	129.67
	Forced electrical shaker motor tests	
11.75 Hz	99.73	103.56
12.25 Hz	94.51	100.31
12.75 Hz	102.93	83.31
	Internal engine shaking forces tests – Idling speed (716 rpm)	
Second order	20.34	22.33
Fourth order	1.34	1.84
Sixth order	0.24	0.3
	Internal engine shaking forces tests – Engine running at 2000 rpm	
Second order	3.47	3.82
Fourth order	0.31	0.4
Sixth order	0.05	0.05
	Transient response tests	
6 mm round bars	160.66	138.82
8 mm round bars	145.96	159.4
12 mm round bars	232.61	231.99
Engine switched off	171.23	250.73
Engine switched on (Predicted)	-	292.38

6 CONCLUSIONS

Vibration was significantly reduced at a vehicle. From the literature survey done, no previous work could be found where a vibration absorber was used at an Engine of a vehicle. The literature survey clearly identified four different resonance conditions at an engine mount system of a typical front-wheel-drive vehicle. These resonance conditions include:

- The wheel hop suspension natural frequency normally coincides with the engine mount system bounce mode natural frequency (10 to 13 Hz).
- The wheel rotation forced frequency coincides with the engine mount system bounce mode natural frequency (10 to 13 Hz) at a certain vehicle speed.
- The uneven road surface normally causes engine vertical excitation on its rubber mounts (10 to 13 Hz).
- Human body natural frequencies (10 to 13 Hz), for example the spinal cord is in this same range and when excited could lead to discomfort.

From the literature it is clear that vibration absorbers used at several other structural applications where resonance takes place, perform extremely well to reduce vibration levels. In this study an Engine Vibration Absorber was successfully designed, manufactured and also experimentally characterised and evaluated.

The design involved the development of mathematical models to determine mainly response and natural frequencies. This was done for a single-degree-of-freedom model where the equation of motion for the Engine on its rubber mounts as excited by a force function was considered. A two-degree-of-freedom model where the Vibration Absorber (relatively smaller rigid body mass with equivalent rubber mount) is attached to the Engine on its rubber mounts was also considered. This included the formulation of two equations of motion with a force function for excitation. The mathematical models were implemented in computer programs developed in a Matlab environment.

The parameters required as input data for the computer programs were experimentally characterised. These parameters included the magnitudes of the Engine mass, Engine rubber mount dynamic properties, Absorber mass, Absorber mount dynamic properties, the different dynamic shaking forces for the investigated operational conditions, and also the position of the Engine's centre of gravity. These operational conditions included road

inputs with several road input forces transmitted to the Engine mount system, and also different Engine speeds with internal engine shaking forces. The output data of the computer simulations included Engine and Absorber time domain response (displacement) under steady state as well as transient conditions. Natural frequency magnitudes were also computed as output data. Steady state conditions included responses from road input forces, as well as from internal engine shaking forces. Transient conditions included responses resulting from road impact forces, Engine starting, and Engine stopping conditions.

From sensitivity computations it was found that the smaller the moving mass magnitude of the Vibration Absorber as a design choice, the larger the response amplitude at the Absorber. On the other hand, the larger the Absorber mass, the less cost effective the Absorber is. Additionally, there is a limit regarding size (mass) due to spatial constraints at the engine compartment of the vehicle. In the design for the Engine Vibration Absorber, it was decided to make the Absorber moving mass 5.8% of the Engine mass, in order to achieve a good compromise between these two diverse design goals. The rubber mounts of this Engine Vibration Absorber was able to accommodate the static displacement caused by the weight of the Absorber, as well as the dynamic displacements caused by the different dynamic forces for all the operational conditions investigated (transient and steady state behaviour).

Regarding the design choice for the amount of damping at the Absorber, the sensitivity computations of this study indicated that the response of the Engine increased when the amount of damping at the Absorber is increased at a pure resonance condition, such as resonance regarding road inputs. However, during transient conditions such as Engine starting and stopping, the engine mount system natural frequency is excited, and under these operational conditions the amount of damping at the Vibration Absorber is very important and more damping thus beneficial to limit the Absorber response. The rubber mounts of this Engine Vibration Absorber provided a good comparison between these two diverse design goals for all the operational conditions investigated (transient and steady state behaviour).

The Engine Vibration Absorber was tuned for a frequency that corresponds to the natural frequency of the Engine mount system. However, it was found that the dynamic properties, mainly the dynamic stiffness, but also the damping coefficients of rubber mounts (elastomeric material) are amplitude excitation dependant. Rubber mounts were

used at the Engine and also at the Absorber, which thus complicated the computer simulations, the characterisation of the rubber mounts used at the Engine and at the Absorber, as well as the practical tuning of the Absorber. These amplitude dependant dynamic mount properties were successfully experimentally characterised nonetheless. This was done for the Absorber mounts and the Engine mounts for different ranges of excitation amplitudes. The measured data was used to compute the dynamic stiffness and damping coefficients of the Absorber mounts based on a mathematical model developed for characterisation as implemented in a computer program.

As criteria of vibration transmitted, the theoretical predicted dynamic force magnitudes transmitted through the Engine mounts to the vehicle's support structure were computed as output data. This was done where the equations of motion were solved with numerical integration and the theoretical vibration responses obtained and subsequently used. These dynamic force magnitudes transmitted were also experimentally determined. This was done where vibration responses were measured, and with the Engine rubber mount properties used, these dynamic force magnitudes were then computed. These predicted and measured dynamic force magnitudes were determined for several operational conditions. It was found that these predicted and measured dynamic force magnitudes compared very well.

The Engine Vibration Absorber very effectively reduced the dynamic force magnitudes transmitted to the vehicle's support structure for all the different road input conditions at or near resonance. The reduction in dynamic force magnitudes transmitted, varied between 50.6% and 71% for these wheel input force conditions. The Engine Vibration Absorber was also evaluated for certain transient conditions. During these conditions the Engine mount system was subject to large displacement responses. The Absorber reduced the large dynamic force magnitudes transmitted to the vehicle's support structure for all the transient conditions investigated extremely well, with the reduction that varied between 12.6% and 40.6%. The effect of the presence of the Absorber was also evaluated when the Engine was running at different rotational speeds, with only internal engine shaking forces that caused excitation. It was found that approximately the same magnitudes of dynamic forces were transmitted to the vehicle's support structure for the Original- and Modified systems, thus with and without the Engine Vibration Absorber. This means that the Engine Vibration Absorber effectively reduced the significantly larger vibration amplitudes caused by road inputs, but with no significant

negative effect regarding any additional dynamic force magnitudes transmitted when the Engine was running.

The predicted and measured natural frequency magnitudes of the two-degree-of-freedom system also corresponded very well, which is additional proof that the mathematical models were reliable.

Noise measurements taken inside the vehicle's compartment at the Original- and the Modified systems indicated a reduction in noise levels for all the steady state operational conditions investigated when the Engine Vibration Absorber was installed.

Vibration Absorbers could have an advantage for several other applications where rigid mass harmonic movement caused by resonance is present, such as

- Tumble dryers and washing machines.
- Passenger seats of vehicles.
- Computer hard drives and fans.
- Air conditioners.

This could be investigated in future research.

For future research on the Engine Vibration Absorber, the dynamic properties could be further optimised by the increase in damping at the Absorber, which could then allow a smaller Absorber mass. The use of an Engine Vibration Absorber with a hydraulic engine mount system may also hold vibration isolation advantages in the higher frequency region, which should be further investigated.

REFERENCES

Alison, E.S., Ken, T.S., Holdgate, A., Ahern, A. & Morris, J. 2011. Noise levels in an Australian emergency department. *Australian Emergency Nursing Journal*, 14:26-31.

Atmaca, E., Peker, I. & Altin, A. 2005. Industrial Noise and Its Effects on Humans. *Polish Journal of Environmental Studies*, 14(6):721-726.

Austrell, P. & Olsson, A.K. 2012. Considering amplitude dependence during cyclic loading elastomers using an equivalent viscoelastic approach. *Polymer Testing*, 31(7):909-915.

Barak, P. 1991. Magic Numbers in Design of Suspensions for Passenger Cars. *SAE international*, SAE paper 911921:53-80.

Bretl, J. 1993. Optimization of Engine Mounting Systems to Minimize Vehicle Vibration. *SAE International*, SAE paper 931322:1822-1829.

Brogan, J., Fortgang, J. & Singhose, W. 2003. Experimental Verification of Vibration Absorbers Combined with Input Shaping for Oscillatory Systems. *Proceedings of the American Control Conference*, 4:3160-3165.

Canales, C.N., López, A.L., Venegas, J.C., Razo-García, J. & Aguilera-Cortés, L.A. 2008. Optimal Design of Stockbridge Dampers. *Ingeniería Mecánica, Tecnología y Desarrollo*, 2(6):193-199.

Cheung, C.K. 2004. Organizational influence on working people's occupational noise protection in Hong Kong. *Journal of Safety Research*, 35(4):465-475.

Colgate, J.E., Chang, C.T., Chiou, Y.C., Liu, W.K. & Keer, L.M. 1995. Modelling of a hydraulic engine mount focusing on response to sinusoidal and composite excitations. *Journal of Sound and Vibration*, 3(184):503-528.

Demic, M. 1990. A Contribution to the Optimization of the Characteristics of Elastodamping Elements of Passenger Cars. *Vehicle System Dynamics*, 19:3-18.

De-Wei, S., Zhi-Gang, C., Guang-Yu, Z. & Eberhard, P. 2011. Modeling and parameter identification of amplitude- and frequency-dependent rubber isolator. *J. Cent. South Univ. Technol.*, 18:672-278.

Du Plooy, N.F. 1999. The development of a vibration absorber for vibrating screens. Pretoria: University of Pretoria. (Dissertation - M. Eng).

Eddy, N. 19 July 2005. Taipei 101's 730-Ton Tuned Mass Damper, Popular Mechanics: http://www.popularmechanics.com/technology/gadgets/news/1612252 Date of access: 30 January 2012.

Fasana, A. & Giorcelli, E. 2009. A vibration absorber for motorcycle handles. *Meccanica*, 45:79-88.

Fischer, O. 2007. Wind-excited vibrations—Solution by passive dynamic vibration absorbers of different types. *Journal of Wind Engineering and Industrial Aerodynamics*, 95:1028-1039.

Fortgang, J., Patrangenaru, V. & Singhose, W. 2006. Scheduling of Input Shaping and Transient Vibration Absorbers for High-Rise Elevators. *Proceedings of the 2006 American Control Conference*:1772-1777.

Fortgang, J. & Singhose, W. 2005. Concurrent design of vibration absorbers and input shapers. *Journal of Dynamic Systems, Measurement, and Control*, 127:329-335.

Garcia, M. 2006. Engineering rubber bushings stiffness formulas including dynamic amplitude dependence. Stockholm: The Marcus Wallenberg Laboratory for Sound and Vibration Research. (Dissertation - M. Eng).

Gielen, L., Van der Linden, P.J.G. & Deges, R. 1996. Identification, Quantification and Reduction of Structural- Borne Road Noise in a Mid-Size Passenger Car. *SAE International*, SAE paper 960195:67-74.

Griffin, M.J. 1981. Biodynamic response to whole-body vibration. *The Shock and Vibration Digest*, 13:3-12.

Griffin, M.J. 2004. Handbook of Human Vibrations. London: Elsevier Academic Press.

Hartog, J.P.D. 1956. Mechanical Vibrations. 4th ed. New York: McGraw-Hill.

Heo, J.W. & Chung, J. 2002. Vibration and noise reduction of an optical disk drive by using a vibration absorber. *IEEE Transactions on Consumer Electronics*, 48(4):874-878.

Heyns, P.S. & Van Niekerk, J.L. 1997. Vibrating screen technology: An overview of vibration control methods. LGI Report no LGI97/075.

Hunt, J.B. 1979. Dynamic Vibration Absorbers. London: Publications LTD.

Hwang, C.H., Lee, B.H. & Jung, P.K. 2009. Reduction of Interior Booming Noise for a Small Diesel Engine Vehicle Without Balance Shaft Module. *SAE International*, SAE paper 2009-01-2121:1-7.

Ishihama, M., Seto, K., Nagamatsu, A. & DOI, K. 1995. Control of Engine Roll and Bounce Vibrations Using Hydraulic Mounts. *JSME International Journal*, 38(1):29-35.

Joseph, L.M., Poon, D. & Shieh, S. 2006. Ingredients of High-Rise Design Taipei 101. http://www.structuremag.org/Archives/2006-6/F-Taipei-101-June-06.pdf Date of access: 2 February 2012.

Karlsson, F. & Persson, A. 2003. Modelling Non-linear Dynamics of Rubber Bushings – Parameter Identification and Validation. Sweden: Lund University. (Dissertation - M. Eng).

Keye, S., Keimer, R. & Homann, S. 2009. A vibration absorber with variable eigenfrequency for turboprop aircraft. *Aerospace Science and Technology*, (13):165-171.

Kim, M.G., Hyun, C.H. & Jeong, H.L. 1994. The Effects of Vehicle Velocity and Engine Mount Stiffness on Ride Comfort. *SAE International*, SAE paper 941045:129-135.

Kim, G. & Singh, R. 1992. Resonance, Isolation and Shock Control Characteristics of Automotive Nonlinear Hydraulic Engine Mounts. *ASME*, 44:165-180.

Kim, N.W., Kim, K.W. & Sin, H. 2007. A Design of a Dynamic Vibration Absorber for a DVD±RW Drive. *IEEE Transactions on Consumer Electronics*, 53(3):956-961.

La Civita, M. & Sestieri, A. 1999. Optimization of an Engine Mounting System for Vibro-acoustic Comfort Improvement. *International Modal Analysis Conference*, 17:1998-2004.

Levak, K. Horvat, M. & Domitrovic, H. 2008. Effects of Noise on Humans. *50th International Symposium*, 2008:333-336.

Lin, T.R., Farag, N.H. & Pan, J. 2005. Evaluation of frequency dependent rubber mount stiffness and damping by impact test. *Applied Acoustics*, 66(7):829-844.

Megahed, S.M. & Abd El-Razik, A.K. 2010. Vibration control of two degrees of freedom system using variable inertia vibration absorbers: Modelling and simulation. *Journal of Sound and Vibration*, 329:4841-4865.

Meillier, J. & Mairesse, P. 1996. Transfer Path Analysis in a Multisource Environment, Application for Road Noise Analysis. *International Modal Analysis Conference*, 14:314-319.

Mndeme, F.G. & Mkoma, S.L. 2012. Assessment of work zone noise levels at a cernent factory in Tanga, Tanzania. *Ethiopian Journal of Environmental Studies and Management,* 5(3):225-231.

Nakahara, K., Nakagawa, N. & Ohta, K. 2008. Dynamic Characteristics of Simple Cylindrical Hydraulic Engine Mount Utilizing Air Compressibility. *Journal of System Design and Dynamics*, 2(5):1118-1136.

Nel, C.B. 2000. Optimisation of engine mount systems at front-wheel-drive vehicles for multiple operational conditions. *ISMA25 Conference*, 2000.

Nel, C.B. & Heyns, P.S. 1996. Experimental verification of an optimization program for a front wheel drive engine mount system. *Noise and Vibration Engineering*, 21(1):1447-1457.

Nel, C.B. & Steyn, A.J. 2012. Stiffness and Damping Characterisation for a Hydraulic Engine Mount. *Proceedings of the International Modal Analysis Conference IMAC XXX*, 6:129-136.

Nel, C.B. & Van Wyngaardt, J. 2014a. Amplitude dependency on dynamic properties of a rubber mount. *Accepted for publication at IMAC XXXII conference 2014.*

Nel, C.B. & Van Wyngaardt, J. 2014b. Dynamic Vibration Absorber Design for a Motor and Pump Assembly. *Accepted for publication at IMAC XXXII conference 2014.*

Nester, T.M., Haddow, A.G. & Shaw, S.W. 2003. Vibration Reduction in a Variable Displacement Engine Using Pendulum Absorbers. *SAE International*, SAE paper 2003-01-1484:1-6.

Ooi, L.E. & Ripin, Z.M. 2011. Dynamic stiffness and loss factor measurement of engine rubber mount by impact test. *Materials & Design*, 32(4):1880-1887.

Prasad, N., Tewari, V.K. & Yadav, R. 1995. Tractor ride vibration – a review. *Journal of Terramechanics*, 32(4):205-219.

Rao, S.S. 2011. Mechanical Vibrations. 5th ed. Singapore: Pearson Prentice Hall.

Roggenkamp, T.J. & Marcella-O'Leary, L. 1996. Case Study: Experimental Low Frequency Structure-borne Coarse Road Noise Model. *International Modal Analysis Conference*, 14:320-325.

Singh, R., Kim, G. & Ravindra, P.V. 1992. Linear analysis of automotive hydro-mechanical mount with emphasis on decoupler characteristics. *Journal of Sound and Vibration*, 158(2):219-243.

Sjöberg, M. 2002. On Dynamic Properties of Rubber Isolators. Stockholm: The Marcus Wallenberg Laboratory for Sound and Vibration Research. (Thesis – PhD).

Steyn, A.J. 2011. Karakterisering en evaluering van `n hidrouliese enjinmonteerstuk. Potchefstroom: North-West University. (Dissertation – M. Eng).

Sun, J.Q., Jolly, M.R. & Norris, M.A. 1995. Passive, adaptive and active tuned vibration absorbers- A survey. *Transactions of the ASME*, 117:234-242.

Van der Linden, P.J.G. & Fun, J.K. 1993. Using Mechanical-Acoustic Reciprocity for Diagnosis of Structure Borne Sound in Vehicles. *SAE International*, SAE paper 931340:1858-1863.

Van der Linden, P.J.G. & Varet, P. 1996. Experimental Determination of Low Frequency Noise Contributions of Interior Vehicle Body Panels in Normal Operation. *SAE International*, SAE paper 960194:61-65.

Verma, H. 2002. The Stockbridge Damper as a Continuous Hysteric System in Single Overhead Transmission Lines. Bombay: Indian Institute of Technology. (Dissertation – M. Eng).

Wang, K.W. & Lai, J.S. 1993. Control of an adaptable dynamic absorber for transient vibration suppression. *Proceedings of the second conference on Recent Advances in Active Control of Sound and Vibration*:506-515.

West, J.P. 1987. Hydraulically-damped engine-mounting. *Automotive Engineer*, 12:17-19.

Wyckaert, K. & Van der Auweraer, H. 1995. Operational Analysis, Transfer Path Analysis, Modal Analysis: Tools to Understand Road Noise Problems in Cars. *SAE International*, SAE paper 951251:139-143.

Yang, Y., Li, D. & Cheng, L. 2011. Dynamic vibration absorbers for vibration control within a frequency band. *Journal of Sound and Vibration*, 330:1582-1598.

APPENDIX A – HARDWARE SPECIFICATIONS

Rubber mount

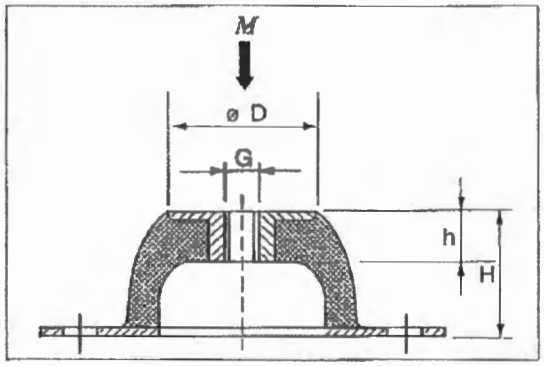

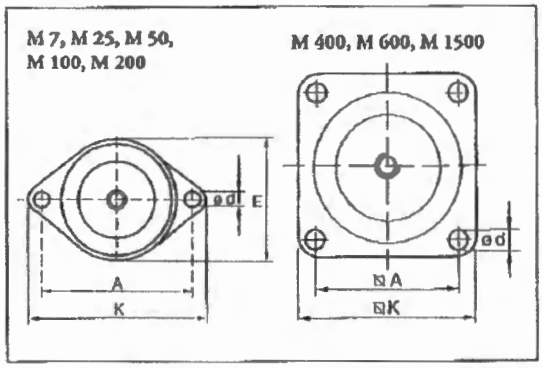

Type	Art.No. 40° IRH	Art.No. 60° IRH	Dimensions in mm D	E	A	K	H	h	d	G	Weight (kg)	*M*-Max(kg) 40° IRH	60° IRH
M 7	2255110	2255120	18	43	50	64	20	7	7.0	M 6	0.02	3.5	9
M 25	1861220	1861230	33	56	66	85	25	11	8.0	M 8	0.07	20	50
M 50	1861240	1861250	45	76	92	114	35	14	10.0	M 10	0.16	40	80
M 100	1861620	1861610	53	96	110	136	40	15	11.5	M 10	0.26	70	150
M 200	1861660	1861670	58	101	124	151	45	13	11.5	M 10	0.42	130	220
M 400	1861680	1861690	78		120	150	63	18	14.5	M 12	1.06	280	500
M 600	1533710	1533720	100		160	200	85	25	14.5	M 16	2.35	380	750
M 1500	1533730	1533740	186		250	310	160	43	18.0	M 24	9.43	1400	2500

Linear guide shafts

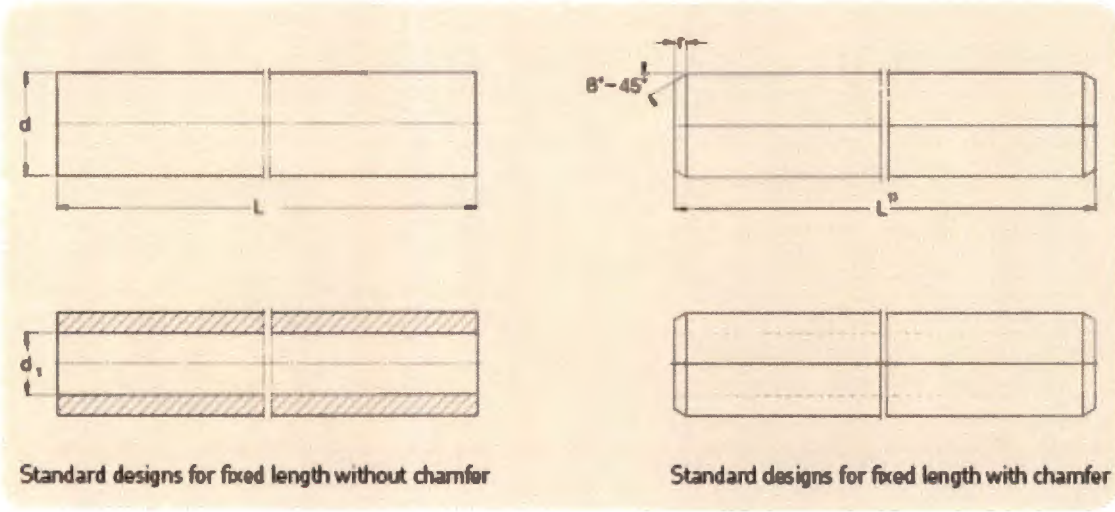

Standard designs for fixed length without chamfer

Standard designs for fixed length with chamfer

Dimension			Mass		Moment of inertia		Cross sectional area		Designations				
			Solid shaft	Hollow shaft	Solid shaft	Hollow shaft	Solid shaft	Hollow shaft	Solid shafts of precision steel	Solid shafts of stainless steel		Solid shafts with high grade steel hard chromium	Hollow shaft high grade steel plated
d	d_1	r_{max}							Cf53/Ck53	X90CrMoV18	X46Cr13	Cf53/Ck53	Ck60/100Cr6
mm			kg/m		cm⁴		mm²						
3	—	0,4	0,06	—	0,0004	—	7,1	—		LJMR 3			
4	—	0,4	0,1	—	0,0013	—	12,6	—		LJMR 4			
5	—	0,8	0,15	—	0,0031	—	19,6	—	LJM 5	LJMR 5	LJMS 5	LJMH 5	
6		0,8	0,22	—	0,0064	—	28,3	—	LJM 6	LJMR 6	LJMS 6	LJMH 6	
8	—	0,8	0,39	—	0,020	—	50,3	—	LJM 8	LJMR 8	LJMS 8	LJMH 8	
10	—	0,8	0,62	—	0,049	—	78,5	—	LJM 10	LJMR 10	LJMS 10	LJMH 10	
12	4	1	0,89	0,79	0,102	—	113	—	LJM 12	LJMR 12	LJMS 12	LJMH 12	LJT 12
14	—	1	1,21	—	0,189	—	154	—	LJM 14	LJMR 14	LJMS 14	LJMH 14	
16	7	1	1,58	1,28	0,322	0,310	201	163	LJM 16	LJMR 16	LJMS 16	LJMH 16	LJT 16
20	14	1,5	2,47	1,25	0,785	0,597	314	160	LJM 20	LJMR 20	LJMS 20	LJMH 20	LJT 20
25	16	1,5	3,86	2,35	1,92	1,64	491	305	LJM 25	LJMR 25	LJMS 25	LJMH 25	LJT 25
30	18	1,5	5,55	3,5	3,98	3,46	707	453	LJM 30	LJMR 30	LJMS 30	LJMH 30	LJT 30
40	28	2	9,86	4,99	12,6	9,96	1 260	685	LJM 40	LJMR 40	LJMS 40	LJMH 40	LJT 40
50	30	2	15,4	9,91	30,7	27,7	1 960	1 350	LJM 50	LJMR 50	LJMS 50	LJMH 50	LJT 50
60	36	2,5	22,2	14,2	63,6	57,1	2 830	1 920	LJM 60	LJMR 60	LJMS 60	LJMH 60	LJT 60
80	57	2,5	39,5	19,43	201	153	5 030	2 565	LJM 80			LJMH 80	LJT 80

Attention:
d_1 can deviate from the value quoted. Please enquire if necessary.
Different shaft diameters and types on request.
The static load capacity has to be decreased by 8 % and the dynamic load capacity by 18 % when using the non corrosion types (HV6) in conjunction with precision steel shafts made of stainless steel.

[1] Width 22 does not correspond to series 1 in ISO standard 10285.
[2] not factory pre-lubricated

Linear guide bearings

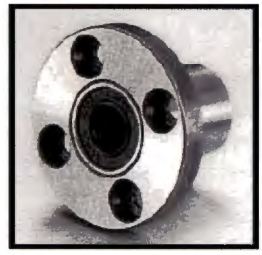

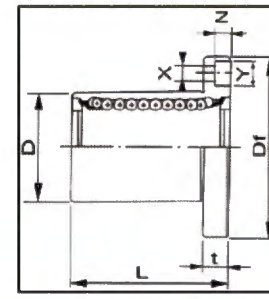

PART	d	D	L	Df	Dp	Circuits	C (N)	Co (N)	Weight(g)
LMF 8 UU	8	15	24	32	24	4	274	392	37
LMF 10 UU	10	19	29	40	29	4	372	549	72
LMF 12 UU	12	21	30	42	32	4	510	784	76
LMF 16 UU	16	28	37	48	38	5	774	1180	120
LMF 20 UU	20	32	42	54	43	5	882	1370	180
LMF 25 UU	25	40	59	62	51	6	980	1570	340
LMF 30 UU	30	45	64	74	60	6	1570	2740	470
LMF 40 UU	40	60	80	96	78	6	2160	4020	1060
LMF 50 UU	50	80	100	116	98	6	3820	7940	2200
LMF 60 UU	60	90	110	134	112	6	4700	10000	3000

Eddy current probe (Ø18)

SPECIFICATIONS	
CALIBRATION MATERIAL	JIS SCM440 flat surface
LINEAR RANGE*3	Over 6mm (begins at approx. 0.3mm from sensor tip)
SENSITIVITY*3	2.5V/mm
SENSITIVITY ERROR*3	Within ±4%
LINEARITY*3	Within ±90μm of 2.5V/mm straight line (if calibrated as a system) Within ±120μm of 2.5V/mm straight line (including interchangeability errors)
FREQUENCY RESPONSE*3	DC to 10kHz (-3dB)
MAX. OUTPUT VOLTAGE*3	Approx -22VDC
OUTPUT IMPEDANCE*3	50Ω
CURRENT CONSUMPTION (10kΩ load)	Max. -13mA
SENSOR TIP DIAMETER	Approx. 18mm dia.
CABLE DIAMETER	Approx. 6mm dia. (with armor : max. 10mm dia.)
CONNECTOR DIAMETER	Approx. 9.5mm dia.
SYSTEM CABLE LENGTH	5m±10% or 9m±10%
OPERATING TEMPERATURE RANGE	Sensor : -40 to +125°C Extension Cable : -40 to +125°C Driver : -38 to +80°C
RANGE OF TEMPERATURE AT EXPLOSION PROOF CONSTRUCTION	EX4 : -20 to +85°C (Sensor, Ext. Cable & Driver) EX5 : -38 to +85°C (Sensor, Ext. Cable & Driver)
TEMPERATURE CHARACTERISTIC	Sensor : Less than ±3% of F.S. Extension Cable : Less than ±3% of F.S. Condition : Gap=3.6mm, Target : JIS SCM440 0 to 80°C (at 20°C standard) Driver : Less than ±4% of F.S. Roop : Less than ±4% of F.S. Condition : Gap=3.6mm, Target : JIS SCM440 0 to 60°C (at 20°C standard)
OPERATING HUMIDITY RANGE	30 to 95% RH (noncondensing, non-submerged) (sensor body : 100%)
POWER SUPPLY	-24VDC ± 10%
DIELECTRIC STRENGTH OF DRIVER	Between each terminal and insulator: 1mA or less at 500VAC for one minute
INSULATION RESISTANCE OF DRIVER	Between each terminal and insulator: 100MΩ or more at 500VDC
SCREWS OF TERMINAL BLOCK	M4
APPLICABLE WIRE GAUGE	0.75 to 2mm^2

*3 The above specifications apply at 25°C with -24VDC power supply and JIS SCM440 target (thickness≥5mm).

NOTICE

1. CALIBRATION MATERIAL
   MODEL VK-602P Transducers are calibrated for JIS SCM440 flat surface (more than 54mm dia.).
   If the measured target is other than JIS SCM440 flat surface, it will present a different characteristics. In such a case, calibration by the connected equipment (e.g. monitor) side should be required for system operation.
2. INSULATORS
   Prior to shipment, the insulators have been installed to the mounting holes of VK driver.
   Be sure to mount VK driver without removing insulators.
   Mounting without insulators could cause noise on driver output.
3. SHIELD WIRE CONNECTION
   Connect shield wire of signal cable (3-wire shielded cable between driver and monitor) to COM terminal.
   If this is not adhered to, noise may be caused.
4. CONNECTOR ISOLATION, etc.
   The connector connecting the sensor cable and the extension cable shall be insulated with the attached insulation sleeve (transparent shrink tube) or fluoro resin insulation tape.
   The vinyl-insulating tape shall not be used, which may cause the wiring trouble in the case of the temperature more than 80°C.
   The connector shall not be located in the oil environment.
   The oil penetration to cable through the connector may cause the sensitivity change, due to the change of the cable capacitance.
5. MEGGER TEST OF SIGNAL CABLE
   If megger test is made on the signal cable (3-wire shielded cable), be sure to discharge the charged electric load before connecting the cable to driver.
   If this caution is not adhered the driver could be damaged.
6. SENSOR INSTALLATION
   Not available for rain water at out door use.
   It may cause the sensitivity change and insulation down.
7. SAFETY BARRIER
   In case of the intrinsically safe specification, the approved following safety barrier is recommended.
   - MTL 796-
8. CALIBRATED AS A SYSTEM
   The sensor, extension cable and driver, which are calibrated as a system, shall be connected with each serial No. as specified in the inspection test report. If this is not adheared the output characteristics may be out of specification.

Other

Eddy current probe (Ø25)

SPECIFICATIONS	
CALIBRATION MATERIAL*3	JIS SCM440 flat surface
LINEAR RANGE*3	Over 13.5mm(begins at approx.3mm from sensor tip)
SENSITIVITY*3	0.8V/mm
SENSITIVITY ERROR*3	Within ± 4%
LINEARITY*3	Within ± 200μm of 0.8V/mm straight line (if calibrated as a system) Within ± 270μm of 0.8V/mm straight line (including interchangeability errors)
FREQUENCY RESPONSE*3	DC to 3kHz (-3dB) at 12mm pk-pk
MAX. OUTPUT VOLTAGE*3	Approx.-22VDC
OUTPUT IMPEDANCE*3	50Ω
CURRENT CONSUMPTION (10kΩ load)	Max. -20mA
SENSOR TIP DIAMETER	Approx. 25mm dia.
CABLE DIAMETER	Approx. 6mm dia. (with armor : max. 10mm dia.)
CONNECTOR DIAMETER	Approx. 9.5mm dia
SYSTEM CABLE LENGTH	5m ± 10% or 9m ± 10%
OPERATING TEMPERATURE RANGE	Sensor : -40 to +125°C Extension Cable : -40 to +125°C Driver : -38 to +80°C
TEMPERATURE CHARACTERISTIC	Sensor : Less than ± 3% of F.S. Extension Cable : Less than ± 2% of F.S. Condition : Gap=11mm, Target : JIS SCM440 0 to 80°C (at 20°C standard) Driver : Less than ± 4% of F.S. Roop : Less than ± 4% of F.S. Condition : Gap=11mm, Target : JIS SCM440 0 to 60°C (at 20°C standard)
OPERATING HUMIDITY RANGE	30 to 95% RH (noncondensing, non-submerged) (sensor body : 100%)
POWER SUPPLY	-24VDC ± 10%
DIELECTRIC STRENGTH OF DRIVER	Between each terminal and insulator: 1mA or less at 500VAC for one minute
INSULATION RESISTANCE OF DRIVER	Between each terminal and insulator: 100MΩ or more at 500VDC
SCREWS OF TERMINAL BLOCK	M4
APPLICABLE WIRE GAUGE	0.75 to 2mm²

*3 The above specifications apply at 25°C with -24VDC power supply and load resistance 10kΩ and JIS SCM440 target (thickness≥5mm).

NOTICE

1. CALIBRATION MATERIAL
   MODEL VK-143P Transducers are calibrated for JIS SCM440 flat surface (more than 155mm dia.).
   If the measured target is other than JIS SCM440 flat surface, it will present a different characteristics. In such a case, calibration by the connected equipment (e.g. monitor) side should be required for system operation.
2. INSULATORS
   Prior to shipment, the insulators have been installed to the mounting holes of VK driver.
   Be sure to mount VK driver without removing insulators.
   Mounting without insulators could cause noise on driver output.
   Special caution to insulaters shall be paid for the intrinsic safety specification so that a system shall be earth grounded only at the barrier strip.
3. SHIELD WIRE CONNECTION
   Connect shield wire of signal cable (3-wire shielded cable between driver and monitor) to COM terminal.
   If this is not adhered to, noise may be caused.
4. CONNECTOR ISOLATION, etc.
   The connector connecting the sensor cable and the extension cable shall be insulated with the attached insulation sleeve (transparent shrink tube) or Teflon insulation tape.
   The vinyl-insulating tape shall not be used, which may cause the wiring trouble in the case of the temperature more than 80°C.
   The connector shall not be located in the oil environment.
   The oil penetration to cable through the connector may cause the sensitivity change, due to the change of the cable capacitance.
5. MEGGER TEST OF SIGNAL CABLE
   If megger test is made on the signal cable (3-wire shielded cable), be sure to discharge the charged electric load before connecting the cable to driver.
   If this caution is not adhered the driver could be damaged.
6. SENSOR INSTALLATION
   Not available for rain water at out door use.
   It may cause the sensitivity change and insulation down.
7. SAFETY BARRIER
   In case of the intrinsically safe specification, the approved following safety barrier shall be used.
   - MTL 796-

   Don't be used except the specified.
8. CALIBRATED AS A SYSTEM
   The sensor, extension cable and driver, which are calibrated as a system, shall be connected with each serial No. as specified in the inspection test report. If this is not adheared the output characteristics may be out of specification.

Other

APPENDIX B – MATLAB COMPUTER PROGRAMS

Noise filter

```
%Frequency domain signals

load JO05a.dat;
f=JO05a(:,2);
af=9.81*JO05a(:,1);

load JO05b.dat;
f1=JO05b(:,2);
af1=9.81*JO05b(:,1);

%%Lt= 256;
%%Lf= 101;
Lf=length(f);
Lf1=length(f1);

figure(1);

subplot(2,1,1);plot(f(1:Lf),af(1:Lf),'b')
ylabel('Mass Acceleration [m/s^2]')
xlabel('Frequency [Hz]')

subplot(2,1,2);plot(f1(1:Lf1),af1(1:Lf1),'b')
ylabel('Base Acceleration [m/s^2]')
xlabel('Frequency [Hz]')

%%%%%%%%%%%%%%%%%%%%%%%%%%%%%%%%%%%%%%%%%%%%%%%%%%%%%%%%%%%%%%%%%%%%%%%%%%%%%%%

%Time domain signals

load JO06a.dat;
t=JO06a(:,2);
Ro=9.81*JO06a(:,1);

load JO06b.dat;
t1=JO06b(:,2);
Rt=9.81*JO06b(:,1);

%%Lt= 256;
%%Lf= 101;
Lt=length(t);
Lt1=length(t1);

figure(2);

subplot(2,1,1);plot(t(1:Lt),Ro(1:Lt),'b')
ylabel('Mass Acceleration [m/s^2]')
xlabel('Time [sec]')

subplot(2,1,2);plot(t1(1:Lt1),Rt(1:Lt1),'b')
ylabel('Base Acceleration [m/s^2]')
xlabel('Time [sec]')
```

```
fs=1/t(2);

%=========================================================================
% Load data
%=========================================================================
% Compute FFTs on two time domain signals
%=========================================================================

np=length(t);
f=fs*(0:np-1)/np;

FRo=fft(Ro);
PRo=abs(FRo)*2/np;
aRo=angle(FRo);

FRt=fft(Rt);
PRt=abs(FRt)*2/np;
aRt=angle(FRt);

%=========================================================================
% Plot spectrum
%=========================================================================

npl=1:(201);

figure(3)

subplot(2,1,1);plot(f(npl),PRo(npl),'b')
ylabel('Abs (Roe) [m/s^2]')
xlabel('Frequency [Hz]')

subplot(2,1,2);plot(f(npl),aRo(npl),'b')
ylabel('Phase (Roe) [rad]')
xlabel('Frequency   [Hz]')

figure(4)

subplot(2,1,1);plot(f(npl),PRt(npl),'b')
ylabel('Abs (Rte) [m/s^2]')
xlabel('Frequency [Hz]')

subplot(2,1,2);plot(f(npl),aRt(npl),'b')
ylabel('Phase (Rte) [rad]')
xlabel('Frequency   [Hz]')

%=========================================================================
% Fourier coefficients
%=========================================================================

datRo=[2*pi*f(npl); PRo(npl)'; aRo(npl)'];
datRt=[2*pi*f(npl); PRt(npl)'; aRt(npl)'];

%=========================================================================
% Reconstruct Time domain signals with noise
%=========================================================================

E=length(t);
```

```
for j=1:E;
Ros(j)=sum(datRo(2,:).*cos(datRo(1,:)*t(j)+datRo(3,:)));
Rts(j)=sum(datRt(2,:).*cos(datRt(1,:)*t(j)+datRt(3,:)));
end

%=========================================================================
% Store Fourier coefficients to folders
%=========================================================================

a=datRo(109)';
b=datRt(109)';

save Ro.dat a -ascii;
save Rt.dat b -ascii;

%=========================================================================
% Reconstruct Time domain signals without noise
%=========================================================================

for j=1:E;
Ros(j)=(datRo(2,109).*cos(datRo(1,109)*t(j)+datRo(3,109)));
Rts(j)=(datRt(2,109).*cos(datRt(1,109)*t(j)+datRt(3,109)));
end

%=========================================================================
% Plot Time domain signals with and without noise
%=========================================================================

figure(5)       %Time domain signals with and without noise.

subplot(2,1,1);plot(t,Ro,'r',t,Ros,'b')
ylabel('Ro [m/s^2]')
xlabel('Time [s]')

subplot(2,1,2);plot(t,Rt,'r',t,Rts,'b')
ylabel('Rt [m/s^2]')
xlabel('Time [s]')

figure(6)       %Time domain signals without noise.

subplot(2,1,1);plot(t,Ros,'b')
ylabel('Ros [m/s^2]')
xlabel('Time [s]')

subplot(2,1,2);plot(t,Rts,'b')
ylabel('Rts [m/s^2]')
xlabel('Time [s]')

phaseRorad = datRo(3,109);
phaseRtrad = datRt(3,109);
phasedifrad1 = phaseRtrad - phaseRorad

%=========================================================================
% Amplitudes at forced Frequency
%=========================================================================

AmplRo1 = datRo(2,109)
AmplRt1 = datRt(2,109)
```

Dynamic characteristics

```
m    = 10.4129;     %Absorber mass [kg]

X = zeros(1,1);
Y = zeros(1,1);
phi = zeros(1,1);
omega = zeros(1,1);
c_mount = zeros(1,1);
k_mount = zeros(1,1);
fre = zeros(1,1)

fre(1,1) = 27;                 %Forced frequency      [Hz]
omega(1,1) = 2*pi*fre(1,1);    %Forced frequency      [rad/s]
X(1,1) =  0.1800;              %Acceleration at mass  [m/s^2]
Y(1,1) = 0.3529;               %Acceleration at base  [m/s^2]
phi(1,1) = -3.4006;            %Phase difference      [rad]


for i = 1:1
    for j = 1:1

syms k c;

eq1 = sqrt((k^2.+(c*omega(i,j))^2.)/((k-m*omega(i,j)^2.)^2.+...
     (c*omega(i,j))^2.))-(X(i,j)/Y(i,j));
eq2 =(m*c*omega(i,j)^3.)/((k*(k-m*omega(i,j)^2.)+...
     (omega(i,j)*c)^2.))-tan(phi(i,j));

[c,k] = solve(eq1,eq2,k,c);

Stiffness1 = double(k);
Damping2 = double(c);

Stiffness = max(Stiffness1);
Damping = max(Damping2);

k_mount(i,j) = Stiffness;
c_mount(i,j) = Damping;

    end
end

Cc(1,1) = 2*sqrt(k_mount(1,1)*m);    %Critical damping coefficient [Ns/m]
psi(1,1) = (c_mount(1,1)/Cc(1,1));   %Damping ratio
XY(1,1) = X(1,1)/Y(1,1);             %Relative movement
Degrees(1,1) = phi(1,1)*((180)/pi);  %Phase difference [Degrees]
```

Runge-Kutta algorithms

Single-degree-of-freedom system – road forces

```
%Subscript 'e' is for the Engine

format long g

m_e=170.5+4.1+4.5              %Engine mass [kg]
k_e=1046.97E3                  %Engine mount stiffness coefficient [N/m]
c_e=1050.94                    %Engine mount damping coefficient [Ns/m]

w=2*pi*12.25                   %Forced frequency [rad/s]
F0=8.292                       %Force acting at base [N]
Y=F0/(sqrt(k_e^2+(c_e*w)^2))   %Displacement at base [m]

%.....................................................................

tspan = [0:0.001:5];     %Integration range
x0 = [0; 0];             %Initial conditions for x0 = [x(1);x(2)]
[t,x] = ode45('funcSDOF_wheels',tspan,x0,[],k_e,m_e,c_e,w,Y);

%.....................................................................
%Compute dynamic forces transmitted

x_e = (x(:, 1))*1000;              %Steady state response of Engine [mm]
max_e = max(x_e(t >= 4 & t <= 5))  %Maximum displacement of Engine
                                   %for steady state response [mm]

Fk_e = k_e*max_e/1000     %Dynamic force transmitted by Engine spring [N]
Fc_e = c_e*w*max_e/1000   %Dynamic force transmitted by Engine damper [N]

Ft_e = sqrt(Fk_e^2 + Fc_e^2)  %Dynamic force transmitted by
                              %Engine mounts [N]

%.....................................................................
%Plot the response

subplot(211);
plot(t,x_e);
xlabel('t [sec]');
ylabel('x_e(t) [mm]');

%.....................................................................

function dxdt = funcSDOF_wheels(t,x,flag,k_e,m_e,c_e,w,Y)

%Reduce the given differential equations to a series of first order
equations
%x(1)=x_e(t); x(2)=dx_e/dt

dxdt = zeros (size(x));     %The array dxdt is the same length as x

dxdt(1) = x(2);
dxdt(2) = ((-k_e*x(1))-(c_e*x(2))+(k_e*Y*sin(w*t))+...
          (c_e*Y*w*cos(w*t)))/m_e;
```

Two-degree-of-freedom system – road forces

```
%Subscript 'e' is for the Engine
%Subscript 'a' is for the Absorber

format long g

m_e= 170.5+4.1+4.5              %Engine mass [kg]
k_e= 1061.27E3                  %Engine mount stiffness coefficient [N/m]
c_e= 1100.98                    %Engine mount damping coefficient [Ns/m]

m_a= 10.4129                    %Absorber mass [kg]
k_a= 90.76E3                    %Absorber mount stiffness coefficient [N/m]
zeta_a= 0.031                   %Absorber mount damping ratio
cc_a=2*sqrt(m_a*k_a)            %Absorber mount critical damping
                                %coefficient [Ns/m]
c_a=zeta_a*cc_a                 %Absorber mount damping coefficient [Ns/m]

w= 12.25*2*pi                   %Forced frequency [rad/s]
F0= 8.292                       %Force acting at base [N]
Y=F0/(sqrt(k_e^2+(c_e*w)^2))    %Displacement at base [m]

%.....................................................................

tspan = [0:0.001:5];   %Integration range
x0 = [0; 0; 0; 0];     %Initial conditions for x0 = [x(1);x(2);x(3);x(4)]
[t,x] = ode45('funcTDOF_wheels',tspan,x0,[],k_e,m_e,k_a,m_a,w,Y,c_e,c_a);

%.....................................................................
%Compute dynamic forces transmitted

x_e=(x(:, 1))*1000;                 %Steady state response of Engine [mm]
max_e = max(x_e(t >= 4 & t <=5 ))   %Maximum displacement of Engine
                                    %for steady state response [mm]

Fk_e=k_e*max_e/1000     %Dynamic force transmitted by Engine spring [N]
Fc_e=c_e*w*max_e/1000   %Dynamic force transmitted by Engine damper [N]

Ft_e=sqrt(Fk_e^2 + Fc_e^2)  %Dynamic force transmitted by
                            %Engine mounts [N]

x_a=(x(:, 3))*1000;                 %Steady state response of Absorber [mm]

%.....................................................................
%Plot the response

subplot(211);
plot(t,x_e);
xlabel('t [sec]');
ylabel('x_e(t) [mm]');

subplot(212);
plot(t,x_a);
xlabel('t [sec]');
ylabel('x_a(t) [mm]');
```

```
%.....................................................................

function dxdt = funcTDOF_wheels(t,x,flag,k_e,m_e,k_a,m_a,w,Y,c_e,c_a)

%Reduce the given differential equations to a series of first order
equations
%x(1)=x_e(t); x(2)=dx_e/dt; x(3)=x_a(t); x(4)=dx_a/dt

dxdt = zeros (size(x));     %The array dxdt is the same length as x

dxdt(1) = x(2);
dxdt(2) = ((-(c_e+c_a)*x(2))+(c_a*x(4))-((k_e+k_a)*x(1))+...
          (k_a*x(3))+(k_e*Y*sin(w*t))+(c_e*Y*w*cos(w*t)))/m_e;

dxdt(3) = x(4);
dxdt(4) = ((c_a*x(2))-(c_a*x(4))+(k_a*x(1))-(k_a*x(3)))/m_a;
```

Single-degree-of-freedom system – internal engine shaking forces

```
%Subscript 'e' is for the Engine

format long g

m_e=170.5+4.1+4.5                %Engine mass [kg]
k_e=1097.78E3                    %Engine mount stiffness coefficient [N/m]
c_e=1419.37                      %Engine mount damping coefficient [Ns/m]

w=23.88*2*pi                     %Forced frequency [rad/s]
F0=55.427                        %Force acting at Engine [N]

%.....................................................................

tspan = [0:0.001:5];      %Integration range
x0 = [0; 0];              %Initial conditions for x0 = [x(1);x(2)]
[t,x] = ode45('funcSDOF_engine',tspan,x0,[],k_e,m_e,F0,w,c_e);

%.....................................................................
%Compute dynamic forces transmitted

x_e = (x(:, 1))*1000;             %Steady state response of Engine [mm]
max_e = max(x(t >= 4 & t <= 5))   %Maximum displacement of Engine
                                  %for steady state response [mm]

Fk_e = k_e*max_e/1000     %Dynamic force transmitted by Engine spring [N]
Fc_e = c_e*w*max_e/1000   %Dynamic force transmitted by Engine damper [N]

Ft_e = sqrt(Fk_e^2 + Fc_e^2)  %Dynamic force transmitted by
                              %Engine mounts [N]

%.....................................................................
%Plot the response

subplot(211);
plot(t,x_e);
xlabel('t [sec]');
ylabel('x_e(t) [mm]');

%.....................................................................

function dxdt = funcSDOF_engine(t,x,flag,k_e,m_e,F0,w,c_e)

%Reduce the given differential equations to a series of first order
equations
%x(1)=x_e(t); x(2)=dx_e/dt

dxdt = zeros (size(x));     %The array dxdt is the same length as x

dxdt(1) = x(2);
dxdt(2) = ((-k_e*x(1))-(c_e*x(2))+(F0*cos(w*t)))/m_e;
```

Two-degree-of-freedom system – internal engine shaking forces

```
%Subscript 'e' is for the Engine
%Subscript 'a' is for the Absorber

format long g

m_e=170.5+4.1+4.5                %Engine mass [kg]
k_e=1097.78E3                    %Engine mount stiffness coefficient [N/m]
c_e=1419.37                      %Engine mount damping coefficient [Ns/m]

m_a=10.4129                      %Absorber mass [kg]
k_a=100.49E3                     %Absorber mount stiffness coefficient [N/m]
zeta_a=0.050                     %Absorber mount damping ratio
cc_a=2*sqrt(m_a*k_a)             %Absorber mount critical damping
                                 %coefficient [Ns/m]
c_a=zeta_a*cc_a                  %Absorber mount damping coefficient [Ns/m]

w=23.88*2*pi                     %Forced Frequency [rad/s]
F0=55.427                        %Force acting at Engine [N]

%.....................................................................

tspan = [0:0.001:5];      %Integration range
x0 = [0; 0; 0; 0];        %Initial conditions for x0 = [x(1);x(2);x(3);x(4)]
[t,x] = ode45('funcTDOF_engine',tspan,x0,[],k_e,m_e,F0,k_a,m_a,w,c_e,c_a);

%.....................................................................
%Compute dynamic forces transmitted

x_e=(x(:, 1))*1000;                 %Steady state response of Engine [mm]
max_e = max(x_e(t >= 4 & t <=5 ))   %Maximum displacement of Engine
                                    %for steady state response [mm]

Fk_e=k_e*max_e/1000     %Dynamic force transmitted by Engine spring [N]
Fc_e=c_e*w*max_e/1000   %Dynamic force transmitted by Engine damper [N]

Ft_e=sqrt(Fk_e^2 + Fc_e^2)  %Dynamic force transmitted by
                            %Engine mounts [N]

x_a=(x(:, 3))*1000;                 %Steady state response of Absorber [mm]

%.....................................................................
%Plot the response

subplot(211);
plot(t,x_e);
xlabel('t [sec]');
ylabel('x_e(t) [mm]');

subplot(212);
plot(t,x_a);
xlabel('t [sec]');
ylabel('x_a(t) [mm]');
```

```
%.....................................................................

function dxdt = funcTDOF_engine(t,x,flag,k_e,m_e,F0,k_a,m_a,w,c_e,c_a)

%Reduce the given differential equations to a series of first order
equations
%x(1)=x_e(t); x(2)=dx_e/dt; x(3)=x_a(t); x(4)=dx_a/dt

dxdt = zeros (size(x));      %The array dxdt is the same length as x

dxdt(1) = x(2);
dxdt(2) = ((-(c_e+c_a)*x(2))+(c_a*x(4))-((k_e+k_a)*x(1))+(k_a*x(3))+...
          (F0*cos(w*t)))/m_e;

dxdt(3) = x(4);
dxdt(4) = ((c_a*x(2))-(c_a*x(4))+(k_a*x(1))-(k_a*x(3)))/m_a;
```

Natural frequencies

```
format long g

m_e=170.5+4.1+4.5                    %Engine mass [kg]
k_e=1072.28E3                        %Engine mount stiffness coefficient [N/m]

m_a=10.4129                          %Absorber mass [kg]
k_a=80.605E3                         %Absorber mount stiffness coefficient [N/m]

%Compute the two natural frequencies in [Hz]

fn1 = sqrt((((k_a*m_e)+((k_e+k_a)*m_a))-sqrt((((k_a*m_e)+((k_e+k_a)*...
      m_a))^2)-(4*m_e*m_a*(((k_e+k_a)*k_e)-k_e^2))))/(8*(pi^2)*m_e*m_a))

fn2 = sqrt((((k_a*m_e)+((k_e+k_a)*m_a))+sqrt((((k_a*m_e)+((k_e+k_a)*...
      m_a))^2)-(4*m_e*m_a*(((k_e+k_a)*k_e)-k_e^2))))/(8*(pi^2)*m_e*m_a))
```

APPENDIX C – DETAILED DRAWINGS

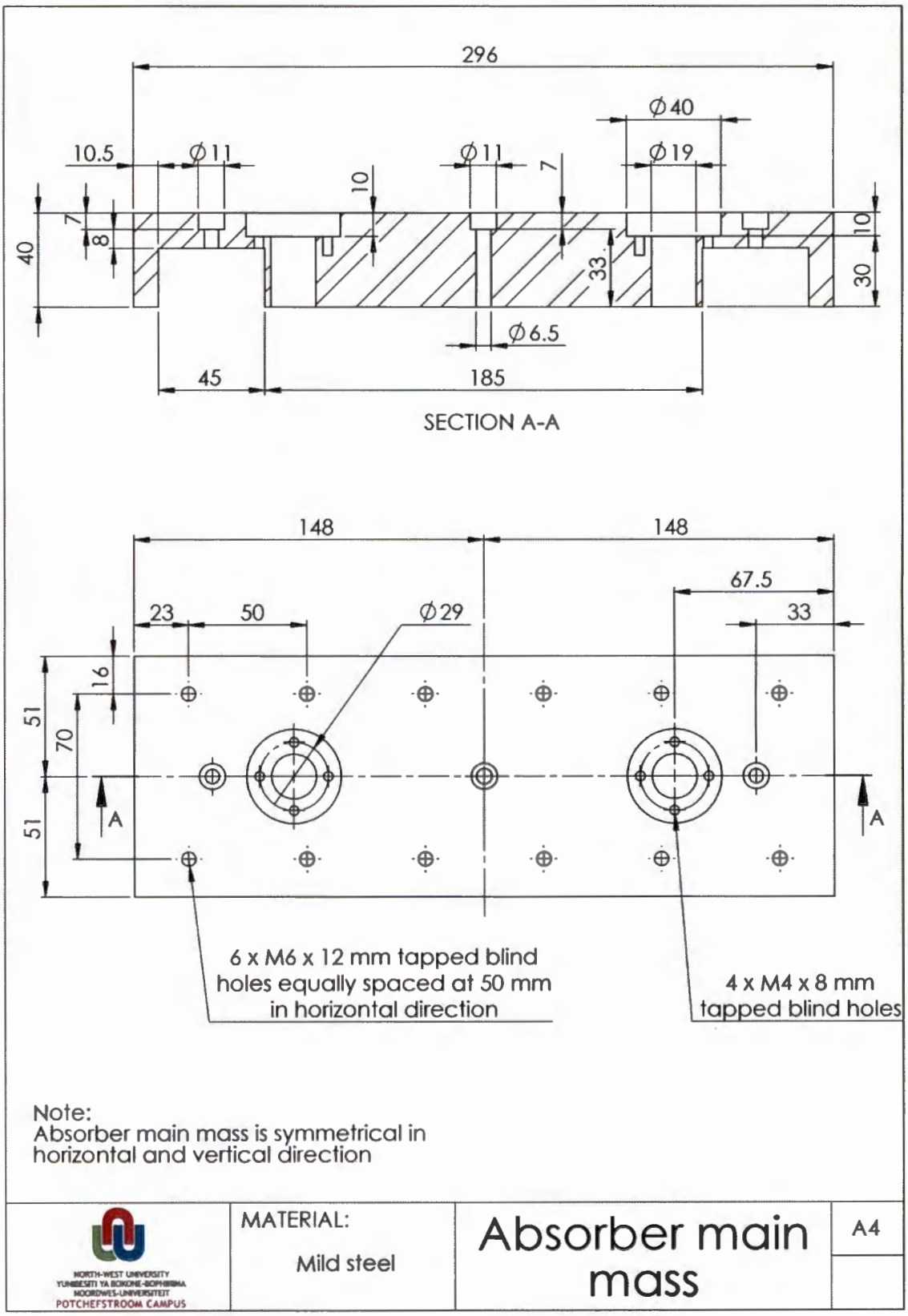

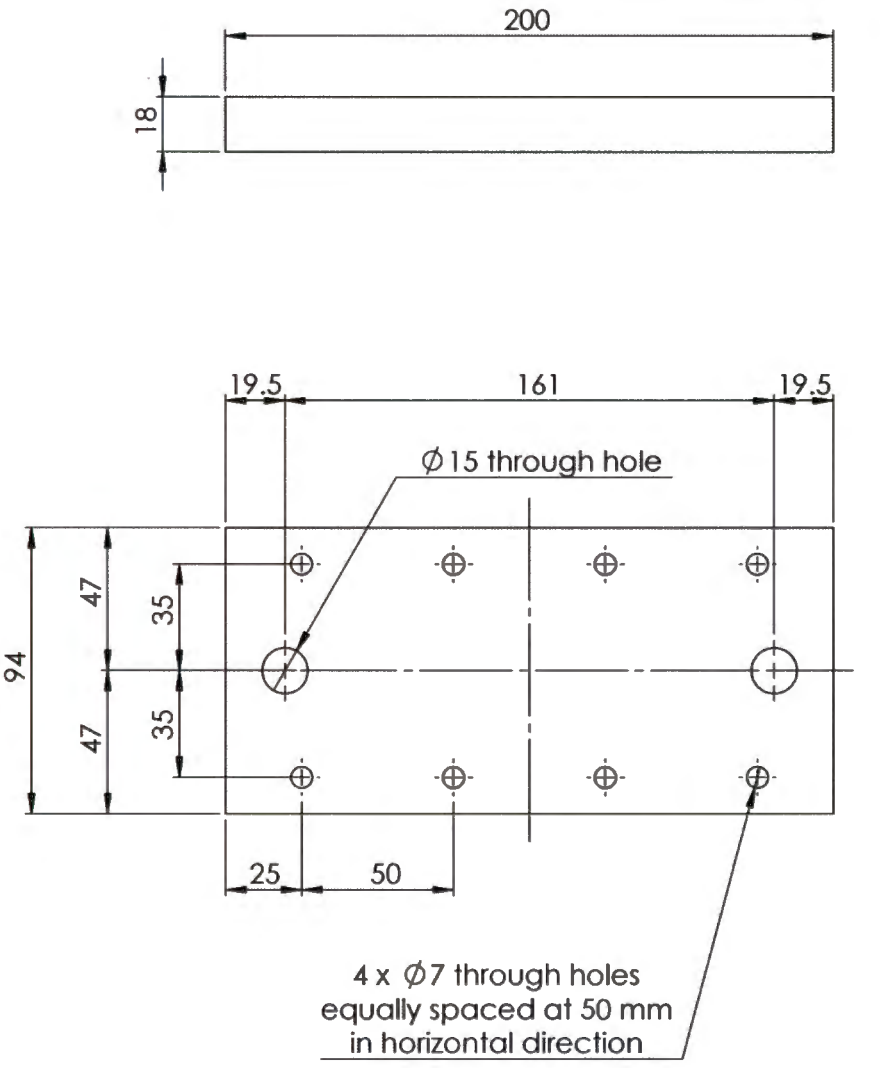

Note:
18 mm tuning mass is symmetrical in horizontal and vertical direction

NORTH-WEST UNIVERSITY YUNIBESITI YA BOKONE-BOPHIRIMA NOORDWES-UNIVERSITEIT POTCHEFSTROOM CAMPUS	MATERIAL: Mild steel	18 mm tuning mass	A4

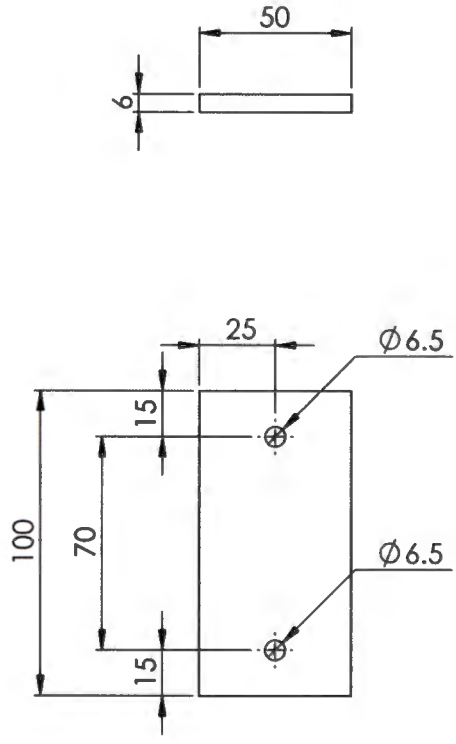

NORTH-WEST UNIVERSITY YUNIBESITI YA BOKONE-BOPHIRIMA NOORDWES-UNIVERSITEIT POTCHEFSTROOM CAMPUS	MATERIAL: Mild steel	6 mm tuning mass	A4

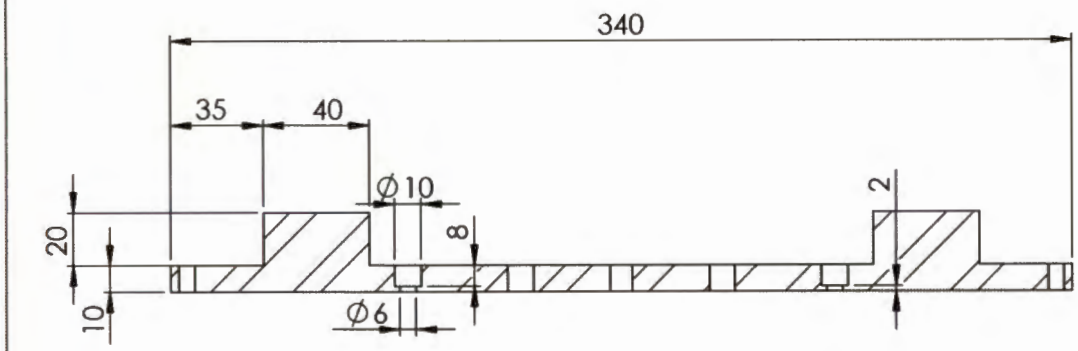

SECTION A-A

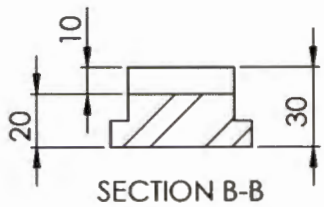

SECTION B-B

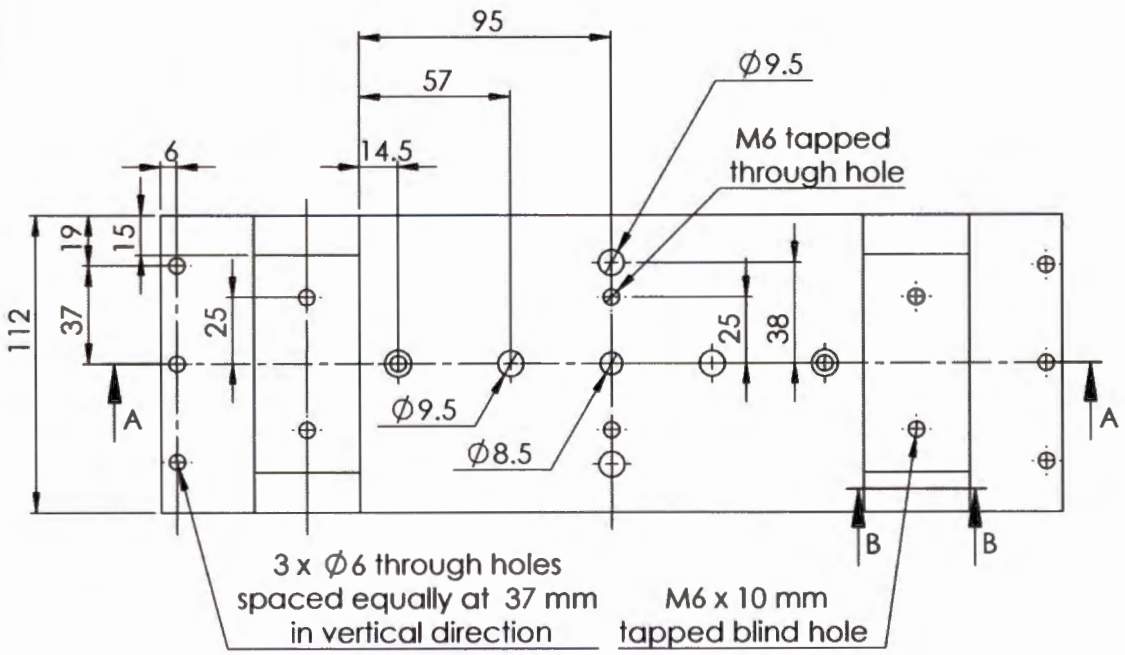

Note:
Absorber base is symmetrical in horizontal and vertical direction

NORTH-WEST UNIVERSITY YUNIBESITI YA BOKONE-BOPHIRIMA NOORDWES-UNIVERSITEIT POTCHEFSTROOM CAMPUS	MATERIAL: Mild steel	Absorber base	A4

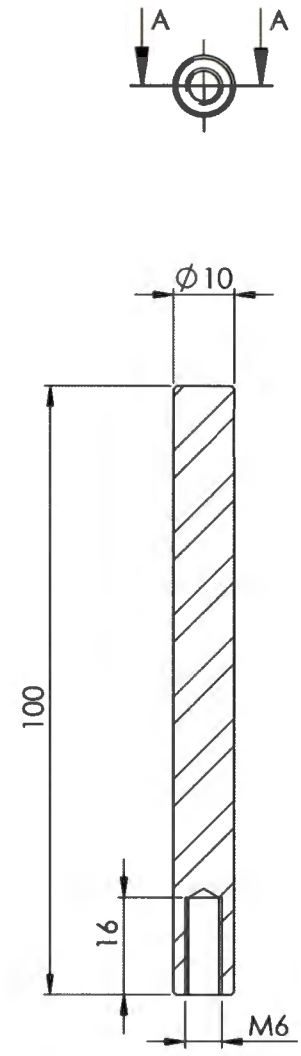

SECTION A-A

NORTH-WEST UNIVERSITY YUNIBESITI YA BOKONE-BOPHIRIMA NOORDWES-UNIVERSITEIT POTCHEFSTROOM CAMPUS	MATERIAL: Steel	Guide shaft	A4

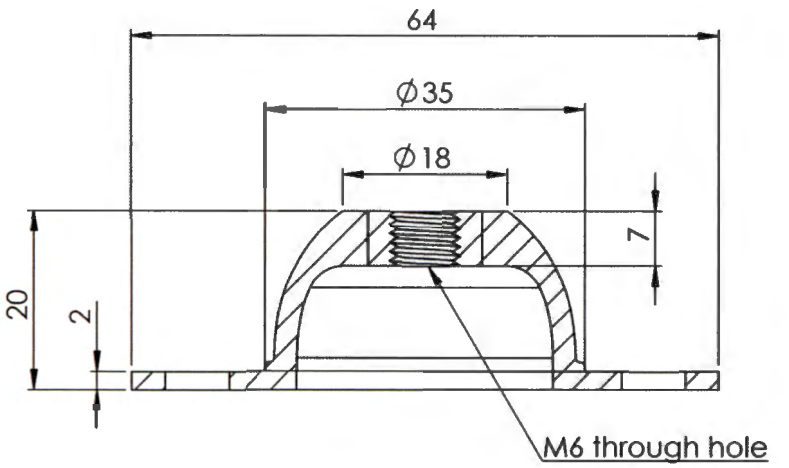

SECTION H-H

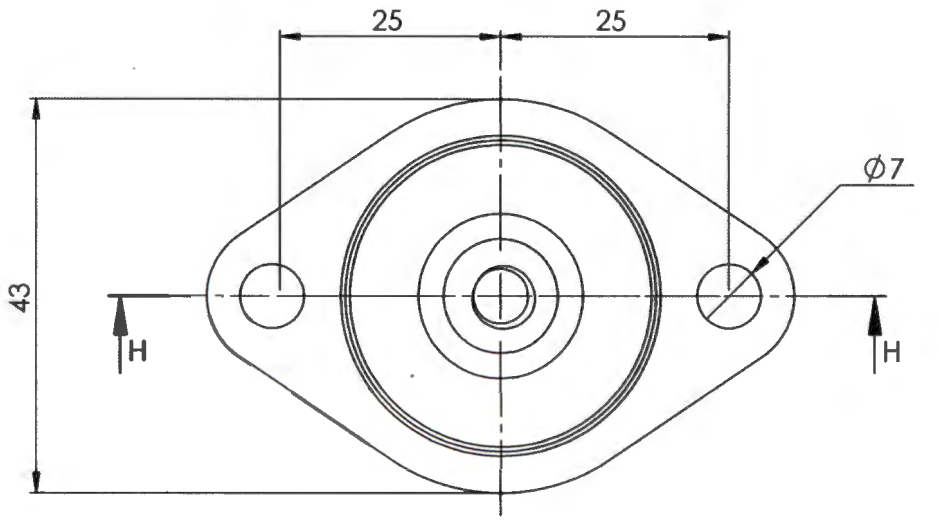

NORTH-WEST UNIVERSITY YUNIBESITI YA BOKONE-BOPHIRIMA NOORDWES-UNIVERSITEIT POTCHEFSTROOM CAMPUS	MATERIAL: N/A	Rubber mount	A4

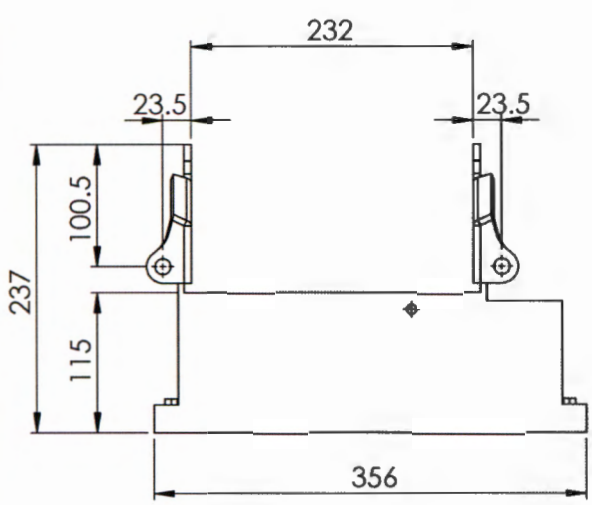

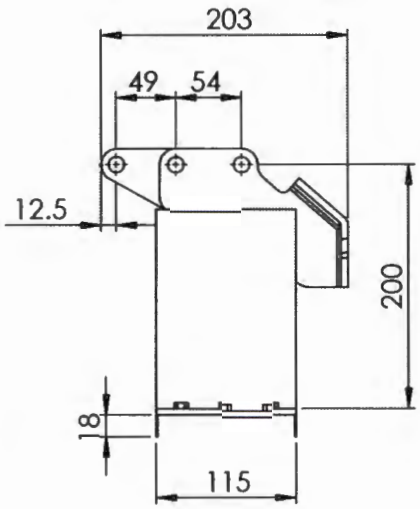

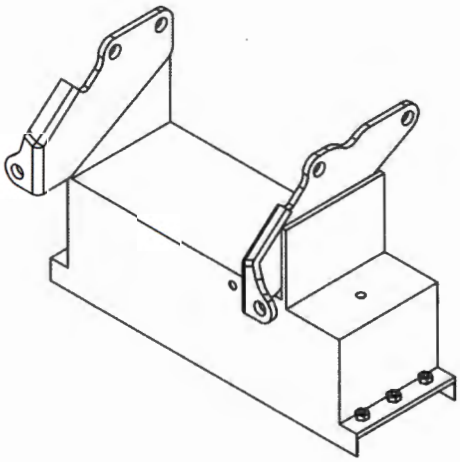

NORTH-WEST UNIVERSITY YUNIBESITI YA BOKONE-BOPHIRIMA NOORDWES-UNIVERSITEIT POTCHEFSTROOM CAMPUS	MATERIAL: Mild steel	Engine attacment bracket	A4

Exploded view

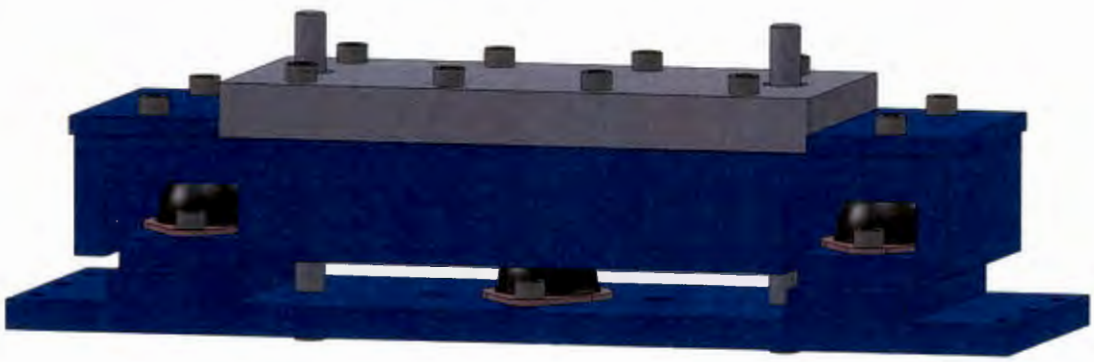

NORTH-WEST UNIVERSITY YUNIBESITI YA BOKONE-BOPHIRIMA NOORDWES-UNIVERSITEIT POTCHEFSTROOM CAMPUS	MATERIAL: N/A	Absorber assembly	A4

APPENDIX D – VIBRATION MEASUREMENTS

Road tests – Original system

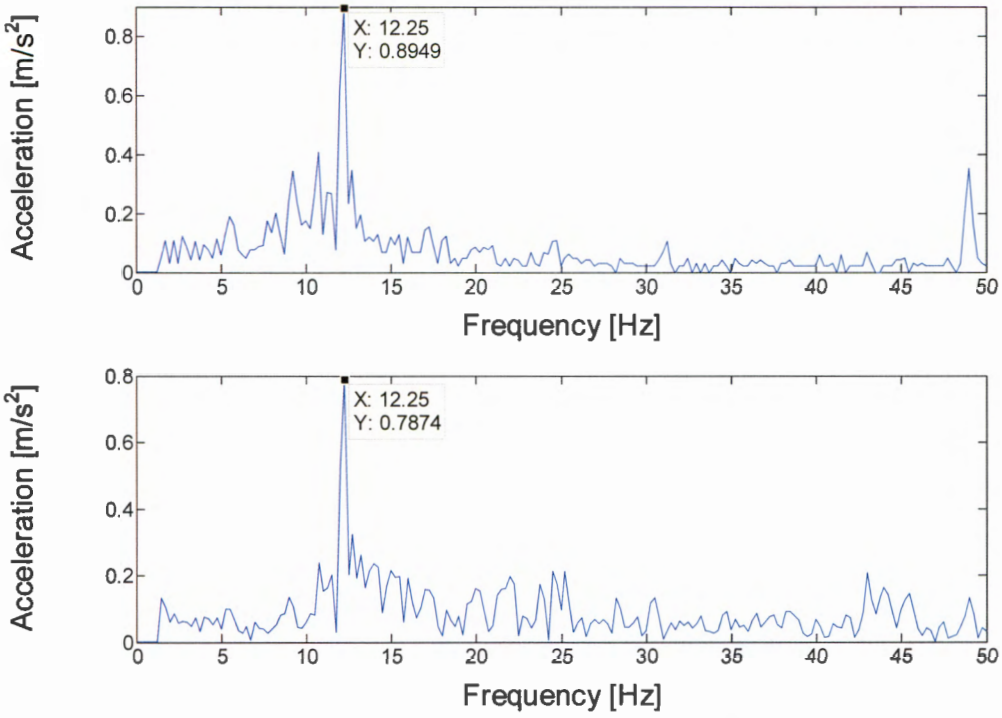

Figure D.1: Engine (top) and structure (bottom) response at 80 km/h with balanced wheels for Original system.

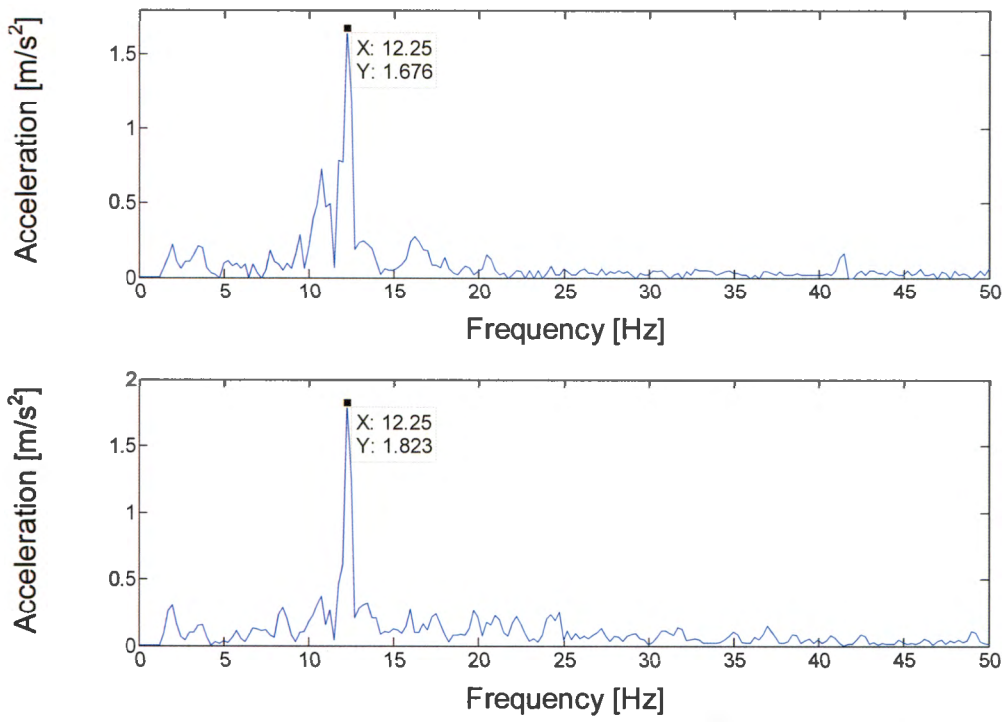

Figure D.2: Engine (top) and structure (bottom) response at 80 km/h with 120 g unbalance for Original system.

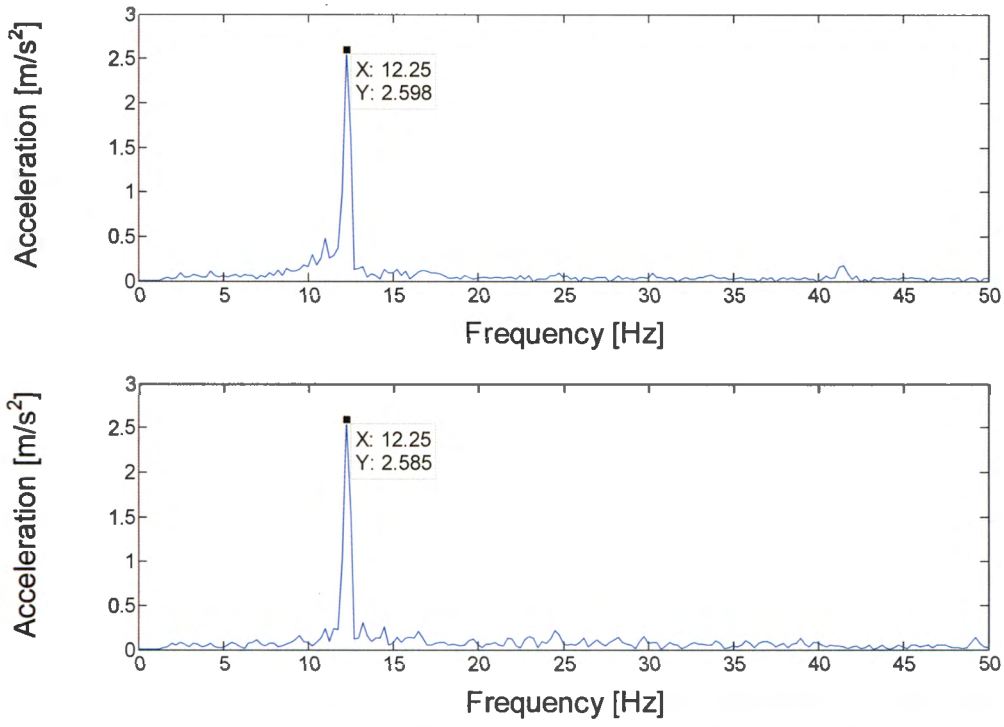

Figure D.3: Engine (top) and structure (bottom) response at 80 km/h with 240 g unbalance for Original system.

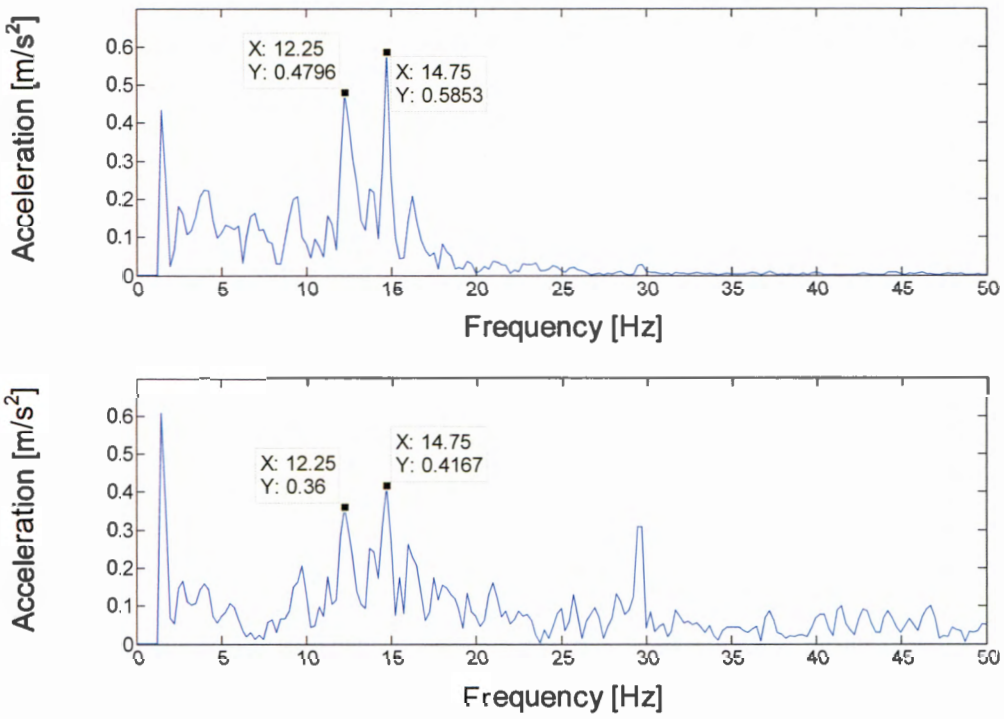

Figure D.4: Engine (top) and structure (bottom) response at 100 km/h with balanced wheels for Original system.

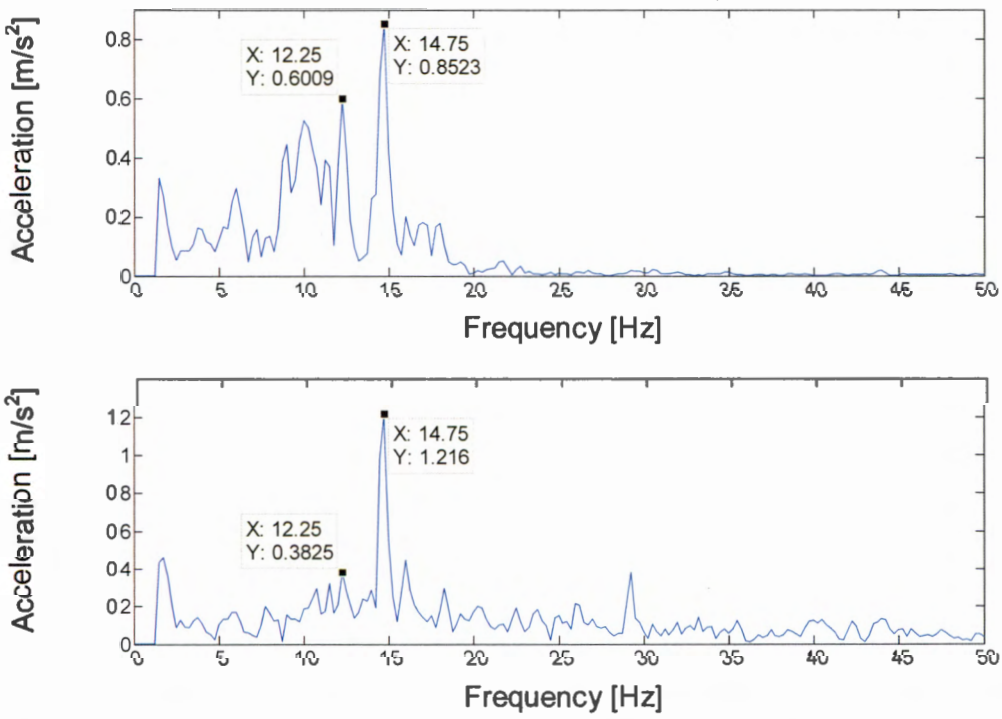

Figure D.5: Engine (top) and structure (bottom) response at 100 km/h with 120 g unbalance for Original system.

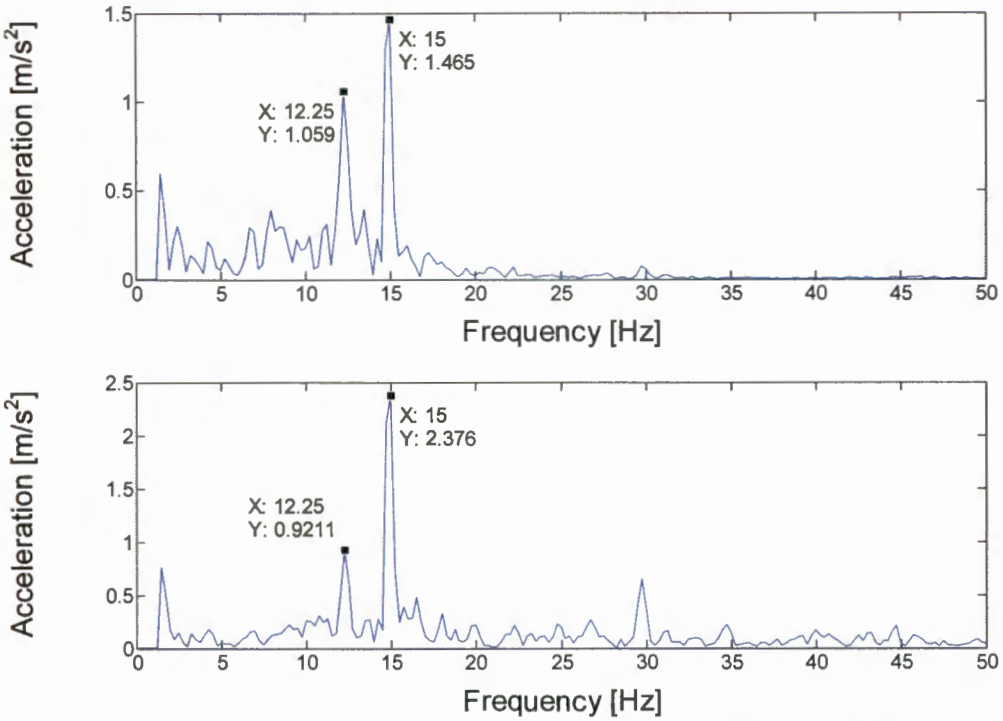

Figure D.6: Engine (top) and structure (bottom) response at 100 km/h with 240 g unbalance for Original system.

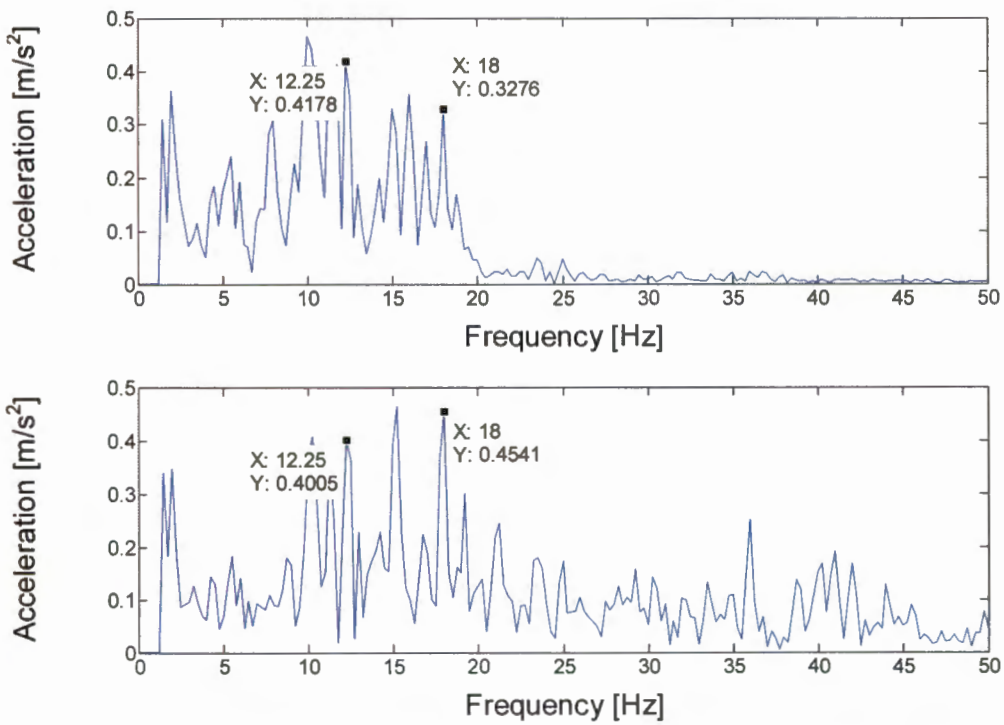

Figure D.7: Engine (top) and structure (bottom) response at 120 km/h with balanced wheels for Original system.

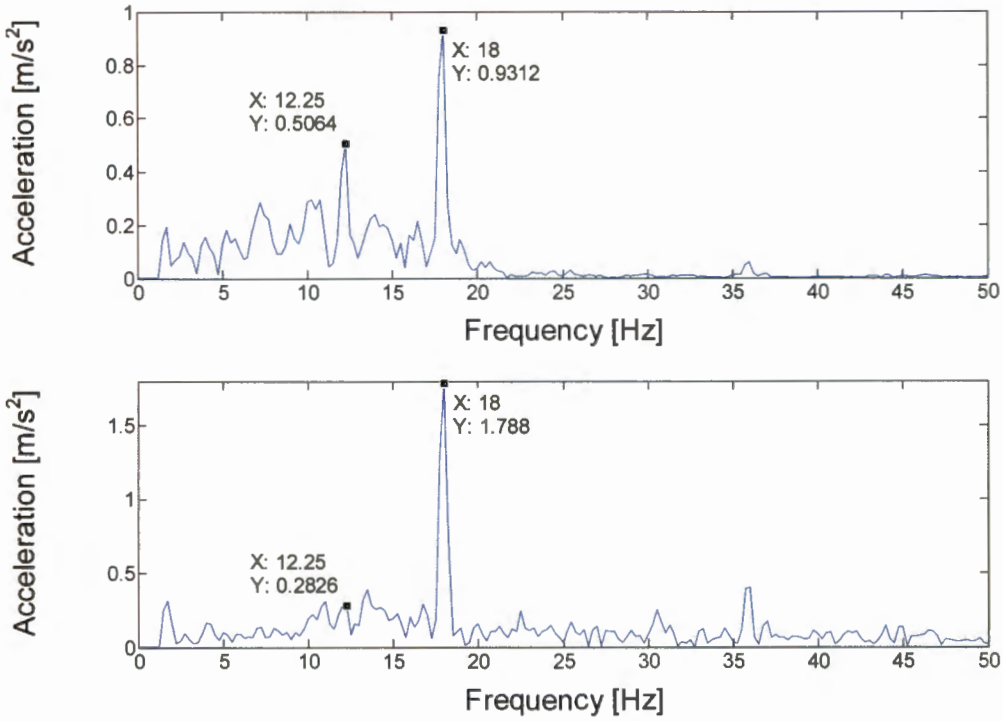

Figure D.8: Engine (top) and structure (bottom) response at 120 km/h with 120 g unbalance for Original system.

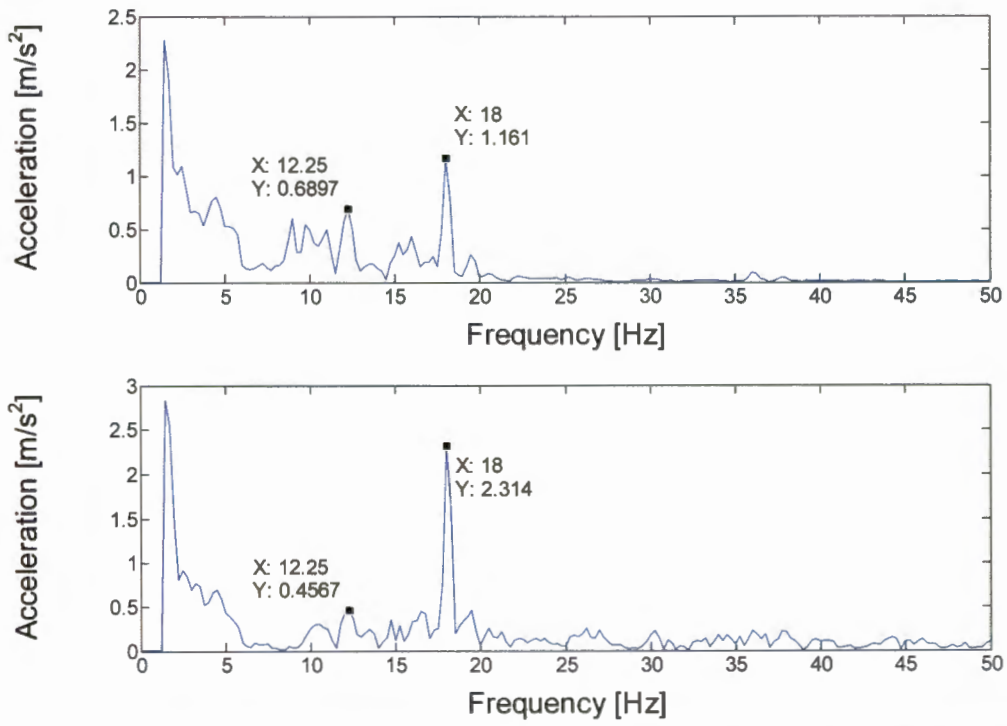

Figure D.9: Engine (top) and structure (bottom) response at 120 km/h with 240 g unbalance for Original system.

Road tests – Modified system

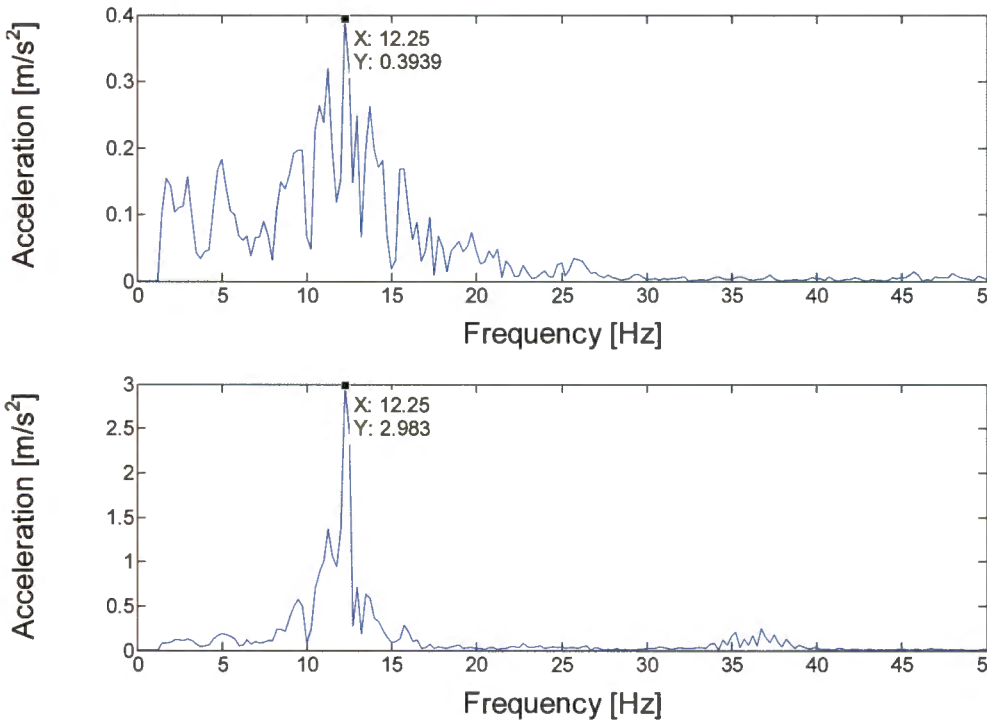

Figure D.10: Engine (top) and Absorber (bottom) response at 80 km/h with balanced wheels for Modified system.

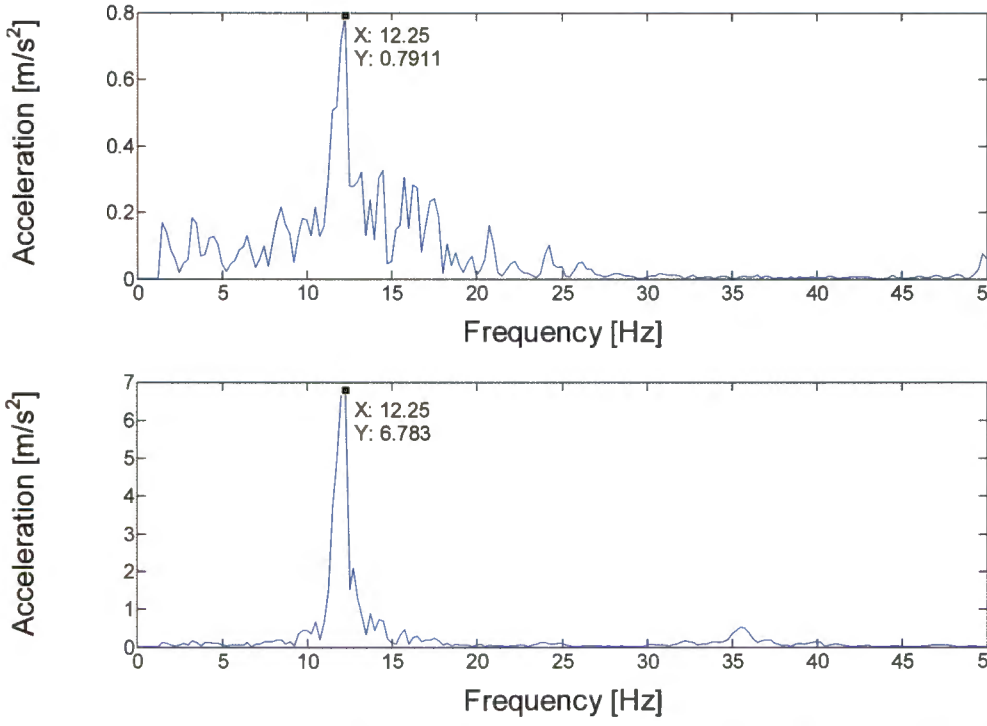

Figure D.11: Engine (top) and Absorber (bottom) response at 80 km/h with 120 g unbalance for Modified system.

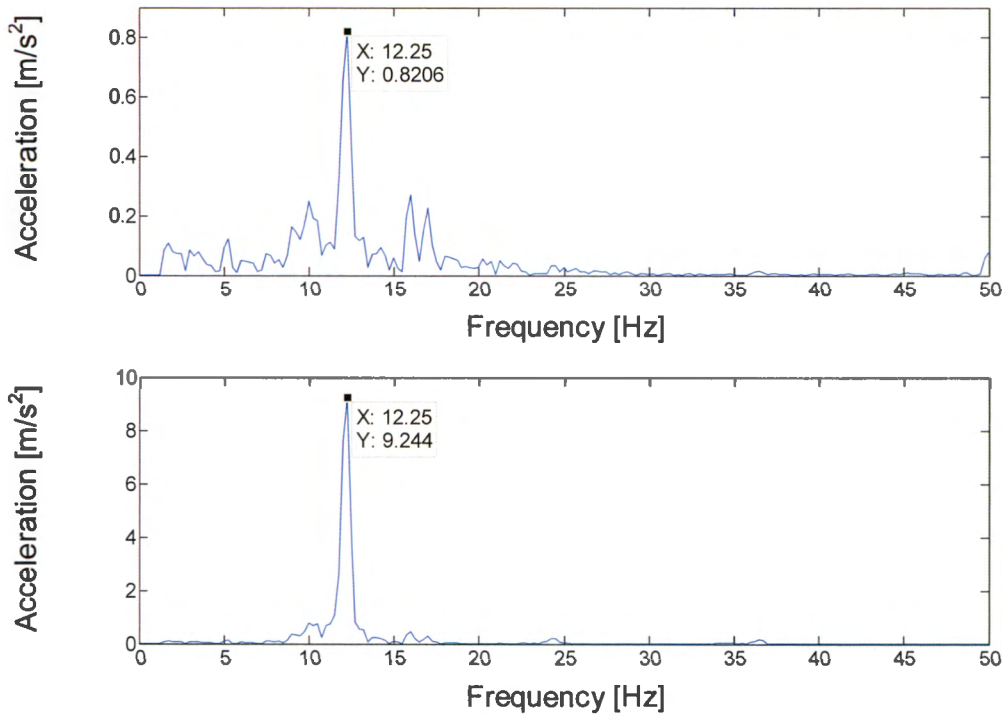

Figure D.12: Engine (top) and Absorber (bottom) response at 80 km/h with 240 g unbalance for Modified system.

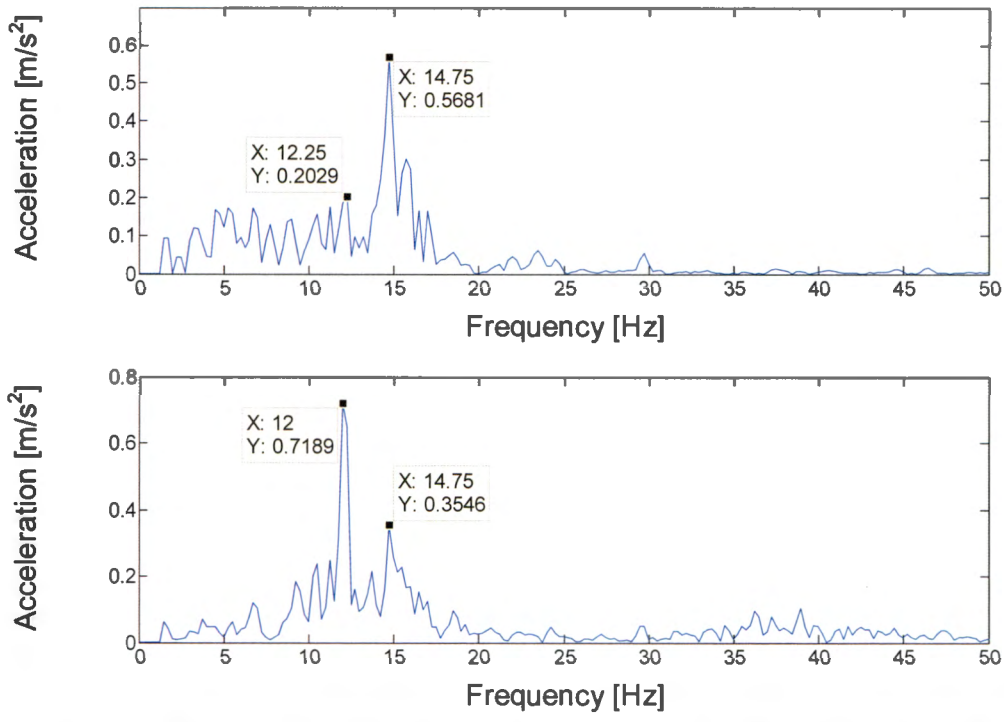

Figure D.13: Engine (top) and Absorber (bottom) response at 100 km/h with balanced wheels for Modified system.

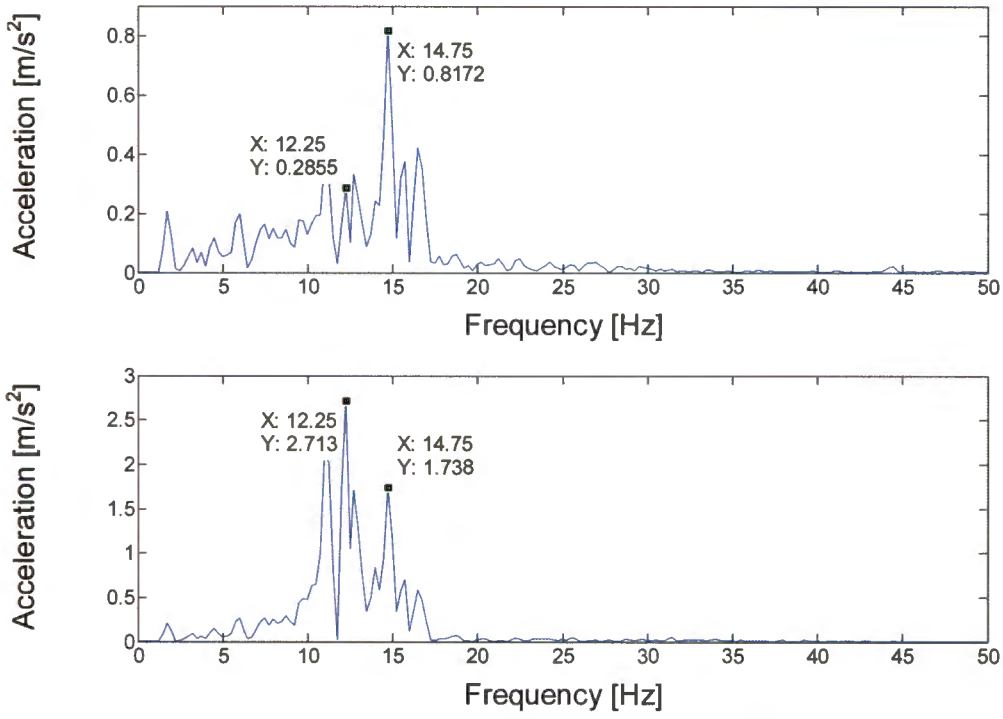

Figure D.14: Engine (top) and Absorber (bottom) response at 100 km/h with 120 g unbalance for Modified system.

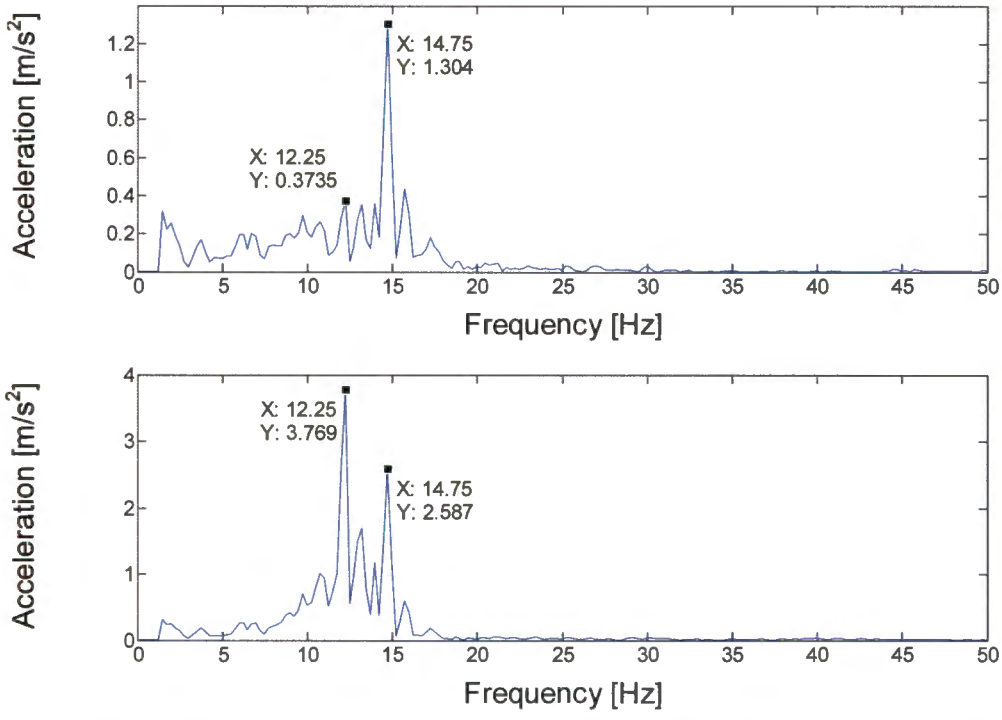

Figure D.15: Engine (top) and Absorber (bottom) response at 100 km/h with 240 g unbalance for Modified system.

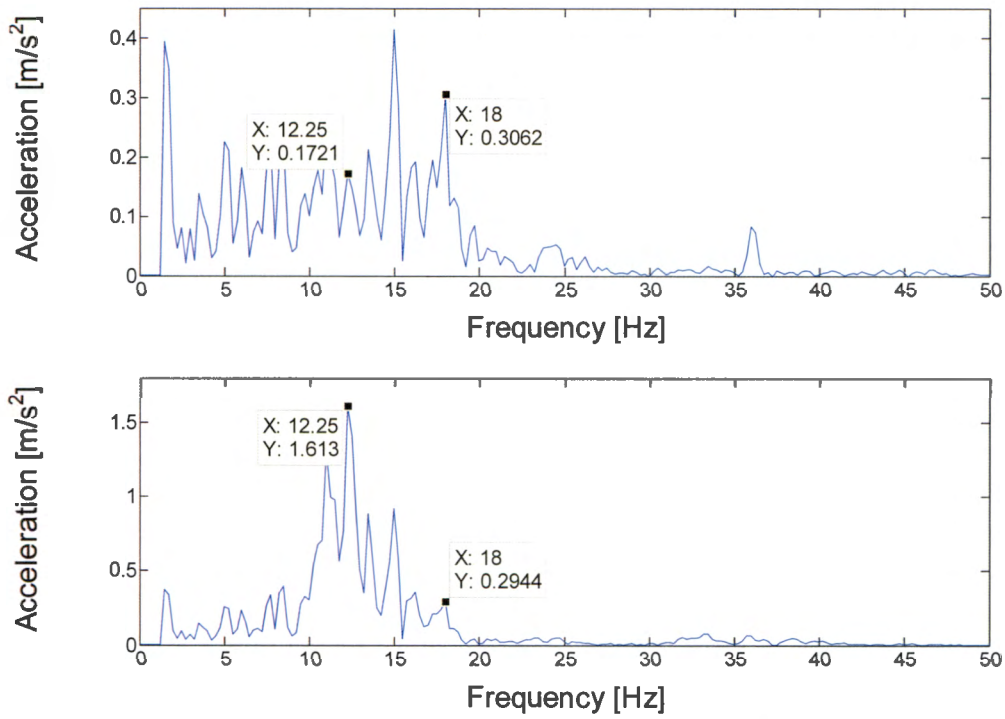

Figure D.16: Engine (top) and Absorber (bottom) response at 120 km/h with balanced wheels for Modified system.

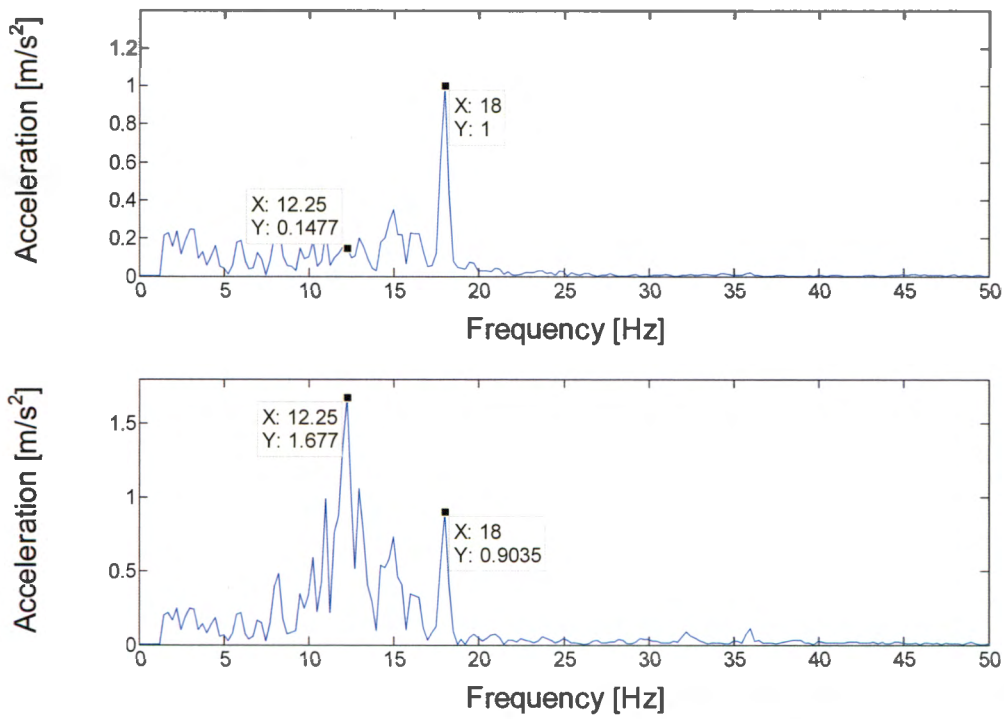

Figure D.17: Engine (top) and Absorber (bottom) response at 120 km/h with 120 g unbalance for Modified system.

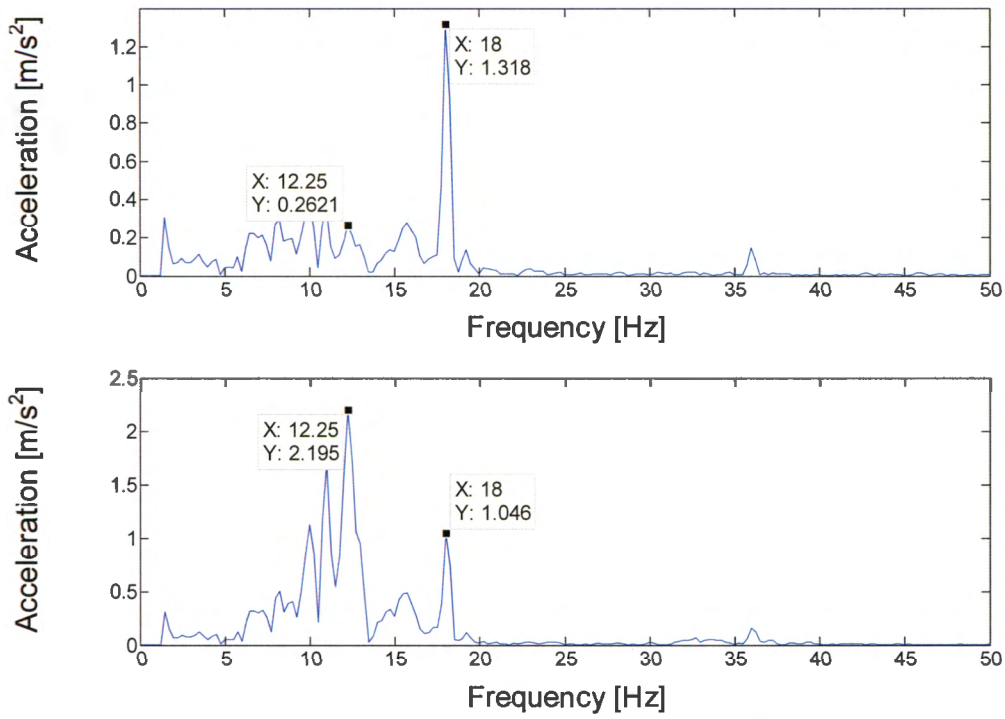

Figure D.18: Engine (top) and Absorber (bottom) response at 120 km/h with 240 g unbalance for Modified system.

Wheel suspension frequency

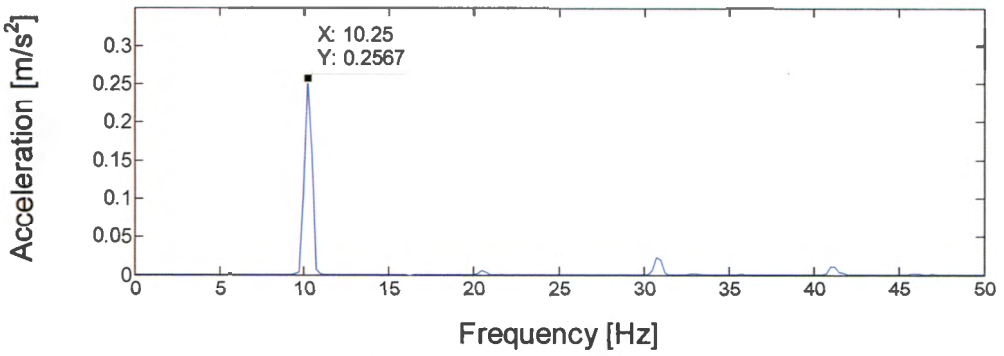

Figure D.19: Wheel suspension response at 10.25 Hz.

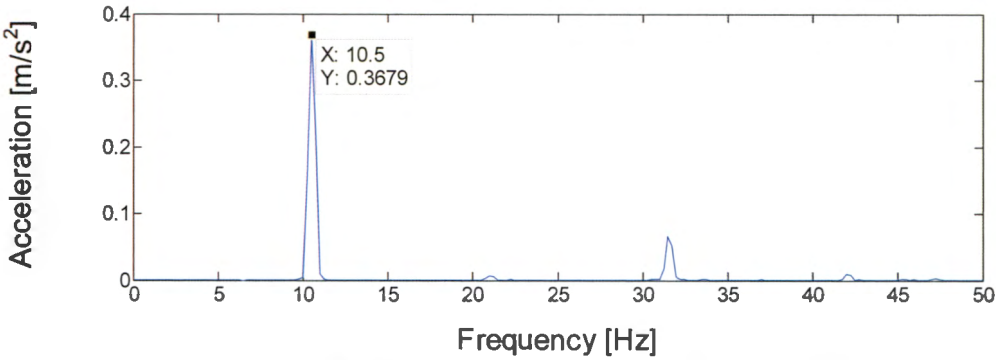

Figure D.20: Wheel suspension response at 10.50 Hz.

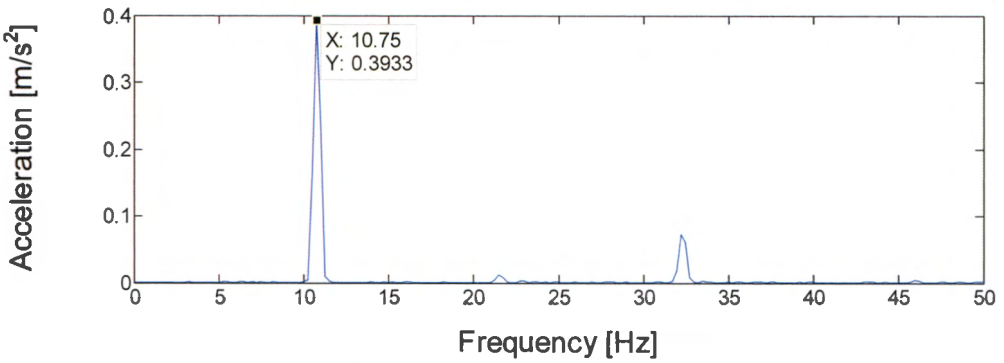

Figure D.21: Wheel suspension at resonance at 10.75 Hz.

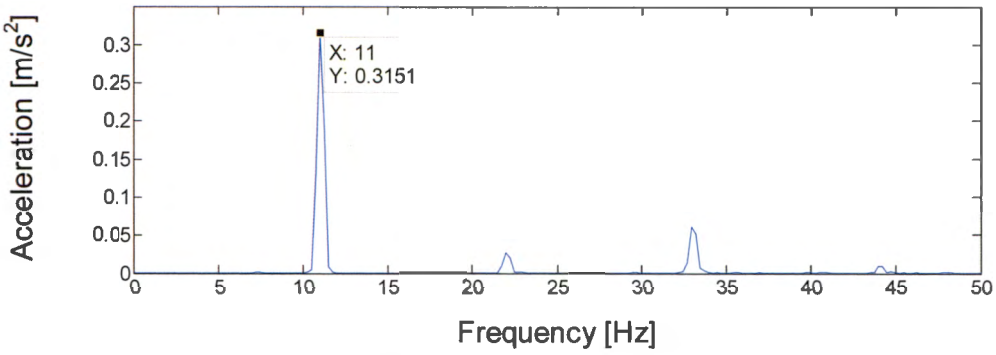

Figure D.22: Wheel suspension response at 11.00 Hz.

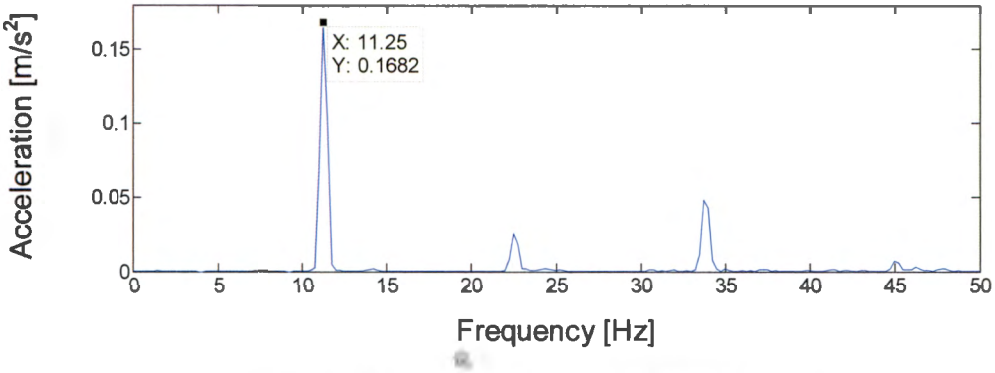

Figure D.23: Wheel suspension response at 11.25 Hz.